ADIPOSE TISSUE DYSFUNCTION

EDITED BY: Dirk Müller-Wieland and Matthias Blüher
PUBLISHED IN: Frontiers in Endocrinology

frontiers Research Topics

ISSN 1664-8714
ISBN 978-2-83250-091-0
DOI 10.3389/978-2-83250-091-0

About Frontiers

Frontiers is more than just an open-access publisher of scholarly articles: it is a pioneering approach to the world of academia, radically improving the way scholarly research is managed. The grand vision of Frontiers is a world where all people have an equal opportunity to seek, share and generate knowledge. Frontiers provides immediate and permanent online open access to all its publications, but this alone is not enough to realize our grand goals.

Frontiers Journal Series

The Frontiers Journal Series is a multi-tier and interdisciplinary set of open-access, online journals, promising a paradigm shift from the current review, selection and dissemination processes in academic publishing. All Frontiers journals are driven by researchers for researchers; therefore, they constitute a service to the scholarly community. At the same time, the Frontiers Journal Series operates on a revolutionary invention, the tiered publishing system, initially addressing specific communities of scholars, and gradually climbing up to broader public understanding, thus serving the interests of the lay society, too.

Dedication to Quality

Each Frontiers article is a landmark of the highest quality, thanks to genuinely collaborative interactions between authors and review editors, who include some of the world's best academicians. Research must be certified by peers before entering a stream of knowledge that may eventually reach the public - and shape society; therefore, Frontiers only applies the most rigorous and unbiased reviews.
Frontiers revolutionizes research publishing by freely delivering the most outstanding research, evaluated with no bias from both the academic and social point of view. By applying the most advanced information technologies, Frontiers is catapulting scholarly publishing into a new generation.

What are Frontiers Research Topics?

Frontiers Research Topics are very popular trademarks of the Frontiers Journals Series: they are collections of at least ten articles, all centered on a particular subject. With their unique mix of varied contributions from Original Research to Review Articles, Frontiers Research Topics unify the most influential researchers, the latest key findings and historical advances in a hot research area! Find out more on how to host your own Frontiers Research Topic or contribute to one as an author by contacting the Frontiers Editorial Office: frontiersin.org/about/contact

ADIPOSE TISSUE DYSFUNCTION

Topic Editors:
Dirk Müller-Wieland, University Hospital RWTH Aachen, Germany
Matthias Blüher, Leipzig University, Germany

Citation: Müller-Wieland, D., Blüher, M., eds. (2022). Adipose Tissue Dysfunction. Lausanne: Frontiers Media SA. doi: 10.3389/978-2-83250-091-0

Table of Contents

frontiers | Frontiers in Endocrinology

TYPE Editorial
PUBLISHED 17 August 2022
DOI 10.3389/fendo.2022.999188

OPEN ACCESS

EDITED AND REVIEWED BY
Katherine Samaras,
St Vincent's Hospital Sydney, Australia

*CORRESPONDENCE
Matthias Blüher
bluma@medizin.uni-leipzig.de
Dirk Muumlller-Wieland
dirmueller@ukaachen.de

SPECIALTY SECTION
This article was submitted to Obesity, a section of the journal Frontiers in Endocrinology

RECEIVED 20 July 2022
ACCEPTED 25 July 2022
PUBLISHED 17 August 2022

CITATION
Blüher M and Müller-Wieland D (2022) Editorial: Adipose tissue dysfunction. *Front. Endocrinol.* 13:999188. doi: 10.3389/fendo.2022.999188

Editorial: Adipose tissue dysfunction

Matthias Blüher[1,2]* and Dirk Müller-Wieland[3]*

[1]Helmholtz Institute for Metabolic, Obesity and Vascular Research (HI-MAG) of the Helmholtz Zentrum München at the University of Leipzig and University Hospital, Leipzig, Germany, [2]Medical Department III – Endocrinology, Nephrology, Rheumatology, University of Leipzig Medical Center, Leipzig, Germany, [3]Department of Cardiology, Angiology and Intensive Care Medicine, University Hospital Aachen, Aachen, Germany

KEYWORDS

adipose tissue, obesity, adipokine, inflammation, lipodystrophy, visceral fat

Editorial on the Research Topic
Adipose tissue dysfunction

For a long time, adipose tissue (AT) has been regarded as a functionally and anatomically simple to understand organ that only contributes to the insulation of the body, thermoregulation, and mechanical organ protection (1–3). Only in the past few decades, it has been recognized that AT is characterized by dynamic adaptations, heterogeneous cell populations, and astonishing plasticity (2–5). With the discovery that adipocytes secrete leptin (6) it became clear that AT is involved in many biological processes including regulation of energy homeostasis, glucose and lipid metabolism, blood pressure, and immune response (1–4).

With the growing interest in better understanding mechanisms causing obesity and obesity-related cardio-metabolic diseases and mortality (7, 8), AT research developed rapidly. Indeed, AT represents the main organ for energy storage under conditions of caloric surplus and releases lipids to protect our bodies against weight loss in prolonged periods of fasting or starvation. Both access to AT in people living with obesity (3, 4, 9), but also deficiency or a complete loss of AT in patients with lipodystrophy or lipoatrophy are associated with conditions that predispose to insulin resistance, type 2 diabetes, fatty liver disease, and other metabolic abnormalities (10, 11). Based on these observations, it has been proposed that impaired expandability of "healthy" subcutaneous AT may be a relevant mechanism linking obesity to its comorbid conditions (12). Supporting this hypothesis, it has been shown that transplantation of AT with a normal function led to beneficial effects on glucose and lipid metabolism in animal models (13).

The risk for many obesity-associated diseases increases linearly with an increase in fat mass (9). However, there are people with obesity who do not develop metabolic or cardiovascular diseases at the expected frequency or age of manifestation. This subgroup of people with metabolically healthy obesity has taught us about potential mechanisms for the link between fat accumulation and cardio-metabolic risk (14, 15). Among the biological mechanisms that link increased body fat mass to cardio-metabolic diseases, AT dysfunction is a major determinant of the individual obesity-associated risk (14, 15).

The concept of AT dysfunction (16) is not novel and has been described as adiposopathy (17), obesity-related adipose tissue disease (OrAD, 18), or sick fat (17). These terms summarize specific symptoms that are associated with abnormal AT function including ectopic fat deposition in visceral depots, the liver, pancreas, and other organs, adipocyte hypertrophy, a higher number of immune cells in AT, AT fibrosis, and secretion of pro-inflammatory, diabetogenic, and atherogenic signals from AT (4, 16, 17).

In principle, AT dysfunction can develop if AT in healthy subcutaneous (e.g. leg and hip fat) depots exceed their storage capacity or have (e.g. genetically determined) limited expandability. The inability of AT to respond to excess energy storage demands with adequate hyperplasia leads to hypertrophy of adipocytes that contributes to hypoxia, inadequate vascularization, AT stress and immune cell infiltration, autophagy, apoptosis, increased production of pro-fibrotic extracellular matrix proteins subsequently causing AT fibrosis.

Current AT research focuses on a better understanding of these mechanisms and specific factors with the ultimate vision to identify targets for the future treatment of obesity and AT dysfunction-related diseases. Within this Research Topic on "*Adipose tissue dysfunction*", the complexity and fascination of AT research are reflected by eleven articles:

Pincu et al. summarize the current knowledge on histopathological characteristics of AT dysfunction and propose the term obesity-related adipose tissue disease (OrAD) to reflect the notion that abnormalities in AT of people with obesity predict future obesity-related endpoints and the response to specific anti-obesity interventions. The authors focus on adipocyte hypertrophy, AT inflammation, and fibrosis as major features of OrAD.

Our readers can find a complimentary review on immune cell regulation of white adipose progenitor cells by Altun et al. The mini-review discusses the heterogeneity in composition and fate of adipose progenitor subtypes and their interactions with different immune cell populations. More specifically, the review article by Zhu and Liu focuses on the role of activated NOD-like receptor family 3 (NLRP3) inflammasome and its interaction with autophagy mechanisms in the development of AT dysfunction.

The importance of AT immune cell infiltration in the context of AT dysfunction has been further elucidated in an original article from Strand et al. The group used a proteomics screen to identify novel surface proteins specific to M1-like- and M2-like macrophages that are fat-depot specifically associated with AT immunophenotypes.

In a sophisticated magnetic resonance imaging study, Zhang et al. support the concept that visceral AT, hepatic fat, pancreatic fat, and preperitoneal AT are associated with cardio-metabolic risk factors independently of BMI.

As lipodystrophy is considered a disease caused by AT dysfunction, our special issue includes an original article by Dattilo et al. in which the authors discovered a predictive role of circulation miRNA-320 for AT function in patients with lipodystrophy.

Ronningen et al. provide novel data on the role of N^6-methyladenosine (m6A) - as one of the most abundant post-transcriptional modifications on mRNA – on fat depot determination.

In a large study of 5,821 adults, Sun et al. (reported that insulin resistance of AT is associated with hyperuricemia, pointing toward a previously unrecognized role AT in uric acid metabolism. The article collection is completed by novel data on associations between obesity subphenotypes and a higher risk of ischemic stroke (Zou et al.) as well as on subcutaneous fat accumulation and increased urinary stone risk in young people (Ye et al.).

We hope that you as our readers enjoy reading our Research Topic on adipose tissue dysfunction and agree with us that AT is a treasure box to identify mechanisms and targets for a better understanding of diseases that involve AT dysfunction.

Author contributions

All authors listed have made a substantial, direct, and intellectual contribution to the work and approved it for publication.

Conflict of interest

MB received honoraria as a consultant and speaker from Amgen, AstraZeneca, Bayer, Boehringer-Ingelheim, Lilly, Novo Nordisk, Novartis and Sanofi. DM-W received honoraria as a consultant and speaker from Amarin, Amgen, AstraZeneca, Bayer, Boehringer-Ingelheim, Daichii-Sankyo, Lilly, Novo Nordisk, Novartis and Sanofi.

Publisher's note

References

1. Arner P. Fat tissue growth and development in humans. *Nestle Nutr Inst Workshop Ser* (2018) 89:37–45. doi: 10.1159/000486491

2. Cinti S. The endocrine adipose organ. *Rev Endocr Metab Disord* (2022) 23 (1):1–4. doi: 10.1007/s11154-022-09709-w

3. Blüher M. Adipose tissue dysfunction contributes to obesity related metabolic diseases. *Best Pract Res Clin Endocrinol Metab* (2013) 27(2):163–77. doi: 10.1016/j.beem.2013.02.005

4. Klöting N, Blüher M. Adipocyte dysfunction, inflammation and metabolic syndrome. *Rev Endocr Metab Disord* (2014) 15(4):277–87. doi: 10.1007/s11154-014-9301-0

5. Emont MP, Jacobs C, Essene AL, Pant D, Tenen D, Colleluori G, et al. A single-cell atlas of human and mouse white adipose tissue. *Nature.* (2022) 603 (7903):926–33. doi: 10.1038/s41586-022-04518-2

6. Zhang Y, Proenca R, Maffei M, Barone M, Leopold L, Friedman JM. Positional cloning of the mouse obese gene and its human homologue. *Nature.* (1994) 372(6505):425–32. doi: 10.1038/372425a0

7. Blüher M. Obesity: global epidemiology and pathogenesis. *Nat Rev Endocrinol* (2019) 15(5):288–98. doi: 10.1038/s41574-019-0176-8

8. Manson JE, Willett WC, Stampfer MJ, Colditz GA, Hunter DJ, Hankinson SE, et al. Body weight and mortality among women. *N Engl J Med* (1995) 333 (11):677–85. doi: 10.1056/NEJM199509143331101

9. Klein S, Gastaldelli A, Yki-Järvinen H, Scherer PE. Why does obesity cause diabetes? *Cell Metab* (2022) 34(1):11–20. doi: 10.1016/j.cmet.2021.12.012

10. Zammouri J, Vatier C, Capel E, Auclair M, Storey-London C, Bismuth E, et al. Molecular and cellular bases of lipodystrophy syndromes. *Front Endocrinol (Lausanne)* (2022) 12:803189. doi: 10.3389/fendo.2021.803189

11. Lim K, Haider A, Adams C, Sleigh A, Savage DB. Lipodistrophy: a paradigm for understanding the consequences of "overloading" adipose tissue. *Physiol Rev* (2021) 101(3):907–93. doi: 10.1152/physrev.00032.2020

12. Rutkowski JM, Stern JH, Scherer PE. The cell biology of fat expansion. *J Cell Biol* (2015) 208(5):501–12. doi: 10.1083/jcb.201409063

13. Tran TT, Yamamoto Y, Gesta S, Kahn CR. Beneficial effects of subcutaneous fat transplantation on metabolism. *Cell Metab* (2008) 7(5):410–20. doi: 10.1016/j.cmet.2008.04.004

14. Stefan N. Causes, consequences, and treatment of metabolically unhealthy fat distribution. *Lancet Diabetes Endocrinol* (2020) 8(7):616–27. doi: 10.1016/S2213-8587(20)30110-8

15. Blüher M. Metabolically healthy obesity. *Endocr Rev* (2020) 41(3):bnaa004. doi: 10.1210/endrev/bnaa004

16. Sun K, Tordjman J, Clément K, Scherer PE. Fibrosis and adipose tissue dysfunction. *Cell Metab* (2013) 18(4):470–7. doi: 10.1016/j.cmet.2013.06.016

17. Bays H, Abate N, Chandalia M. Adiposopathy: sick fat causes high blood sugar, high blood pressure and dyslipidemia. *Future Cardiol* (2005) 1(1):39–59. doi: 10.1517/14796678.1.1.39

frontiers in Endocrinology

ORIGINAL RESEARCH
published: 21 September 2021
doi: 10.3389/fendo.2021.713357

Heterogeneous miRNA-mRNA Regulatory Networks of Visceral and Subcutaneous Adipose Tissue in the Relationship Between Obesity and Renal Clear Cell Carcinoma

*Yuyan Liu[1,2], Yang Liu[1], Jiajin Hu[1], Zhenwei He[1], Lei Liu[1], Yanan Ma[3] and Deliang Wen[1]**

[1] Institute of Health Sciences, China Medical University, Shenyang, China, [2] Department of Clinical Epidemiology, The Fourth Affiliated Hospital of China Medical University, Shenyang, China, [3] Department of Biostatistics and Epidemiology, School of Public Health, China Medical University, Shenyang, China

Background: Clear cell renal cell carcinoma (ccRCC) is one of the most lethal urologic cancer. Associations of both visceral adipose tissue (VAT) and subcutaneous adipose tissue (SAT) with ccRCC have been reported, and underlying mechanisms of VAT perhaps distinguished from SAT, considering their different structures and functions. We performed this study to disclose different miRNA-mRNA networks of obesity-related ccRCC in VAT and SAT using datasets from Gene Expression Omnibus (GEO) and The Cancer Genome Atlas (TCGA); and find out different RNAs correlated with the prognosis of ccRCC in VAT and SAT.

Methods: We screened out different expressed (DE) mRNAs and miRNAs of obesity, in both VAT and SAT from GEO datasets, and constructed miRNA-mRNA networks of obesity-related ccRCC. To evaluate the sensitivity and specificity of RNAs in networks of obesity-related ccRCC in both VAT and SAT, Receiver Operating Characteristic (ROC) analyses were conducted using TCGA datasets. Spearman correlation analyses were then performed to find out RNA pairs with inverse correlations. We also performed Cox regression analyses to estimate the association of all DE RNAs of obesity with the overall survival.

Results: 136 and 185 DE mRNAs of obesity in VAT and SAT were found out. Combined with selected DE miRNAs, miRNA-mRNA networks of obesity-related ccRCC were constructed. By performing ROC analyses, RNAs with same trend as shown in networks and statistically significant ORs were selected to be paired. Three pairs were finally remained in Spearman correlation analyses, including hsa-miR-182&ATP2B2, hsa-miR-532&CDH2 in VAT, and hsa-miR-425&TFAP2B in SAT. Multivariable Cox regression analyses showed that several RNAs with statistically significant adjusted HRs remained consistent trends as shown in DE analyses of obesity. Risk score analyses using selected RNAs showed that the overall survival time of patients in the low-risk group was significantly longer than that in the high-risk group regardless of risk score models.

OPEN ACCESS

Edited by:
Matthias Blüher,
Leipzig University, Germany

Reviewed by:
Carlo Augusto Mallio,
Campus Bio-Medico University, Italy
Sebastián Chapela,
University of Buenos Aires, Argentina

***Correspondence:**
Deliang Wen
dlwen@cmu.edu.cn

Specialty section:
This article was submitted to Obesity, a section of the journal Frontiers in Endocrinology

Received: *22 May 2021*
Accepted: *01 September 2021*
Published: *21 September 2021*

Citation:
Liu Y, Liu Y, Hu J, He Z, Liu L, Ma Y and Wen D (2021) Heterogeneous miRNA-mRNA Regulatory Networks of Visceral and Subcutaneous Adipose Tissue in the Relationship Between Obesity and Renal Clear Cell Carcinoma. Front. Endocrinol. 12:713357. doi: 10.3389/fendo.2021.713357

Conclusions: We found out different miRNA-mRNA regulatory networks of obesity-related ccRCC for both VAT and SAT; and several DE RNAs of obesity-related ccRCC were found to remain consistent performance in terms of ccRCC prognosis. Our findings could provide valuable evidence on the targeted therapy of obesity-related ccRCC.

Keywords: renal clear cell carcinoma, obesity, adipose tissue, micro RNA, messenger RNA

INTRODUCTION

Renal cell carcinoma (RCC) is one of the most lethal urologic cancer (1), encompassing histological subtypes of cancers derived from renal tubular epithelial cells (2). Approximately 2% of incidence and mortality of malignances can be attributed to RCC (3). Clear cell renal cell carcinoma (ccRCC) is the most common subtype of RCC, accounting for over 70% of cases (4). Obesity has been identified as one of the independent modifiable risk factors of RCC, and is involved in the development of more than 30%-40% of RCC cases (5). Published studies demonstrated that ccRCC risk was 1.5-fold higher in people with obesity than those with normal weight (6). Another longitudinal cohort study found that after an average follow-up of 11.3 years, large body mass index (BMI) at baseline was associated with the increased risk of ccRCC, hazard ratio (HR) per 1 kg/m^2 increase of BMI was 1.09 with the 95% confidence interval (CI) of (1.02, 1.16) (7). Inflammatory cytokines released from adipose tissue has been considered playing a key role in the pathophysiology of obesity-related ccRCC (6). Results from a case-control study including 682 ccRCC cases implied that insulin resistance and inflammation driven by several obesity-related biomarkers might underlie the relationship between obesity and ccRCC (8).

Abdominal adipose tissue, including visceral adipose tissue (VAT) and subcutaneous adipose tissue (SAT), is not only a main storage of fat in mammals, but also an important endocrine organ secreting adipokines, such as cytokines, interleukins and other biologically active molecules (9). Both VAT and SAT have been reported to be positively associated with the prevalence/incidence of several cardiovascular diseases (10) and cancers (11, 12), including ccRCC. Greco, et al. found that both VAT and SAT areas measured using computed tomography (CT) were larger in ccRCC group compared to controls (13). However, no study has revealed if the mechanism of VAT underlying the relationship between obesity and ccRCC distinguished from that of SAT. We thought such heterogeneity perhaps existed, considering differences in levels of lipid mobilization, adipokine production and adipocyte differentiation between VAT and SAT (14, 15).

It has been well proven that gene expression profiles estimated using message RNA (mRNA) level could be an effective method to predict the pathophysiological mechanisms of several cancers (16–18). For an instance, a bioinformatic analysis performed by Zhou et al., showed that 5 genes, such as IGHA1 and IGKC were correlated with ccRCC (19). In addition, micro RNA (miRNA) is a class of well-characterized RNA without protein encoding potential. miRNAs can bind to their target genes, typically resulting in gene silencing by triggering the degradation of the target mRNAs, and associations of miRNAs with ccRCC have been reported (20–22). However, no miRNA-mRNA regulatory network relative to obesity-related ccRCC was given. On the other hand, whether ccRCC-relevant RNAs were different between VAT and SAT remained unknown.

Therefore, as shown in **Figure 1**, we performed this study aiming to disclose different miRNA-mRNA networks of obesity-related ccRCC in VAT and SAT using datasets from Gene Expression Omnibus (GEO); verify the obtained miRNA-mRNA pairs relevant to ccRCC using the dataset of The Cancer Genome Atlas (TCGA); and find out different mRNAs and miRNAs correlated with the prognosis of ccRCC in VAT and SAT. Findings in this study would be helpful to distinguish the molecular mechanisms of obesity-related ccRCC between VAT and SAT, and provide valuable evidence on the targeted therapy of obesity-related ccRCC.

METHODS

Selecting Microarray Datasets and Collecting Data

We first downloaded the microarray dataset (GSE24883) of mRNA expression profiles in both VAT and SAT based on the platform of GPL4133 from the GEO (https://www.ncbi.nlm.nih.gov/geo/) (23). The GSE24883 dataset included 64 samples of VAT, as well as paired SAT from 32 female participants, who were divided in 4 subgroups according to BMI, and the presence of the metabolic syndrome (MS) (24), i.e. lean (8/32), overweight (8/32), obesity (8/32), and obesity with MS (8/32). Whole transcriptome analysis was performed using DNA microarrays on VAT and SAT samples, and total RNA was hybridized to Agilent 44k whole human genome microarray (Agilent, Santa Clara, CA). Thereafter, miRNA expression profiles of VAT and SAT were obtained from datasets of GSE50574 (GPL16384) and GSE25402 (GPL8786), respectively. In GSE50574 datasets, 7 obese (BMI: 33-50 kg/m^2) and 5 lean (BMI: 22-25 kg/m^2) samples were included. Adipocyte-exosomal total RNA was extracted from VAT, and only mature human miRNAs were retained as Affymetrix 3.0 miRNA arrays (Affymetrix, Santa Clara, CA) (25). GSE25402 dataset included 30 obese (BMI> 30 kg/m^2) and 26 non-obese samples (BMI< 30 kg/m^2) healthy samples. Total RNA was extracted from abdominal subcutaneous white adipose tissue, and miRNAs were retained as Affymetrix multispecies miRNA-1 array (Affymetrix) (26). In addition, mRNA expression profiles of ccRCC (GSE46699,

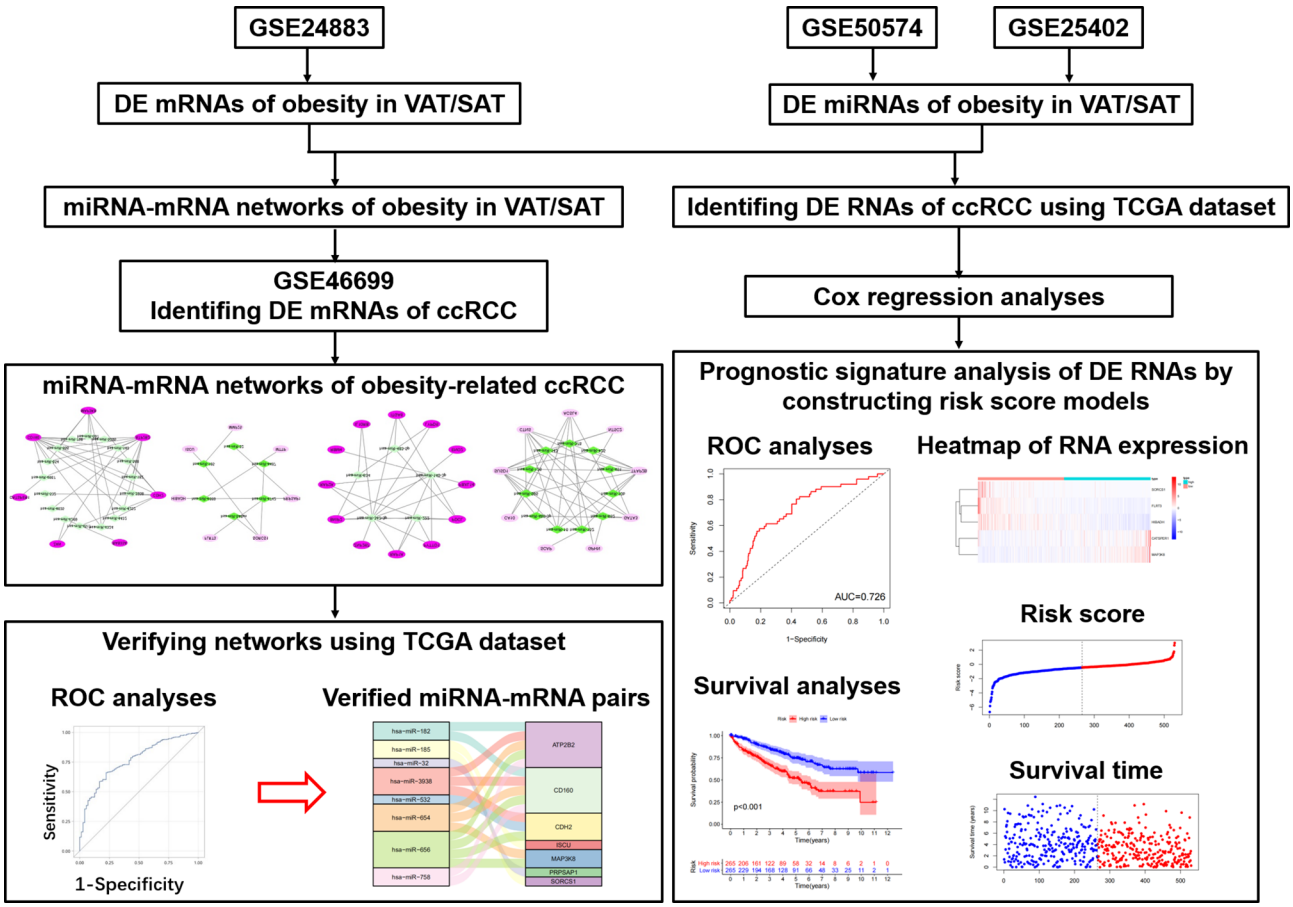

FIGURE 1 | Flow chart of this study.

GPL570) was downloaded, and only 24 samples (patient-matched tumors and adjacent-normal tissues) from 12 obese participants (BMI> 30 kg/m^2) were used for the following analyses, considering that we would like to find out if differentially expressed (DE) mRNAs of obesity in both VAT and SAT datasets were correlated with the presence of obesity-related ccRCC (27).

Identifying DE mRNAs and miRNAs of Obesity in VAT and SAT

Firstly, we downloaded the series matrix file of GSE24883 and the platform file of GPL4133. In accordance with the annotations, probe IDs in the matrix file were transformed into the gene symbols, and probes that did not correspond to the mRNA symbols were excluded. The average value of mRNA correlated with more than one probe was used as the final expression value (28). We then normalized the data of mRNA expression profiles using robust multi-array average (RMA) based on the limma package in R (v.4.0.3) software (29). Since samples in GSE24883 were divided into 4 subgroups, statistical comparisons were respectively performed between lean and other 3 subgroups with different obese statuses using the Bayesian method in limma package. By setting a cutoff threshold of P-value < 0.05 and |log$_2$fold change (FC)| > 2, DE mRNAs of overweight, obesity and obesity with metabolic syndrome (MS) in both VAT and SAT were revealed. Consistent methods as above mentioned were respectively repeated in both GSE50574 and GSE25402 datasets to obtain the DE miRNA of obesity in VAT and SAT using the cutoff of P value < 0.05 and |FC| > 1.2 (25). Relevant volcano plots and heatmaps of both mRNAs and miRNAs were given using R software. Furthermore, for DE mRNAs of 3 obese statuses, Venn diagrams were generated using VennDiagram R package to disclose the common DE mRNAs in 3 obese statuses in both VAT and SAT.

Constructing miRNA-mRNA Networks of Obesity in VAT and SAT

Based on the up- and down-regulated DE miRNAs of obesity in VAT and SAT, miRNA-mRNA pairs were predicted using Targetscan database (30), followed by performing VennDiagram R package to obtain the intersections between predicted mRNAs in miRNA-mRNA pairs and DE ones of obesity in VAT and SAT, respectively. Secondly, we screened

out the pairs including the DE mRNAs in the intersection, and then only retained those showing inverse relationship between miRNA and mRNA as the final miRNA-mRNA network considering the specific role of miRNA in degrading their target mRNAs (31, 32). Results were visualized using the Cytoscape software (v3.8.0). To investigate a comprehensive set of functional annotation of target mRNAs in networks of obesity, Kyoto Encyclopedia of Genes and Genomes (KEGG) pathway analyses (33) and gene ontology (GO) term enrichment analyses (34) were performed by using the Clusterprofiler package. The KEGG pathway and GO enrichment analyses of genes were based on the threshold of P-value < 0.05.

Identifying DE mRNAs of ccRCC From miRNA-mRNA Networks of Obesity

Target mRNAs of miRNA-mRNA networks obtained from the former step in both VAT and SAT were respectively analyzed in the specific samples from obese participants of GSE46699 dataset. By running Bayesian method in limma R package, we identified the DE mRNAs of ccRCC in obesity with P-value < 0.05, and furthermore screened out those with same trends (up- or down-regulated) as shown in networks of obesity. Thereafter, miRNA-mRNA networks of obesity-related ccRCC in both VAT and SAT were constructed, and visualized using Cytoscape software.

TCGA Data Collection

The RNA sequencing (RNAseq) data from Illumina HiSeq RNA-Seq platform and corresponding clinical follow-up information were downloaded from TCGA (https://portal.gdc.cancer.gov/) database. Fragments Per Kilobase Million (FPKM) values of both mRNA and miRNA data were collected. For mRNA data, we transferred ENSAMBL IDs in the matrix file into gene symbols. As a result, 611 and 616 samples were respectively selected for mRNA and miRNA analyses from TCGA database by searching KIRC (kidney renal clear cell carcinoma), while clinical follow-up information were only collected among 537 samples.

Receiver Operating Characteristic Curve Analysis of RNAs in Networks of Obesity-Related ccRCC

To evaluate the sensitivity and specificity of both mRNAs and miRNAs in networks of obesity-related ccRCC in both VAT and SAT for distinguishing between normal and cancer tissues, ROC curve analyses were respectively conducted for mRNAs and miRNAs, and the area under curve (AUC) was calculated by running the code of "proc logistic" in the SAS software (v9.4). DE RNAs with both statistically significant odds ratios (ORs) and same trends as shown in previous obtained networks were retained to construct the updated networks in VAT and SAT. Sankey diagrams of networks were given using R software. To further verify the relationship of miRNA-mRNA pairs shown in Sankey diagrams, we then performed Spearman correlation analyses focusing on the specific RNAs in networks by selecting samples with both mRNA and miRNA data in TCGA dataset. miRNA-mRNA pairs with inverse correlation coefficients ($r < 0$ and P-value < 0.05) were considered as final networks.

Prognostic Signature Analysis of DE RNAs of Obesity-Related ccRCC

To differentiate the ccRCC prognostic signatures of DE RNAs of obesity between VAT and SAT, we performed Cox regression analyses to estimate the association of all DE mRNAs and miRNAs of obesity (which were not limited to those in networks) with the overall survival using the TCGA dataset of ccRCC. 530 and 516 samples with ccRCC were respectively selected for the analyses of mRNAs and miRNAs. Multivariable Cox proportional hazards regression analyses were performed by running SAS code of "proc phreg", HR and relevant 95% CI were given. Regression models included unadjusted model and multi-adjusted model (adjusted for age, gender, as well as the tumor stage according to the tumor-node-metastasis (TNM) staging system of ccRCC). mRNA and miRNA with both statistical significant HRs (P-value < 0.05) and same trends as shown in previously performed DE analyses were then remained as candidates to calculate a risk score for each patient using regression coefficients of these eligible RNAs derived from Cox regression models. The formula was shown as follows: Risk score= expRNA1 * βRNA1 + expRNA2 * βRNA2 + expRNA3 * βRNA3 +……+ expRNAn * βRNAn, expRNA implies the expression value of RNA, and βRNA implies the regression coefficient of Cox regression model (17). In accordance with the risk scores, patients were divided into high- and low-risk groups, and 1-year ROC as well as Kaplan-Meier survival curves of the two groups were generated by running "timeROC", "survival", and "surviminer" R packages. Simultaneously, scatter plots of risk scores and survival time among patients, as well as heatmaps of RNA components used for calculating the risk score were given using R software.

RESULTS

Identification of DE mRNAs of Obesity in VAT and SAT

By running limma R package among 64 samples in the dataset of GSE24833, we obtained DE mRNAs of overweight, obesity and obesity with MS in both VAT and SAT (**Supplemental Tables 1** and **2**). Volcano plots and heatmaps of DE mRNAs in VAT and SAT were respectively shown in **Figure 2** and **Figure 3**. The amount of DE mRNAs of obesity in VAT was 136 (35 for overweight, 54 for obesity, and 61 for obesity with MS), and only 2 mRNAs (IQCF6 and FRAG1) were shared by all these 3 obesity components as shown in Venn diagram (**Figure 2D**). For SAT, the amount of DE mRNAs of obesity was 185 (50 for overweight, 54 for obesity, and 107 for obesity with MS), and only 3 mRNAs (JSRP1, MRS2 and STK40) were shared by all these 3 obesity components as shown in Venn diagram (**Figure 3D**).

Construction of miRNA-mRNA Networks of Obesity in VAT and SAT

In the dataset of GSE50574, we screened out 52 DE miRNAs of obesity in VAT by comparing 7 obese to 5 lean samples. On the other hand, 25 miRNAs of obesity in SAT were obtained in the dataset of GSE25402. Values of |log2FC| and P were shown in

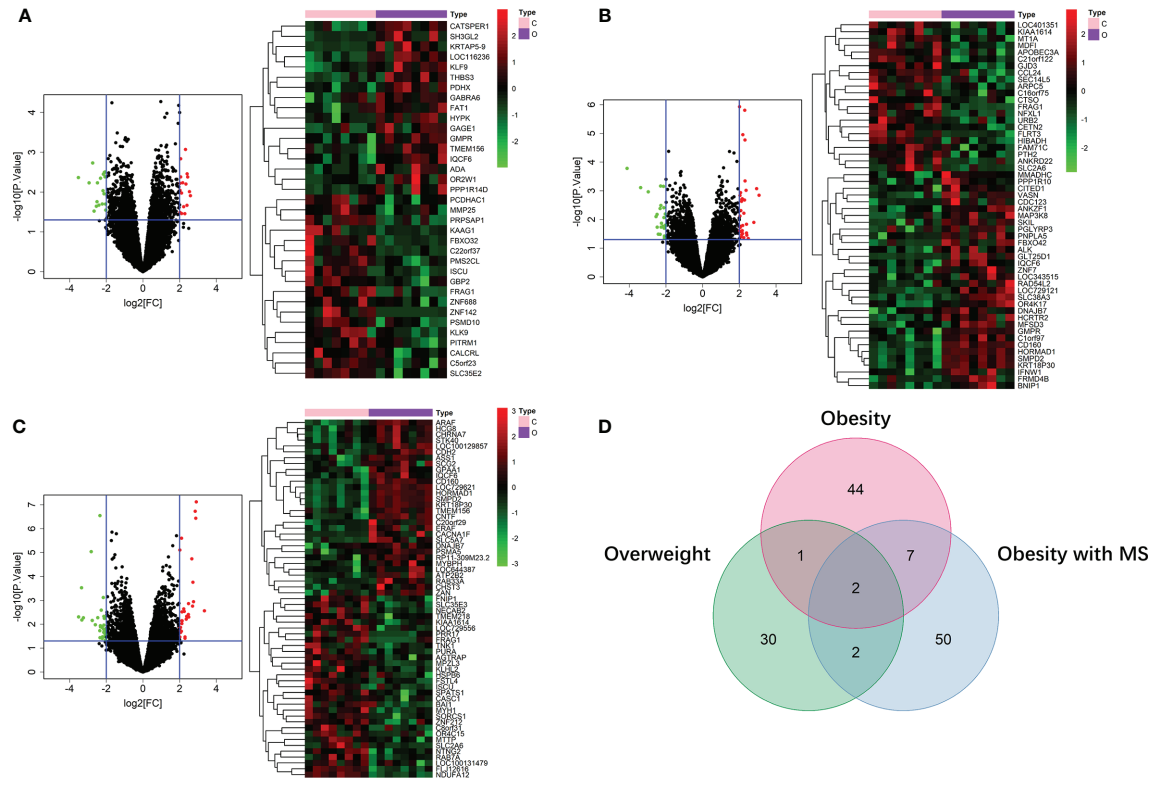

FIGURE 2 | DE mRNAs of overweight **(A)**, obesity **(B)**, and obesity with MS **(C)** in VAT. The red points in the volcano plots represent upregulation and the green plots represent downregulation. The color in heatmaps from green to red shows the progression from low expression to high expression. The amount of DE mRNAs of obesity in VAT was 136 (35 for overweight, 54 for obesity, and 61 for obesity with MS). Venn diagram **(D)** shows that only 2 mRNAs (IQCF6 and FRAG1) were shared by all these 3 obesity components.

Supplemental Table 3. Volcano plots and heatmaps of DE miRNAs of obesity in VAT and SAT were shown in **Figures 4A, B**. According to the miRNA-mRNA pairs predicted using Targetscan database, 17,423 and 16,612 target mRNAs were respectively obtained for 52 DE miRNA of obesity in VAT and 25 in SAT. By performing VennDiagram R package, the intersections of DE mRNAs of obesity and predicted target mRNAs in miRNA-mRNA pairs were 99 (**Figure 4C**) and 118 (**Figure 4D**) for VAT and SAT, respectively. By further screening out inverse miRNA-mRNA pairs including mRNAs in the intersection, the networks of obesity in VAT and SAT were constructed as shown in **Supplemental Figure 1**. In the network of VAT, 87 mRNAs and 27 miRNAs were included. In the network of SAT, 101 mRNAs and 16 miRNAs were included.

Functional Annotation of DE mRNAs in Networks of Obesity in VAT and SAT

To gain insights into the different biological features of miRNA-mRNA networks of obesity in VAT and SAT, KEGG and GO analyses were respectively performed for target mRNAs. As shown in **Table 1**, target mRNAs in the miRNA-mRNA network of obesity in VAT were enriched in 6 pathways as following: nicotine addiction (hsa05033; genes: CHRNA7 and GABRA6); cholinergic synapse (hsa04725; genes: CACNA1F, CHRNA7, and SLC5A7); vascular smooth muscle contraction (hsa04270; genes: ARAF, CACNA1F, and CALCRL); mineral absorption (hsa04978; genes: ATP2B2 and MT1A); non-small cell lung cancer (hsa05223; genes: ALK and ARAF); arrhythmogenic right ventricular cardiomyopathy (hsa05412; genes: CACNA1F and CDH2). For the network of SAT, target mRNAs were enriched in 4 pathways as following: pancreatic secretion (hsa04972; genes: ATP1A2, PLA2G1B, and RAP1A); synthesis and degradation of ketone bodies (hsa00072; genes: HMGCS2); PPAR signaling pathway (hsa03320; genes: ACSL4 and HMGCS2); RNA degradation (hsa03018; genes: ENO2 and WDR61). Results of GO enrichment analyses were shown in **Supplemental Figure 2**. In brief, biological process (BP) functional enrichment found that target mRNAs of network of obesity in VAT were enriched in functions like cellular response to glucocorticoid stimulus, cellular response to corticosteroid stimulus, and eosinophil chemotaxis. Target mRNAs in SAT were enriched in functions such as cellular response to drug, DNA methylation or demethylation, and regulation of histone H3-K9 acetylation.

Construction of miRNA-mRNA Networks of Obesity-Related ccRCC in VAT and SAT

In 24 samples (patient-matched tumors and adjacent-normal tissues) from 12 obese participants the dataset of ccRCC (GSE46699), we screened out 28 DE mRNAs of ccRCC

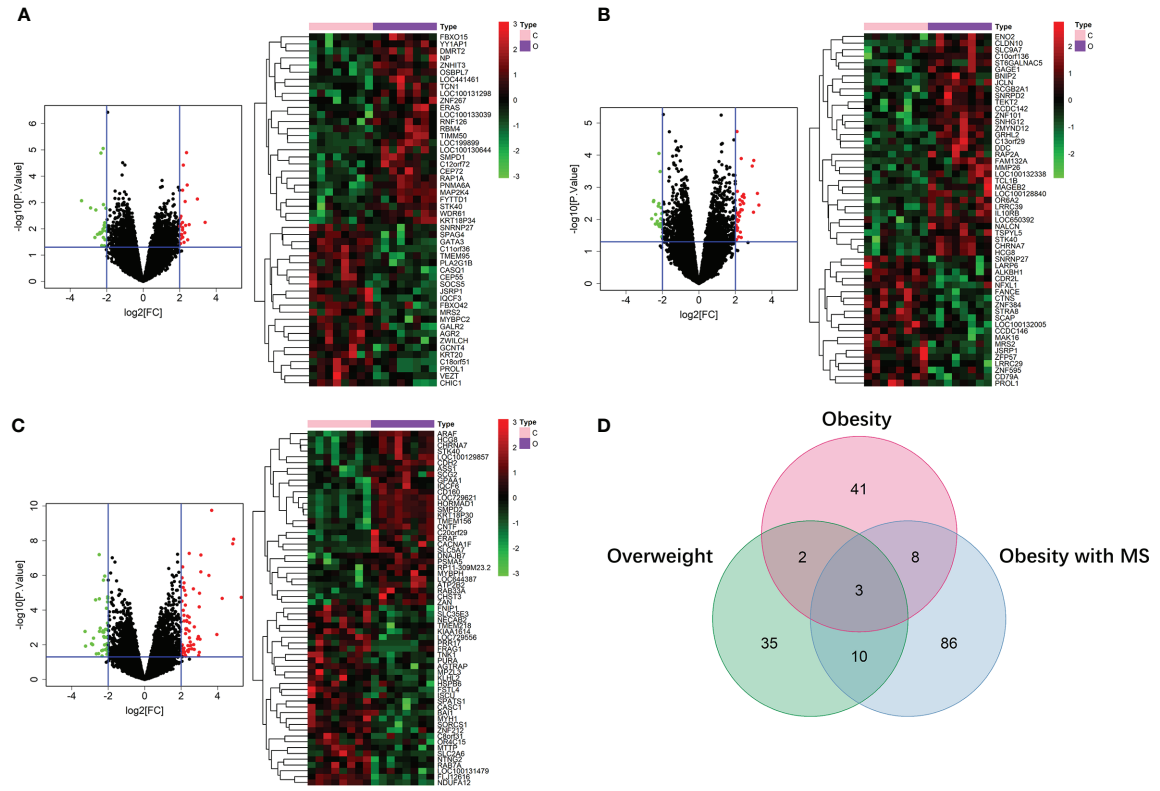

FIGURE 3 | DE mRNAs of overweight **(A)**, obesity **(B)**, and obesity with MS **(C)** in SAT. The red points in the volcano plots represent upregulation and the green plots represent downregulation. The color in heatmaps from green to red shows the progression from low expression to high expression. The amount of DE mRNAs of obesity in VAT was 185 (50 for overweight, 54 for obesity, and 107 for obesity with MS). Venn diagram **(D)** shows that only 3 mRNAs (JSRP1, MRS2 and STK40) were shared by all these 3 obesity components.

(P-value < 0.05) among 87 target mRNAs in the network of obesity in VAT (**Supplemental Table 4**). By further selecting those with same trends (up- or down-regulated) as shown in the network of obesity, 14 mRNAs were retrained. In accordance with these 14 mRNAs, a miRNA-mRNA network of obesity-related ccRCC in VAT was constructed and visualized as **Figure 5A**. In this network, 23 miRNAs were included. Consistent methods were repeated among 101 target mRNAs in the network of obesity in SAT, and 21 mRNAs were finally retrained. By using these 21 mRNAs and 16 paired miRNAs, the miRNA-mRNA network of obesity-related ccRCC in SAT was constructed (**Figure 5B**).

Verification of miRNA-mRNA Networks of Obesity-Related ccRCC Using TCGA Dataset

We respectively selected 611 samples (including 72 controls) and 616 samples (including 71 controls) in the TCGA dataset of ccRCC to evaluate the sensitivity and specificity of both mRNAs and miRNAs in networks of obesity-related ccRCC. Among 14 target mRNAs and 23 miRNAs in the network of obesity-related ccRCC in VAT, 13 mRNAs and 8 miRNAs with same trends as shown in the network had statistically significant ORs (shown in **Supplemental Table 5**). Seven of 13 mRNAs that could be paired with 8 selected miRNAs were retrained, and ROCs were shown in **Figures 6A, B**. By performing consistent methods, 17 mRNAs and 2 miRNAs were respectively selected from 21 target mRNAs and 16 miRNAs in the network of obesity-related ccRCC in SAT, ORs and 95%CI were shown in **Supplemental Table 5**. Among 17 mRNAs, 3 were found to be paired with 2 miRNAs, and ROCs of them were shown in **Figures 6C, D**. Sankey diagrams of miRNA-mRNA networks were shown in **Figure 6E**, 18 and 5 miRNA-mRNA pairs in both VAT and SAT were included. Furthermore, 588 samples (71 controls) with both mRNA and miRNA data in TCGA dataset were selected to perform Spearman correlation analyses among these RNA pairs. After adjusted for group (tumor or adjacent tissue), 3 pairs showed inverse relationship with statistically significant correlation coefficients, including hsa-miR-182&ATP2B2 (r = -0.154, P-value < 0.001) in VAT, hsa-miR-532&CDH2 (r = -0.085, P-value =0.039) in VAT, and hsa-miR-425&TFAP2B (r = -0.125, P-value =0.002) in SAT (**Figure 6F**). By searching these 3 target mRNAs in GSE24833, all of them were DE mRNAs of obesity with MS.

Construction of Prognostic Signature Based on DE RNAs of Obesity-Related ccRCC

We firstly screened out the DE RNAs (mRNAs and miRNAs) of ccRCC among DE RNAs of obesity. From 136 DE mRNAs and 52 DE miRNAs of obesity in VAT (shown in **Figures 2** and **3A**), 17 DE mRNAs and 44 DE miRNAs of ccRCC were respectively

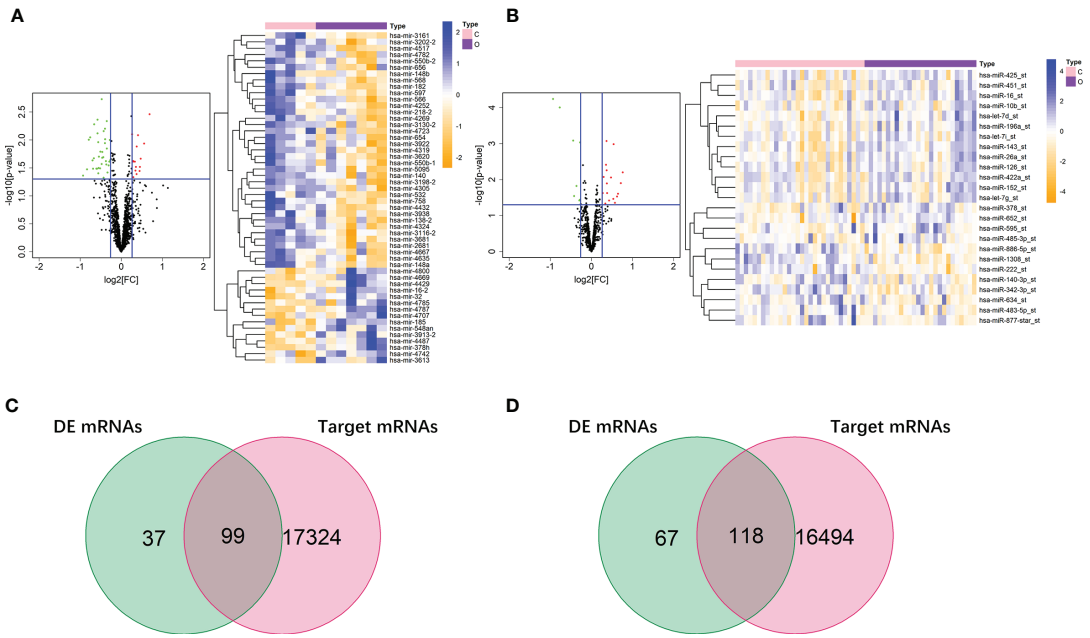

FIGURE 4 | DE miRNAs of obesity in VAT and SAT. 52 DE miRNAs of obesity were screened out in VAT **(A)**, and 25 were screened out in SAT **(B)**. The red points in the volcano plots represent upregulation and the green plots represent downregulation. The color in heatmaps from blue to yellow shows the progression from low expression to high expression. Venn diagrams **(C, D)** shows that the intersections of DE mRNAs of obesity and predicted target mRNAs in miRNA-mRNA pairs were 99 and 118 for VAT **(C)** and SAT **(D)**, respectively.

selected using the TCGA dataset. For DE RNAs of obesity in SAT, 24 mRNAs and 11 miRNAs were finally remained. Multivariable Cox regression analyses were performed among these eligible RNAs, crude and adjusted HRs for each RNA were shown in **Supplemental Table 6**. As results showed, 5 DE mRNAs (SORCS1, FLRT3, HIBADH, CATSPER1, and MAP3K8) and 5 DE miRNAs (hsa-miR-3130-2, hsa-miR-148b, hsa-miR-2681, hsa-miR-4487, and hsa-miR-3613) of obesity-related ccRCC with statistically significant adjusted HRs remained consistent trends (up- and down-regulated) as shown in DE analyses of obesity in VAT. For DE RNAs of obesity-related ccRCC in SAT, 4 mRNAs (ENO2, YY1AP1, FAP, IL10RB) and 1 miRNA (hsa-miR-425) were eligible for the following risk score analyses. By utilizing adjusted regression coefficients of these RNAs, we calculated risk scores of both mRNAs and miRNAs for each patient. Formulas were shown as following:

$$\text{Risk score of mRNAs in VAT} = \text{SORCS1} * (-0.936) + \text{FLRT3} * (-0.055) + \text{HIBADH} * (0.016) + \text{CATSPER1} * (0.832) + \text{MAP3K8} * (0.133);$$

$$\text{Risk score of miRNAs in VAT} = \text{hsa} - \text{miR} - 3130 - 2 * (-0.200) + \text{hsa} - \text{miR} - 148\text{b} * (0.335) + \text{hsa} - \text{miR} - 2681 * (-0.519) + \text{hsa} - \text{miR} - 4487 * (0.628) + \text{hsa} - \text{miR} - 3613 * (0.268);$$

$$\text{Risk score of mRNAs in SAT} = \text{ENO2} * (0.006) + \text{YY1AP1} * (0.090) + \text{FAP} + (0.113) + \text{IL10RB} * (0.036)$$

We divided patients into high- and low-risk groups according to the medians of risk scores. As shown in **Figure 7A**, AUCs of risk score models were 0.726 (mRNAs in VAT), 0.631 (miRNAs in VAT), and 0.680 (mRNAs in SAT). In addition, overall survival time of patients in the low-risk group was significantly long than that in the high-risk group regardless of risk score models (P-values < 0.001, **Figure 7B**). Distributions of RNA expressions, risk scores, and survival statuses for each patient were shown in **Figures 7C–E**.

DISCUSSION

In recent years, obesity has become a worldwide health problem. Emerging evidence shows that obesity is a risk factor of various non-communicable diseases, including cancers (35), and main mechanisms could be partially attributed to the inflammation triggered by excess adipose tissue. Abdominal adipose tissue is a major storage of body fat, consisting of VAT and SAT. Differences in abdominal locations, structural compositions, metabolic activities, and functional significances between VAT and SAT implied that their pathophysiological mechanisms might be different (36), while no study has disclosed such

TABLE 1 | KEGG enrichments of target mRNAs in miRNA-mRNA networks of obesity in VAT and SAT.

ID	Description	GeneRatio	P-value	geneID	Count
VAT					
hsa05033	Nicotine addiction	2/37	0.014244	CHRNA7/ GABRA6	2
hsa04725	Cholinergic synapse	3/37	0.014618	CACNA1F/ CHRNA7/ SLC5A7	3
hsa04270	Vascular smooth muscle contraction	3/37	0.022488	ARAF/ CACNA1F/ CALCRL	3
hsa04978	Mineral absorption	2/37	0.029596	ATP2B2/ MT1A	2
hsa05223	Non-small cell lung cancer	2/37	0.042611	ALK/ARAF	2
hsa05412	Arrhythmogenic right ventricular cardiomyopathy	2/37	0.048094	CACNA1F/ CDH2	2
SAT					
hsa04972	Pancreatic secretion	3/36	0.010288	ATP1A2/ PLA2G1B/ RAP1A	3
hsa00072	Synthesis and degradation of ketone bodies	1/36	0.043658	HMGCS2	1
hsa03320	PPAR signaling pathway	2/36	0.044704	ACSL4/ HMGCS2	2
hsa03018	RNA degradation	2/36	0.04793	ENO2/ WDR61	2

KEGG, Kyoto Encyclopedia of Genes and Genomes; VAT, visceral adipose tissue; SAT, subcutaneous adipose tissue.

heterogeneity. In our study, 136 and 185 DE mRNAs of obesity were respectively found in VAT and SAT using GEO datasets, while no RNA was overlapped between these two adipose tissues. DE genes between VAT and SAT have been reported in several published studies (37–39), our result was in line with previous findings, and implied that VAT and SAT perhaps differed in pathophysiological functions. Simultaneously, in accordance with miRNA datasets of GEO, different miRNA-mRNA regulatory networks of obesity in VAT and SAT were obtained. To further explore the heterogeneity in biological functions between VAT and SAT, KEGG and GO analyses were performed among mRNAs in obtained miRNA-mRNA networks of obesity. As we found, 6 and 4 non-overlapped biological pathways were respectively enriched for mRNAs in networks of both VAT and SAT. Results from enrichment analyses indicated that miRNA-mRNA regulatory networks we screened out were biologically functional, and also disclosed different pathophysiological mechanisms of obesity-related diseases potentially existing in VAT and SAT.

The association of ccRCC with excessively accumulated adipose tissue has been revealed in several studies. In a newly published study, both VAT and SAT areas measured using CT were found to be positively associated with ccRCC among Caucasian patients with different genetic background (40). There is a multi-center study from Chinese population showing that the mean VAT area measured by CT in ccRCC group was larger than that in non-ccRCC group by 25 cm^2, and such difference was statistically significant (41). In another study, statistical differences of both VAT and SAT were found between ccRCC cases and controls, and smaller P-value (<0.001) for VAT was shown (13). Additionally, it has been reported that individuals with high levels of C-peptide, interleukin-6 (IL-6), tumor necrosis factor-α (TNF-α), as well as low level of adiponectin had significantly higher risk of ccRCC, all these biomarkers are obesity-related (8, 42). Even though associations of ccRCC with both biochemical and image-based indices of obesity have been estimated, relevant bioinformatic studies still remained limited. Zhou, et al. performed a data-mining study by combining GEO with TCGA datasets, and 5 genes correlated with both ccRCC and obesity were found (IGHA1 and IGKC were oncogenes, and MAOA, MUC20 and TRPM3 were tumor suppressor genes) (19). However, if RNAs regarding to obesity-related ccRCC were different between VAT and SAT still remained underdetermined. On the other hand, miRNAs from both plasma and tissue samples have been reported to be associated with ccRCC (22, 43), while miRNA-mRNA regulatory networks of obesity-related ccRCC were not given in the above mentioned bioinformatic study.

In our study, based on the obtained miRNA-mRNA networks of obesity in VAT and SAT, we only included samples of obese participants from the GEO dataset of ccRCC, and screened out specific networks of obesity-related ccRCC (14 mRNAs and 23 miRNAs were included in the network of VAT; 21 mRNAs and 16 miRNAs were included in the network of SAT). After further verified using TCGA dataset, 18 and 5 miRNA-mRNA pairs were respectively screened out for VAT and SAT, and only 3 pairs remained inverse relationship in Spearman correlation analyses (hsa-miR-182&ATP2B2, hsa-miR-532&CDH2 in VAT; and hsa-miR-425&TFAP2B in SAT). All these 3 miRNAs were shown to be associated with ccRCC, despite that reported target genes distinguished from those we found. For example, hsa-miR-182, and hsa-miR-532 could suppresses RCC migration and proliferation respectively *via* targeting insulin-like growth factor 1 receptor (IGF1R), or nucleosome assembly protein 1-like 1 (NAP1L1) (44, 45). In contrast, hsa-miR-425 could perform an oncogenic effect by promoting invasion and migration of RCC cell lines (46). Although all 3 genes of ATP2B2, CDH2 and TFAP2B have been reported to play a role in pathophysiology of various cancers (47–49), reports referring to the association with RCC remained limited. Zhang, et al. found that the elevation of CDH2 could promote growth, migration, and invasion abilities of RCC cells (49). According to the published evidence as above mentioned, all these 3 miRNA-mRNA pairs we screened out in VAT and SAT perhaps could play some potential roles in the pathogenesis of obesity-related ccRCC, while the following experimental studies verifying their regulatory relationships are still necessary.

Even though obesity have been generally identified as a risk factor of ccRCC, the paradox between obesity and ccRCC prognosis was still frequently disclosed (22, 50, 51). Sanchez, et al. combined 3 cohort studies (COMPARZ trial, TCGA cohort, and MSK immunotherapy study) and obtained the consistent results of survival advantage in obese patients with ccRCC (51). Findings from this study implied that the peritumoral

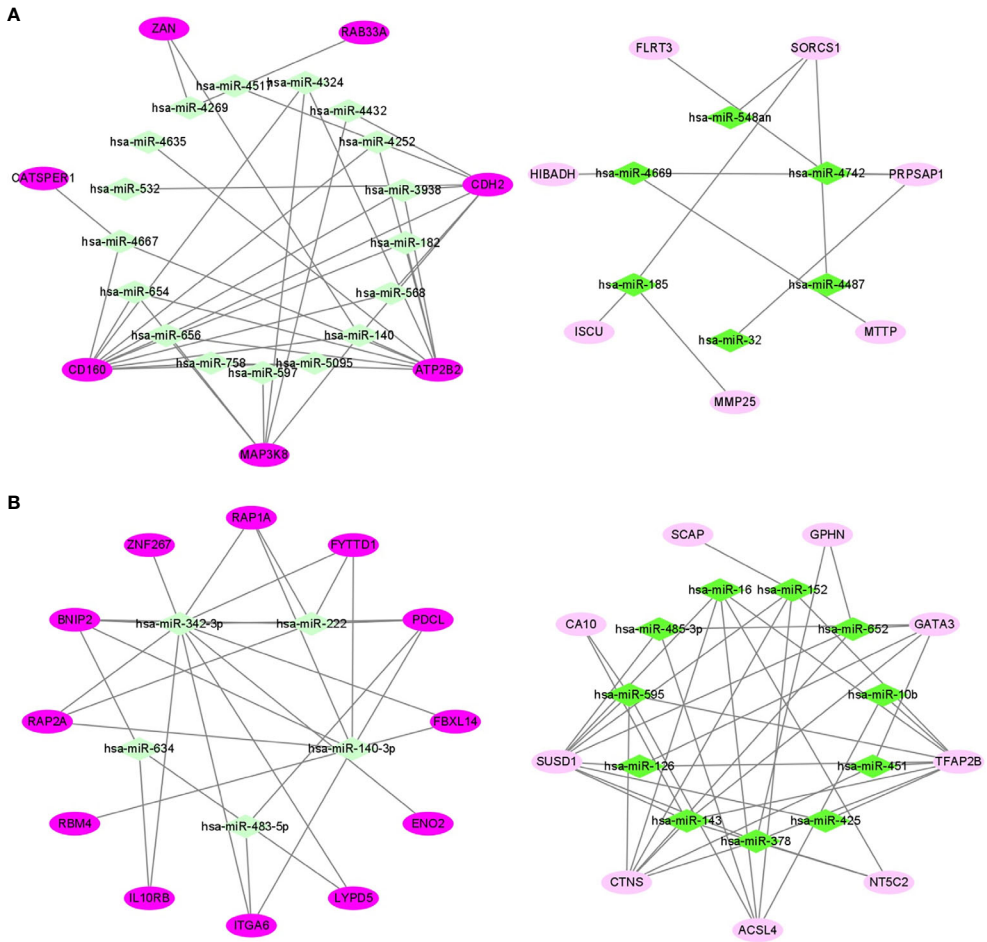

FIGURE 5 | miRNA-mRNA networks of obesity-related ccRCC in VAT **(A)** and SAT **(B)**. In VAT **(A)**, 14 mRNAs and 23 miRNAs were included. In SAT **(B)**, 21 mRNAs and 16 miRNAs were included. Green diamonds represent miRNAs, and pink ellipses represent mRNAs. The color from dark to light respectively represents up- and down-regulated.

adipose tissue might contribute to the better prognosis of ccRCC by acting as an immune reservoir. However, the potential roles of abdominal adipose tissue, as the main storage of fat, in the prognosis of ccRCC still remained unknown. Based on previously published findings showing the excess accumulated VAT and SAT were positively associated with the prevalence of ccRCC (13, 41), as well as what we found in this current study, we hypothesized that there probably could exist some DE RNAs of obesity-related ccRCC in VAT and SAT remaining consistent performance in terms of ccRCC prognosis, i.e. up-regulated DE RNAs of obesity-related ccRCC could be correlated with poor prognosis, and down-regulated ones could be correlated with better prognosis. As we found in the survival analyses, 5 DE mRNAs (SORCS1, FLRT3, HIBADH, CATSPER1, and MAP3K8) and 5 DE miRNAs (hsa-miR-3130-2, hsa-miR-148b, hsa-miR-2681, hsa-miR-4487, and hsa-miR-3613) of obesity-related ccRCC were found in VAT. For DE RNAs of obesity in SAT, 4 mRNAs (ENO2, YY1AP1, FAP, IL10RB) and 1 miRNA (hsa-miR-425) were found. Most of selected RNAs were reported to be relevant to prognosis of various cancers, while studies referring to their associations with RCC prognosis are still limited. Sun, et al. found that ENO2, i.e. enolase 2, was associated with worsened prognosis in papillary RCC and was related to glycolysis (52). hsa-miR-3613 and hsa-miR-425 were also shown to be associated with poor prognosis of ccRCC and chromophobe RCC, respectively (53, 54). Our subsequent risk score analyses by utilizing above selected RNAs also found that patients in the low-risk group survived significantly longer than those in the high-risk group regardless of risk score models. Findings in our survival analyses implied that there probably existed some potential mechanisms underlying the association between obesity and poor prognosis of ccRCC. However, factors correlated with ccRCC prognosis were complicated, and biological functions of relevant RNAs found in this study should be further verified.

Cautions should be paid when interpreting our findings. Firstly, although DE RNAs of obesity were estimated based on

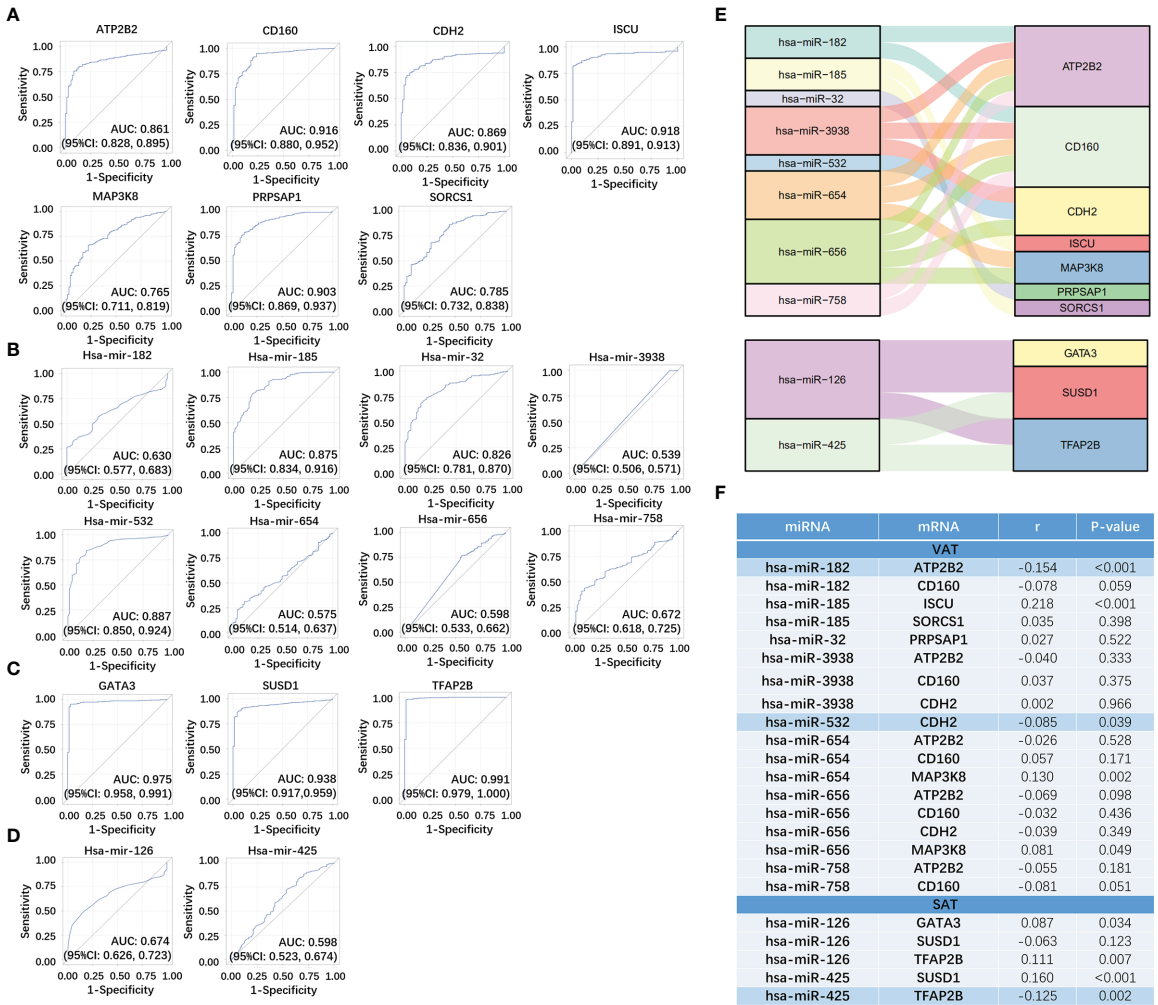

F

miRNA	mRNA	r	P-value
VAT			
hsa-miR-182	ATP2B2	-0.154	<0.001
hsa-miR-182	CD160	-0.078	0.059
hsa-miR-185	ISCU	0.218	<0.001
hsa-miR-185	SORCS1	0.035	0.398
hsa-miR-32	PRPSAP1	0.027	0.522
hsa-miR-3938	ATP2B2	-0.040	0.333
hsa-miR-3938	CD160	0.037	0.375
hsa-miR-3938	CDH2	0.002	0.966
hsa-miR-532	CDH2	-0.085	0.039
hsa-miR-654	ATP2B2	-0.026	0.528
hsa-miR-654	CD160	0.057	0.171
hsa-miR-654	MAP3K8	0.130	0.002
hsa-miR-656	ATP2B2	-0.069	0.098
hsa-miR-656	CD160	-0.032	0.436
hsa-miR-656	CDH2	-0.039	0.349
hsa-miR-656	MAP3K8	0.081	0.049
hsa-miR-758	ATP2B2	-0.055	0.181
hsa-miR-758	CD160	-0.081	0.051
SAT			
hsa-miR-126	GATA3	0.087	0.034
hsa-miR-126	SUSD1	-0.063	0.123
hsa-miR-126	TFAP2B	0.111	0.007
hsa-miR-425	SUSD1	0.160	<0.001
hsa-miR-425	TFAP2B	-0.125	0.002

FIGURE 6 | Verification of miRNA-mRNA networks of obesity-related ccRCC using TCGA dataset. For VAT, 7 mRNA **(A)** and 8 paired miRNAs **(B)** with statistically significant ORs were retrained. For SAT, 3 mRNA **(C)** and 2 paired miRNAs **(D)** with statistically significant ORs were retrained. miRNA-mRNA networks of obesity-related ccRCC were visualized using Sankey Diagram **(E)**. Spearman correlation analyses **(F)** found that 3 miRNA-mRNA pairs showed inverse relationship with statistically significant correlation coefficients, including hsa-miR-182&ATP2B2 in VAT, hsa-miR-532&CDH2 in VAT, and hsa-miR-425&TFAP2B in SAT.

the adipose tissue samples (VAT or SAT), both GEO and TCGA datasets of ccRCC consist of samples only from tumor or adjacent tissues. Therefore, some RNAs only highly expressed in adipose tissue but not in tumor tissues perhaps could be eliminated. However, it was still reasonable to consider that the eventually selected DE RNAs of obesity-related ccRCC might have some potential pathophysiological effects underlying the association between obesity and ccRCC. Further studies directly focusing on the selected RNAs from adipose tissues of both ccRCC cases and controls would be necessary. Secondly, there are several noncoding RNAs such as circular RNA (circRNA) and long non-coding RNA (lncRNA), which could compete for miRNA binding, and thereafter regulate the expression of mRNA. However, we only constructed the miRNA-mRNA networks in this study since that datasets of circRNA or lncRNA cannot be simultaneously found for both VAT and SAT. Thirdly, only ccRCC was considered in our study, while the biological functions of VAT and SAT might be different in terms of other subtypes of renal cancer. The association of DE RNAs and miRNA-mRNA networks selected in our study with other renal cancers should be further estimated.

CONCLUSIONS

In this study, we respectively constructed specific miRNA-mRNA regulatory networks of obesity-related ccRCC for both VAT and SAT, and 3 RNA pairs (i.e. hsa-miR-182&ATP2B2, hsa-miR-532&CDH2 in VAT; and hsa-miR-425&TFAP2B in SAT) were finally screened out. This finding indicated that VAT and SAT might perform distinct functions in the pathogenesis of obesity-related ccRCC. On the other hand,

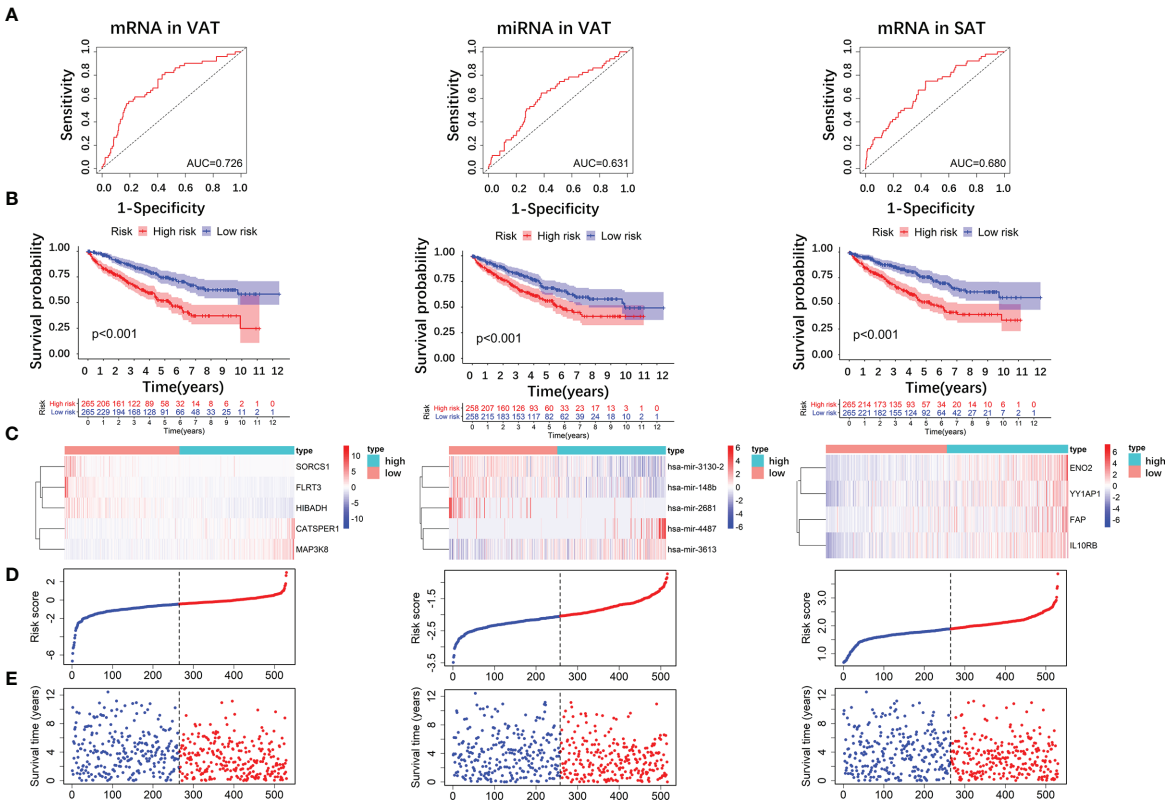

FIGURE 7 | Risk score analyses of DE RNAs of obesity-related ccRCC in the prognosis of ccRCC. 5 DE mRNAs (SORCS1, FLRT3, HIBADH, CATSPER1, and MAP3K8), 5 DE miRNAs (hsa-miR-3130-2, hsa-miR-148b, hsa-miR-2681, hsa-miR-4487, and hsa-miR-3613) of obesity-related ccRCC in VAT, and 4 mRNAs (ENO2, YY1AP1, FAP, IL10RB) in SAT were used to calculate risk scores. AUC of risk score of mRNAs in VAT was larger than those of miRNAs in VAT, and mRNAs in SAT **(A)**. Overall survival time of patients in the low-risk group was significantly longer than in the high-risk group regardless of risk score models **(B)**. Distributions of RNA expressions, risk scores, and survival statuses for each patient were also shown **(C–E)**.

several DE RNAs of obesity-related ccRCC were found to remain consistent performance in terms of ccRCC prognosis, implying that there probably existed some potential mechanisms underlying the association between obesity and poor prognosis of ccRCC. What we found disclosed heterogeneous molecular mechanisms between VAT and SAT in relation to the prevalence and prognosis of ccRCC, and could provide valuable evidence on the targeted therapy of obesity-related ccRCC.

DATA AVAILABILITY STATEMENT

The datasets presented in this study can be found in online repositories. The names of the repository/repositories and accession number(s) can be found in the article/**Supplementary Material**.

AUTHOR CONTRIBUTIONS

YuL and YM: conception and design. YuL: development of methodology. YuL and YM: analysis and interpretation of data. YuL: writing of the manuscript. YaL, JH, and LL: review of the manuscript. DW: study supervision. All authors contributed to the article and approved the submitted version.

FUNDING

This research was supported by the National Key R&D Program of China [Grant#2018YFC1311600].

ACKNOWLEDGMENTS

We thank all relevant investigators, staff, and participants for their important contribution to this work.

SUPPLEMENTARY MATERIAL

The Supplementary Material for this article can be found online at: https://www.frontiersin.org/articles/10.3389/fendo.2021.713357/full#supplementary-material

Supplementary Figure 1 | miRNA-mRNA networks of obesity in VAT **(A)** and SAT **(B)**. In the network of VAT **(A)**, 87 mRNAs and 27 miRNAs were included. In the network of SAT **(B)**, 101 mRNAs and 16 miRNAs were included. Blue and green ellipses represent mRNAs, and pink diamonds represent miRNAs. The color from dark to light respectively represents up- and down-regulated.

Supplementary Figure 2 | Results of GO enrichment analyses in VAT **(A–C)** and SAT **(D–F)**. **(A, D)**: results of biological process (BP) functional enrichment in mRNAs of VAT **(A)** and SAT **(D)**; **(B, E)**: results of molecular function (MF) functional enrichment in mRNAs of VAT **(B)** and SAT **(E)**; **(C, F)**: results of cellular component (CC) functional enrichment in mRNAs of VAT **(C)** and SAT **(F)**. The color from red to blue represents p-values.

REFERENCES

1. Sung H, Siegel RL, Torre LA, Pearson-Stuttard J, Islami F, Fedewa SA, et al. Global Patterns in Excess Body Weight and the Associated Cancer Burden. *CA Cancer J Clin* (2019) 69:88–112. doi: 10.3322/caac.21499
2. Hsieh JJ, Purdue MP, Signoretti S, Swanton C, Albiges L, Schmidinger M, et al. Renal Cell Carcinoma. *Nat Rev Dis Primers* (2017) 3:17009. doi: 10.1038/nrdp.2017.9
3. Ferlay J, Soerjomataram I, Dikshit R, Eser S, Mathers C, Rebelo M, et al. Cancer Incidence and Mortality Worldwide: Sources, Methods and Major Patterns in GLOBOCAN 2012. *Int J Cancer* (2015) 136:E359–86. doi: 10.1002/ijc.29210
4. Banks RE, Tirukonda P, Taylor C, Hornigold N, Astuti D, Cohen D, et al. Genetic and Epigenetic Analysis of Von Hippel-Lindau (VHL) Gene Alterations and Relationship With Clinical Variables in Sporadic Renal Cancer. *Cancer Res* (2006) 66:2000–11. doi: 10.1158/0008-5472.CAN-05-3074
5. Chow WH, Dong LM, Devesa SS. Epidemiology and Risk Factors for Kidney Cancer. *Nat Rev Urol* (2010) 7:245–57. doi: 10.1038/nrurol.2010.46
6. McGuire BB, Fitzpatrick JM. BMI and the Risk of Renal Cell Carcinoma. *Curr Opin Urol* (2011) 21:356–61. doi: 10.1097/MOU.0b013e32834962d5
7. Smits KM, Schouten LJ, Hudak E, Verhage B, van Dijk BA, Hulsbergen-van de Kaa CA, et al. Body Mass Index and Von Hippel-Lindau Gene Mutations in Clear-Cell Renal Cancer: Results of the Netherlands Cohort Study on Diet and Cancer. *Ann Epidemiol* (2010) 20:401–4. doi: 10.1016/j.annepidem.2010.01.010
8. Wang Q, Tu H, Zhu M, Liang D, Ye Y, Chang DW, et al. Circulating Obesity-Driven Biomarkers Are Associated With Risk of Clear Cell Renal Cell Carcinoma: A Two-Stage, Case-Control Study. *Carcinogenesis* (2019) 40:1191–97. doi: 10.1093/carcin/bgz074
9. Gustafson B. Adipose Tissue, Inflammation and Atherosclerosis. *J Atheroscler Thromb* (2010) 17:332–41. doi: 10.5551/jat.3939
10. Abraham TM, Pedley A, Massaro JM, Hoffmann U, Fox CS. Association Between Visceral and Subcutaneous Adipose Depots and Incident Cardiovascular Disease Risk Factors. *Circulation* (2015) 132:1639–47. doi: 10.1161/CIRCULATIONAHA.114.015000
11. Xiao X, Wang Y, Gao Y, Xie Q, Zhou X, Lin L, et al. Abdominal Visceral Adipose Tissue Is Associated With Unsuspected Pulmonary Embolism on Routine CT Scans in Patients With Gastrointestinal Cancer. *Br J Radiol* (2019) 92:20190526. doi: 10.1259/bjr.20190526
12. Bradshaw PT, Cespedes Feliciano EM, Prado CM, Alexeeff S, Albers KB, Chen WY, et al. Adipose Tissue Distribution and Survival Among Women With Nonmetastatic Breast Cancer. *Obes (Silver Spring)* (2019) 27:997–1004. doi: 10.1002/oby.22458
13. Greco F, Quarta LG, Grasso RF, Beomonte Zobel B, Mallio CA. Increased Visceral Adipose Tissue in Clear Cell Renal Cell Carcinoma With and Without Peritumoral Collateral Vessels. *Br J Radiol* (2020) 93:20200334. doi: 10.1259/bjr.20200334
14. Wajchenberg BL. Subcutaneous and Visceral Adipose Tissue: Their Relation to the Metabolic Syndrome. *Endocr Rev* (2000) 21:697–738. doi: 10.1210/edrv.21.6.0415
15. Dusserre E, Moulin P, Vidal H. Differences in mRNA Expression of the Proteins Secreted by the Adipocytes in Human Subcutaneous and Visceral Adipose Tissues. *Biochim Biophys Acta* (2000) 1500:88–96. doi: 10.1016/s0925-4439(99)00091-5
16. Qi X, Lin Y, Liu X, Chen J, Shen B. Biomarker Discovery for the Carcinogenic Heterogeneity Between Colon and Rectal Cancers Based on lncRNA-Associated ceRNA Network Analysis. *Front Oncol* (2020) 10:535985. doi: 10.3389/fonc.2020.535985
17. Liu J, Nie S, Gao M, Jiang Y, Wan Y, Ma X, et al. Identification of EPHX2 and RMI2 as Two Novel Key Genes in Cervical Squamous Cell Carcinoma by an Integrated Bioinformatic Analysis. *J Cell Physiol* (2019) 234:21260–73. doi: 10.1002/jcp.28731
18. Zhao X, Sun S, Zeng X, Cui L. Expression Profiles Analysis Identifies a Novel three-mRNA Signature to Predict Overall Survival in Oral Squamous Cell Carcinoma. *Am J Cancer Res* (2018) 8:450–61.
19. Zhou J, Yang Z, Wu X, Zhang J, Zhai W, Chen Y. Identification of Genes That Correlate Clear Cell Renal Cell Carcinoma and Obesity and Exhibit Potential Prognostic Value. *Transl Androl Urol* (2021) 10:680–91. doi: 10.21037/tau-20-891
20. Lin Y, Wu W, Sun Z, Shen L, Shen B. MiRNA-BD: An Evidence-Based Bioinformatics Model and Software Tool for microRNA Biomarker Discovery. *RNA Biol* (2018) 15:1093–105. doi: 10.1080/15476286.2018.1502590
21. Chen J, Zhang D, Zhang W, Tang Y, Yan W, Guo L, et al. Clear Cell Renal Cell Carcinoma Associated microRNA Expression Signatures Identified by an Integrated Bioinformatics Analysis. *J Transl Med* (2013) 11:169. doi: 10.1186/1479-5876-11-169
22. Shu X, Hildebrandt MA, Gu J, Tannir NM, Matin SF, Karam JA, et al. MicroRNA Profiling in Clear Cell Renal Cell Carcinoma Tissues Potentially Links Tumorigenesis and Recurrence With Obesity. *Br J Cancer* (2017) 116:77–84. doi: 10.1038/bjc.2016.392
23. Klimcakova E, Roussel B, Marquez-Quinones A, Kovacova Z, Kovacikova M, Combes M, et al. Worsening of Obesity and Metabolic Status Yields Similar Molecular Adaptations in Human Subcutaneous and Visceral Adipose Tissue: Decreased Metabolism and Increased Immune Response. *J Clin Endocrinol Metab* (2011) 96:E73–82. doi: 10.1210/jc.2010-1575
24. Alberti KG, Zimmet P, Shaw JGroup IDFETFC. The Metabolic Syndrome–a New Worldwide Definition. *Lancet* (2005) 366:1059–62. doi: 10.1016/S0140-6736(05)67402-8
25. Ferrante SC, Nadler EP, Pillai DK, Hubal MJ, Wang Z, Wang JM, et al. Adipocyte-Derived Exosomal miRNAs: A Novel Mechanism for Obesity-Related Disease. *Pediatr Res* (2015) 77:447–54. doi: 10.1038/pr.2014.202
26. Arner E, Mejhert N, Kulyte A, Balwierz PJ, Pachkov M, Cormont M, et al. Adipose Tissue microRNAs as Regulators of CCL2 Production in Human Obesity. *Diabetes* (2012) 61:1986–93. doi: 10.2337/db11-1508
27. Eckel-Passow JE, Serie DJ, Bot BM, Joseph RW, Hart SN, Cheville JC, et al. Somatic Expression of ENRAGE Is Associated With Obesity Status Among Patients With Clear Cell Renal Cell Carcinoma. *Carcinogenesis* (2014) 35:822–7. doi: 10.1093/carcin/bgt485
28. Tian M, Dong J, Yuan B, Jia H. Identification of Potential circRNAs and circRNA-miRNA-mRNA Regulatory Network in the Development of Diabetic Foot Ulcers by Integrated Bioinformatics Analysis. *Int Wound J* (2020) 18:323–31. doi: 10.1111/iwj.13535
29. Papadopoulou SK. Sarcopenia: A Contemporary Health Problem Among Older Adult Populations. *Nutrients* (2020) 12:1293–7. doi: 10.3390/nu12051293
30. Agarwal V, Bell GW, Nam JW, Bartel DP. Predicting Effective microRNA Target Sites in Mammalian mRNAs. *Elife* (2015) 4:e05005. doi: 10.7554/eLife.05005
31. Bartel DP. MicroRNAs: Genomics, Biogenesis, Mechanism, and Function. *Cell* (2004) 116:281–97. doi: 10.1016/S0092-8674(04)00045-5
32. Espinoza-Lewis RA, Wang D-Z. Chapter Ten - MicroRNAs in Heart Development. *Curr Top Dev Biol* (2012) 100:279–317. doi: 10.1016/B978-0-12-387786-4.00009-9
33. Yu G, Wang LG, Han Y, He QY. Clusterprofiler: An R Package for Comparing Biological Themes Among Gene Clusters. *OMICS* (2012) 16:284–7. doi: 10.1089/omi.2011.0118
34. Peng J, Wang H, Lu J, Hui W, Wang Y, Shang X. Identifying Term Relations Cross Different Gene Ontology Categories. *BMC Bioinf* (2017) 18:573. doi: 10.1186/s12859-017-1959-3

35. Neeland IJ, Ayers CR, Rohatgi AK, Turer AT, Berry JD, Das SR, et al. Associations of Visceral and Abdominal Subcutaneous Adipose Tissue With Markers of Cardiac and Metabolic Risk in Obese Adults. *Obes (Silver Spring)* (2013) 21:E439–47. doi: 10.1002/oby.20135
36. Bays HE, Gonzalez-Campoy JM, Bray GA, Kitabchi AE, Bergman DA, Schorr AB, et al. Pathogenic Potential of Adipose Tissue and Metabolic Consequences of Adipocyte Hypertrophy and Increased Visceral Adiposity. *Expert Rev Cardiovasc Ther* (2008) 6:343–68. doi: 10.1586/14779072.6.3.343
37. Vohl MC, Sladek R, Robitaille J, Gurd S, Marceau P, Richard D, et al. A Survey of Genes Differentially Expressed in Subcutaneous and Visceral Adipose Tissue in Men. *Obes Res* (2004) 12:1217–22. doi: 10.1038/oby.2004.153
38. Korsic M, Gotovac K, Nikolac M, Dusek T, Skegro M, Muck-Seler D, et al. Gene Expression in Visceral and Subcutaneous Adipose Tissue in Overweight Women. *Front Biosci (Elite Ed)* (2012) 4:2734–44. doi: 10.2741/e587
39. Ronquillo MD, Mellnyk A, Cardenas-Rodriguez N, Martinez E, Comoto DA, Carmona-Aparicio L, et al. Different Gene Expression Profiles in Subcutaneous & Visceral Adipose Tissues From Mexican Patients With Obesity. *Indian J Med Res* (2019) 149:616–26. doi: 10.4103/ijmr.IJMR_1165_17
40. Greco F, Mallio CA. Relationship Between Visceral Adipose Tissue and Genetic Mutations (VHL and KDM5C) in Clear Cell Renal Cell Carcinoma. *Radiol Med* (2021) 126:645–51. doi: 10.1007/s11547-020-01310-y
41. Wang HK, Song XS, Cheng Y, Qu YY, Zhang SL, Dai B, et al. Visceral Fat Accumulation Is Associated With Different Pathological Subtypes of Renal Cell Carcinoma (RCC): A Multicentre Study in China. *BJU Int* (2014) 114:496–502. doi: 10.1111/bju.12592
42. Wang H, Wu J, Gu W, Wang B, Wan F, Dai B, et al. Serum Adiponectin Level May Be an Independent Predictor of Clear Cell Renal Cell Carcinoma. *J Cancer* (2016) 7:1340–6. doi: 10.7150/jca.14716
43. Chanudet E, Wozniak MB, Bouaoun L, Byrnes G, Mukeriya A, Zaridze D, et al. Large-Scale Genome-Wide Screening of Circulating microRNAs in Clear Cell Renal Cell Carcinoma Reveals Specific Signatures in Late-Stage Disease. *Int J Cancer* (2017) 141:1730–40. doi: 10.1002/ijc.30845
44. Zhai W, Ma J, Zhu R, Xu C, Zhang J, Chen Y, et al. MiR-532-5p Suppresses Renal Cancer Cell Proliferation by Disrupting the ETS1-Mediated Positive Feedback Loop With the KRAS-Nap1l1/P-ERK Axis. *Br J Cancer* (2018) 119:591–604. doi: 10.1038/s41416-018-0196-5
45. Wang X, Li H, Cui L, Feng J, Fan Q. MicroRNA-182 Suppresses Clear Cell Renal Cell Carcinoma Migration and Invasion by Targeting IGF1R. *Neoplasma* (2016) 63:717–25. doi: 10.4149/neo_2016_508
46. Quan J, Li Y, Pan X, Lai Y, He T, Lin C, et al. Oncogenic miR-425-5p Is Associated With Cellular Migration, Proliferation and Apoptosis in Renal Cell Carcinoma. *Oncol Lett* (2018) 16:2175–84. doi: 10.3892/ol.2018.8948
47. Varga K, Hollosi A, Paszty K, Hegedus L, Szakacs G, Timar J, et al. Expression of Calcium Pumps Is Differentially Regulated by Histone Deacetylase Inhibitors and Estrogen Receptor Alpha in Breast Cancer Cells. *BMC Cancer* (2018) 18:1029. doi: 10.1186/s12885-018-4945-x
48. Raap M, Gierendt L, Kreipe HH, Christgen M. Transcription Factor AP-2beta in Development, Differentiation and Tumorigenesis. *Int J Cancer* (2021) 149:1221–7. doi: 10.1002/ijc.33558
49. Zhang D, Yang XJ, Luo QD, Fu DL, Li ZL, Zhang P, et al. Down-Regulation of Circular RNA_000926 Attenuates Renal Cell Carcinoma Progression Through miRNA-411-Dependent CDH2 Inhibition. *Am J Pathol* (2019) 189:2469–86. doi: 10.1016/j.ajpath.2019.06.016
50. Parker AS, Lohse CM, Cheville JC, Thiel DD, Leibovich BC, Blute ML. Greater Body Mass Index Is Associated With Better Pathologic Features and Improved Outcome Among Patients Treated Surgically for Clear Cell Renal Cell Carcinoma. *Urology* (2006) 68:741–6. doi: 10.1016/j.urology.2006.05.024
51. Sanchez A, Furberg H, Kuo F, Vuong L, Ged Y, Patil S, et al. Transcriptomic Signatures Related to the Obesity Paradox in Patients With Clear Cell Renal Cell Carcinoma: A Cohort Study. *Lancet Oncol* (2020) 21:283–93. doi: 10.1016/S1470-2045(19)30797-1
52. Sun C, Liu M, Zhang W, Wang S, Qian G, Wang M, et al. Overexpression of Enolase 2 Is Associated With Worsened Prognosis and Increased Glycikolysis in Papillary Renal Cell Carcinoma. *J Cell Physiol* (2021) 236:3821–31. doi: 10.1002/jcp.30130
53. Qin S, Shi X, Wang C, Jin P, Ma F. Transcription Factor and miRNA Interplays Can Manifest the Survival of ccRCC Patients. *Cancers (Basel)* (2019) 11:1668–88. doi: 10.3390/cancers11111668
54. Ge YZ, Xin H, Lu TZ, Xu Z, Yu P, Zhao YC, et al. MicroRNA Expression Profiles Predict Clinical Phenotypes and Prognosis in Chromophobe Renal Cell Carcinoma. *Sci Rep* (2015) 5:10328. doi: 10.1038/srep10328

Conflict of Interest: The authors declare that the research was conducted in the absence of any commercial or financial relationships that could be construed as a potential conflict of interest.

Publisher's Note: All claims expressed in this article are solely those of the authors and do not necessarily represent those of their affiliated organizations, or those of the publisher, the editors and the reviewers. Any product that may be evaluated in this article, or claim that may be made by its manufacturer, is not guaranteed or endorsed by the publisher.

frontiers in Endocrinology

ORIGINAL RESEARCH
published: 01 December 2021
doi: 10.3389/fendo.2021.750999

Deciphering the Irregular Risk of Stroke Increased by Obesity Classes: A Stratified Mendelian Randomization Study

*Xuelun Zou[1], Leiyun Wang[2,3], Linxiao Xiao[4], Zihao Xu[1], Tianxing Yao[1], Minxue Shen[5], Yi Zeng[6] and Le Zhang[1]**

[1] Department of Neurology, Xiangya Hospital, Central South University, Changsha, China, [2] Department of Clinical Pharmacology, Xiangya Hospital, Central South University, Changsha, China, [3] Institute of Clinical Pharmacology, Central South University, Hunan Key Laboratory of Pharmacogenetics, Changsha, China, [4] Department of Spine Surgery and Orthopaedics, Xiangya Hospital, Central South University, Changsha, China, [5] Department of Epidemiology and Health Statistics, Xiangya School of Public Health, Central South University, Changsha, China, [6] Department of Geriatrics, Second Xiangya Hospital, Central South University, Changsha, China

OPEN ACCESS

Edited by:
Jeff M. P. Holly, University of Bristol, United Kingdom

Reviewed by:
Zhiguo Zhang, First Affiliated Hospital of Jilin University, China
Safaa Hisham Hammoud, Beirut Arab University, Lebanon

***Correspondence:**
Le Zhang
zlzdzlzd@csu.edu.cn

Specialty section:
This article was submitted to Obesity, a section of the journal Frontiers in Endocrinology

Received: *31 July 2021*
Accepted: *08 November 2021*
Published: *01 December 2021*

Citation:
Zou X, Wang L, Xiao L, Xu Z, Yao T, Shen M, Zeng Y and Zhang L (2021) Deciphering the Irregular Risk of Stroke Increased by Obesity Classes: A Stratified Mendelian Randomization Study. Front. Endocrinol. 12:750999. doi: 10.3389/fendo.2021.750999

Background: To investigate the relationship between different classes of obesity and stroke, we conducted a stratified Mendelian randomization (MR) study.

Methods: The body mass index (BMI) data of 263,407 Europeans with three classes of obesity (obesity class I, 30 kg/m^2 ≤ BMI < 35 kg/m^2; obesity class II, 35 kg/m^2 ≤ BMI < 40 kg/m^2; obesity class III, 40 kg/m^2 ≤ BMI) were extracted from the Genetic Investigation of ANthropometric Traits (GIANT) consortium. Summary-level data of stroke and its subtypes [ischemic stroke (IS) and intracerebral hemorrhage (ICH)] were obtained from the genome-wide association study (GWAS) meta-analysis, which was performed by the MEGASTROKE consortium. MR methods were used to identify the causal relationships.

Results: The MR analysis revealed that both obesity class I [odds ratio (OR) = 1.08, 95% CI: 1.05–1.12, $p = 1.0 \times 10^{-5}$] and obesity class II (OR = 1.06, 95% CI: 1.03–1.09, $p = 1 \times 10^{-4}$) were significantly positively related to IS, while obesity class III was not (OR = 1.01, 95% CI: 0.96–1.06, $p = 0.65$). In contrast to IS, there was no class of obesity associated with ICH risk. Further examination of the relationship between obesity classification and IS subtypes revealed that certain degrees of obesity were related to large artery stroke (LAS) (OR = 1.14, 95% CI: 1.04–1.24, $p = 2.8 \times 10^{-3}$ for class I; OR = 1.08, 95% CI: 1.01–1.16, $p = 0.002$ for class II) and cardioembolic stroke (CES) (OR = 1.11, 95% CI: 1.02–1.20, $p = 0.02$ for class I; OR = 1.08, 95% CI: 1.02–1.15, $p = 0.007$ for class II).

Conclusions: A higher risk of IS, but not ICH, could be linked to obesity classes I and II. A strong association between LAS and CES and obesity was observed among all IS subtypes in the obese population.

Keywords: stroke, obesity, Mendelian randomization, body mass index, genome-wide association study

INTRODUCTION

Stroke, the second leading cause of death and disability worldwide, has put huge economic pressure and healthcare burden on patients worldwide (1, 2). In 2017, there were about 6 million deaths due to stroke and a loss of 132.1 million stroke-related disability-adjusted life years (95% CI: 126.5–137.4) (2). A growing number of studies have confirmed the correlation between stroke and modifiable or non-modifiable risk factors such as smoking, drinking, hypertension, diabetes, and genetics (3). There is no doubt that the prevention and control of these risk factors will reduce the disease burden of stroke.

Obesity caused by abnormal metabolism, as one of the major health threats to all populations, is also viewed as a potential risk factor for stroke (4). As reported by the World Health Organization (WHO), approximately 1.9 billion adults are obese or overweight worldwide (5), and 3 million people died of obesity-related diseases in 2018 (6). Therefore, a large part of the disease burden of stroke may arise from obese people. Conventional observational studies may be affected by many confounders when investigating the causal relationship between exposure factors (obesity) and outcome effects (stroke). Factors such as the distribution of fat and the condition of health are difficult to control using typical analytic methods.

These shortcomings can be eliminated using Mendelian randomization (MR) studies. MR studies as nature's randomized controlled trials are widely applied to assess the causality between exposure factors and outcome diseases (7). The MR method utilizes genetic variations, namely, single-nucleotide polymorphisms (SNPs), as mediating variables, which are objective factors free of influence from various confounding factors (8, 9). In MR studies, SNPs are used to determine whether an observational relationship between an exposure factor and an outcome disease is aligned with a causal effect (9). Therefore, MR studies have outstanding advantages in exploring the causal relationship between exposure factors and outcome diseases.

Previous studies have shown that obesity can lead to the accumulation of many human body adipose tissues, and adipose tissue can release a large number of inflammatory cytokines and anti-inflammatory factors, cytokines, and other factors (10–13). It also leads to a lack of oxygen to the body, oxidative stress, and chronic inflammation, causing blood vessel damage and extracellular matrix remodeling, such as pathological changes in vascular fibrosis (10, 13–16). All of these are potential stroke triggers that can accelerate brain vessel damage (17, 18). Observational studies have reported that obesity is associated with stroke, but the causality between them remains controversial (19, 20). Furthermore, in a previous MR study, abdominal adiposity has been shown to cause pathological processes in cerebrovascular diseases (21). Moreover, central adiposity has been reported to increase the risk of stroke (22). However, three other MR analyses (21–23) indicated that the BMI of obesity may not be related to stroke and its subtypes. This discrepancy may hinder the discovery of the inner links between obesity and stroke, which may be due to the irregular physiological status, different classes of obesity, or various subtypes of stroke. As reported in a genome-wide association meta-analysis study, different obesity classes presented obvious differences in genetics (24). Therefore, we speculated that only some obese people are at a higher risk of stroke, which may be due to genetic differences in their obesity classification. To confirm this assumption, we performed a stratified MR study to explore the causality between the classes of obesity and the risk of stroke.

Since the causal relationship between different obesity classes and risk of stroke with its subtypes is unclear, we conducted this stratified MR study to study the causal relationship.

METHODS

Summary of Genome-Wide Association Study Data

The information on obesity exposure factors was acquired from the Genetic Investigation of ANthropometric Traits (GIANT) consortium (24), which is a publicly available database taken from the magnanimous data of genome-wide association study (GWAS). In detail, 263 and 407 Europeans were included to study the genetic factors associated with obesity (24). Obesity was divided into obesity class I (30 $kg/m^2 \leq$ BMI < 35 kg/m^2; 32,858 cases and 65,839 controls), obesity class II (35 $kg/m^2 \leq$ BMI < 40 kg/m^2; 9,889 cases and 62,657 controls), and obesity class III (40 $kg/m^2 \leq$ BMI; 2,896 cases and 47,468 controls) (24).

The data on stroke and its subtypes in this study were acquired from the MEGASTROKE consortium (25) and the Common Metabolic Diseases Knowledge Portal (26). The summary statistics data of stroke were obtained from 446,696 subjects (40,585 cases and 406,111 controls). Among them, patients were ranked as having ischemic stroke (IS) (34,217 cases), large artery stroke (LAS) (4,373 cases), cardioembolic stroke (CES) (7,193 cases), and small vessel stroke (SVS) (5,386 cases) (25). Another common subtype of stroke is ICH, which was collected from another GWAS meta-analysis of 3,026 Europeans (about 1,545 cases and 1,481 controls) (26). Considering the different locations of hemorrhage, ICH was subtyped into lobar ICH (LICH, 686 cases) and non-lobar ICH (NLICH, 909 cases). Since this study was a retrospective study based on the public GWAS database as the published source, ethics approval was not required.

Instrumental Single-Nucleotide Polymorphism Inclusion Criteria

SNPs related to obesity were selected from a meta-analysis of GWAS data. Information including age, sex, height, hip circumference, waist–hip ratio, and health condition of these obese patients was also acquired. Different SNPs related to the obesity classes were selected to evaluate the causal relationship between obesity and stroke (including IS and ICH). We also relaxed the selection criteria to $p < 1 \times 10^{-6}$ to retain enough SNPs, which could be included for downstream studies and make our results more reliable, as reported in a previous study (7). The parameters $r^2 = 0.01$ and kb = 10,000 were chosen to remove the SNPs that could not pass the linkage disequilibrium test.

Stratified Mendelian Randomization Analysis

Three R platform-supported packages, Mendelian randomization, TwoSampleMR (27), and Mendelian Randomization Pleiotropy RESidual Sum and Outlier (MR-PRESSO) (28), were utilized in this study. All analyses were completed using R (version 4.0.3) and R studio software.

The inverse-variance weighted (IVW) method was chosen as the primary method for analysis (29), which can obtain an accurate and stable estimate when the directional pleiotropy is of poor statistical significance (30). MR-Egger regression (31), weighted median estimation (WME) (32), and other robust MR methods were also used to show the causal association between each variable. MR-Egger regression methods can provide a robust estimate of the causal relationship when some instrumental variables violate the supposed selection criteria (31, 33). When the intercept term is close to zero, directional pleiotropy does not exist, and the results of the MR-Egger regression method will verge on IVW. WME has an advantage in controlling the Type 1 error rates of finite samples and has a stable estimator, although the invalid instrumental variables include values up to 50% (32).

In addition, to ensure the reliability and effectiveness of the MR study, the heterogeneity test, which can inspect the differences in all kinds of SNPs using Cochran's Q statistics, was utilized to test the existence of heterogeneity (34). If there was heterogeneity in the larger sample, we needed to eliminate the SNPs that had small *p*-values by utilizing a random-effects model to assess the effect of MR. Therefore, we conducted a random-effects model to analyze the association between obesity class II and SVS, while the rest of the analyses adopted a fixed-effects model in this stratified MR analysis. Pleiotropy tests were performed in two ways: the intercept term of the MR-Egger regression method and the global and distortion test in the MR-PRESSO method (28). MR-PRESSO global and distortion tests, which could delete the SNPs gradually, were utilized to determine the presence or absence of abnormal values and to determine how to handle these accordingly (28). The leave-one-out sensitivity test was used to appraise whether the MR results were sensitized to single SNP changes (35). All of these parameters for model selection are listed in **Table 3**.

Assumptions of the Mendelian Randomization Study

Three core assumptions must be satisfied to obtain valid results from MR studies (36, 37). 1) Instrumental variables (SNPs) must not correlate with confounders. To estimate this assumption, we checked each instrument variable in phewascatalog.org (38), where no statistical significance ($p < 1 \times 10^{-6}$) of association was detected. In addition, we carefully checked the exposure factors in the GWAS Catalog database and found no correlation with previously reported confounding factors ($p < 1 \times 10^{-6}$) (39). We defined smoking, unhealthy diet, physical activity, and sedentary time as associated confounding factors (40–42). 2) The direct association between instrumental variables (SNPs) and exposure (obesity) must be reliable. As shown in **Supplementary Tables S1–S3**, we found that all included SNPs were significantly related to exposure (obesity). To assess the pleiotropy of the selected SNPs, F statistics was used (43). When $F \leq 10$, the selected SNPs were viewed as weak instrument biases, and thus they could not explain the observed exposure associations well (44). The F values of the instrumental variables selected based on the exposure variable ranged from 22 to 306, the details of which can be found in **Supplementary Tables S1–S3**. 3) Instrumental variables (SNPs) should affect the outcome (stroke) only by exposure (obesity), and there should be no other pathways. In order to eliminate the impact of other potential paths, we conducted the MR-Egger regression method and MR-PRESSO global test and found no existence of pleiotropy. The influence of potential pathways was also excluded, as presented in the *Results* section below (**Table 3**) (36). All assumptions are shown in **Figure 1**.

Statistical Analyses

The statistical significance of the *p*-value in the multiple comparisons was defined as 0.0056, contributing to a Bonferroni correction of nine tests in the primary analysis. Three exposures (obesity class I, obesity class II, and obesity class III) and three main outcomes (stroke, IS, and ICH) were counted. Since the total causal relationship was confirmed in the primary analysis and was only used for exploratory analyses, the subtype analysis was performed without conducting *p*-value corrections (45).

RESULTS

In our study, MR analysis was used to explore the causal relationship between different classes of obesity and stroke with its subtypes, such as IS and ICH, as shown in **Figure 1**. SNPs were selected as instrumental variables, and different classes of obesity were viewed as exposure factors, while stroke and its subtypes were regarded as the outcome diseases in this study. Data for this study were derived from the different classes of obesity GWAS including 263,407 European populations and a 446,696 European stroke population.

Selected Single-Nucleotide Polymorphisms

The instrumental variable SNPs between the different classes of obesity and the risk of IS subtypes were screened (**Supplementary Tables S1–S3**). As a result, 29 SNPs, 21 SNPs, and five SNPs passed the screening rules for obesity class I, obesity class II, and obesity class III, respectively. Among them, rs13130484 was not detected in the GWAS of CES. Therefore, this variation was excluded from the analysis of the causal relationship between obesity classes I and II and CES. The instrumental variables of SNPs that matched ICH were selected from the obesity data. Consequently, there were 24 SNPs found for obesity class I, 19 SNPs for obesity class II, and four SNPs for obesity class III. In obesity class I with risk of ICH, rs1514177, rs17203351, rs523288, rs8028313, and rs9816226

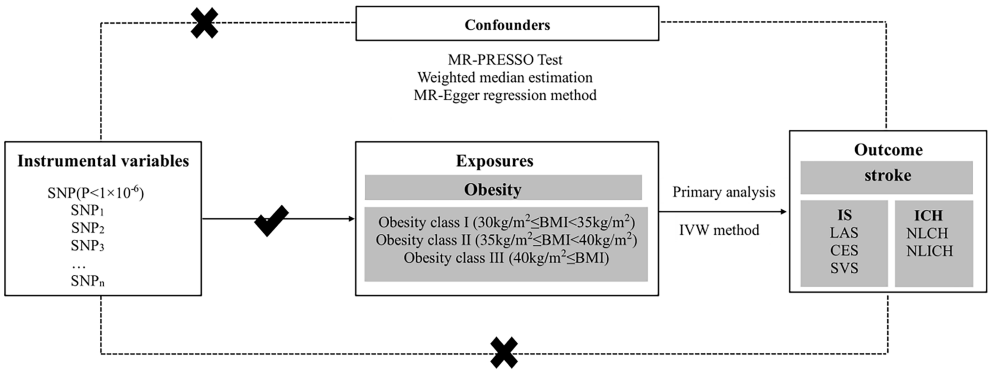

FIGURE 1 | Conceptual framework figure of exploring the causal relationship in different obesity classes and stroke with its subtypes in the MR analysis. MR, Mendelian randomization; IS, ischemic stroke; LAS, large artery stroke; CES, cardioembolic stroke; SVS, small vessel stroke; ICH, intracerebral hemorrhage; LICH, lobar intracerebral hemorrhage; NLICH, non-lobar intracerebral hemorrhage; IVW, inverse-variance weighted; WME, weighted median estimation; MR-PRESSO, MR pleiotropy residual sum and outlier.

were removed because they were palindromic with intermediate allele frequencies, and rs7531118 was not detected in the GWAS of ICH. rs7538571 was removed for intermediate allele frequencies in obesity class II and ICH. In obesity class III with a risk of ICH, rs13104545 was not detected in the GWAS of ICH.

Obesity Classes I and II but Not III Were Significantly Associated With the Risk of Ischemic Stroke

The IVW method was utilized for stratified MR analysis to assess the association between obesity and stroke. We found that the SNPs of obesity class I (OR = 1.08, 95% CI: 1.05–1.12, $p = 7.4 \times 10^{-6}$) and obesity class II (OR = 1.05, 95% CI: 1.02–1.08, $p = 7 \times 10^{-4}$) significantly increased the risk of stroke but not obesity class III (OR = 1.00, 95% CI: 0.94–1.06, $p = 0.96$). To determine the association between obesity classes and IS, which is one of the two common subtypes of stroke, we performed stratified MR analysis and found that genetic predispositions to obesity class I (OR = 1.08, 95% CI: 1.05–1.12, $p = 1.0 \times 10^{-5}$) and obesity class II (OR = 1.06, 95% CI: 1.03–1.09, $p = 1 \times 10^{-4}$) were positively associated with the risk of IS. However, no statistically significant causal relationship between obesity class III and the risk of IS could be established (OR = 1.01, 95% CI: 0.96–1.06, $p = 0.65$). These results are shown in **Table 1**. The power values of the relationship between stroke and obesity classes I, II, and III were 0.88, 0.66, and 0.82, respectively, which indicates that our negative observation for obesity class III is reliable.

In the stratified MR analysis for all three IS subtypes (LAS, CES, and SVS), we found that obesity class I (OR = 1.14, 95% CI: 1.04–1.24, $p = 2.8 \times 10^{-3}$) and obesity class II (OR = 1.08, 95% CI: 1.01–1.16, $p = 0.002$) could increase the risk of LAS but not obesity class III (OR = 1.04, 95% CI: 0.80–1.36, $p = 0.75$). The risk of CES was increased by obesity class I (OR = 1.11, 95% CI: 1.02–1.20, $p = 0.02$) and obesity class II (OR = 1.08, 95% CI: 1.02–1.15, $p = 0.007$) but was not related to obesity class III (OR = 1.02, 95% CI: 0.93–1.12, $p = 0.64$). Interestingly, obesity class I (OR = 1.07, 95% CI: 0.97–1.17, $p = 0.17$), obesity class II (OR = 1.03, 95% CI: 0.95–1.13, $p = 0.42$), and obesity class III (OR = 1.07, 95% CI: 0.98–1.17, $p = 0.12$) presented no causal relationship with SVS. The intercept from the MR-Egger regression (heterogeneity test) and Cochran's Q statistics (pleiotropy test) did not show statistical significance between obesity class I, obesity class II, and obesity class III and the risk of stroke, IS, and other IS subtypes (**Table 3**).

TABLE 1 | MR stratification analysis of obesity classes I, II, and III with the risk of IS and IS subtypes using the IVW method.

		Obesity class I (n = 29)		Obesity class II (n = 21)		Obesity class III (n = 5)	
		OR (95% CI)	*p* value	OR (95%CI)	*p* value	OR (95% CI)	*p* value
Stroke		1.08 (1.05–1.12)	**7.4×10^{-6}**	1.05 (1.02–1.08)	**7×10^{-4}**	1.00 (0.94–1.06)	0.96
IS		1.08 (1.05–1.12)	**1.0×10^{-5}**	1.06 (1.03–1.09)	**1×10^{-4}**	1.01 (0.96–1.06)	0.65
	LAS	1.14 (1.04–1.24)	**2.8×10^{-3}**	1.08 (1.01–1.16)	**0.002**	1.04 (0.80–1.36)	0.75
	CES	1.11 (1.02–1.20)	**0.02**	1.08 (1.02–1.15)	**0.007**	1.02 (0.93–1.12)	0.64
	SVS	1.07 (0.97–1.17)	0.17	1.03 (0.95–1.13)	0.42	1.07 (0.98–1.17)	0.12

IS, ischemic stroke; LAS, large artery stroke; CES, cardioembolic stroke; SVS, small vessel stroke; IVW, inverse-variance weighted method.
Power $_{obesity\ class\ I}$ = 0.88, Power $_{obesity\ class\ II}$ = 0.66, Power $_{obesity\ class\ III}$ = 0.82.
All values which are lower than 0.05 are marked in the bold font, indicating that they are statistically significant.

Obesity Was Not Associated With Intracerebral Hemorrhage and Its Subtypes

As **Table 2** shows, no causal relationship between obesity class I (OR = 1.05, 95% CI: 0.80–1.37, $p = 0.75$), obesity class II (OR = 1.07, 95% CI: 0.88–1.32, $p = 0.49$), and obesity class III (OR = 0.93, 95% CI: 0.76–1.11, $p = 0.43$) with a risk of ICH was found through the IVW analysis. Moreover, obesity class I (OR = 1.10, 95% CI: 0.81–1.51, $p = 0.53$), obesity class II (OR = 1.01, 95% CI: 0.80–1.28, $p = 0.94$), and obesity class III (OR = 0.95, 95% CI: 0.68–1.30, $p = 0.74$) were not related to the ICH subtype of LICH. Obesity class I (OR = 1.06, 95% CI: 0.78–1.45, $p = 0.70$), obesity class II (OR = 1.19, 95% CI: 0.91–1.55, $p = 0.21$), and obesity class III (OR = 0.98, 95% CI: 0.88–1.09, $p = 0.89$) were not associated with NLICH. No heterogeneity and pleiotropy could be detected between obesity classes I, II, and III and the risk of ICH and its subtypes, which indicated the reliability of our analysis (**Table 3**).

Validation of the Associations Using Various Stratified Mendelian Randomization Methods

To ensure the stability and reliability of the results, we used three other methods, MR-PRESSO, WME, and MR-Egger, to test whether the classes of obesity were associated with the risk of IS and ICH. As expected, obesity class I had a causal relationship with the risk of IS in the MR-PRESSO (OR = 1.08, 95% CI: 1.02–1.12, $p = 2.0 \times 10^{-4}$) and WME (OR = 1.08, 95% CI: 1.02–1.14, $p = 5.9 \times 10^{-3}$) analyses. Similarly, the MR-PRESSO (OR = 1.06, 95% CI: 1.03–1.09, $p = 1.0 \times 10^{-3}$) and WME (OR = 1.06, 95% CI: 1.01–1.11, $p = 9.0 \times 10^{-3}$) analyses confirmed the causal effect of obesity class II on the risk of IS. Obesity class III showed no association with the risk of IS in the MR-PRESSO, WME, and MR-Egger analyses, which is in agreement with our results calculated using the IVW method. Likewise, obesity classes I, II, and III were not correlated with ICH in the MP-PRESSO, WEM, or MR-Egger analyses. All these results were consistent

TABLE 2 | MR stratification analysis of obesity classes I, II, and III with the risk of ICH and ICH subtypes using the IVW method.

		Obesity class I (n = 24)		Obesity class II (n = 19)		Obesity class III (n = 4)	
		OR (95% CI)	*p* value	OR (95% CI)	*p* value	OR (95% CI)	*p* value
Stroke		1.08 (1.05–1.12)	**7.4×10^{-6}**	1.05 (1.02–1.08)	**7×10^{-4}**	1.00 (0.94–1.06)	0.96
ICH		1.05 (0.80–1.37)	0.75	1.07 (0.88–1.32)	0.49	0.96 (0.76–1.31)	0.81
	LICH	1.10 (0.81–1.51)	0.53	1.01 (0.80–1.28)	0.94	0.96 (0.73–1.25)	0.74
	NLICH	1.06 (0.78–1.45)	0.70	1.19 (0.91–1.55)	0.21	1.02 (0.72–1.46)	0.89

ICH, intracerebral hemorrhage; LICH, lobar intracerebral hemorrhage; NLICH, non-lobarintracerebral hemorrhage; IVW, inverse-variance weighted method.
All values which are lower than 0.05 are marked in the bold font, indicating that they are statistically significant.

TABLE 3 | The outcome of the sensitivity analysis of obesity with the risk of stroke.

Method		Cochran's Q	HT (*p*)	intercept	PT (*p*)	GT (RSSobs)	GT (*p*)
Obesity class I	**Stroke**	20.7	0.84	-0.0001	0.97	24.9	0.77
	IS	26.5	0.55	-0.0017	0.74	30.8	0.49
	LAS	23.2	0.72	-0.0080	0.49	24.9	0.77
	CES	35.5	0.13	0.0112	0.35	40.6	0.11
	SVS	35.7	0.10	-0.0103	0.39	39.9	0.11
	ICH	31.1	0.12	-0.0029	0.94	36.2	0.23
	LICH	24.3	0.39	-0.0094	0.82	29.1	0.52
	NLICH	28.7	0.19	0.0034	0.93	33.6	0.30
Obesity class II	**Stroke**	23.2	0.28	0.0035	0.58	24.8	0.32
	IS	23.0	0.29	0.0040	0.55	24.7	0.32
	LAS	17.8	0.60	-0.0012	0.94	19.2	0.63
	CES	16.8	0.66	0.0148	0.25	19.3	0.64
	SVS	39.5	0.00	-0.0020	0.91	43.5	0.00
	ICH	21.2	0.15	0.0540	0.23	29.9	0.13
	LICH	15.3	0.57	0.0317	0.54	17.9	0.59
	NLICH	29.4	0.05	0.0828	0.16	35.2	0.04
Obesity class III	**Stroke**	6.39	0.17	-0.0220	0.37	8.71	0.24
	IS	4.21	0.37	-0.0160	0.46	5.81	0.49
	LAS	8.52	0.07	-0.0890	0.18	11.9	0.14
	CES	1.79	0.77	0.0388	0.37	3.67	0.69
	SVS	4.82	0.31	-0.0235	0.63	7.21	0.34
	ICH	6.75	0.08	-0.1036	0.64	9.57	0.17
	LICH	2.13	0.54	-0.0699	0.67	3.03	0.64
	NLICH	6.38	0.09	-0.0770	0.76	9.14	0.20

IS, ischemic stroke; LAS, large artery stroke; CES, cardioembolic stroke; SVS, small vessel stroke; ICH, intracerebral hemorrhage; LICH, lobar intracerebral hemorrhage; NLICH, non-lobar intracerebral hemorrhage; SNP, single-nucleotide polymorphism; IVW, inverse-variance weighted; WME, weighted median estimation; MR-PRESSO, MR pleiotropy residual sum and outlier; HT, heterogeneity test; PT, pleiotropy test; GT, MR-PRESSO global test.

with the IVW analyses in the previous section and are summarized in **Figure 2**.

Single-Nucleotide Polymorphisms Affect the Causal Relationship Between Obesity Class I/Class II and Ischemic Stroke/ Cardioembolic Stroke

As shown in **Figure 3**, IS, LAS, and CES were significantly associated with obesity classes I and II. As most MR studies reported, the SNPs that contributed to obesity class I and obesity class II also presented similar causality associations with IS and its subtypes (**Figure 4**). In the forest plot containing each SNP effect value, we found that all 29 SNPs were associated with the causal relationship between obesity class I and IS (**Figure 4A**). Among them, two SNPs (rs9816226 and rs8028313) of obesity class I may have contributed to the incidence of IS to a great degree. Similarly, three SNPs (rs17381664, rs12914773, rs2207139), which are the causes of obesity class II, can significantly increase the risk of IS, as shown in **Figure 4B**. Furthermore, we found that three SNPs (rs7138803, rs7141420, and rs527248) may be the potential reasons for why obesity class I can increase the risk of CES (**Figure 4C**), and one SNP (rs7138803) from obesity class II played an outstanding role in CES (**Figure 4D**).

In addition, no outliers could be gauged in the leave-one-out analysis between obesity and the risk of IS. In addition, no outliers were found between obesity classes I, II, or III and stroke and all subtypes in the MR-PRESSO global test (**Table 3**).

DISCUSSION

To the best of our knowledge, this is the first study to investigate the causal relationship between different obesity classes and the risk of stroke and its subtypes, particularly conducted using the epidemiology data of a large number of patients from GWAS meta-analysis findings. Our findings confirmed that obesity classes I and II were associated with IS. Among the subtypes of IS, obesity classes I and II significantly influenced LAS and CES. Although suggested by their genetic characteristics, the causal relationship between obesity class III and stroke was not observed in our MR study. Whether the relationship between obesity class III and stroke exists in other populations needs to be confirmed with further research. In addition, ICH and its subtypes did not reach statistical significance with any class of obesity in this stratified MR analysis.

As our study indicated, there was no causal relationship between obesity class III and stroke, which is consistent with previous studies (22, 23). However, our results confirmed a specific correlation between obesity class I, obesity class II, and the risk of stroke, which is different from the results of previous studies (22–24). Our study focused on the relationship between different subtypes of obesity and found that only a certain degree of obesity increased the risk of stroke. This is in line with the common knowledge that different degrees of obesity have different effects on the metabolism and blood vessels of the body. Moreover, previous GWASs on obesity also confirmed genetic differences in obesity classification (24). Therefore, our findings on the association between obesity and stroke are potentially related to the degrees of obesity studied. Further studies are needed to explore the mechanism between different degrees of obesity and the occurrence of IS.

Different IS subtypes have different pathogenesis mechanisms; therefore, we further explored the influence of different obesity classifications on IS subtypes. In the subtype analysis of IS, obesity likely plays a critical role in the mechanisms of morbidity in LAS, which can be attributed to the atherosclerosis of large and medium-sized vessels due to the destruction of the microenvironment induced by the deposition of cholesterol *via* a macrophage-sterol-responsive network triggered by obesity (46, 47). Subsequently, the incidence of atherosclerosis can increase susceptibility to ischemic events (48–50) and LAS. In addition, abnormal massive accumulation of adipocytes in obese patients results in increased secretion of leptin, adiponectin, and pro-inflammatory cytokines, which subsequently aggravate the progression of atherosclerosis and

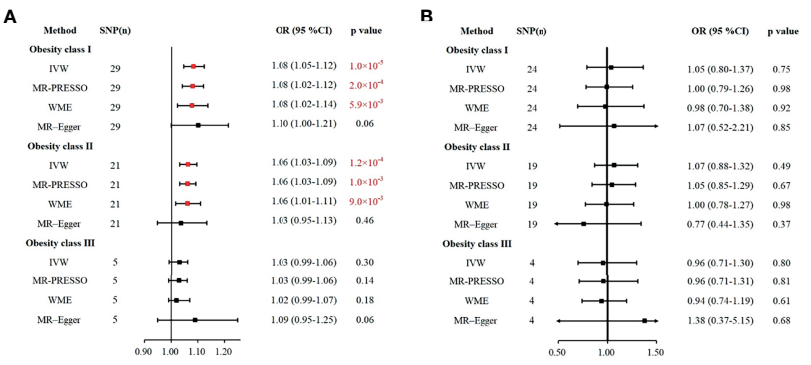

FIGURE 2 | Various methods to assess the impacts of obesity class I, obesity class II, and obesity class III on IS **(A)** and ICH **(B)**. **(A)** The causal effect of obesity and risk of IS. **(B)** The causal effect of obesity and the risk of ICH. IS, ischemic stroke; ICH, intracerebral hemorrhage; IVW, inverse-variance weighted; WME, weighted median estimation; MR-PRESSO, MR pleiotropy residual sum and outlier.

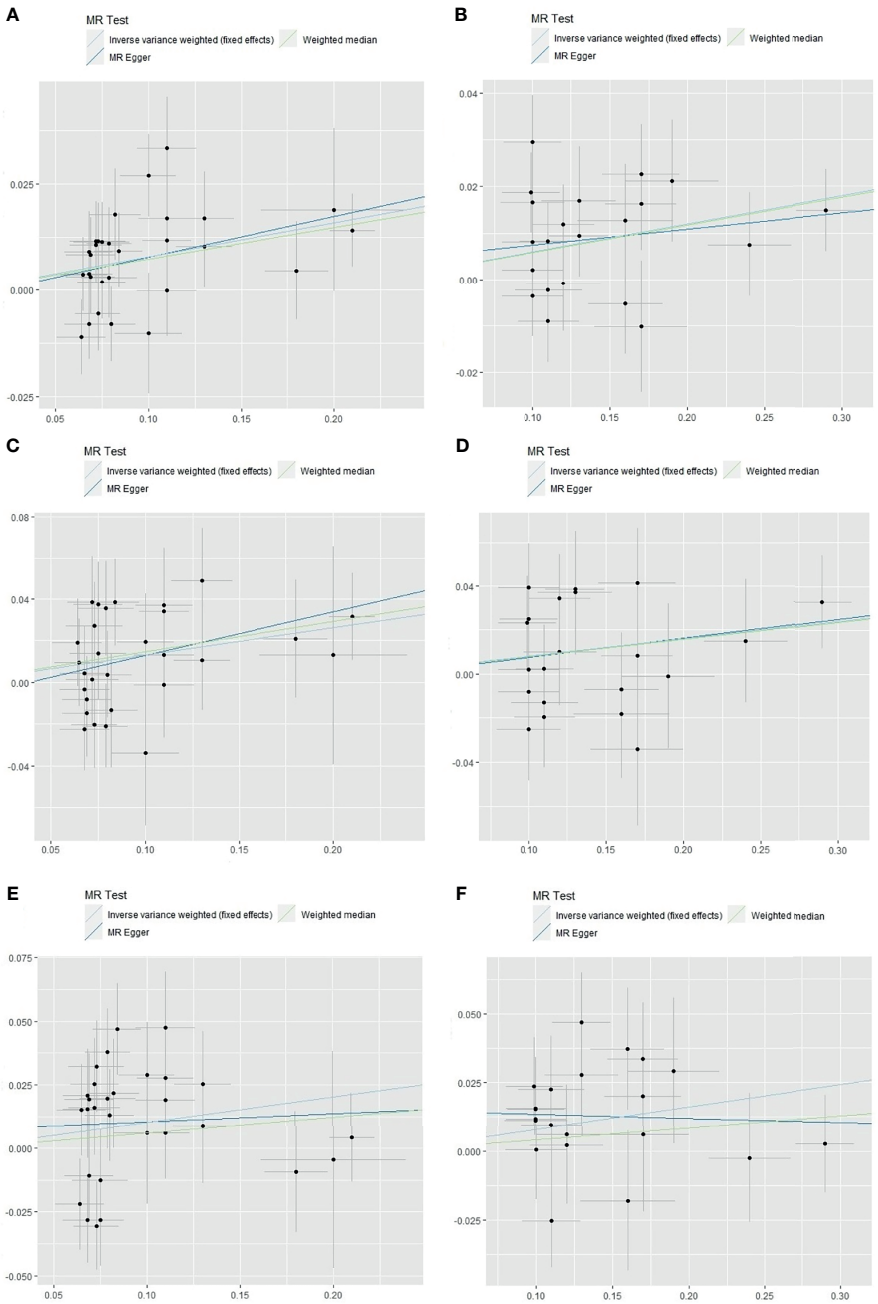

FIGURE 3 | The scatter plot of obesity classes I and II with the risk of IS, LAS, and CES in the MR analysis. **(A)** Analysis of obesity class I and risk of IS. **(B)** Analysis of obesity class II and risk of IS. **(C)** Analysis of obesity class I and risk of LAS. **(D)** Analysis of obesity class II and risk of LAS. **(E)** Analysis of obesity class I and risk of CES. **(F)** Analysis of obesity class II and risk of CES. IS, ischemic stroke; LAS, large artery stroke; CES, cardioembolic stroke; MR, Mendelian randomization.

thrombosis of cardiac and cerebral vessels and accelerate the development of LAS (49, 51, 52).

An association between genetic predisposition to obesity class I and the risk of CES was revealed in this study through MR analysis. Obesity is one of the most important predictors of atrial fibrillation and is associated with a decrease in systemic vascular resistance and an increase in cardiac output (53). A continuous state of the supercycle is prone to left ventricular diastolic dysfunction and left artery embolism, which could trigger atrial fibrillation and thus cause CES (53–55). The influence of obesity on atrial fibrillation frequently depends on the degree and duration of obesity (53, 56). In contrast, our study provided no significant evidence for an association between obesity and SVS (all $p > 0.05$). Convincing evidence has shown that obese

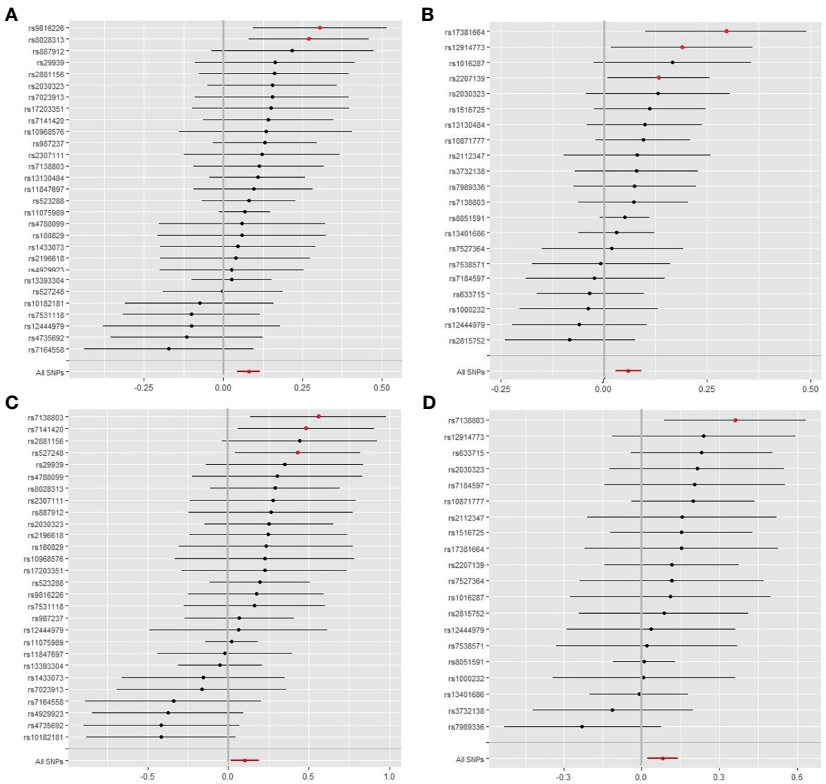

FIGURE 4 | Forest plot of SNPs of obesity classes I and II correlated with the risk of IS and CES. **(A)** The single effect of the SNPs in obesity class I and the risk of IS. **(B)** Single effects of the SNPs on obesity class II and the risk of IS. **(C)** Single effects of the SNPs on obesity class I and risk of CES. **(D)** Single effects of the SNPs on obesity class II and the risk of CES. IS, ischemic stroke; CES, cardioembolic stroke; SNP, single-nucleotide polymorphism.

individuals are more susceptible to atherosclerosis and insulin resistance (48, 57), while the association between SVS and insulin resistance and atherosclerosis has not been established (58).

Interestingly, we also found that a higher degree of obesity was not associated with a higher risk of stroke at the genetic level. Our MR analysis indicated that a higher BMI was only associated with a higher risk of stroke within a certain BMI range (30 kg/m^2 ≤ BMI < 40 kg/m^2), which is in contrast to a previous study (59). A systematic review and meta-analysis of BMI and stroke also showed that the relationship between BMI and stroke has a J-type distribution. With a BMI >25 kg/m^2, the risk of stroke rapidly increases (60). The difference between our findings and the above report could be attributed to the potential influence of mediating variables in stroke such as hypertension and smoking (61, 62). Another potential interpretation is that morbid obesity (BMI >40 kg/m^2) leads to a decrease in endothelial cell shear stress, which reduces the risk of atherosclerosis due to increases in blood vessel diameters and reductions of injuries in vascular endothelial cells (49, 63). In addition, an animal model study on the obesity paradox indicated that extremely obese mice were deficient in microRNA-155 (64), which acts on the 3-terminal noncoding region of nitric oxide synthase in vascular endothelial cells and regulates the function of vascular endothelial cells (65). Deficiency in microRNA-155 reduces the risk of atherosclerosis by improving the generation rate of vascular endothelium (64, 65). Moreover, in morbidly obese people, some factors secreted by adipocytes may play different roles. Adiponectin is an exceptive adipokine that can reduce the risk of atherosclerosis in the morbidly obese population by regulating the inflammatory reaction of the endothelium, inhibiting the scavenger receptor of macrophages, and inhibiting the transformation of macrophages to foam cells (49, 66, 67). Finally, the risk of stroke is reduced by the low occurrence of atherosclerosis in the morbidly obese population.

Although our study found that obesity class III was not associated with genetic risk of stroke, some studies have shown that obesity disrupts the balance between pro-inflammatory adipokines and anti-inflammatory adipokines (10–13). The equilibrium is transformed into pro-inflammatory mediators, and pro-inflammatory factors such as leptin, resistin, chemerin, visfatin, retinol binding protein 4, and lipocalin 2 may increase sharply, leading to chronic inflammation of the blood vessels (10, 68, 69). Chronic vascular inflammation and immune cell infiltration can promote remodeling of the extracellular matrix and vascular fibrosis (16, 70, 71). Therefore, class III obesity does not protect against stroke. Obesity classes I and II are associated with stroke, but the effects of unhealthy lifestyle obesity on the risk of stroke should be avoided.

Our study found that no class of obesity was related to ICH and its subtypes, which is different from previous observational studies. These may imply the existence of confounding factors in observational studies that interfere with causality (72, 73). Although several observational studies have considered various adjustments for confounding factors, some unknown confounders may not have been found (74). Taken together with previous reports (72, 75), hypertension, hyperlipidemia, diabetes, and other factors, but not obesity, may be the direct causes of ICH. In addition, a previous MR study confirmed that hypertension plays a role in mediating causality in abdominal obesity-induced stroke (21). Moreover, we carefully compared the previously published GWAS data on hypertension with the data on obesity included in this study and found that the genetic loci were different (24, 76). This also confirms that there is no genetic association between obesity and ICH and that hypertension may be the main cause of ICH. All these confounders may contribute more to ICH than the SNPs analyzed in our MR study.

The obvious advantages of our study lie in the following points. First, this MR analysis is the first study to explore the relationship between different obesity grades and stroke and its subtypes in a large sample size using the MR method. We also tested the heterogeneity, directional pleiotropy, and outliers using a variety of sensitivity analysis methods to confirm our results. Second, this study uncovered the association of class I and class II but not class III obesity with stroke for the first time. Finally, we found that some SNP sites could be potential predictors of IS and CES in class I and class II obese populations. These SNPs may be clinically significant for the prevention and treatment of IS and CES in obese people in the future.

This study had some limitations. First, the population was derived from Europe. To our knowledge, ethnic and regional differences can influence the incidence and prevalence of stroke and obesity (77). Developing regions such as Asia and Africa have higher stroke burdens (1) and have higher incidence and fatality rates due to stroke (2). However, current GWAS data for stroke in Asians and Africans were limited, which hampers the downstream analyses for other populations. Therefore, our results should be generalized with caution to other populations that are not of European descent, and further GWASs and MR studies for other populations are warranted to determine the causal relationship between obesity and the risk of stroke. Second, we found that some of the SNPs in obesity classes I and II were positively associated with IS, especially CES. These SNPs and their impact on the predisposition to stroke warrant close attention for stroke prevention in the obese population in further research. In clinical practice, these SNPs may have great significance in the prevention of IS, especially CES, for obese people with a certain BMI distribution ($30\ kg/m^2 \leq BMI < 40\ kg/m^2$). Third, some personalized features of obese patients were not available in this study. For example, information about the distribution of fat and the diet of these obese patients would be helpful if available. As some studies reported, the differences between general obesity and central obesity also showed different impacts on the stroke risks (22). This also confirms the contribution of different obesity subgroups like patients with different fat distributions and indicated that the importance of analyzing from different obesity perspectives can explore the effects of different obesity classes on stroke. Therefore, in the future, the inclusion of different personalized characteristics can be considered in obese patients to explore the causal relationship between obesity and stroke in more detail.

CONCLUSION

In summary, we found that not all subtypes of stroke are associated with obesity, namely, ICH and its subtypes. Interestingly, different classes of obesity did not contribute equally to stroke, as obesity classes I and II were more likely to be the cause of stroke. Moreover, we found that some SNPs in class I and II obesity patients may be the possible culprits of IS, especially CES, in these populations. Future studies focusing on the function or intervention of these SNPs may provide a preventive solution for stroke in obese populations.

DATA AVAILABILITY STATEMENT

The original contributions presented in the study are included in the article/**Supplementary Material**. Further inquiries can be directed to the corresponding author.

AUTHOR CONTRIBUTIONS

LZ and XZ designed the research and determined the structure of the paper. XZ, LX, and LW selected the references and contributed to the writing. XZ, LX, LW, ZX, and TY helped to analyze the results of the study. YZ, MS, and LZ contributed to the revision and finalization of the article. All authors contributed to the article and approved the submitted version.

FUNDING

This project was supported by the National Science and Technology Foundational Resource Investigation Program of China (Grant No. 2018FY100900) and the National Natural Science Foundation of China (Grant No. 2016JJ2164).

ACKNOWLEDGMENTS

We thank the Genetic Investigation of GIANT Consortium, the MEGASTROKE GWAS dataset, and the International Stroke Genetics Consortium and all concerned investigators for sharing GWAS summary statistics on obesity and stroke.

SUPPLEMENTARY MATERIAL

The Supplementary Material for this article can be found online at: https://www.frontiersin.org/articles/10.3389/fendo.2021.750999/full#supplementary-material

REFERENCES

1. Krishnamurthi RV, Feigin VL, Forouzanfar MH, Mensah GA, Connor M, Bennett DA, et al. Global Burden of Diseases, Injuries, Risk Factors Study 2010 (GBD 2010); GBD Stroke Experts Group. Global and Regional Burden of First-Ever Ischaemic and Hemorrhagic Stroke During 1990-2010: Findings From the Global Burden of Disease Study 2010. *Lancet Glob Health* (2013) 1 (5):e259–81. doi: 10.1016/S2214-109X(13)70089-5
2. Krishnamurthi RV, Ikeda T, Feigin VL. Global, Regional and Country-Specific Burden of Ischaemic Stroke, Intracerebral Haemorrhage and Subarachnoid Haemorrhage: A Systematic Analysis of the Global Burden of Disease Study 2017. *Neuroepidemiology* (2020) 54(2):171–9. doi: 10.1159/000506396
3. Boehme AK, Esenwa C, Elkind MS. Stroke Risk Factors, Genetics, and Prevention. *Circ Res* (2017) 120(3):472–95. doi: 10.1161/CIRCRESAHA.116.308398
4. Kachur S, Lavie CJ, de Schutter A, Milani RV, Ventura HO. Obesity and Cardiovascular Diseases. *Minerva Med* (2017) 108(3):212–28. doi: 10.23736/S0026-4806.17.05022-4
5. World Health Organization. *Obesity and Overweight. World Health Organization Website* (2018). Available at: http://www.who.int/news-room/fact-sheets/detail/obesity-and-overweight (Accessed November 13, 2018).
6. World Health Organization. *Global Health Observatory (GHO) Data: Obesity Situation and Trends* (2018). World Health Organization Website. Available at: http://www.who.int/gho/ncd/risk_factors/obesity_text/en/ (Accessed November 13, 2018).
7. Cai H, Cai B, Zhang H, Sun W, Wang Y, Zhou S, et al. Major Depression and Small Vessel Stroke: A Mendelian Randomization Analysis. *J Neurol* (2019) 266(11):2859–66. doi: 10.1007/s00415-019-09511-w
8. Smith GD, Ebrahim S. 'Mendelian Randomization':can Genetic Epidemiology Contribute to Understanding Environmental Determinants of Disease? *Int J Epidemiol* (2003) 32(1):1–22. doi: 10.1093/ije/dyg070
9. Emdin CA, Khera AV, Kathiresan S. Mendelian Randomization. *JAMA* (2017) 318(19):1925–6. doi: 10.1001/jama.2017.17219
10. AlZaim I, Hammoud SH, Al-Koussa H, Ghazi A, Eid AH, El-Yazbi AF. Adipose Tissue Immunomodulation: A Novel Therapeutic Approach in Cardiovascular and Metabolic Diseases. *Front Cardiovasc Med* (2020) 7:602088. doi: 10.3389/fcvm.2020.602088
11. Stolarczyk E. Adipose Tissue Inflammation in Obesity: A Metabolic or Immune Response? *Curr Opin Pharmacol* (2017) 37:35–40. doi: 10.1016/j.coph.2017.08.006
12. Trayhurn P, Wood IS. Signalling Role of Adipose Tissue: Adipokines and Inflammation in Obesity. *Biochem Soc Trans* (2005) 33(Pt 5):1078–81. doi: 10.1042/BST0331078
13. Ohashi K, Shibata R, Murohara T, Ouchi N. Role of Anti-Inflammatory Adipokines in Obesity-Related Diseases. *Trends Endocrinol Metab* (2014) 25 (7):348–55. doi: 10.1016/j.tem.2014.03.009
14. Alcalá M, Calderon-Dominguez M, Bustos E, Ramos P, Casals N, Serra D, et al. Increased Inflammation, Oxidative Stress and Mitochondrial Respiration in Brown Adipose Tissue From Obese Mice. *Sci Rep* (2017) 7(1):16082. doi: 10.1038/s41598-017-16463-6
15. Bouloumie A, Marumo T, Lafontan M, Busse R. Leptin Induces Oxidative Stress in Human Endothelial Cells. *FASEB J* (1999) 13(10):1231–8. doi: 10.1096/fasebj.13.10.1231
16. Lin D, Chun TH, Kang L. Adipose Extracellular Matrix Remodelling in Obesity and Insulin Resistance. *Biochem Pharmacol* (2016) 119:8–16. doi: 10.1016/j.bcp.2016.05.005
17. Tang XN, Liebeskind DS, Towfighi A. The Role of Diabetes, Obesity, and Metabolic Syndrome in Stroke. *Semin Neurol* (2017) 37(3):267–73. doi: 10.1055/s-0037-1603753
18. Yawoot N, Govitrapong P, Tocharus C, Tocharus J. Ischemic Stroke, Obesity, and the Anti-Inflammatory Role of Melatonin. *Biofactors* (2021) 47(1):41–58. doi: 10.1002/biof.1690
19. Liu S, Gao Z, Dai Y, Guo R, Wang Y, Sun Z, et al. Association of General and Abdominal Obesity and Their Changes With Stroke in Chinese Adults: Results From an 11.8-Year Follow-Up Study. *Nutr Metab Cardiovasc Dis* (2020) 30(11):2001–7. doi: 10.1016/j.numecd.2020.06.011
20. Mitchell AB, Cole JW, McArdle PF, Cheng YC, Ryan KA, Sparks MJ, et al. Obesity Increases Risk of Ischemic Stroke in Young Adults. *Stroke* (2015) 46 (6):1690–2. doi: 10.1161/STROKEAHA.115.008940
21. Marini S, Merino J, Montgomery BE, Malik R, Sudlow CL, Dichgans M, et al. International Stroke Genetics Consortium. Mendelian Randomization Study of Obesity and Cerebrovascular Disease. *Ann Neurol* (2020) 87(4):516–24. doi: 10.1002/ana.25686
22. Dale CE, Fatemifar G, Palmer TM, White J, Prieto-Merino D, Zabaneh D, et al. Causal Associations of Adiposity and Body Fat Distribution With Coronary Heart Disease, Stroke Subtypes, and Type 2 Diabetes Mellitus: A Mendelian Randomization Analysis. *Circulation* (2017) 135(24):2373–88. doi: 10.1161/CIRCULATIONAHA.116.026560
23. Larsson SC, Bäck M, Rees JMB, Mason AM, Burgess S. Body Mass Index and Body Composition in Relation to 14 Cardiovascular Conditions in UK Biobank: A Mendelian Randomization Study. *Eur Heart J* (2020) 41(2):221–6. doi: 10.1093/eurheartj/ehz388
24. Berndt SI, Gustafsson S, Mägi R, Ganna A, Wheeler E, Feitosa MF, et al. Genome-Wide Meta-Analysis Identifies 11 New Loci for Anthropometric Traits and Provides Insights Into Genetic Architecture. *Nat Genet* (2013) 45 (5):501–12. doi: 10.1038/ng.2606
25. Malik R, Chauhan G, Traylor M, Sargurupremraj M, Okada Y, Mishra A, et al. Multiancestry Genome-Wide Association Study of 520, 000 Subjects Identifies 32 Loci Associated With Stroke and Stroke Subtypes. *Nat Genet* (2018) 50 (4):524–37. doi: 10.1038/s41588-018-0058-3
26. Woo D, Falcone GJ, Devan WJ, Brown WM, Biffi A, Howard TD, et al. International Stroke Genetics Consortium. Meta-Analysis of Genome-Wide Association Studies Identifies 1q22 as a Susceptibility Locus for Intracerebral Hemorrhage. *Am J Hum Genet* (2014) 94(4):511–21. doi: 10.7554/eLife.34408
27. Hemani G, Zheng J, Elsworth B, Wade KH, Haberland V, Baird D, et al. The MR-Base Platform Supports Systematic Causal Inference Across the Human Phenome. *Elife* (2018) 7:e34408. doi: 10.7554/eLife.34408
28. Verbanck M, Chen CY, Neale B, Do R. Detection of Widespread Horizontal Pleiotropy in Causal Relationships Inferred From Mendelian Randomization Between Complex Traits and Diseases. *Nat Genet* (2018) 50(5):693–8. doi: 10.1038/s41588-018-0099-7
29. Baiocchi M, Cheng J, Small DS. Instrumental Variable Methods for Causal Inference. *Stat Med* (2014) 33:2297–340. doi: 10.1002/sim.6128
30. Choi KW, Chen CY, Stein MB, Klimentidis YC, Wang MJ, Koenen KC, et al. Major Depressive Disorder Working Group of the Psychiatric Genomics Consortium. Assessment of Bidirectional Relationships Between Physical Activity and Depression Among Adults: A 2-Sample Mendelian Randomization Study. *JAMA Psychiatry* (2019) 76(4):399–408. doi: 10.1001/jamapsychiatry.2018.4175
31. Bowden J, Del Greco MF, Minelli C, Davey Smith G, Sheehan NA, Thompson JR. Assessing the Suitability of Summary Data for Two-Sample Mendelian Randomization Analyses Using MR-Egger Regression: The Role of the I2 Statistic. *Int J Epidemiol* (2016) 45(6):1961–74. doi: 10.1093/ije/dyw220
32. Bowden J, Davey Smith G, Haycock PC, Burgess S. Consistent Estimation in Mendelian Randomization With Some Invalid Instruments Using a Weighted Median Estimator. *Genet Epidemiol* (2016) 40(4):304–14. doi: 10.1002/gepi.21965
33. Bowden J, Davey Smith G, Burgess S. Mendelian Randomization With Invalid Instruments: Effect Estimation and Bias Detection Through Egger Regression. *Int J Epidemiol* (2015) 44(2):512–25. doi: 10.1093/ije/dyv080
34. Greco MF, Minelli C, Sheehan NA, Thompson JR. Detecting Pleiotropy in Mendelian Randomization Studies With Summary Data and a Continuous Outcome. *Stat Med* (2015) 34:2926–40. doi: 10.1002/sim.6522
35. Hemani G, Bowden J, Davey Smith G. Evaluating the Potential Role of Pleiotropy in Mendelian Randomization Studies. *Hum Mol Genet* (2018) 27 (R2):R195–208. doi: 10.1093/hmg/ddy163
36. Emdin CA, Khera AV, Kathiresan S. Mendelian Randomization. *JAMA* (2017) 318(19):1925–6. doi: 10.1001/jama.2017.17219
37. Baumeister SE, Karch A, Bahls M, Teumer A, Leitzmann MF, Baurecht H. Physical Activity and Risk of Alzheimer Disease: A 2-Sample Mendelian Randomization Study. *Neurology* (2020) 95(13):e1897–905. doi: 10.1212/WNL.0000000000010013

38. Huang JY, Labrecque JA. From GWAS to PheWAS: The Search for Causality in Big Data. *Lancet Digit Health* (2019) 1(3):e101–3. doi: 10.1016/S2589-7500(19)30059-7
39. Buniello A, MacArthur JAL, Cerezo M, Harris LW, Hayhurst J, Malangone C, et al. The NHGRI-EBI GWAS Catalog of Published Genome-Wide Association Studies, Targeted Arrays and Summary Statistics 2019. *Nucleic Acids Res* (2019) 47(D1):D1005–12. doi: 10.1093/nar/gky1120
40. Boehme AK, Esenwa C, Elkind MS. Stroke Risk Factors, Genetics, and Prevention. *Circ Res* (2017) 120(3):472–95. doi: 10.1161/CIRCRESAHA.116.308398
41. An SJ, Kim TJ, Yoon BW. Epidemiology, Risk Factors, and Clinical Features of Intracerebral Hemorrhage: An Update. *J Stroke* (2017) 19(1):3–10. doi: 10.5853/jos.2016.00864
42. García-Cabo C, López-Cancio E. Exercise and Stroke. *Adv Exp Med Biol* (2020) 1228:195–203. doi: 10.1007/978-981-15-1792-1_13
43. Pierce BL, Ahsan H and V anderweele TJ. Power and Instrument Strength Requirements for Mendelian Randomization Studies Using Multiple Genetic Variants. *Int J Epidemiol* (2011) 40:740–52. doi: 10.1093/ije/dyq151
44. Palmer TM, Lawlor DA, Harbord RM, Sheehan NA, Tobias JH, Timpson NJ, et al. Using Multiple Genetic Variants as Instrumental Variables for Modifiable Risk Factors. *Stat Methods Med Res* (2012) 21:223–42. doi: 10.1177/0962280210394459
45. Marouli E, Kus A, Del Greco MF, Chaker L, Peeters R, Teumer A, et al. Thyroid Function Affects the Risk of Stroke *via* Atrial Fibrillation: A Mendelian Randomization Study. *J Clin Endocrinol Metab* (2020) 105(8):2634–41. doi: 10.1210/clinem/dgaa239
46. Yurdagul A Jr, Finney AC, Woolard MD, Orr AW. The Arterial Microenvironment: The Where and Why of Atherosclerosis. *Biochem J* (2016) 473(10):1281–95. doi: 10.1042/BJ20150844
47. Chaturvedi S, Bhattacharya P. Large Artery Atherosclerosis: Carotid Stenosis, Vertebral Artery Disease, and Intracranial Atherosclerosis. *Continuum (Minneap Minn)* (2014) 20(2 Cerebrovascular Disease):323–34. doi: 10.1212/01.CON.0000446104.90043.a5
48. van Rooy MJ, Pretorius E. Obesity, Hypertension and Hypercholesterolemia as Risk Factors for Atherosclerosis Leading to Ischemic Events. *Curr Med Chem* (2014) 21(19):2121–9. doi: 10.2174/0929867321666131227162950
49. Brodsky SV, Barth RF, Mo X, Yildiz V, Allenby P, Ivanov I, et al. An Obesity Paradox: An Inverse Correlation Between Body Mass Index and Atherosclerosis of the Aorta. *Cardiovasc Pathol* (2016) 25(6):515–20. doi: 10.1016/j.carpath.2016.09.002
50. Kim CK, Kwon HM, Lee SH, Kim BJ, Ryu WS, Kwon HT, et al. Association of Obesity With Cerebral Microbleeds in Neurologically Asymptomatic Elderly Subjects. *J Neurol* (2012) 259(12):2599–604. doi: 10.1007/s00415-012-6546-y
51. Molica F, Morel S, Kwak BR, Rohner-Jeanrenaud F, Steffens S. Adipokines at the Crossroad Between Obesity and Cardiovascular Disease. *Thromb Haemost* (2015) 113(3):553–66. doi: 10.1160/TH14-06-0513
52. Ruscica M, Baragetti A, Catapano AL, Norata GD. Translating the Biology of Adipokines in Atherosclerosis and Cardiovascular Diseases: Gaps and Open Questions. *Nutr Metab Cardiovasc Dis* (2017) 27(5):379–95. doi: 10.1016/j.numecd.2016.12.005
53. Lavie CJ, Pandey A, Lau DH, Alpert MA, Sanders P. Obesity and Atrial Fibrillation Prevalence, Pathogenesis, and Prognosis: Effects of Weight Loss and Exercise. *J Am Coll Cardiol* (2017) 70(16):2022–35. doi: 10.1016/j.jacc.2017.09.002
54. Miki K, Nakano M, Aizawa K, Hasebe Y, Kimura Y, Morosawa S, et al. Risk Factors and Localization of Silent Cerebral Infarction in Patients With Atrial Fibrillation. *Heart Rhythm* (2019) 16(9):1305–13. doi: 10.1016/j.hrthm.2019.03.013
55. Alpert MA, Omran J, Bostick BP. Effects of Obesity on Cardiovascular Hemodynamics, Cardiac Morphology, and Ventricular Function. *Curr Obes Rep* (2016) 5(4):424–34. doi: 10.1007/s13679-016-0235-6
56. Abed HS, Samuel CS, Lau DH, Kelly DJ, Royce SG, Alasady M, et al. Obesity Results in Progressive Atrial Structural and Electrical Remodeling: Implications for Atrial Fibrillation. *Heart Rhythm* (2013) 10(1):90–100. doi: 10.1016/j.hrthm.2012.08.043
57. Reaven GM. Insulin Resistance: The Link Between Obesity and Cardiovascular Disease. *Med Clin North Am* (2011) 95(5):875–92. doi: 10.1016/j.mcna.2011.06.002
58. Dearborn JL, Schneider AL, Sharrett AR, Mosley TH, Bezerra DC, Knopman DS, et al. Obesity, Insulin Resistance, and Incident Small Vessel Disease on Magnetic Resonance Imaging: Atherosclerosis Risk in Communities Study. *Stroke* (2015) 46(11):3131–6. doi: 10.1161/STROKEAHA.115.010060
59. Guo Y, Yue XJ, Li HH, Song ZX, Yan HQ, Zhang P, et al. Overweight and Obesity in Young Adulthood and the Risk of Stroke: A Meta-Analysis. *J Stroke Cerebrovasc Dis* (2016) 25(12):2995–3004. doi: 10.1016/j.jstrokecerebrovasdis
60. Liu X, Zhang D, Liu Y, Sun X, Hou Y, Wang B, et al. A J-Shaped Relation of BMI and Stroke: Systematic Review and Dose-Response Meta-Analysis of 4.43 Million Participants. *Nutr Metab Cardiovasc Dis* (2018) 28(11):1092–9. doi: 10.1016/j.numecd.2018.07.004
61. Winsløw UC, Rode L, Nordestgaard BG. High Tobacco Consumption Lowers Body Weight: A Mendelian Randomization Study of the Copenhagen General Population Study. *Int J Epidemiol* (2015) 44(2):540–50. doi: 10.1093/ije/dyu276
62. Jayedi A, Rashidy-Pour A, Khorshidi M, Shab-Bidar S. Body Mass Index, Abdominal Adiposity, Weight Gain and Risk of Developing Hypertension: A Systematic Review and Dose-Response Meta-Analysis of More Than 2.3 Million Participants. *Obes Rev* (2018) 19(5):654–67. doi: 10.1111/obr.12656
63. Barth RF, Maximilian Buja L, Cao L, Brodsky SV. An Obesity Paradox: Increased Body Mass Index Is Associated With Decreased Aortic Atherosclerosis. *Curr Hypertens Rep* (2017) 19(7):55. doi: 10.1007/s11906-017-0753-y
64. Virtue A, Johnson C, Lopez-Pastraña J, Shao Y, Fu H, Li X, et al. MicroRNA-155 Deficiency Leads to Decreased Atherosclerosis, Increased White Adipose Tissue Obesity, and Non-Alcoholic Fatty Liver Disease: A NOVEL MOUSE MODEL OF OBESITY PARADOX. *J Biol Chem* (2017) 292(4):1267–87. doi: 10.1074/jbc.M116.739839
65. Donners MM, Wolfs IM, Stöger LJ, van der Vorst EP, Pöttgens CC, Heymans S, et al. Hematopoietic Mir155 Deficiency Enhances Atherosclerosis and Decreases Plaque Stability in Hyperlipidemic Mice. *PloS One* (2012) 7(4):e35877. doi: 10.1371/journal.pone.0035877
66. Mattu HS, Randeva HS. Role of Adipokines in Cardiovascular Disease. *J Endocrinol* (2013) 216(1):T17–36. doi: 10.1530/JOE-12-0232
67. Ouchi N, Kihara S, Arita Y, Nishida M, Matsuyama A, Okamoto Y, et al. Adipocyte-Derived Plasma Protein, Adiponectin, Suppresses Lipid Accumulation and Class A Scavenger Receptor Expression in Human Monocyte-Derived Macrophages. *Circulation* (2001) 103(8):1057–63. doi: 10.1161/01.cir.103.8.1057
68. Alaaeddine RA, AlZaim I, Hammoud SH, Arakji A, Eid AH, Abd-Elrahman KS, et al. The Pleiotropic Effects of Antithrombotic Drugs in the Metabolic-Cardiovascular-Neurodegenerative Disease Continuum: Impact Beyond Reduced Clotting. *Clin Sci (Lond)* (2021) 135(8):1015–51. doi: 10.1042/CS20201445
69. Mancuso P. The Role of Adipokines in Chronic Inflammation. *Immunotargets Ther* (2016) 5:47–56. doi: 10.2147/ITT.S73223
70. Takikawa T, Ohashi K, Ogawa H, Otaka N, Kawanishi H, Fang L, et al. Adipolin/C1q/Tnf-Related Protein 12 Prevents Adverse Cardiac Remodeling After Myocardial Infarction. *PloS One* (2020) 15(12):e0243483. doi: 10.1371/journal.pone.0243483
71. Crewe C, An YA, Scherer PE. The Ominous Triad of Adipose Tissue Dysfunction: Inflammation, Fibrosis, and Impaired Angiogenesis. *J Clin Invest* (2017) 127(1):74–82. doi: 10.1172/JCI88883
72. Pezzini A, Grassi M, Paciaroni M, Zini A, Silvestrelli G, Iacoviello L, et al. Multicentre Study on Cerebral Hemorrhage in Italy (MUCH-Italy) Investigators. Obesity and the Risk of Intracerebral Hemorrhage: The Multicenter Study on Cerebral Hemorrhage in Italy. *Stroke* (2013) 44(6):1584–9. doi: 10.1161/STROKEAHA.111.000069
73. Silventoinen K, Tynelius P, Rasmussen F. Weight Status in Young Adulthood and Survival After Cardiovascular Diseases and Cancer. *Int J Epidemiol* (2014) 43(4):1197–204. doi: 10.1093/ije/dyu091
74. Gill D, Brewer CF, Del Greco MF, Sivakumaran P, Bowden J, Sheehan NA, et al. Age at Menarche and Adult Body Mass Index: A Mendelian Randomization Study. *Int J Obes (Lond)* (2018) 42(9):1574–81. doi: 10.1038/s41366-018-0048-7

75. An SJ, Kim TJ, Yoon BW. Epidemiology, Risk Factors, and Clinical Features of Intracerebral Hemorrhage: An Update. *J Stroke* (2017) 19(1):3–10. doi: 10.5853/jos.2016.00864
76. Elsworth BL, Lyon MS, Alexander T, Liu Y, Hemani G. The MRC IEU OpenGWAS Data Infrastructure. *Biorxiv* (2020), 1–22. doi: 10.1101/2020.08.10.244293
77. Gardener H, Sacco RL, Rundek T, Battistella V, Cheung YK, Elkind MSV. Race and Ethnic Disparities in Stroke Incidence in the Northern Manhattan Study. *Stroke* (2020) 51(4):1064–9. doi: 10.1161/STROKEAHA.119.028806

Conflict of Interest: The authors declare that the research was conducted in the absence of any commercial or financial relationships that could be construed as a potential conflict of interest.

Publisher's Note: All claims expressed in this article are solely those of the authors and do not necessarily represent those of their affiliated organizations, or those of the publisher, the editors and the reviewers. Any product that may be evaluated in this article, or claim that may be made by its manufacturer, is not guaranteed or endorsed by the publisher.

frontiers in Endocrinology

ORIGINAL RESEARCH
published: 07 December 2021
doi: 10.3389/fendo.2021.778875

m6A Regulators in Human Adipose Tissue - Depot-Specificity and Correlation With Obesity

*Torunn Rønningen[1], Mai Britt Dahl[2], Tone Gretland Valderhaug[3], Akin Cayir[1,4], Maria Keller[5,6], Anke Tönjes[5], Matthias Blüher[5,6] and Yvonne Böttcher[1,2,6]**

[1] Clinical Molecular Biology (EpiGen), Division of Medicine, Akershus Universitetssykehus, Lørenskog, Norway, [2] Department of Clinical Molecular Biology (EpiGen), Institute of Clinical Medicine, University of Oslo, Oslo, Norway, [3] Department of Endocrinology, Akershus Universitetssykehus, Lørenskog, Norway, [4] Vocational Health College, Canakkale Onsekiz Mart University, Canakkale, Turkey, [5] Department of Medicine, University of Leipzig, Leipzig, Germany, [6] Helmholtz Institute for Metabolic, Obesity and Vascular Research (HI-MAG) of the Helmholtz Zentrum München at the University of Leipzig and University Hospital, Leipzig, Germany*

Background: N^6-methyladenosine (m6A) is one of the most abundant post-transcriptional modifications on mRNA influencing mRNA metabolism. There is emerging evidence for its implication in metabolic disease. No comprehensive analyses on gene expression of m6A regulators in human adipose tissue, especially in paired adipose tissue depots, and its correlation with clinical variables were reported so far. We hypothesized that inter-depot specific gene expression of m6A regulators may differentially correlate with clinical variables related to obesity and fat distribution.

Methods: We extracted intra-individually paired gene expression data (omental visceral adipose tissue (OVAT) *N*=48; subcutaneous adipose tissue (SAT) *N*=56) of m6A regulators from an existing microarray dataset. We also measured gene expression in another sample set of paired OVAT and SAT (*N*=46) using RT-qPCR. Finally, we extracted existing gene expression data from peripheral mononuclear blood cells (PBMCs) and single nucleotide polymorphisms (SNPs) in *METTL3* and *YTHDF3* from genome wide data from the Sorbs population (*N*=1049). The data were analysed for differential gene expression between OVAT and SAT; and for association with obesity and clinical variables. We further tested for association of SNP markers with gene expression and clinical traits.

Results: In adipose tissue we observed that several m6A regulators (*WTAP*, *VIRMA*, *YTHDC1* and *ALKBH5*) correlate with obesity and clinical variables. Moreover, we found adipose tissue depot specific gene expression for *METTL3*, *WTAP*, *VIRMA*, *FTO* and *YTHDC1*. In PBMCs, we identified *ALKBH5* and *YTHDF3* correlated with obesity. Genetic markers in *METTL3* associate with BMI whilst SNPs in *YTHDF3* are associated with its gene expression.

Conclusions: Our data show that expression of m6A regulators correlates with obesity, is adipose tissue depot-specific and related to clinical traits. Genetic variation in m6A regulators adds an additional layer of variability to the functional consequences.

Keywords: RNA methylome, m6A methylation, epitranscriptome, obesity, transcription, fat distribution

OPEN ACCESS

Edited by:
Katherine Samaras, St Vincent's Hospital Sydney, Australia

Reviewed by:
Hongyan Qiu, Affiliated Hospital of Weifang Medical University, China
Qianyan He, First Affiliated Hospital of Jilin University, China

****Correspondence:***
Yvonne Böttcher
yvonne.bottcher@medisin.uio.no

Specialty section:
This article was submitted to Obesity, a section of the journal Frontiers in Endocrinology

Received: *17 September 2021*
Accepted: *15 November 2021*
Published: *07 December 2021*

Citation:
Rønningen T, Dahl MB, Valderhaug TG, Cayir A, Keller M, Tönjes A, Blüher M and Böttcher Y (2021) m6A Regulators in Human Adipose Tissue - Depot-Specificity and Correlation With Obesity. Front. Endocrinol. 12:778875. doi: 10.3389/fendo.2021.778875

INTRODUCTION

Obesity is a major health burden predisposing to a variety of serious co-morbidities including metabolic disorders (1). Increased fat storage in omental visceral adipose tissue (OVAT) strongly correlates with a higher risk of metabolic sequelae [such as insulin resistance, type 2 diabetes (T2D)], whilst accumulation of subcutaneous adipose tissue (SAT) is less correlated to metabolic alterations (2–4). Due to its multifactorial, complex nature, obesity is subject to regulation by genetic and non-genetic factors (5). In addition to dynamic epigenetic signatures regulating gene expression and function, epitranscriptomic regulation represent an additional layer of variability adding to the complexity of gene regulation and function (6). Among multiple mRNA modifications N6-methyladenosine (m6A) is the most abundant (7, 8) and is a reversible, epitranscriptomic mark, playing an essential role in RNA processing, particularly in regulating RNA stability and decay, RNA export, translation and splicing (9). Similar to DNA methylation and other dynamic epigenetic modifications, m6A is regulated by a number of regulators entitled as "writers", "readers" and "erasers" (10). The abundance of m6A in mRNA is determined by the activity of the "writer" and "eraser" proteins. A multi-protein "writer" complex consisting of the two methyltransferases methyltransferase-like 3 and 14 (METTL3 and METTL14), along with several other co-regulators such as Wilms tumor 1-associated protein (WTAP), and vir like m6A methyltransferase associated (VIRMA) installs m6A predominantly at stop codons, 3′and 5′UTR regions (11). Further, m6A is dynamically removed by specific demethylases or "erasers" including fat mass and obesity associated (FTO) and AlkB homologue 5 (ALKBH5) (12, 13). Multiple "reader" proteins including YTH family proteins and insulin like growth factor 2 binding proteins (IGF2BPs) are responsible for translating m6A deposition into function (12). Readers such as YTHDF2 and YTHDF3 increase transcript decay, while in contrast IGFBPs (IGF2BP1, 2 and 3) function by stabilizing mRNA. Furthermore, YTHDF1 and YTHDF3 modify translation efficiency, while YTHDC1 influence alternative splicing and nuclear export of mRNA (14). The functional consequence of m6A is therefore highly dependent on the associated reader protein. Several studies indicated that m6A regulators are important players in metabolic diseases (15–18). Interestingly, genetic variants within the *FTO* gene are strongly associated with obesity (19) and robustly replicated in many studies (20). FTO-dependent m6A demethylation is functionally linked to adipogenesis in 3T3-L1 mouse adipocytes by overlooking alternative splicing (21). Zhao et al. (2014) further reported that m6A levels negatively correlate to *FTO* expression in adipogenesis and *FTO* siRNA knock down inhibits 3T3-L1 adipocyte differentiation. Recently, it was suggested that m6A modifications may be involved in adipose tissue expansion (22–24). So far, to the best of our knowledge, no attempts have been undertaken to investigate the role of m6A regulators in intra-individually paired samples of human visceral vs subcutaneous adipose tissue, their role in obesity and potential differential depot-specific correlation with anthropometric and metabolic traits. Here, we set out to describe **(i)** the gene expression profile of m6A writers, readers and erasers in visceral vs subcutaneous adipose tissue with a potential depot-specificity perspective; **(ii)** to analyze its relationship to clinically relevant traits of obesity in several well-described cohorts and **(iii)** to test whether SNP markers in m6A regulators associate with gene expression and clinical traits.

METHODS

Study Populations

Adipose Tissue Leipzig Cohort

We have used data from the Adipose tissue Leipzig cohort (*N*=63, mean age 53 ± 16 years, mean BMI 36.1 ± 13.9 kg/m^2) (25, 26), for which genome wide gene expression data are available for intra-individually paired samples of subcutaneous (SAT) and omental visceral adipose tissue (OVAT). Samples were taken at metabolic surgery or other procedures such as cholecystectomy as reported previously (25, 27). Patients were categorized based on BMI according to the WHO classification: lean ≥18; <25 kg/m^2; overweight ≥25; <30 kg/m^2; obese≥ 30 kg/m^2. This cohort comprises lean (*N*=23), overweight (*N*=3) and obese individuals (*N*=37). A range of anthropometric and metabolic variables available for this cohort were used in the here presented work. By using computed tomography measurements subjects with obesity were categorized in subcutaneous or visceral obese (CT-ratio represents the ratio of visceral/subcutaneous fat area). Another sample set of *N*=46 paired adipose tissue samples from SAT and OVAT from obese patients was used to support observed gene expression effects (10 samples overlapped with the initial Adipose tissue Leipzig cohort). RNA was extracted by using standard approaches (SIGMA ALDRICH, Saint Louis, USA and Qiagen, Hilden, Germany). RNA integrity and concentration were examined using Agilent 2100 Bioanalyzer (Agilent Technologies, CA, USA). RNA samples with RNA integrity values (RIN) of less than 5 were excluded from further analysis. All characteristics of the study populations are summarized in **Table 1**. The ethics committee of the University of Leipzig and the Regional Committee for Medical and Health Research Ethics for South Eastern Norway have approved all study protocols and written informed consents were collected from all study participants.

Sorbs Cohort

In the present study a total of 1049 individuals from the Sorbs population, a German minority of Slavonic origin, were included (28). Of those, *N*=900 non-diabetic individuals (mean age 48 ± 16 and mean BMI 26.9 ± 4.9 kg/m^2) were used for statistical analysis and a portfolio of clinical variables was available, including anthropometric and metabolic variables. The main study population characteristics are summarized in **Table 1**. The ethics committee of the University of Leipzig has approved the study protocols and written informed consents were collected from all study participants.

TABLE 1 | Main characteristics of the study populations.

	Adipose tissue Leipzig cohort				Sorbs cohort			
	Total	**Lean**	**Obese**	***N* per trait (total/lean/obese)**	**Total**	**Lean**	**Obese**	***N* per trait (total/lean/obese)**
N	63	23	37		1049	387	232	
sex (m/f)	16/47	7/16	7/30		418/617	114/273	86/146	
T2D (yes/no)	14/49	1/22	13/24		106/900	12/365	57/169	
age (years)	53 ± 16	65 ± 11	45 ± 13	63/23/37	48 ± 16	39 ± 15	58 ± 13	1035/387/232
BMI (kg/m2)	36.1 ± 13.9	22.8 ± 1.7	45.1 ± 11.2	63/23/37	26.9 ± 4.9	22.3 ± 1.7	34 ± 3.8	1022/387/232
visceral fat area (cm²)	164 ± 128	66 ± 88	252 ± 94	55/23/29	n.a.	n.a.	n.a.	n.a.
subcutanoues fat area (cm²)	583 ± 635	100 ± 232	1016 ± 570	55/23/29	n.a.	n.a.	n.a.	n.a.
CT-ratio (vis./subc. fat area)	0.62 ± 0.51	0.95 ± 0.59	0.33 ± 0.22	55/23/29	n.a.	n.a.	n.a.	n.a.
Waist (cm)	104 ± 30	78 ± 17	126 ± 21	54/22/29	90.9 ± 14	78 ± 8	107 ± 12	1012/377/230
Hip (cm)	109 ± 24	89 ± 10	126 ± 18	54/22/29	104 ± 9	97 ± 6	115 ± 9	1005/387/226
Waist-to-hip ratio	0.95 ± 0.15	0.88 ± 0.11	1.01 ± 0.15	54/22/29	0.87 ± 0.10	0.81 ± 0.08	0.93 ± 0.09	1002/376/226
body fat %	35.44 ± 13.87	21.66 ± 7.52	43.75 ± 9.87	43/14/27	21.45 ± 9.54	14.96 ± 5.36	32.86 ± 9.31	1008/380/226
Fasting Plasma Glucose (mmol/l)	5.86 ± 1.31	5.47 ± 1.01	6.16 ± 1.45	63/23/37	5.55 ± 1.20	5.06 ± 0.69	6.28 ± 1.64	1021/382/229
Fasting Plasma Insulin (pmol/l)	94.70 ± 141.1	22.64 ± 65.53	148.52 ± 158.75	32/5/26	42.39 ± 27.96	31.21 ± 18.55	62.96 ± 36.18	1025/385/228
HbA1c %	5.71 ± 0.66	5.28 ± 0.29	6.03 ± 0.67	61/23/35	n.a.	n.a.	n.a.	n.a.
HDL Cholesterol (mmol/l)	1.33 ± 0.39	1.6 ± 0.47	1.17 ± 0.25	47/16/28	1.63 ± 0.40	1.83 ± 0.39	1.49 ± 0.36	1006/377/226
LDL Cholesterol (mmol/l)	3.28 ± 1.29	2.78 ± 1.00	3.63 ± 1.39	48/17/28	3.37 ± 0.96	2.95 ± 0.91	3.56 ± 0.90	1006/377/226
Triglycerids (mmol/l)	1.19 ± 0.5	1.01 ± 0.28	1.37 ± 0.57	31/12/2017	1.31 ± 0.88	0.96 ± 0.53	1.72 ± 1.10	1006/377/226

All data are shown as mean ± S.D. (standard deviation). N, Number of subjects; T2D, diagnosed type 2 diabetes; BMI, body mass index (WHO classification: lean≥18; <25 kg/m²; <30 kg/m²obese≥ 30 kg/m²); n.a., not available; m, male; f, female.

Extraction of Gene Expression Data

mRNA expression data for all described m6A regulators in paired human adipose tissue samples were extracted for the Adipose tissue Leipzig cohort from our own work published previously elsewhere (25) for a total of *N*=63 with expression data available for SAT in *N*=56 and OVAT in *N*=48 (overlapping data in SAT and OVAT *N*=41). Further, mRNA expression data from peripheral blood mononuclear cells (PBMCs) for m6A regulators were available for the Sorbs cohort and were extracted from a genome wide data set for *N*=1049 subjects (29). Briefly, Illumina human HT-12 expression chips were used to generate mRNA expression data for both studies. Expression data were background-corrected, log-transformed and quantile-normalized. Differential expression analysis was performed using the R package oposSOM (30).

Extraction of SNP Data

Genotype data of 41 single nucleotide polymorphisms (SNP) markers (24 SNPs in the *METTL3* locus; 17 SNPs in the *YTHDF3* locus) were extracted from a genome wide SNP data set available for 840 non-diabetic individuals from the German Sorbs population (31). All genotype data were analysed for being in Hardy-Weinberg equilibrium (HWE). We excluded one SNP marker in *METTL3* and five SNP markers in *YTHDF3* from further analyses because of being significantly different from HWE with $p<0.05$. Moreover, 14 SNP markers in *METTL3* and six SNPs in *YTHDF3* were in linkage disequilibrium (LD) and excluded from further analyses (**Supplementary Figure 1**).

Expression Measurements by Using Reverse Transcriptase Quantitative PCR (RT-qPCR)

RT-qPCR was performed in triplicates on a Quantstudio 7 Flex system (ThermoFisher Scientific) using target specific primers (**Supplementary Table 1**) and PowerUp SYBR green (ThermoFisher Scientific). Gene expression levels were calculated by relative quantification with *PPIA* as housekeeping gene ($2^{(-CT\ gene\ of\ interest\ -\ CT\ PPIA)}$). Primers were designed to cover all main transcript variants of the genes and to cross exon-intron borders.

Statistical Analyses

All statistical analyses were performed using SPSS statistics software 26 (SPSS, Inc. Chicago, IL) and GraphPad Prism 8 (GraphPad, San Diego, Ca, USA). Prior to analyses, data were tested for normal distribution by using both visual inspection of histograms and one-sample Kolmogorov-Smirnov test. Non-normally distributed variables were either logarithmically transformed to approximate normal distribution or non-parametric test were applied. Data are presented as mean ± standard deviation if not stated otherwise. Paired Student's t-tests or Wilcoxon's signed rank test were used to test for adipose tissue depot-specific gene expression whilst independent group statistics was used to test for differences between lean subjects and individuals with obesity. Linear regression analyses adjusted for age, gender and ln_BMI were performed to test for linear relationship between gene expression levels or SNPs and clinical

variables (except for BMI in analyses where BMI was used as an independent variable). Genetic association analyses were performed for additive (mm vs Mm vs MM) or dominant (mm + Mm vs MM) mode of inheritance (m=minor allele; M=major allele). Different significance thresholds were applied to different sections of the work. For comparisons of means between lean and obese or SAT and OVAT, P<0.05 was used. When testing for correlations with clinical variables in two adipose tissue depots Bonferroni correction was used to take into account multiple testing (0.05/6 (highly correlated traits were reduced to three x 2 tissue depots=number of tests=6)). We lowered the study-specific significance threshold for these tests in adipose tissue to *P*=0.0083. All P-values > 0.0083 but < 0.05 were considered to be of nominal statistical significance. For genetic association analyses in the Sorbs cohort, we also applied Bonferroni correction taking into account clinical traits (*N*=3 after aggregating highly correlated traits) and the number of SNP markers tested (*N*=15). We lowered the study-specific significance threshold for this part of the analyses to *P*=0.0011 (0.05/45). All P-values > 0.0011 but < 0.05 were considered to be of nominal statistical significance. All P-values given are uncorrected for multiple testing.

RESULTS

Expression of m6A Writers, Erasers and Readers in Human Adipose Tissue Differs Between Lean and Obese and Correlates With Clinical Variables

To evaluate the impact of gene expression level of m6A regulators on clinically relevant traits of obesity, we first tested whether m6A writers, erasers, and readers are significantly different expressed between individuals with obesity and lean subjects.

Gene Expression of m6A Writers, Erasers and Readers Correlates with Obesity

From our previously published genome-wide data set (Keller M et al., 2016), we extracted paired gene expression data from OVAT and SAT for 11 m6A regulators (**Table 2** and **Supplementary Figure 2**). In OVAT, we identified by using independent t-tests or Mann-Whitney-U tests, the writers *WTAP* (ILMN_2279339; *P*=0.011) and *VIRMA* (*P*=0.028) as differentially expressed between lean and obese (**Table 2**). Further, we found the eraser *ALKBH5* (*P*=0.023, **Table 2**) as well as the readers *YTHDF1* (*P*=0.007), and *YTHDF2* (*P*=0.045) differentially expressed between lean and obese. The most significant differences between the two groups were, however, found in SAT at the writer *VIRMA* (*P*=0.005) and the reader *YTHDC1* (ILMN_1707506; $P=9.26\text{x}10^{-5}$), both being significantly lower expressed in individuals with obesity. All data are summarized in **Table 2**. No significant relationship of gene expression of m6A regulators with T2D was observed (data not shown).

Gene Expression Correlates Differentially With Measures of Obesity and Fat Distribution

The statistically significant association between gene expression of a number of m6A regulators and obesity led us to hypothesize that gene expression of these regulators correlates also with continuous traits related to obesity and fat distribution. Indeed, among non-diabetic individuals we find that gene expression of *WTAP* in OVAT correlates with body mass index (BMI) (*P*=0.003) and waist circumference (*P*=0.009). In line with this, expression of *VIRMA*in OVAT, which associates with obesity, shows a negative correlation with BMI (*P*=0.040). The expression of the eraser *ALKBH5* in OVAT shows a nominal significant correlation with the amount of subcutaneous fat area (*P*=0.013) as well as the ratio of visceral to subcutaneous fat area (CT-ratio, *P*=0.004). All these bivariate correlations withstand adjustment for age and sex in linear regression analyses (all adjusted *P*-values are shown in **Figure 1A**).

In line with reduced gene expression of *VIRMA* in patients with obesity, we find in SAT gene expression of *VIRMA* correlated to BMI (*P*=0.021), waist to hip ratio (WHR) (*P*=0.012), percentage of body fat (*P*=0.0003), maximal adipocyte diameter in SAT (*P*=0.009) and OVAT (*P*=0.011), and leptin serum levels (*P*=0.016). Further, to substantiate evidence for a linear relationship, we performed linear regression analysis adjusted for covariates such as age and sex. All described correlations are also significant after such adjustment. All adjusted *P*-values are shown in **Figure 1B**.

These data indicate that expression of certain m6A regulators in adipose tissue is associated with obesity and a range of continuous clinical variables related to obesity and fat distribution. However, this seems also dependent on the respective adipose tissue depot. Therefore, we next tested the hypothesis that the expression of m6A regulators may be adipose tissue depot-specific.

Inter-Depot Specific Adipose Tissue Expression Between SAT and OVAT

By using paired statistics, we observed that gene expression of a number of m6A regulators is significantly different between OVAT and SAT (**Table 3**). We show that the writers *METTL3* (*P*=0.014), *WTAP* (probe ILMN_2279339 *P*=0.031; and probe ILMN_1734544 *P*=0.022) and *VIRMA* (*P*=0.002) confer significant inter-depot specificity, with highest significance for *VIRMA* (**Table 3**). Moreover, highly significant differences were identified for the eraser *FTO* ($P=2.257\text{x}10^{-4}$), the strongest obesity candidate gene identified in genetic studies (19). Further, two probes targeting the reader *YTHDC1* (probe ILMN_1666111 *P*=0.047; and probe ILMN_1707506 *P*=0.045) showed borderline significance between the two adipose tissue depots. All data are summarized in **Table 3**. Among those five m6A regulator genes exhibiting significant depot specificity, the gene encoding the catalytic subunit of the m6A methyltransferase complex, *METTL3*, shows higher expression in OVAT whilst other subunits of the methyltransferase complex *WTAP* and *VIRMA* show higher expression in SAT. *FTO* is

TABLE 2 | Comparison of mean gene expression of m6A regulators between lean and obese in adipose tissue.

Gene	Probe	Depot	N	Lean		Obese		p-value
			Lean/Obese	Mean	SD of Mean	Mean	SD of Mean	
m6A writers								
METTL3	ILMN_1655635	SAT	20/34	-0.0135	0.0588	-0.0116	0.0619	n.s.[2]
		OVAT	15/31	0.0022	0.06	0.0246	0.1103	n.s.[2]
METTL14	ILMN_22124523	SAT	20/34	0.0004	0.061	-0.0029	0.0423	n.s.[1]
		OVAT	15/31	0.0035	0.0498	0.0048	0.0512	n.s.[1]
WTAP	1: ILMN_2279339	SAT	20/34	0.0126	0.1093	0.0263	0.1193	n.s.[2]
		OVAT	15/31	-0.0839	0.0807	0.0063	0.1082	**0.011**[2]
	2: ILMN_2260725	SAT	20/34	-0.0046	0.0576	0.0078	0.0565	n.s.[1]
		OVAT	15/31	-0.0151	0.083	0.0017	0.0708	n.s.[1]
	3: ILMN_2356559	SAT	20/34	-0.0196	0.0649	0.0044	0.0765	n.s.[1]
		OVAT	15/31	-0.0102	0.0577	-0.0033	0.0558	n.s.[1]
	4: ILMN_1734544	SAT	20/34	0.0165	0.0911	0.0116	0.0818	n.s.[2]
		OVAT	15/31	-0.0167	0.1356	-0.0182	0.065	n.s.[2]
	5: ILMN_1657618	SAT	20/33	0.0403	0.1046	-0.0177	0.0805	**0.041**[1]
		OVAT	15/31	0.032	0.078	-0.0025	0.0944	n.s.1
VIRMA	ILMN_1813635	SAT	20/34	0.0568	0.0808	-0.0059	0.0621	**0.005**[1]
		OVAT	15/31	0.0147	0.0705	-0.0343	0.0582	**0.028**[1]
m6A erasers								
FTO	ILMN_2288070	SAT	20/34	0.0212	0.0513	0.0311	0.0637	n.s.[1]
		OVAT	15/31	-0.0311	0.0717	-0.0285	0.0637	n.s.[1]
ALKBH5	ILMN_1657283	SAT	20/34	-0.0213	0.0483	0.0083	0.0356	**0.021**[2]
		OVAT	15/31	-0.0179	0.0399	0.0113	0.0385	**0.023**[2]
m6A readers								
YTHDF1	ILMN_1753885	SAT	20/34	0.0046	0.0546	-0.0082	0.0398	n.s.[2]
		OVAT	15/30	-0.025	0.0468	0.015	0.049	**0.007**[2]
YTHDF2	ILMN_1730658	SAT	20/34	-0.0163	0.0487	0.0112	0.0659	n.s.[1]
		OVAT	15/31	-0.0293	0.0546	0.0071	0.0569	**0.045**[1]
YTHDF3	ILMN_1657470	SAT	20/34	-0.0078	0.0518	0.0013	0.0577	n.s.[1]
		OVAT	15/31	-0.0031	0.0405	0.0037	0.0649	n.s.[1]
YTHDC1	1: ILMN_1666111	SAT	20/34	-0.008	0.0674	0.0201	0.0777	n.s.[1]
		OVAT	15/31	-0.019	0.1035	-0.0133	0.0763	n.s.[1]
	2: ILMN_1670878	SAT	20/34	-0.0049	0.074	0.009	0.0664	n.s.[1]
		OVAT	15/31	0.0153	0.0613	-0.0133	0.0684	n.s.[1]
	3: ILMN_1707506	SAT	20/34	0.0403	0.0647	-0.0359	0.055	**9.262x10^{-5}** [1]
		OVAT	15/31	0.0133	0.0631	0.0016	0.0782	n.s.[1]
IGF2BP2	ILMN_1702447	SAT	20/34	-0.0082	0.1097	0.0009	0.1306	n.s.[1]
		OVAT	15/31	-0.0313	0.1112	0.005	0.1637	n.s.[1]

P-values were calculated using 1) independent t-test for normally distributed variables and 2) Mann-Whitney-U test for not normally distributed variables; SAT, Subcutaneous adipose tissue; OVAT, Omental visceral adipose tissue; SD, Standard deviation; n.s., not significant.
P-values < 0.05 are highlighted in bold.

significantly higher expressed in SAT confirming previous data (32) whilst we found gene expression for two different probes targeting the reader *YTHDC1* either increased or decreased in OVAT. All data are summarized in **Figure 2**.

To verify these results, we performed RT-qPCR in another sample set (N=46) of intra-individually paired human adipose tissue samples of OVAT and SAT. Gene expression was measured for the following genes: writers: *METTL3*, *METTL14*, *WTAP* and *VIRMA*, erasers: *FTO* and *ALKBH5* and readers: *YTHDF1*, *YTHDF2*, *YTHDC1* and *IGF2BP2*. Interestingly, we confirm our finding of inter-depot specific expression for *METTL3* (P=0.001, **Figure 3**) showing the same effect direction with higher expression in OVAT. In addition, we observed increased OVAT expression of the second main component of the methyltransferase complex *METTL14* (P=0.012, **Figure 3**). No other differences were identified in this cohort. All data are summarized in **Table 4**.

Gene Expression of m6A Erasers and Readers in PBMCs Correlates With Obesity

Based on our data from adipose tissue showing that gene expression of several m6A regulators correlates with obesity and clinical variables, we hypothesized that gene expression of m6A writers, readers and erasers in PBMCs might also be different between lean subjects and individuals with obesity. Therefore, we extracted gene expression data for m6A regulators from our existing genome wide data set (29) and tested for differences of the mean expression values between lean and obese by using independent t-test statistics. Our data show that none of the covered probes for the writers are different between the two groups (**Table 5**). However, we find a strong difference for the eraser *ALKBH5* showing higher expression in obese (P=5.80x10^{-5}), as well as for the two readers *YTHDF1* (P=0.049) and *YTHDF3* (P=0.003) both showing higher

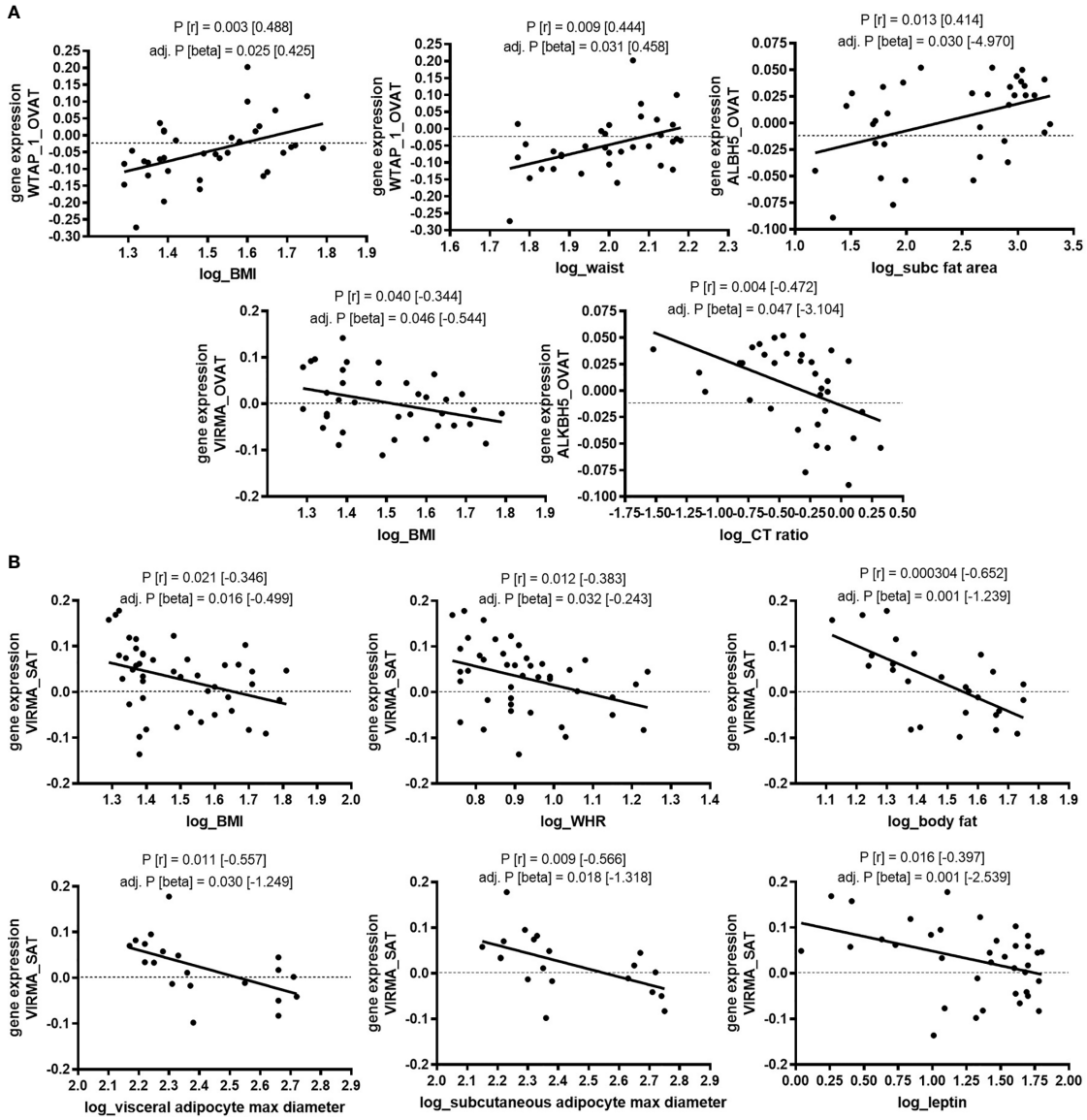

FIGURE 1 | Association of gene expression with clinical variables of obesity and fat distribution in non-diabetic subjects (adipose tissue Leipzig cohort). Correlation of gene expression (log transformed, normalized intensities) with clinical variables of obesity and fat distribution in non-diabetic subjects. **(A)** in OVAT and **(B)** in SAT. *P*-values were calculated by using bivariate Pearson or Spearman correlation. Significant correlation results are shown for correlations that survive adjustment for age, and sex in linear regression analysis. BMI, body mass index; WHR, waist to hip ratio; OVAT, omental visceral adipose tissue; SAT, subcutaneous adipose tissue; Beta, non-standardized regression coefficient from linear regression; *P*=*P*-value; r, correlation coefficient from bivariate correlation.

expression in lean individuals. To better understand whether the observed differences of means reflect an association of gene expression with BMI, we performed linear regression analysis adjusted for age and sex as additional confounders. These analyses resulted for *YTHDF3* in a *P*=0.012 (beta -0.055; [-0.098; -0.012]), whilst no nominal significance was found for *ALKBH5* and *YTHDF1*. **Figure 4** illustrates the negative linear relationship between *YTHDF3* expression and BMI. No significant association of gene expression of m6A regulators with T2D was observed (data not shown).

Genetic Variants in *METTL3* and *YTHDF3* Associate With Anthropometric and Metabolic Variables Related to Obesity

Our data have shown so far that **(i)** *METTL3* expression is adipose tissue depot-specific with higher expression levels in OVAT in two sample sets and, **(ii)** that *YTHDF3* gene expression in PBMCs differs between lean and obese and is negatively associated with BMI. To test the hypothesis that the observed effects may be at interplay with genetic variation, we analysed genotypes of 15 SNP markers (9 SNPs for *METTL3* and 6 SNPs

TABLE 3 | Differential gene expression of m6A regulators between SAT and OVAT.

Gene	Probe	N	SAT		OVAT		p-value
			Mean	SD of Mean	Mean	SD of mean	
m6A writers							
METTL3	ILMN_1655635	41	-0.01387	0.063791	0.02829	0.093343	**0.014**[b]
METTL14	ILMN_22124523	41	0.0006	0.046264	0.00673	0.051285	n.s[a]
WTAP	1: ILMN_2279339	41	0.02405	0.115028	-0.02073	0.110101	**0.031**[b]
	2: ILMN_2260725	41	0.00559	0.053769	-0.00879	0.071324	n.s[a]
	3: ILMN_2356559	41	0.0044	0.075411	-0.00279	0.054819	n.s[a]
	4: ILMN_1734544	41	0.02897	0.082764	-0.0077	0.09224	**0.022**[b]
	5: ILMN_1657618	40	-0.01555	0.071808	0.00402	0.084863	n.s[a]
VIRMA	ILMN_1813635	41	0.01375	0.076048	-0.0173	0.067723	**0.002**[a]
m6A erasers							
FTO	ILMN_2288070	41	0.03308	0.05702	-0.02831	0.068946	**2.257x10^{-4}** [a]
ALKBH5	ILMN_1657283	41	0.00433	0.038695	0.00376	0.041619	n.s[b]
m6A readers							
YTHDF1	ILMN_1753885	40	-0.00949	0.04035	0.00177	0.050554	n.s[b]
YTHDF2	ILMN_1730658	41	0.01221	0.057429	-0.00354	0.057748	n.s[a]
YTHDF3	ILMN_1657470	41	0.0049	0.0515	0.0062	0.05516	n.s[a]
YTHDC1	1: ILMN_1666111	41	0.02307	0.067122	-0.00951	0.08985	**0.047**[a]
	2: ILMN_1670878	41	0.005	0.066725	-0.00409	0.070425	n.s[a]
	3: ILMN_1707506	41	-0.02831	0.063662	0.00131	0.07475	**0.045**[a]
IGF2BP2	ILMN_1702447	41	-0.01219	0.122958	-0.00586	0.152985	n.s[a]

P-values were calculated using a) paired t-tests for normally distributed variable and b) Wilcoxon signed rank test for non-normally distributed variables. WHO classification: lean ≥18; <25 kg/m²; overweight ≥25; <30 kg/m²; obese≥ 30 kg/m²; N (lean/overweight/obese)=12/1/28; SAT, Subcutaneous adipose tissue; OVAT, Omental visceral adipose tissue; SD, Standard deviation; n.s., not significant.

P-values < 0.05 are highlighted in bold.

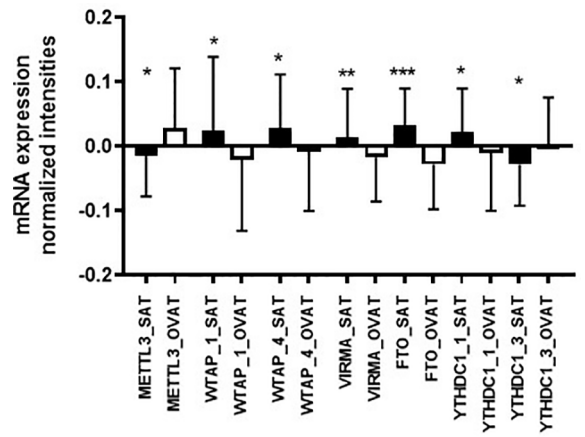

FIGURE 2 | Adipose tissue depot-specific differences in gene expression of m6A writers, reader and erasers (adipose tissue Leipzig cohort). Differences in gene expression (log transformed, normalized intensities) between SAT and OVAT. Data are presented as mean ± SD. *P*-values were calculated using paired samples t-tests or Wilcoxon signed rank test in n=41 and given as asterix (*P < 0.05; **P < 0.01; ***P < 0.001). OVAT, omental visceral adipose tissue; SAT, subcutaneous adipose tissue. The following Illumina probes are presented: METTL3=ILMN_1655635; WTAP_1=ILMN_2279339; WTAP_4=ILMN_1734544; VIRMA=ILMN_1813635; FTO=ILMN_2288070; YTHDC1_1=ILMN_1666111; YTHDC1_3=ILMN_1707506.

for *YTHDF3*) extracted from our existing genome wide data set (31). We performed genetic association analyses of these markers in *N*=840 non-diabetic individuals with anthropometric and metabolic variables available in the Sorbs (**Table 1**). We identified two SNP markers in the locus of the m6A reader *YTHDF3* (rs2241754 upstream variant, and rs1435457 intronic variant) correlating with *YTHDF3* gene expression. Carriers of the minor G allele of rs2241754 show nominal significantly lower expression levels compared to carriers of the major A allele (**Figure 5A**). Similar results were obtained for rs1435457 with decreased expression levels in minor A allele carriers (**Figure 5A**). Further, we observed that two SNP markers in *METTL3* (rs1139130 intragenic coding and rs2242526 intronic variant) associate with BMI (**Figure 5B**), though these effects were not strong enough to withstand logistic regression analysis for obesity adjusted for age and sex (data not shown). These results imply that genetic variation in *METTL3* and *YTHDF3* is related to either BMI or gene expression which may potentially modulate a relationship between gene expression of m6A regulators and variables of obesity and fat distribution.

DISCUSSION

In this work, we studied the gene expression profiles of major players of the m6A writer complex, several readers and the two known erasers in human adipose tissue and in PBMCs from different cohorts. This is the first report analysing m6A regulators in paired human adipose tissue biopsies (SAT and OVAT) and our results show, that **(i)** gene expression of some m6A regulators correlates with obesity and clinical variables; **(ii)** several regulators are differentially expressed between the two adipose tissue depots and **(iii)** genetic variation in selected regulators is related to both gene expression levels and BMI.

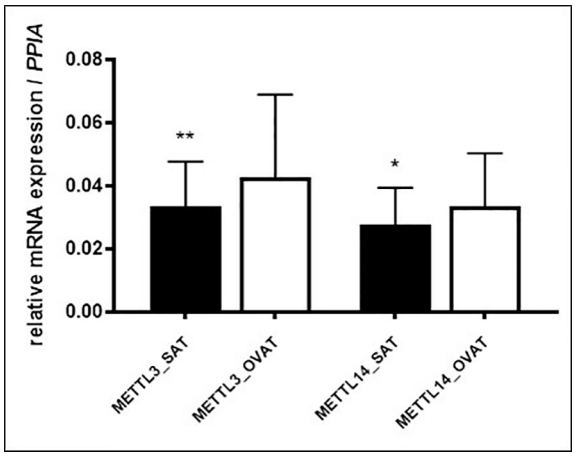

FIGURE 3 | m6A writers showing significant differential gene expression in SAT vs. OVAT (RT-qPCR validation). Differences in gene expression between SAT and OVAT measured by RT-qPCR. Relative expression values using *PPIA* as housekeeping gene. Data are presented as mean ± SD. *P*-values were calculated using Wilcoxon signed rank test in n=46 individuals. (*P < 0.05; **P < 0.01). OVAT, omental visceral adipose tissue; SAT, subcutaneous adipose tissue.

m6A Regulators in Adipose Tissue Correlate With Obesity and Clinical Variables

By comparing gene expression of m6A regulators in adipose tissue between individuals with obesity and lean controls, we identify several genes that associate with obesity in SAT and/or OVAT. These include the writers *WTAP* and *VIRMA*, the eraser *ALKBH5*, and genes encoding reader proteins such as *YTHDF1, YTHDF2* and *YTHDC1*. These results imply a relationship of gene expression with weight and prompted us to further test for a correlation with clinical variables related to obesity. We observed significant correlations with clinical parameters for *VIRMA, WTAP* and *ALKBH5*.

VIRMA, (also known as *KIAA1429*) encodes a subunit of the m6A methyltransferase complex and is together with WTAP, METTL3 and METTL14, required for its methyltransferase activity (33). VIRMA acts as a scaffolding protein, guiding region-selective methylation by recruiting the catalytic core components METTL3/METTL14/WTAP to stop codons and 3'UTR regions, influencing alternative polyadenylation and splicing (34). VIRMA is dysregulated in several cancer types, influencing cell proliferation in both a m6A-dependent and a m6A-independent manner (35). Interestingly, we find that gene expression of *VIRMA* associates with obesity both in SAT and OVAT showing lower expression in obesity. In line with this, expression of *VIRMA* negatively correlates with BMI both in SAT and VAT. Moreover, SAT expression of *VIRMA* is consistently negatively correlated with WHR, body fat percentage, adipocyte diameter and leptin levels, all being clinical variables related to fat distribution and obesity. Collectively, these data imply that altered levels of this writer complex subunit, which may contribute to altered m6A deposition, is involved in obesity. To our knowledge, so far nothing is known regarding VIRMA in the context of adipose tissue and metabolic dysfunction in obesity. Our results suggest a role for VIRMA in adipose tissue biology and metabolism, particularly in SAT, and further functional studies are required to investigate the role of this m6A writer in obesity.

WTAP is another main subunit of the m6A writer complex (36). In adipose tissue originating from omental visceral depots *WTAP* expression is higher among individuals with obesity. In line with this, we also find a positive correlation of *WTAP* expression in OVAT with BMI and waist circumference implying a depot-specific role in obesity. Indeed, *WTAP* is differentially expressed between the two depots. However, among the 5 probes available in our dataset such correlations were only found for one probe (ILMN_2279339). In support of our data, WTAP has been shown to have an essential role in adipogenic differentiation in mouse 3T3-L1 preadipocytes (17), and may be involved in adipose tissue dysfunction observed in morbidly obese individuals.

TABLE 4 | Differential gene expression of m6A writers, erasers and readers between SAT and OVAT measured by RT-qPCR.

Gene	N	SAT		OVAT		p-value
		Mean	SD of Mean	Mean	SD of Mean	
m6A writers						
METTL3	46	0.0333	0.01434	0.0427	0.02628	**0.001**
METTL14	46	0.0277	0.01165	0.0335	0.01681	**0.012**
WTAP	46	0.1485	0.12453	0.1218	0.07448	n.s
VIRMA	46	0.0527	0.02732	0.0542	0.02878	n.s
m6A erasers						
FTO	46	0.0705	0.0724	0.0769	0.07478	n.s
ALKBH5	46	0.0818	0.05545	0.0852	0.05669	n.s
m6A readers						
YTHDF1	46	0.0286	0.01545	0.0273	0.01374	n.s
YTHDF2	46	0.1382	0.16016	0.1298	0.11158	n.s
YTHDC1	46	0.0656	0.03214	0.0696	0.03237	n.s
IGF2BP2	46	0.0318	0.01897	0.0275	0.01739	n.s

P-values were calculated using Wilcoxon signed rank test for non-normally distributed variables. WHO classification: lean ≥18; <25 kg/m²; overweight ≥25; <30 kg/m²; obese≥ 30 kg/m²; SD, Standard deviation; SAT, Subcutaneous adipose tissue; OVAT, Omental visceral adipose tissue; n.s., not significant.
P-values < 0.05 are highlighted in bold.

TABLE 5 | Comparison of mean gene expression of m6A regulators between lean and obese in the Sorbs cohort.

Gene	Probe	N	Lean		Obese		p-value
		Lean/Obese	Mean	SD of Mean	Mean	SD of Mean	
m6A writers							
METTL3	ILMN_1655635	382/227	8.740326	0.3575872	8.73174	0.3787329	n.s
METTL14	ILMN_22124523	382/227	7.144649	0.2171319	7.14253	0.2632073	n.s
WTAP	1: ILMN_2279339	382/227	9.370565	0.2706417	9.33891	0.254263	n.s
	2: ILMN_2260725	382/227	6.527478	0.2282255	6.52325	0.2277159	n.s
	3: ILMN_2356559	382/227	6.881981	0.3160953	6.92075	0.312121	n.s
	4: ILMN_1734544	382/227	6.470573	0.2863549	6.46303	0.2961954	n.s
	5: ILMN_1657618	382/227	6.526426	0.2998339	6.47908	0.2864933	n.s
m6A erasers							
FTO	ILMN_2288070	382/227	7.49235	0.2440247	7.48991	0.2792386	n.s
ALKBH5	ILMN_1657283	382/227	12.00184	0.1602151	12.0582	0.1688926	**$5.80x10^{-5}$**
m6A readers							
YTHDF1	ILMN_1753885	382/227	9.568409	0.1794507	9.5409	0.1582593	**0.049**
YTHDF2	ILMN_1730658	382/227	9.570496	0.2648845	9.58526	0.2376172	n.s
YTHDF3	ILMN_1657470	382/226	8.548154	0.2412513	8.49755	0.1997413	**0.005**
YTHDC1	1: ILMN_1666111	382/227	6.836997	0.4142519	6.86563	0.4287415	n.s
	2: ILMN_1670878	382/227	5.974073	0.1735351	5.98633	0.1975569	n.s
	3: ILMN_1707506	382/227	11.429733	0.2175373	11.4067	0.222591	n.s
IGF2BP2	ILMN_1702447	382/227	8.156624	0.3614102	8.15192	0.3238712	n.s

P-values were calculated using independent t-test for normally distributed variables. WHO classification: lean ≥18; <25 kg/m²; overweight ≥25; <30 kg/m²; obese≥ 30 kg/m²; SD, Standard deviation; n.s., not significant. P-values < 0.05 are highlighted in bold.

ALKBH5 gene encodes one of the two known m6A demethylases and is reportedly involved in multiple biological mechanisms related to cancer such as proliferation (37) or metastasis (38). However, no direct role in metabolic diseases such as obesity is described so far. In adipose tissue, we find that subjects with obesity exhibit higher gene expression of *ALKBH5* in both fat depots compared to lean individuals. Further, expression in OVAT is positively correlated with subcutaneous fat area and negatively related to CT-ratio, both measures of fat distribution. These data imply a potential role of ALKBH5 in obesity and its clinical variables, which warrants further functional studies.

Collectively, our results add to and support previously published data from porcine models, demonstrating that m6A levels associate with fat mass and are involved in adipogenesis and lipid metabolism, suggesting a possible role for m6A writers in obesity (39). No significant relationship of gene expression of m6A regulators with T2D was observed in our data set.

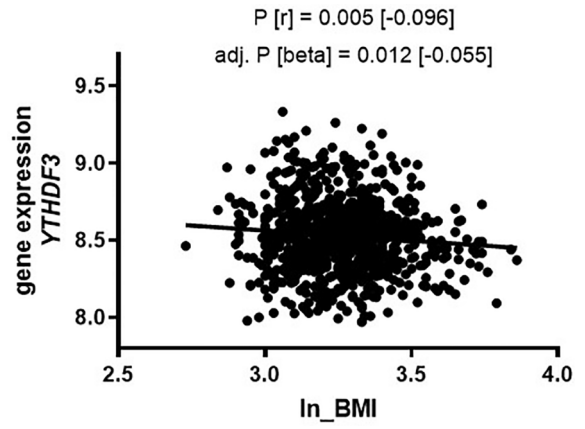

FIGURE 4 | Gene expression of *YTHDF3* (PBMCs) in the Sorbs cohort correlates with BMI. Correlation of gene expression with BMI in the Sorbs population in non-diabetic subjects (*N*=875). *P*-values were calculated by using bivariate Spearman correlation (top *P*-value) and linear regression analysis for ln_BMI adjusted for age and sex (bottom line). BMI, body mass index; Beta=non-standardized regression coefficient from linear regression; *P*=*P*-value, r=correlation coefficient from bivariate correlation.

Adipose Tissue Depot-Specific Gene Expression of Major m6A Regulators

By comparing gene expression data from intra-individually paired adipose tissue depots, we find that multiple m6A regulators are differentially expressed between SAT and OVAT. Particularly, genes encoding the m6A writers show depot specific expression, with significant differences in almost all examined target genes. *METTL3*, *WTAP* (two out of 5 probes: ILMN_2279339 and ILMN_1734544) and *VIRMA* are all differentially expressed between SAT and OVAT in the microarray dataset. Depot specific gene expression of *METTL3* was confirmed in another sample set of adipose tissue analyzed by RT-qPCR. Moreover, we find also for *METTL14* a higher expression in OVAT compared to SAT. Several studies have reported an important role for m6A writer proteins in adipogenesis. METTL3, METTL14 and WTAP have been shown to be required for adipogenesis in mouse pre-adipocytes regulating mitotic clonal expansion (17, 40). Contrary to these data, adipogenic differentiation of porcine bone marrow derived stem cells is inhibited *via* METTL3 (41). Although contradictory results have been reported, results point towards an important role of m6A writers in metabolic disease and in adipogenesis, a role that may be dependent on species, fat depot or on the

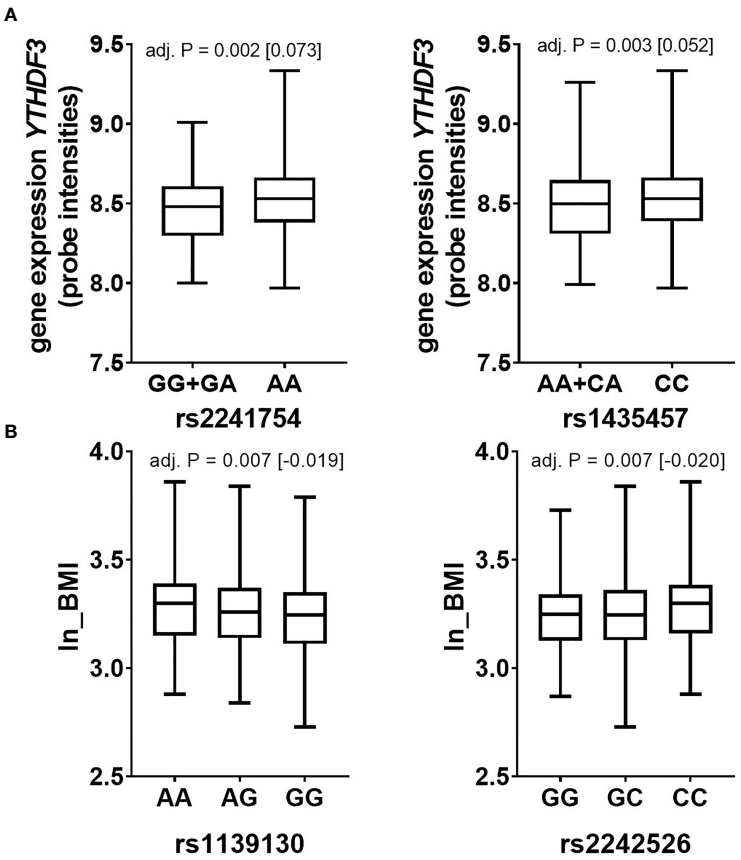

FIGURE 5 | Genetic variation in *YTHDF3* and *METTL3* associates with expression and BMI respectively (Sorbs cohort). Data are presented as boxplots with median and quartile distribution for SNPs in **(A)** *YTHDF3* and **(B)** *METTL3*. *P*-values were calculated by using linear regression analyses adjusted for age, sex and BMI (except for ln_BMI) by using an additive or dominant mode of inheritance. Numbers of subjects per SNP are as following: *METTL3*: rs1139130 AA=209, AG=390, GG=241; rs2242526 GG=151, GC=415, CC=274; *YTHDF3*: rs2241754 AA=733, GG+GA= 107; rs1435457 CC=586, AA+AC=254. *P*=*P*-value; BMI-body mass index.

cellular context. Moreover, expression of *METTL3*, *METTL14*, and *WTAP* was reported to be increased in blood from patients with type 2 diabetes (T2D) (42), whilst METTL3 was reported to increase hepatic lipid accumulation through YTHDF2 dependent stabilization of PPARα (43). No evidence for differential gene expression in adipose tissue of *VIRMA* was previously reported, and collectively, our data indicate that inter-depot specific gene expression of m6A writers is involved in obesity.

In addition to writers, we also identified depot specific expression of the m6A eraser *FTO*, with higher expression in SAT, in line with previously published data (32) and data from the Genotype-Tissue Expression (GTEx) consortium (https://gtexportal.org). FTO-dependent de-methylation is reported to be essential for adipogenic differentiation (21), suggesting that depot specific expression may be involved in the reduced adipogenic capacity of OVAT (44). Further, the reader *YTHDC1* is also differentially expressed between SAT and OVAT, showing differential expression in 2 out of 3 probes, however with different effect directions between the two probes (ILMN_1666111: higher expression in SAT, ILMN_1707506: higher expression in OVAT). As the probes target different transcripts of *YTHDC1*, these results may suggest that different transcript variants and alternative splicing of this gene may contribute to depot-specific differences. Further transcript variant specific studies are needed to validate potential depot specific expression of *YTHDC1* isoforms. YTHDC1 is located in the cell nucleus, where it is involved in the nuclear export of m6A modified mRNAs as well as in m6A guided regulation of chromatin organization (45, 46). Differential expression of *YTHDC1* may, therefore, potentially also influence chromatin organization in an adipose tissue depot-specific manner, adding another level of complexity to gene regulation by m6A.

Taken together, these results indicate a depot specific role of m6A regulators, potentially introducing inter-depot-specific variability in mRNA metabolism. Such variability may potentially impact on adipogenesis, adipose tissue expansion capacity or metabolism, reflected by its correlation with clinical variables. Whether the observed expression differences have such functional consequences, either by targeting specific transcripts in the different tissues or by inducing global differences in m6A deposition remains to be investigated.

The Role of m6A Regulators in Peripheral Blood Mononuclear Cells

In line with expression differences in adipose tissue between lean and obese individuals, we also found expression of m6A regulators associated with obesity in a dataset from PBMCs from the Sorbs population. In PBMCs, the eraser *ALKBH5* and the readers *YTHDF1* and *YTHDF3* associate with obesity. *ALKBH5* shows higher gene expression among individuals with obesity compared to lean subjects which is in line with our results from adipose tissue and thus, adding weight to a potential implication of *ALKBH5* in obesity. YTHDF3 is together with YTHDF1 and YTHDF2 a cytoplasmic reader protein facilitating transcript turnover and translation (47). In contrast to our data from adipose tissue, we do not find similar effect directions for these reader proteins in PBMCs. However, in line with an association with obesity, expression of *YTHDF3* is correlated to BMI. Altered gene expression of reader proteins in obesity may induce tissue specific functional consequences of m6A methylation and thus on RNA metabolism. However, no significant association of gene expression of any m6A regulator with T2D as a potential consequence of obesity was observed and functional studies are warranted to further evaluate potential biological consequences on RNA metabolism.

Taken together, these results show that expression of a number of m6A regulators is associated with obesity, both in adipose tissue and in PBMCs, suggesting that the m6A machinery is altered in obesity. However, what genes are affected appears to be tissue type dependent. Mapping of m6A modified transcripts and characterization of m6A readers and functional studies are required to further elucidate consequences of the observed differences.

Genetic Variation in m6A Regulators

METTL3 is differentially expressed between SAT and OVAT, whilst *YTHDF3* associates with obesity and BMI in blood. Thus, we then performed genetic analyses of these selected m6A regulators in the Sorbs. We observe a correlation of two SNP markers in the *YTHDF3* locus with its gene expression level suggesting that genetic variation underlying this reader protein may further impact on its potential role in obesity. However, no further relationships with any other clinical variables are observed and further genetic studies are needed to support or reject our results. Two SNP markers within the *METTL3* gene correlate with BMI implying that genetic variability in *METTL3* encoding the catalytic subunit of the m6A methyltransferase complex may influence clinical variables of obesity. No other clinical variables are related to the two SNPs. Our genetic data reveal a potential relationship of genetic variation in genes encoding m6A regulators with either clinical variables or gene expression. Whether such genetic variability impacts on the function of m6A regulators remains to be elucidated.

Limitations

This is to our knowledge the first study analyzing gene expression of m6A regulators in paired samples from different human adipose tissue depots. Further, to support our findings we have included another cohort for which both gene expression data from PBMCs and genetic data were available. Despite these strengths, we are well aware of several limitations at different aspects in our study. First, adipose tissue is a heterogeneous tissue consisting of many cell types other than adipocytes. We performed our analyses on whole adipose tissue and potential effects from cell type composition cannot be either excluded or estimated. No data are available to account for cell type differences or blood cell count by using bioinformatic approaches. Further studies measuring expression in purified adipocytes or performing single cell gene expression profiling are warranted to provide deeper insights into the contribution of different cell types in the tissue. Second, the cohorts used in this study are relatively small which may have led to false positive or false negative results. The effect sizes of the observed differences are small and further studies are required to elucidate whether results from this study are of biological significance. Therefore, the results presented here need to be interpreted with caution to avoid overestimating the observed effects.

Conclusion

Collectively, our data show that expression of m6A regulators is adipose tissue depot-specific and differentially related to clinical traits. We further show that several m6A regulators are associated with obesity. Taken together, these results point towards a potential role of m6A regulators in obesity and imply that expression of genes encoding writers, erasers and readers in adipose tissue may exert depot-specific effects on important pathways potentially related to adipogenesis or adipose tissue expansion. Genetic variation in m6A regulators adds an additional layer of variability to the functional consequences.

DATA AVAILABILITY STATEMENT

The original contributions presented in the study are included in the article/**Supplementary Material**. Further inquiries can be directed to the corresponding author.

ETHICS STATEMENT

The ethics committee of the University of Leipzig and the Regional Committee for Medical and Health Research Ethics for South Eastern Norway have approved all study protocols and written informed consents were collected from all study participants. The patients/participants provided their written informed consent to participate in this study.

AUTHOR CONTRIBUTIONS

TR performed data analysis, statistical work and contributed to the manuscript draft. MD performed RT-qPCR analyses. TV, AC, and MK have critically contributed to the discussion. AT is the PI of the Sorbs cohort. MB is the PI of the adipose tissue

cohort. YB initiated, conceived and designed the study, contributed to critical data discussion and wrote the final version of the manuscript. All authors contributed to the final manuscript by proof reading, editing and critical discussing the obtained results. All authors contributed to the article and approved the submitted version.

FUNDING

TR and AC are funded by Helse-SørØst grants to YB. Further support of this work came from the Kompetenznetz Adipositas to MB (Competence network for Obesity) funded by the Federal Ministry of Education and Research (German Obesity Biomaterial Bank; FKZ 01GI1128). A grant by the Deutsche Forschungsgemeinschaft for a Collaborative Research Center (CRC 1052/2) further supported this work: 'Obesity mechanisms' project number 20993838 - SFB1052 (to AT and MB).

ACKNOWLEDGEMENTS

The authors thank all individuals who participated in the study. We very much appreciate the help from Arne Klungland, who provided primers for a variety of m6A regulators as a gift. We further thank Lydia Hopp and Hans Binder (Interdisciplinary Centre for Bioinformatics, University of Leipzig) for pre-processing and analysis of the mRNA expression data (27). We are grateful to Arne Dietrich, Michael R. Schön, Daniel Gärtner, Tobias, Lohmann und Miriam Dreßler who contributed adipose tissue samples.

SUPPLEMENTARY MATERIAL

The Supplementary Material for this article can be found online at: https://www.frontiersin.org/articles/10.3389/fendo.2021.778875/full#supplementary-material

Supplementary Table 1 | Primer sequences used for RT-qPCR analyses.

Supplementary Figure 1 | Heatmap matrix of pairwise linkage disequilibrium. Heatmap matrix of pairwise linkage disequilibrium statistics (r2 and D') of SNP markers in **(A)** the *YTHDF3* locus and **(B)** the *METTL3* locus. The figure was created by using "LDlink – An interactive webtool for exploring linkage disequilibrium in population groups (https://ldlink.nci.nih.gov/?tab=ldmatrix provided by NIH, National Cancer Institute). Data are represented for Europeans (CEU; Utah residents from North and Western Europe).

Supplementary Figure 2 | Work flow and study design. Figure illustrates the stepwise study design.

REFERENCES

1. Blüher M. Obesity: Global Epidemiology and Pathogenesis. *Nat Rev Endocrinol* (2019) 15(5):288–98. doi: 10.1038/s41574-019-0176-8
2. Björntorp P. Metabolic Implications of Body Fat Distribution. *Diabetes Care* (1991) 14(12):1132–43. doi: 10.2337/diacare.14.12.1132
3. Snijder MB, Visser M, Dekker JM, Goodpaster BH, Harris TB, Kritchevsky SB, et al. Low Subcutaneous Thigh Fat is a Risk Factor for Unfavourable Glucose and Lipid Levels, Independently of High Abdominal Fat. *Health ABC Study Diabetologia* (2005) 48(2):301–8. doi: 10.1007/s00125-004-1637-7
4. Tran TT, Yamamoto Y, Gesta S, Kahn CR. Beneficial Effects of Subcutaneous Fat Transplantation on Metabolism. *Cell Metab* (2008) 7(5):410–20. doi: 10.1016/j.cmet.2008.04.004
5. Rohde K, Keller M, la Cour Poulsen L, Blüher M, Kovacs P, Böttcher Y. Genetics and Epigenetics in Obesity. *Metabolism: Clin Exp* (2019) 92:37–50. doi: 10.1016/j.metabol.2018.10.007
6. Boccaletto P, Machnicka MA, Purta E, Piatkowski P, Baginski B, Wirecki TK, et al. MODOMICS: A Database of RNA Modification Pathways. 2017 Update. *Nucleic Acids Res* (2018) 46(D1):D303–d7. doi: 10.1093/nar/gkx1030
7. Desrosiers R, Friderici K, Rottman F. Identification of Methylated Nucleosides in Messenger RNA From Novikoff Hepatoma Cells. *Proc Natl Acad Sci USA* (1974) 71(10):3971–5. doi: 10.1073/pnas.71.10.3971
8. Tuck MT. The Formation of Internal 6-Methyladenine Residues in Eucaryotic Messenger RNA. *Int J Biochem* (1992) 24(3):379–86. doi: 10.1016/0020-711X(92)90028-Y
9. Li Y, Wang J, Huang C, Shen M, Zhan H, Xu K. RNA N6-Methyladenosine: A Promising Molecular Target in Metabolic Diseases. *Cell Bioscience* (2020) 10:19. doi: 10.1186/s13578-020-00385-4
10. Chen XY, Zhang J, Zhu JS. The Role of M(6)A RNA Methylation in Human Cancer. *Mol Cancer* (2019) 18(1):103. doi: 10.1186/s12943-019-1033-z
11. Liu J, Yue Y, Han D, Wang X, Fu Y, Zhang L, et al. A METTL3-METTL14 Complex Mediates Mammalian Nuclear RNA N6-Adenosine Methylation. *Nat Chem Biol* (2014) 10(2):93–5. doi: 10.1038/nchembio.1432
12. Deng X, Su R, Weng H, Huang H, Li Z, Chen J. RNA N(6)-Methyladenosine Modification in Cancers: Current Status and Perspectives. *Cell Res* (2018) 28(5):507–17. doi: 10.1038/s41422-018-0034-6
13. Gerken T, Girard CA, Tung YC, Webby CJ, Saudek V, Hewitson KS, et al. The Obesity-Associated FTO Gene Encodes a 2-Oxoglutarate-Dependent Nucleic Acid Demethylase. *Sci (New York NY)* (2007) 318(5855):1469–72. doi: 10.1126/science.1151710
14. Shi H, Wei J, He C. Where, When, and How: Context-Dependent Functions of RNA Methylation Writers, Readers, and Erasers. *Mol Cell* (2019) 74(4):640–50. doi: 10.1016/j.molcel.2019.04.025
15. Chen X, Luo Y, Jia G, Liu G, Zhao H, Huang Z. FTO Promotes Adipogenesis Through Inhibition of the Wnt/β-Catenin Signaling Pathway in Porcine Intramuscular Preadipocytes. *Anim Biotechnol* (2017) 28(4):268–74. doi: 10.1080/10495398.2016.1273835
16. De Jesus DF, Zhang Z, Kahraman S, Brown NK, Chen M, Hu J, et al. M(6)A mRNA Methylation Regulates Human β-Cell Biology in Physiological States and in Type 2 Diabetes. *Nat Metab* (2019) 1(8):765–74. doi: 10.1038/s42255-019-0089-9
17. Kobayashi M, Ohsugi M, Sasako T, Awazawa M, Umehara T, Iwane A, et al. The RNA Methyltransferase Complex of WTAP, METTL3, and METTL14 Regulates Mitotic Clonal Expansion in Adipogenesis. *Mol Cell Biol* (2018) 38(16). doi: 10.1128/MCB.00116-18
18. Xie W, Ma LL, Xu YQ, Wang BH, Li SM. METTL3 Inhibits Hepatic Insulin Sensitivity *via* N6-Methyladenosine Modification of Fasn mRNA and Promoting Fatty Acid Metabolism. *Biochem Biophys Res Commun* (2019) 518(1):120–6. doi: 10.1016/j.bbrc.2019.08.018
19. Frayling TM, Timpson NJ, Weedon MN, Zeggini E, Freathy RM, Lindgren CM, et al. A Common Variant in the FTO Gene is Associated With Body Mass Index and Predisposes to Childhood and Adult Obesity. *Sci (New York NY)* (2007) 316(5826):889–94. doi: 10.1126/science.1141634
20. Locke AE, Kahali B, Berndt SI, Justice AE, Pers TH, Day FR, et al. Genetic Studies of Body Mass Index Yield New Insights for Obesity Biology. *Nature* (2015) 518(7538):197–206. doi: 10.1038/nature14177
21. Zhao X, Yang Y, Sun BF, Shi Y, Yang X, Xiao W, et al. FTO-Dependent Demethylation of N6-Methyladenosine Regulates mRNA Splicing and is Required for Adipogenesis. *Cell Res* (2014) 24(12):1403–19. doi: 10.1038/cr.2014.151
22. Jiang Q, Sun B, Liu Q, Cai M, Wu R, Wang F, et al. MTCH2 Promotes Adipogenesis in Intramuscular Preadipocytes *via* an M(6)A-YTHDF1-

Dependent Mechanism. *FASEB J Off Publ Fed Am Societies Exp Biol* (2019) 33 (2):2971–81. doi: 10.1096/fj.201801393RRR
23. Wu R, Wang X. Epigenetic Regulation of Adipose Tissue Expansion and Adipogenesis by N(6) -Methyladenosine. *Obes Rev an Off J Int Assoc Study Obes* (2021) 22(2):e13124. doi: 10.1111/obr.13124
24. Zhang GH, Lu JX, Chen Y, Zhao YQ, Guo PH, Yang JT, et al. Comparison of the Adipogenesis in Intramuscular and Subcutaneous Adipocytes From Bamei and Landrace Pigs. *Biochem Cell Biol = Biochimie Biologie Cellulaire* (2014) 92 (4):259–67. doi: 10.1139/bcb-2014-0019
25. Keller M, Hopp L, Liu X, Wohland T, Rohde K, Cancello R, et al. Genome-Wide DNA Promoter Methylation and Transcriptome Analysis in Human Adipose Tissue Unravels Novel Candidate Genes for Obesity. *Mol Metab* (2017) 6(1):86–100. doi: 10.1016/j.molmet.2016.11.003
26. Klöting N, Fasshauer M, Dietrich A, Kovacs P, Schön MR, Kern M, et al. Insulin-Sensitive Obesity. *Am J Physiol Endocrinol Metab* (2010) 299(3): E506–15. doi: 10.1152/ajpendo.00586.2009
27. Rohde K, Keller M, la Cour Poulsen L, Rønningen T, Stumvoll M, Tönjes A, et al. (Epi)genetic Regulation of CRTC1 in Human Eating Behaviour and Fat Distribution. *EBioMedicine* (2019) 44:476–88. doi: 10.1016/j.ebiom.2019.05.050
28. Veeramah KR, Tönjes A, Kovacs P, Gross A, Wegmann D, Geary P, et al. Genetic Variation in the Sorbs of Eastern Germany in the Context of Broader European Genetic Diversity. *Eur J Hum Genet EJHG* (2011) 19(9):995–1001. doi: 10.1038/ejhg.2011.65
29. Tönjes A, Scholz M, Breitfeld J, Marzi C, Grallert H, Gross A, et al. Genome Wide Meta-Analysis Highlights the Role of Genetic Variation in RARRES2 in the Regulation of Circulating Serum Chemerin. *PloS Genet* (2014) 10(12): e1004854. doi: 10.1371/journal.pgen.1004854
30. Löffler-Wirth H, Kalcher M, Binder H. oposSOM: R-Package for High-Dimensional Portraying of Genome-Wide Expression Landscapes on Bioconductor. *Bioinf (Oxford England)* (2015) 31(19):3225–7. doi: 10.1093/bioinformatics/btv342
31. Tönjes A, Koriath M, Schleinitz D, Dietrich K, Böttcher Y, Rayner NW, et al. Genetic Variation in GPR133 is Associated With Height: Genome Wide Association Study in the Self-Contained Population of Sorbs. *Hum Mol Genet* (2009) 18(23):4662–8. doi: 10.1093/hmg/ddp423
32. Klöting N, Schleinitz D, Ruschke K, Berndt J, Fasshauer M, Tönjes A, et al. Inverse Relationship Between Obesity and FTO Gene Expression in Visceral Adipose Tissue in Humans. *Diabetologia* (2008) 51(4):641–7. doi: 10.1007/s00125-008-0928-9
33. Schwartz S, Mumbach MR, Jovanovic M, Wang T, Maciag K, Bushkin GG, et al. Perturbation of M6a Writers Reveals Two Distinct Classes of mRNA Methylation at Internal and 5' Sites. *Cell Rep* (2014) 8(1):284–96. doi: 10.1016/j.celrep.2014.05.048
34. Yue Y, Liu J, Cui X, Cao J, Luo G, Zhang Z, et al. VIRMA Mediates Preferential M(6)A mRNA Methylation in 3'UTR and Near Stop Codon and Associates With Alternative Polyadenylation. *Cell Discov* (2018) 4:10. doi: 10.1038/s41421-018-0019-0
35. Zhu W, Wang JZ, Wei JF, Lu C. Role of M6a Methyltransferase Component VIRMA in Multiple Human Cancers (Review). *Cancer Cell Int* (2021) 21 (1):172. doi: 10.1186/s12935-021-01868-1
36. Ping XL, Sun BF, Wang L, Xiao W, Yang X, Wang WJ, et al. Mammalian WTAP is a Regulatory Subunit of the RNA N6-Methyladenosine Methyltransferase. *Cell Res* (2014) 24(2):177–89. doi: 10.1038/cr.2014.3
37. Chao Y, Shang J, Ji W. ALKBH5-M(6)A-FOXM1 Signaling Axis Promotes Proliferation and Invasion of Lung Adenocarcinoma Cells Under Intermittent Hypoxia. *Biochem Biophys Res Commun* (2020) 521(2):499–506. doi: 10.1016/j.bbrc.2019.10.145
38. Li XC, Jin F, Wang BY, Yin XJ, Hong W, Tian FJ. The M6a Demethylase ALKBH5 Controls Trophoblast Invasion at the Maternal-Fetal Interface by Regulating the Stability of CYR61 mRNA. *Theranostics* (2019) 9(13):3853–65. doi: 10.7150/thno.31868
39. Wang X, Sun B, Jiang Q, Wu R, Cai M, Yao Y, et al. mRNA M(6)A Plays Opposite Role in Regulating UCP2 and PNPLA2 Protein Expression in Adipocytes. *Int J Obes* (2018) 42(11):1912–24. doi: 10.1038/s41366-018-0027-z
40. Liu Q, Zhao Y, Wu R, Jiang Q, Cai M, Bi Z, et al. ZFP217 Regulates Adipogenesis by Controlling Mitotic Clonal Expansion in a METTL3-M(6) A Dependent Manner. *RNA Biol* (2019) 16(12):1785–93. doi: 10.1080/15476286.2019.1658508
41. Yao Y, Bi Z, Wu R, Zhao Y, Liu Y, Liu Q, et al. METTL3 Inhibits BMSC Adipogenic Differentiation by Targeting the JAK1/STAT5/C/EBPbeta Pathway *via* an M(6)A-YTHDF2-Dependent Manner. *FASEB J* (2019) 33 (6):7529–44. doi: 10.1096/fj.201802644R
42. Yang Y, Shen F, Huang W, Qin S, Huang JT, Sergi C, et al. Glucose is Involved in the Dynamic Regulation of M6a in Patients With Type 2 Diabetes. *J Clin Endocrinol Metab* (2018) 14(3):665–73. doi: 10.1210/jc.2018-00619
43. Zhong X, Yu J, Frazier K, Weng X, Li Y, Cham CM, et al. Circadian Clock Regulation of Hepatic Lipid Metabolism by Modulation of M(6)A mRNA Methylation. *Cell Rep* (2018) 25(7):1816–28.e4. doi: 10.1016/j.celrep.2018.10.068
44. Porro S, Genchi VA, Cignarelli A, Natalicchio A, Laviola L, Giorgino F, et al. Dysmetabolic Adipose Tissue in Obesity: Morphological and Functional Characteristics of Adipose Stem Cells and Mature Adipocytes in Healthy and Unhealthy Obese Subjects. *J Endocrinological Invest* (2021) 44(5):921–41. doi: 10.1007/s40618-020-01446-8
45. Li Y, Xia L, Tan K, Ye X, Zuo Z, Li M, et al. N(6)-Methyladenosine Co-Transcriptionally Directs the Demethylation of Histone H3k9me2. *Nat Genet* (2020) 52(9):870–7. doi: 10.1038/s41588-020-0677-3
46. Roundtree IA, Luo GZ, Zhang Z, Wang X, Zhou T, Cui Y, et al. YTHDC1 Mediates Nuclear Export of N(6)-Methyladenosine Methylated mRNAs. *Elife* (2017) 6. doi: 10.7554/eLife.31311
47. Shi H, Wang X, Lu Z, Zhao BS, Ma H, Hsu PJ, et al. YTHDF3 Facilitates Translation and Decay of N(6)-Methyladenosine-Modified RNA. *Cell Res* (2017) 27(3):315–28. doi: 10.1038/cr.2017.15

Conflict of Interest: The authors declare that the research was conducted in the absence of any commercial or financial relationships that could be construed as a potential conflict of interest.

Publisher's Note: All claims expressed in this article are solely those of the authors and do not necessarily represent those of their affiliated organizations, or those of the publisher, the editors and the reviewers. Any product that may be evaluated in this article, or claim that may be made by its manufacturer, is not guaranteed or endorsed by the publisher.

frontiers in Endocrinology

MINI REVIEW
published: 29 March 2022
doi: 10.3389/fendo.2022.859044

Immune Cell Regulation of White Adipose Progenitor Cell Fate

Irem Altun[1,2†], *Xiaocheng Yan*[1,2†] *and Siegfried Ussar*[1,2,3*]

[1] Research Group Adipocytes and Metabolism, Institute for Diabetes and Obesity, Helmholtz Diabetes Center, Helmholtz Zentrum München, German Research Center for Environmental Health GmbH, Neuherberg, Germany, [2] German Center for Diabetes Research (DZD), Neuherberg, Germany, [3] Department of Medicine, Technische Universität München, Munich, Germany

Adipose tissue is essential for energy storage and endocrine regulation of metabolism. Imbalance in energy intake and expenditure result in obesity causing adipose tissue dysfunction. This alters cellular composition of the stromal cell populations and their function. Moreover, the individual cellular composition of each adipose tissue depot, regulated by environmental factors and genetics, determines the ability of the depots to expand and maintain its endocrine and storage function. Thus, stromal cells modulate adipocyte function and vice versa. In this mini-review we discuss heterogeneity in terms of composition and fate of adipose progenitor subtypes and their interactions with and regulation by different immune cell populations. Immune cells are the most diverse cell populations in adipose tissue and play essential roles in regulating adipose tissue function *via* interaction with adipocytes but also with adipocyte progenitors. We specifically discuss the role of macrophages, mast cells, innate lymphoid cells and T cells in the regulation of adipocyte progenitor proliferation, differentiation and lineage commitment. Understanding the factors and cellular interactions regulating preadipocyte expansion and fate decision will allow the identification of novel mechanisms and therapeutic strategies to promote healthy adipose tissue expansion without systemic metabolic impairment.

Keywords: preadipocyte, immune cells, proliferation, differentiation, adipose tissue expansion, obesity, adipose precursor cells

OPEN ACCESS

Edited by:
Matthias Blüher,
Leipzig University, Germany

Reviewed by:
Zoi Michailidou,
University of Edinburgh, United Kingdom
Assaf Rudich,
Ben-Gurion University of the Negev, Israel

***Correspondence:**
Siegfried Ussar
Siegfried.ussar@helmholtz-munich.de

[†]These authors have contributed equally to this work and share first authorship

Specialty section:
This article was submitted to Obesity, a section of the journal Frontiers in Endocrinology

Received: *20 January 2022*
Accepted: *28 February 2022*
Published: *29 March 2022*

Citation:
Altun I, Yan X and Ussar S (2022) Immune Cell Regulation of White Adipose Progenitor Cell Fate. Front. Endocrinol. 13:859044. doi: 10.3389/fendo.2022.859044

INTRODUCTION

White adipose tissue (WAT) is an important endocrine organ playing a key role in energy homeostasis and insulin action (1–4). Therefore, its development and expansion is crucial to establish and maintain a functional metabolism. However, excessive fat accumulation results in obesity, predisposing most people to the development of insulin resistance and the metabolic syndrome. A gain in fat mass results in various changes in adipose depots including remodeling of the extracellular matrix (ECM), recruitment and activation of immune cells, upregulation of pro-inflammatory cytokines and changes in adipogenesis and adipocyte function (5). However, a number of studies described a metabolically healthy obese (MHO) phenotype (6–9). One characteristic of these subjects is that in contrast to metabolically unhealthy obesity (MUO), these individuals accumulate fat preferentially in the subcutaneous rather than visceral depots. Despite their adiposity MHO individuals are insulin sensitive, glucose tolerant and do not display

ectopic lipid accumulation in organs such as the liver or skeletal muscle (7, 8). The underlying mechanisms and temporal stability of healthy adipose tissue expansion are still incompletely understood. However, it appears that there are principle mechanisms available allowing the metabolically safe storage of very large quantities of energy in adipose tissue without impairing adipose or systemic metabolic function. Various genetic polymorphisms, altering adipocyte function, could contribute to the MHO phenotype (10, 11). Differences in the preadipocyte pool, its size, composition and proliferative capacity as well as the interaction with other cells of the stromal compartment, especially the diverse immune cell populations could also play an important role in the MHO phenotype. However, these interactions in regulation of healthy adipose tissue expansion are less understood. In addition to white adipose tissue function, differences in brown fat function could also play a role in MHO. Brown adipocytes, in contrast to white adipocytes, do not act as site of energy storage, but rather dissipate energy to produce heat through UCP-1 mediated mitochondrial uncoupling (12, 13). Others and we have identified heterogeneity within murine brown adipocyte progenitors and brown adipocytes modulating overall brown fat activity and systemic metabolism (14, 15). Thus, inter-individual differences in brown adipocyte composition could also modulate the physiological response to weight gain. Moreover, the role of beige adipocytes, which refers to brown adipocyte-like cells within white adipose tissue depots, has also not been extensively studied in the context of MHO. However, in this review we will focus on factors and cell populations that regulate the fate of white adipose progenitor cells (APCs), preadipocytes and tissue homeostasis with a main focus on immune cells.

ADIPOSE TISSUE DURING DEVELOPMENT AND OBESITY

In humans, white adipose tissue starts to develop around 14 weeks of gestation as mesenchymal lobules that differentiate into primitive fat lobules. This is initiated by mesenchymal cell condensation resulting in the development of a capillary network and vascularization, followed by the proliferation of preadipocytes and formation of definitive fat lobules, which can be observed before week 28. The number of fat lobules is determined by week 23, while the size continuous to increase until week 29 (16, 17). In mice, subcutaneous white adipose tissue (sWAT) develops prenatally, starting between E14 and E18, while visceral white adipose tissue (vWAT) develops starting at P1 (18). In humans, the total number of adipocytes increases during childhood and adolescence, reaching a constant number at around 20 years of age, irrespective of the overall fat mass stored in a person. This indicates that inter-individual differences in adipocyte numbers are defined early in life and not by weight gain in adulthood (19, 20). However, obesity can also increase the estimated number of adipocytes, albeit it remains unclear how the subjects in this study differ from those in other studies that have not observed this increase in adipocyte numbers in adulthood (21).

Regardless, turnover of adipocytes and progenitor proliferation appear much more dynamic. In mice, around 5% of preadipocytes replicate and 1-5% of adipocytes are replaced per day. In humans the annual adipocyte turnover is around 10% (19, 22). Thus, adipocyte death, *de novo* differentiation and proliferation of adipocyte progenitors need to be tightly regulated to maintain a constant adipocyte number throughout life. Moreover, species differences in turnover of adipocytes and adipocyte progenitor proliferation should be considered when translating murine research data to humans. This is especially true for any therapeutic strategies aiming to increase the number of thermogenic beige adipocytes in WAT through *de novo* differentiation or promoting hyperplasia over hypertrophy.

In addition, obese individuals generate a higher number of new adipocytes every year compared to lean individuals. Conversely, significant body fat loss can also induce proliferation of adipocyte progenitor cells, as this was observed following bariatric surgery (19, 21). Thus, both weight gain and loss can have effects on the adipocyte progenitor pool. In mice, two weeks of high fat diet (HFD) feeding increased the proliferation of preadipocytes in visceral adipose tissue either compared to mice fed a chow diet (CD) or switched to a CD from a HFD (23). This effect was lost after 7 weeks of HFD feeding. However, prolonged HFD feeding increased the number of *de novo* differentiated adipocytes. Thus, there are complex interactions between a hypercaloric state requiring additional storage of energy in fat, progenitor expansion, and adipose tissue growth by either increasing the number of adipocytes (hyperplasia) or increasing adipocyte size (hypertrophy) (19, 24).

Expansion of adipose tissue through an increase in adipocyte number requires regulated proliferation of the adipocyte progenitor population to prevent progenitor exhaustion enabling continued adipogenesis throughout life. Thus, a variety of cell types, such as immune, endothelial and nerve cells interact with different subpopulations of APCs and preadipocytes to regulate adipose tissue function and growth, as well as homeostasis of the preadipocyte pool.

HETEROGENEITY AND HIERARCHY IN ADIPOSE PROGENITOR CELLS

The definition of what exactly is an adipocyte progenitor cell is often unclear. As previously discussed, various cell types, such as mesenchymal stem cell, pericytes, endothelial cells and others can give rise to adipocytes (5). Moreover, advances in genetic lineage tracing and single cell technologies have identified intermediate states and distinct adipocyte progenitor lineages, giving rise to distinct adipocyte subpopulations (25–27). Following the definitions suggested by Sakers et al., we use the term preadipocytes to refer to cells with the general ability to differentiate into adipocytes (25). In addition, we distinguish,

where possible, APCs that have a higher proliferative capacity, stem like properties and are able to maintain the progenitor niche in the tissue. In the following sections, we use the more general term preadipocytes whenever it is unclear if APCs or preadipocytes were studied.

Analysis of the stromal vascular fraction (SVF) from WAT identified adipocyte progenitor populations that are Lin^{-}:$CD34^{+}$:$CD29^{+}$:Sca-1^{+}:$CD24^{+}$ ($CD24^{+}$) or Lin^{-}:$CD34^{+}$:$CD29^{+}$:Sca-1^{+}:$CD24^{-}$ ($CD24^{-}$), which was confirmed using PDGFRα-cre dependent reporter mice. Around 53% of the stromal vascular cells are $CD24^{-}$ preadipocytes, while only 0.08% were $CD24^{+}$ APCs. These studies established a principle hierarchy where CD24 expressing APCs give rise to committed $CD24^{-}$ preadipocytes (**Figure 1**) (28, 29). Moreover, transplantation of $CD24^{+}$ APCs but not $CD24^{-}$ preadipocytes into A-zip lipodystrophic mice were able to form a complete functional WAT, demonstrating the role of APCs in regulating stromal interactions and tissue homeostasis. Moreover, Jiang et al. described differences in *'developmental'* and *'adult'* APCs, regulating adipose tissue development and maintenance, respectively (30). PDGFRα^{+} stromal cells are necessary for tissue formation and adipose tissue (AT) expansion during tissue development, whereas other APC populations contributed to adipocyte turnover and tissue homeostasis during adulthood (31). Additional studies identified further subtypes within the PDGFRα^{+} cell population, based on the

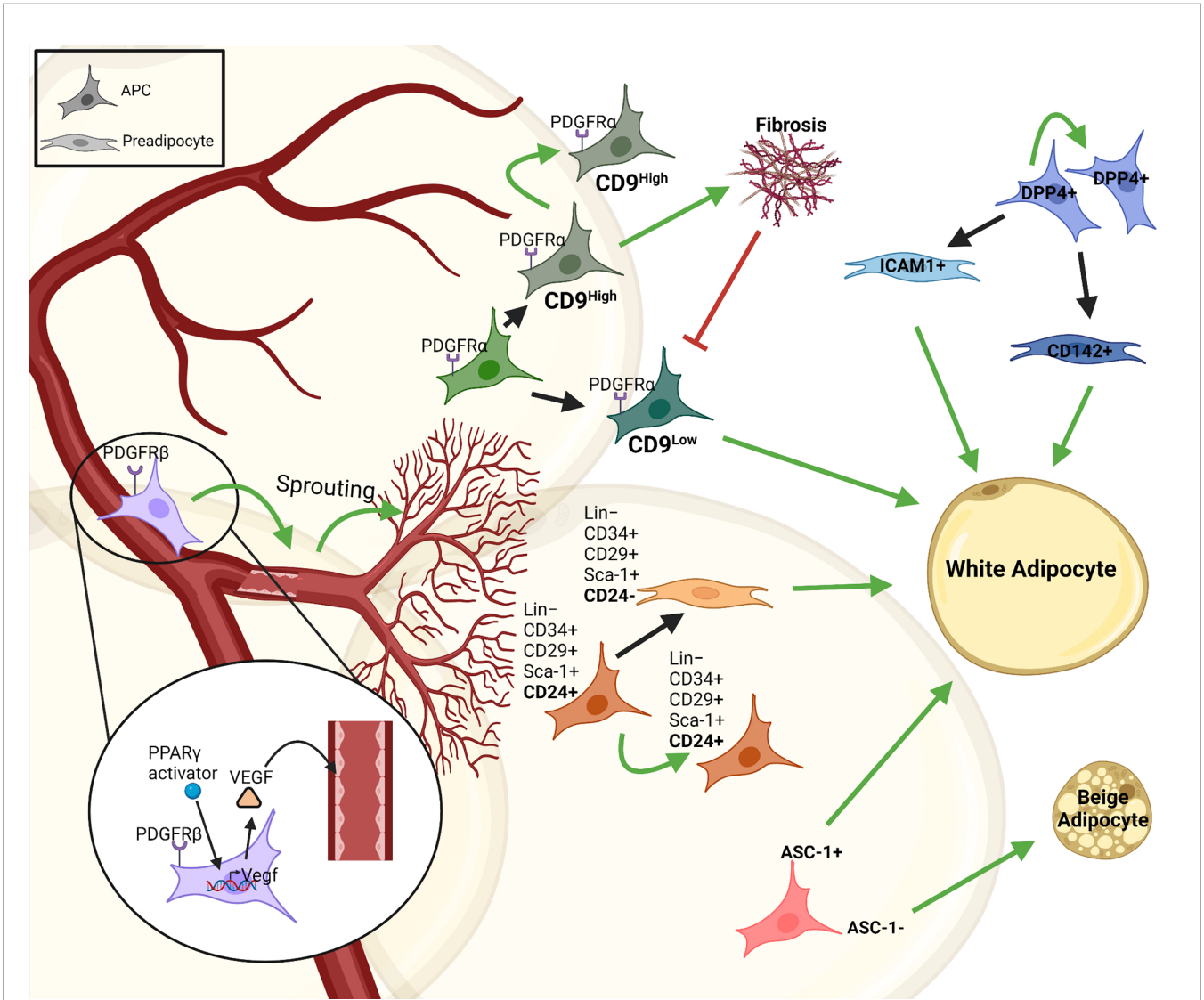

FIGURE 1 | Heterogeneity and interactions of adipose progenitor cells. There are different subtypes of APCs with self-renewal properties in adipose tissue that give rise to various subpopulations of committed preadipocytes (e.g. $CD24^{-}$, $ICAM1^{+}$ or $CD142^{+}$ cells). This proliferative/self-renewal capacity is represented by a green arrow that give rise to the same cell type. Some of these progenitors generate preadipocytes that differentiate into white adipocytes, such as; $ASC1^{+}$, $CD24^{+}$, $DPP4^{+}$, while some are responsible for vascular-APC interaction including PDGFRβ^{+}PPARγ^{+}, others contribute to fibrosis in the tissue like PDGFRα^{+}CD9^{high} cells and some like ASC-1^{-} cells give rise to beige adipocytes. The figure was generated using BioRender.com.

effects of PDGFRα signaling to induce fibrosis (32). PDGFRα$^+$ CD9^{high} cells were proliferative and induced fibrosis, whereas PDGFRα$^+$ CD9^{low} cells showed an upregulation in pro-adipogenic transcription factors (**Figure 1**). However, PDGFRα$^+$ CD9^{low} cells almost completely disappeared with AT fibrosis upon HFD feeding (33). Recently, a highly proliferative dipeptidyl peptidase-4 (DPP4)$^+$ APC population was identified that gives rise to highly adipogenic ICAM1$^+$ preadipocytes as well as a CD142$^+$ adipogenic cell population, which was further studied by DPP4-Cre mediated lineage tracing experiments (**Figure 1**) (26, 34). Moreover, various other cell surface molecules have been described to distinguish APC and preadipocyte populations and we recently showed that the amino acid transporter ASC-1 regulates the commitment of APCs to become either white or beige adipocytes (35, 36). These findings highlight the heterogeneity within adipose progenitors that gives rise to different subsets of committed preadipocytes in AT. It is important to understand the complexity and diversity that is created by these subpopulation of cells to understand the mechanisms underlying tissue homeostasis and expansion. Moreover, these cells also interact with and are regulated by other cell types, especially immune cells, resident in AT.

INTERACTION OF PREADIPOCYTES WITH OTHER STROMAL CELLS

The nervous-endocrine-immune system is an integrated regulatory network playing an essential role in maintaining homeostasis of the organism, including the adipose tissue (37, 38). The vasculature and neurons supply the adipose tissue with essential inputs such as nutrients, growth factors and signals from the autonomic nervous system. Thus, it is not surprising that in addition to adipocytes also APCs and preadipocytes continuously interact with other stromal cell types to regulate their function. APCs interact with endothelial cells through PPARγ mediated expression of VEGF, inducing vascular sprouting (**Figure 1**). This explains the perivascular localization of APCs (39). APCs also express PDGFRβ regulating APC-vascular niche interactions. These interactions are reciprocal as APCs are essential for vascular expansion, while vascular sprouting is essential for APC maintenance and differentiation. Most importantly, however, these interactions are necessary for adipogenesis and AT expansion (39).

In addition to the systemic inputs, immune cells modulate adipocyte function, as well as preadipocyte proliferation and differentiation either directly or indirectly (40–43). Many studies described adverse effects of chronic inflammation during obesity associated adipose tissue expansion (44). However, local inflammation is also, to some extent, necessary for healthy adipose tissue expansion and the MHO phenotype. Inhibition of pro-inflammatory pathways impairs adipogenesis, leading to ectopic lipid accumulation and systemic glucose intolerance (45, 46). The underlying mechanisms are still incompletely understood, but immune cell mediated reconfiguration of the ECM is certainly important for adipose tissue expansion. Moreover, the integration of various hormones and cytokines, in addition to nutritional cues, regulate processes of progenitor quiescence, proliferation and differentiation. To this end, we discuss some of the key regulatory inputs of different immune cell types on preadipocyte proliferation, differentiation and lineage (white versus beige adipocyte) commitment.

Macrophages

Macrophages are abundantly present and extensively studied in adipose tissue (47, 48). They play an important role in tissue homeostasis and hypertrophy induced adipose tissue inflammation and the initiation of local and systemic insulin resistance (49, 50). In general, accumulation of macrophages in adipose tissue is associated with insulin resistance and MUO (51). More recently, this was further refined as specific macrophage subtypes in visceral adipose tissue were found to be increased in diabetic obese compared to non-diabetic obese subjects (52). Previously, based on *in vitro* data, macrophages in adipose tissue were categorized as either M1 or M2. M1 macrophages originate from the stimulation with lipopolysaccharide (LPS), interferon (IFN)-γ or TNF-α, mediating pro-inflammatory actions by producing TNF-α, IL-6, IL-1β and nitric oxide (NO). M2 macrophages originate from the stimulation with IL-4, IL-10, IL-13, showing an anti-inflammatory phenotype by producing IL-4 and IL-10 (**Figure 2**) (53, 54). However, albeit widely used, the M1/M2 classification was recently challenged (55). Thus, previous *in vitro* data might not directly translate to the role of macrophages in adipose tissue *in vivo*. scRNAseq analysis of human white adipose tissues identified resident macrophages with an M1/M2-like phenotype. In contrast to the classical description of macrophages in *in vitro* studies, these subtypes were referred to as perivascular, inflammatory and lipid-associated macrophages. However, the interaction of these macrophage subtypes on progenitor cell fate has not been studied (47, 48, 52). Nevertheless, macrophages regulate tissue function through modulating preadipocyte expansion and commitment.

Relatively little is known on the role of macrophages and their secretome in regulating preadipocyte proliferation. Lacasa et al. used macrophage conditioned medium derived from *in vitro* differentiated blood monocytes of overweight patients. They showed increased proliferation but reduced differentiation of preadipocytes from non-obese donors when treated with the conditioned medium (56). Conversely, another human study found reduced preadipocyte proliferation when preadipocytes were exposed to macrophage conditioned media, which could be improved by antioxidant treatment (57). The discrepancy could be based on the different source of macrophages, as well as the physiologic and genetic background of the donors. A more detailed analysis of the impact of individual macrophage subtypes on preadipocytes is required to uncover the context specific role of macrophages on preadipocyte fate in humans.

Proliferation and differentiation are tightly linked with each other, as cell cycle exit is a prerequisite for adipocyte differentiation. Human and murine studies showed that M1

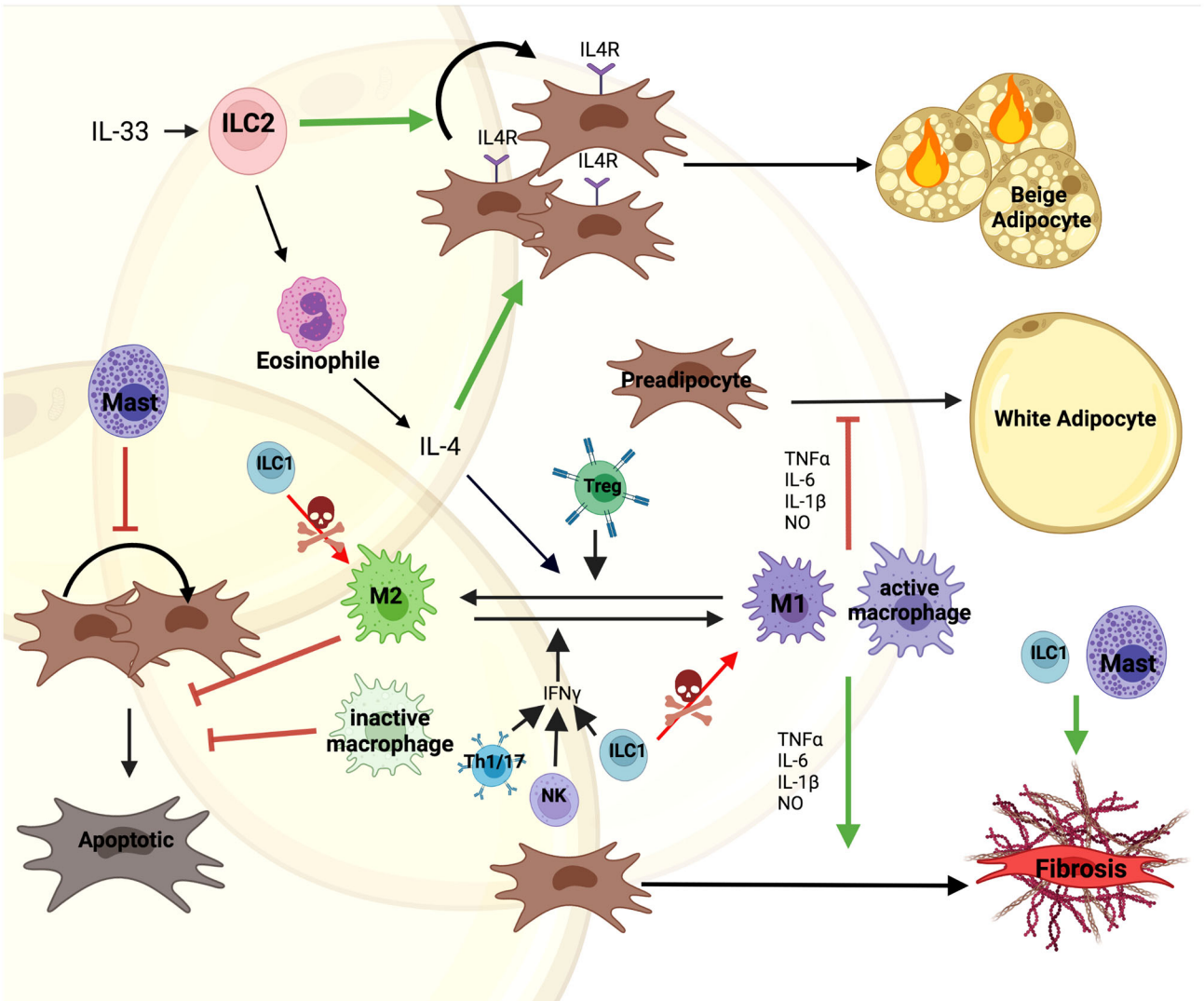

FIGURE 2 | Direct and indirect interactions of immune cell with preadipocytes. Immune cells are one of the most diverse cell types constituting the microenvironment of AT. IL-33 mediated Type 2 Innate Lymphoid Cell (ILC2) activation induces secretion of IL-4 by eosinophils. This promotes both proliferation of IL4R expressing preadipocytes and their differentiation into beige adipocytes. Moreover, IL-4 along with Tregs promotes M1 to M2 macrophage polarization supporting M2 controlled survival of preadipocytes. On the other hand, Th1/17, Type 1 Innate Lymphoid Cells (ILC1) and Natural Killer (NK) cells secrete IFN-γ stimulating macrophage to polarize to the M1 phenotype, secreting pro-inflammatory factors, such as; TNFα, IL-6, IL-1β and nitric oxide (NO). This inhibits preadipocyte differentiation into white adipocytes and together with Mast cells induces a fibrotic phenotype. Mast cells also block proliferation of preadipocytes. Additionally, ILC1s kill macrophages and induce fibrosis in the tissue. The figure was generated using BioRender.com.

macrophages, the pro-inflammatory or classically activated macrophages, secrete factors inhibiting preadipocyte differentiation (56, 58, 59). The inhibitory effect was further confirmed by culturing $CD14^+$ macrophages with preadipocytes of obese individuals, mediated by IKKβ/NF-κB signaling (60, 61). The block in differentiation was due to an impairment in the clonal expansion phase by inhibiting expression of cell cycle proteins such as; cyclin A, cyclin-dependent kinase 2, retinoblastoma protein, etc. (62, 63). Moreover, M1, pro-inflammatory macrophages promote preadipocytes to acquire a fibrotic phenotype, which is mediated through cytokines such as; TNF-α, IL-6 and IL-1β (**Figure 2**). This contributes to increased inflammation and tissue fibrosis impairing adipogenesis in both human and mice (56, 61, 64–66). However, these negative effects on preadipocyte differentiation were improved by growth hormone down-regulating IL-1β in macrophages (67).

Jang et al. compared high fat diet fed wild type to iNOS knockout mice and demonstrated that M1 macrophages produce nitric oxide impairing mitochondrial function by suppressing PGC1α expression. This inhibited adipocyte differentiation and

promoted conversion of preadipocytes to a fibrotic phenotype (68). Furthermore, macrophages secrete the apoptosis inhibitor of macrophage, which also inhibited adipogenesis (69). In addition to proliferation and differentiation, maintenance and survival of existing preadipocytes is also controlled by macrophages, as macrophage conditioned medium promoted preadipocyte survival in a PDGF-dependent manner, which strongly stimulates PI3K-Akt and MEK-ERK1/2 pathways (70, 71). This effect was observed in M2 macrophages, activated by IL-4, but not activated M1 macrophages (72). Thus, the activation state of macrophages can have profound effects on preadipocyte survival, proliferation and differentiation and thereby shape the ability of the organism to store surplus energy in the future.

Mast Cells

Mast cells (MCs) are tissue resident cells of the innate immune system that accumulate in adipose tissue with obesity (73). As previously reviewed, MC recruitment and activation has pleiotropic effects on adipose tissue (74). Importantly, MC-released IFN-γ, chymase, tryptase, IL-6, and cysteinyl cathepsins promote adipogenesis as well as angiogenesis through direct actions on adipocytes and endothelial cells as well as macrophages (52, 75, 76). Moreover, MCs play an important role in the reconfiguration of the extracellular matrix. Thus, MCs are a highly dynamic and important part of the nervous-endocrine-immune system regulating adipose function. Current data on the role of mast cells on preadipocyte differentiation are restricted to murine studies and controversial. Hirai et al. showed that mast cell protease 6 (MCP-6) secreted by mature mast cells induces collagen V expression in obese adipose tissue, contributing to adipose tissue fibrosis inhibiting preadipocyte differentiation (**Figure 2**) (77). Mast cell deficient $Kit^{w\text{-}sh/w\text{-}sh}$ mice, which are fertile and non-anemic but also lack additional cell types mainly, melanocytes, and interstitial cells of Cajal, confirmed these previous findings and showed upregulated adipogenic capacity and preadipocyte proliferation (78). Similarly, mice where MCs were chemically inhibited as well as $Kit^{w\text{-}sh/w\text{-}sh}$ mice showed an increase in sWAT PDGFRα$^+$ APC proliferation and induced beige (thermogenic) adipocyte differentiation (79). However, stimulation of MCs by calcium or high-glucose induced adipogenesis in 3T3-L1 preadipocytes through the production of 15-deoxy-delta-12, 14-prostaglandin J2 acting as an activator of PPARγ (80). Furthermore, Chen et al. demonstrated that mast cell derived heparin could act as the endogenous factor initiating fascial adipogenesis (81). These findings suggest an adipose depot specific effect of mast cells on adipocyte progenitors, dependent on other immune cells and the metabolic state of the organism. Moreover, available data on the role of MCs on adipocyte progenitors focus on studies in rodents, while the role in humans remains to be determined.

Innate Lymphoid Cells

Type 2 innate lymphoid cells (ILC2), which are part of the first line of the innate immune system, regulate type 2 immunity during tissue damage, parasite infection, and allergy (82–87). Apart from their role in wound healing, ILC2s also exhibit positive effects on metabolic homeostasis in visceral WAT, where they regulate eosinophils and alternatively activate macrophages (88). IL-33 mediated activation of ILC2s promote proliferation and commitment of APCs to become beige rather than white adipocytes (**Figure 2**) (89). In addition, an alternative pathway was described through the interaction of ILC2s with eosinophils, promoting secretion of IL-4, which activated IL-4R signaling in preadipocytes (89, 90). In the steady state, lacking IL-33, co-culture of adipose-derived ILC2s with 3T3-L1 cells induced adipocyte differentiation and lipid accumulation (91). Moreover, apart from ILC2s, ILC1s as well as NK cells play an important indirect role in modulating adipocyte-immune cell interactions. ILC1s kill adipose tissue macrophages and maintain macrophage homeostasis (**Figure 2**). However, this effect is abolished in obesity (92). Furthermore, adipose ILC1 secreted IFN-γ contributes to M1 macrophage polarization under HFD feeding (93, 94). Similar effects are also seen by NK cell activation (95, 96). Co-culture of ILC1 from obese subjects with lean stromal vascular cells upregulated the expression of fibrosis-related genes and ECM regulators, indicating that ILC1s promote fibrosis in obese adipose tissue (93).

T Cells

The direct effects of T cells on preadipocytes is unclear. Pan et al. showed that senescent T cells inhibit brown preadipocyte differentiation by secreting high levels of IFN-γ (97). Co-culture of active pan T cells with 3T3-L1 preadipocytes *in vitro* significantly suppressed differentiation (98). However, individual T cell subtypes play distinct roles in regulating inflammation in adipose tissue by modulating the switch between macrophage phenotypes. Pro-inflammatory T cells, such as; Th1 and Th17, activate pro-inflammatory macrophages by secreting IFNγ and IL-17. However, anti-inflammatory T cells, like Th2 and Foxp3$^+$ Treg induced macrophage differentiation into the anti-inflammatory macrophages by secreting IL-4 and IL-13 (**Figure 2**) (99). Interestingly, the percentage of naive CD4$^+$ and CD8$^+$ T cells were significantly higher in insulin sensitive compared to insulin resistant obese individuals, whereas activated T cells and IL-6 levels were reduced (100). This suggests that T cells contribute to the low-grade inflammation observed in MUO, albeit the link to alterations in adipose tissue has to be made.

Here we provide an overview of selected adipose tissue resident immune cells and their role in modulating preadipocyte fate directly or indirectly (**Figure 2**). Due to the complex regulations between immune cells and with the various adipocyte precursor populations, the impact of these interactions on the MHO phenotype remains to be determined. Moreover, adipose tissue depot specific differences in progenitors and immune cell composition need to be considered to evaluate the role of individual immune cell populations on healthy AT expansion. Furthermore, it will be exciting to see additional *in vivo* data on the regulations and interdependence of progenitor cell proliferation and differentiation on each other.

CONCLUSION AND FUTURE PERSPECTIVE

There is a rapidly increasing number of studies investigating adipocyte-preadipocyte-immune cell interaction. Thus, more and more details on the cellular subtypes and their regulation in obesity and the metabolic syndrome become available. Various computational approaches based on large–omics datasets are and will provide exciting new insights into the complex multidimensional spatial and temporal interactions of cell types, endocrine and nutritional inputs (47). This will allow a more holistic view on adipose tissues and their cellular interactions. However, these analyses are limited by the quality of the input data. Irrespective of the technical aspects of data acquisition, several points will need to be considered/improved to significantly advance our understanding of the control of adipocyte progenitor fate. One of the biggest limitations is the use of *in vitro* systems. Although simplification is important to identify molecular mechanism, the use of poorly defined progenitor or immune cell populations often results in data that cannot be translated to *in vivo*. Moreover, 2D cell culture models, most often do not allow "natural" cell-cell interactions, disregarding the effects of the ECM and biophysical properties such as oxygenation etc. Conversely, studying these mechanisms *in vivo* is also complex due to the lack of specific genetic models and low sample sizes. Moreover, the use of different mouse strains, in different life science disciplines, such as immunology and metabolism research also complicate the comparison of research data. To this end, novel developments such as spatial transcriptomics and single cell proteomics, could provide elegant ways to establish cell-cell interactions *in vivo*, most importantly in humans. Once these technical difficulties are solved, it will be fascinating to elucidate the reciprocal interaction of obesity and the metabolic syndrome with adipose stromal cell composition, function and activity. In summary, the expansion of adipose tissue, as well as the metabolic consequences of it in the context of MHO and MUO rely on a complex interplay between all cellular components, which should be studied as networks rather than linear interactions.

AUTHOR CONTRIBUTIONS

All authors listed have made a substantial, direct, and intellectual contribution to the work, and approved it for publication.

FUNDING

XY received support from China Scholarship Council (No. 201908370218).

ACKNOWLEDGMENTS

We would like to thank Yasuhiro Onogi fruitful discussion. The figures were created with a licensed version of BioRender.com.

REFERENCES

1. Friedman JM. Leptin and the Endocrine Control of Energy Balance. *Nat Metab* (2019) 1(8):754–64. doi: 10.1038/s42255-019-0095-y
2. Scheja L, Heeren J. The Endocrine Function of Adipose Tissues in Health and Cardiometabolic Disease. *Nat Rev Endocrinol* (2019) 15(9):507–24. doi: 10.1038/s41574-019-0230-6
3. Funcke JB, Scherer PE. Beyond Adiponectin and Leptin: Adipose Tissue-Derived Mediators of Inter-Organ Communication. *J Lipid Res* (2019) 60 (10):1648–84. doi: 10.1194/jlr.R094060
4. Kershaw EE, Flier JS. Adipose Tissue as an Endocrine Organ. *J Clin Endocrinol Metab* (2004) 89(6):2548–56. doi: 10.1210/jc.2004-0395
5. Schoettl T, Fischer IP, Ussar S. Heterogeneity of Adipose Tissue in Development and Metabolic Function. *J Exp Biol* (2018) 221(Pt Suppl 1):1–17. doi: 10.1242/jeb.162958
6. Bluher M. Metabolically Healthy Obesity. *Endocr Rev* (2020) 41(3):1–16. doi: 10.1210/endrev/bnaa004
7. Loos RJF, Kilpelainen TO. Genes That Make You Fat, But Keep You Healthy. *J Intern Med* (2018) 284(5):450–63. doi: 10.1111/joim.12827
8. Ahl S, Guenther M, Zhao S, James R, Marks J, Szabo A, et al. Adiponectin Levels Differentiate Metabolically Healthy Vs Unhealthy Among Obese and Nonobese White Individuals. *J Clin Endocrinol Metab* (2015) 100(11):4172–80. doi: 10.1210/jc.2015-2765
9. Stefan N, Haring HU, Hu FB, Schulze MB. Metabolically Healthy Obesity: Epidemiology, Mechanisms, and Clinical Implications. *Lancet Diabetes Endocrinol* (2013) 1(2):152–62. doi: 10.1016/S2213-8587(13)70062-7
10. Justice AE, Karaderi T, Highland HM, Young KL, Graff M, Lu Y, et al. Protein-Coding Variants Implicate Novel Genes Related to Lipid Homeostasis Contributing to Body-Fat Distribution. *Nat Genet* (2019) 51(3):452–69. doi: 10.1038/s41588-018-0334-2
11. Shungin D, Winkler TW, Croteau-Chonka DC, Ferreira T, Locke AE, Magi R, et al. New Genetic Loci Link Adipose and Insulin Biology to Body Fat Distribution. *Nature* (2015) 518(7538):187–96. doi: 10.1038/nature14132
12. Harms M, Seale P. Brown and Beige Fat: Development, Function and Therapeutic Potential. *Nat Med* (2013) 19(10):1252–63. doi: 10.1038/nm.3361
13. Cannon B, Nedergaard J. Brown Adipose Tissue: Function and Physiological Significance. *Physiol Rev* (2004) 84(1):277–359. doi: 10.1152/physrev.00015.2003
14. Karlina R, Lutter D, Miok V, Fischer D, Altun I, Schottl T, et al. Identification and Characterization of Distinct Brown Adipocyte Subtypes in C57bl/6j Mice. *Life Sci Alliance* (2021) 4(1):1–19. doi: 10.26508/lsa.202000924
15. Song A, Dai W, Jang MJ, Medrano L, Li Z, Zhao H, et al. Low- and High-Thermogenic Brown Adipocyte Subpopulations Coexist in Murine Adipose Tissue. *J Clin Invest* (2020) 130(1):247–57. doi: 10.1172/JCI129167
16. Desoye G, Herrera E. Adipose Tissue Development and Lipid Metabolism in the Human Fetus: The 2020 Perspective Focusing on Maternal Diabetes and Obesity. *Prog Lipid Res* (2021) 81:101082. doi: 10.1016/j.plipres.2020.101082
17. Poissonnet CM, Burdi AR, Bookstein FL. Growth and Development of Human Adipose Tissue During Early Gestation. *Early Hum Dev* (1983) 8 (1):1–11. doi: 10.1016/0378-3782(83)90028-2
18. Wang QA, Tao C, Gupta RK, Scherer PE. Tracking Adipogenesis During White Adipose Tissue Development, Expansion and Regeneration. *Nat Med* (2013) 19(10):1338–44. doi: 10.1038/nm.3324
19. Spalding KL, Arner E, Westermark PO, Bernard S, Buchholz BA, Bergmann O, et al. Dynamics of Fat Cell Turnover in Humans. *Nature* (2008) 453 (7196):783–7. doi: 10.1038/nature06902
20. Knittle JL, Timmers K, Ginsberg-Fellner F, Brown RE, Katz DP. The Growth of Adipose Tissue in Children and Adolescents. Cross-Sectional and Longitudinal Studies of Adipose Cell Number and Size. *J Clin Invest* (1979) 63(2):239–46. doi: 10.1172/JCI109295
21. Petrus P, Mejhert N, Corrales P, Lecoutre S, Li Q, Maldonado E, et al. Transforming Growth Factor-Beta3 Regulates Adipocyte Number in

Subcutaneous White Adipose Tissue. *Cell Rep* (2018) 25(3):551–60 e5. doi: 10.1016/j.celrep.2018.09.069
22. Rigamonti A, Brennand K, Lau F, Cowan CA. Rapid Cellular Turnover in Adipose Tissue. *PloS One* (2011) 6(3):e17637. doi: 10.1371/journal.pone.0017637
23. Kulenkampff E, Wolfrum C. Proliferation of Nutrition Sensing Preadipocytes Upon Short Term Hfd Feeding. *Adipocyte* (2019) 8(1):16–25. doi: 10.1080/21623945.2018.1521229
24. Hirsch J, Han PW. Cellularity of Rat Adipose Tissue: Effects of Growth, Starvation, and Obesity. *J Lipid Res* (1969) 10(1):77–82. doi: 10.1016/S0022-2275(20)42651-3
25. Sakers A, De Siqueira MK, Seale P, Villanueva CJ. Adipose-Tissue Plasticity in Health and Disease. *Cell* (2022) 185(3):419–46. doi: 10.1016/j.cell.2021.12.016
26. Merrick D, Sakers A, Irgebay Z, Okada C, Calvert C, Morley MP, et al. Identification of a Mesenchymal Progenitor Cell Hierarchy in Adipose Tissue. *Science* (2019) 364(6438):1–11. doi: 10.1126/science.aav2501
27. Lee KY, Luong Q, Sharma R, Dreyfuss JM, Ussar S, Kahn CR. Developmental and Functional Heterogeneity of White Adipocytes Within a Single Fat Depot. *EMBO J* (2019) 38(3):1–19. doi: 10.15252/embj.201899291
28. Berry R, Rodeheffer MS. Characterization of the Adipocyte Cellular Lineage *in Vivo*. *Nat Cell Biol* (2013) 15(3):302–8. doi: 10.1038/ncb2696
29. Rodeheffer MS, Birsoy K, Friedman JM. Identification of White Adipocyte Progenitor Cells *In Vivo*. *Cell* (2008) 135(2):240–9. doi: 10.1016/j.cell.2008.09.036
30. Jiang Y, Berry DC, Tang W, Graff JM. Independent Stem Cell Lineages Regulate Adipose Organogenesis and Adipose Homeostasis. *Cell Rep* (2014) 9(3):1007–22. doi: 10.1016/j.celrep.2014.09.049
31. Shin S, Pang Y, Park J, Liu L, Lukas BE, Kim SH, et al. Dynamic Control of Adipose Tissue Development and Adult Tissue Homeostasis by Platelet-Derived Growth Factor Receptor Alpha. *Elife* (2020) 9:1–21. doi: 10.7554/eLife.56189
32. Iwayama T, Steele C, Yao L, Dozmorov MG, Karamichos D, Wren JD, et al. Pdgfralpha Signaling Drives Adipose Tissue Fibrosis by Targeting Progenitor Cell Plasticity. *Genes Dev* (2015) 29(11):1106–19. doi: 10.1101/gad.260554.115
33. Marcelin G, Ferreira A, Liu Y, Atlan M, Aron-Wisnewsky J, Pelloux V, et al. A Pdgfralpha-Mediated Switch Toward Cd9(High) Adipocyte Progenitors Controls Obesity-Induced Adipose Tissue Fibrosis. *Cell Metab* (2017) 25(3):673–85. doi: 10.1016/j.cmet.2017.01.010
34. Stefkovich M, Traynor S, Cheng L, Merrick D, Seale P. Dpp4+ Interstitial Progenitor Cells Contribute to Basal and High Fat Diet-Induced Adipogenesis. *Mol Metab* (2021) 54:101357. doi: 10.1016/j.molmet.2021.101357
35. Onogi Y, Khalil A, Ussar S. Identification and Characterization of Adipose Surface Epitopes. *Biochem J* (2020) 477(13):2509–41. doi: 10.1042/BCJ20190462
36. Suwandhi L, Altun I, Karlina R, Miok V, Wiedemann T, Fischer D, et al. Asc-1 Regulates White Versus Beige Adipocyte Fate in a Subcutaneous Stromal Cell Population. *Nat Commun* (2021) 12(1):1588. doi: 10.1038/s41467-021-21826-9
37. Larabee CM, Neely OC, Domingos AI. Obesity: A Neuroimmunometabolic Perspective. *Nat Rev Endocrinol* (2020) 16(1):30–43. doi: 10.1038/s41574-019-0283-6
38. Libretti S, Puckett Y. Physiology, Homeostasis. In: *Statpearls*. Treasure Island, FL: StatPearls Publishing [Internet] (2022).
39. Jiang Y, Berry DC, Jo A, Tang W, Arpke RW, Kyba M, et al. A Ppargamma Transcriptional Cascade Directs Adipose Progenitor Cell-Niche Interaction and Niche Expansion. *Nat Commun* (2017) 8:15926. doi: 10.1038/ncomms15926
40. Cinkajzlova A, Mraz M, Haluzik M. Adipose Tissue Immune Cells in Obesity, Type 2 Diabetes Mellitus and Cardiovascular Diseases. *J Endocrinol* (2021) 252(1):R1–R22. doi: 10.1530/JOE-21-0159
41. Weinstock A, Moura Silva H, Moore KJ, Schmidt AM, Fisher EA. Leukocyte Heterogeneity in Adipose Tissue, Including in Obesity. *Circ Res* (2020) 126(11):1590–612. doi: 10.1161/CIRCRESAHA.120.316203
42. Villarroya F, Cereijo R, Gavalda-Navarro A, Villarroya J, Giralt M. Inflammation of Brown/Beige Adipose Tissues in Obesity and Metabolic Disease. *J Intern Med* (2018) 284(5):492–504. doi: 10.1111/joim.12803
43. Guzik TJ, Skiba DS, Touyz RM, Harrison DG. The Role of Infiltrating Immune Cells in Dysfunctional Adipose Tissue. *Cardiovasc Res* (2017) 113(9):1009–23. doi: 10.1093/cvr/cvx108
44. Kawai T, Autieri MV, Scalia R. Adipose Tissue Inflammation and Metabolic Dysfunction in Obesity. *Am J Physiol Cell Physiol* (2021) 320(3):C375–C91. doi: 10.1152/ajpcell.00379.2020
45. Wernstedt Asterholm I, Tao C, Morley TS, Wang QA, Delgado-Lopez F, Wang ZV, et al. Adipocyte Inflammation Is Essential for Healthy Adipose Tissue Expansion and Remodeling. *Cell Metab* (2014) 20(1):103–18. doi: 10.1016/j.cmet.2014.05.005
46. Lilja HE, Morrison WA, Han XL, Palmer J, Taylor C, Tee R, et al. An Adipoinductive Role of Inflammation in Adipose Tissue Engineering: Key Factors in the Early Development of Engineered Soft Tissues. *Stem Cells Dev* (2013) 22(10):1602–13. doi: 10.1089/scd.2012.0451
47. Hildreth AD, Ma F, Wong YY, Sun R, Pellegrini M, O'Sullivan TE. Single-Cell Sequencing of Human White Adipose Tissue Identifies New Cell States in Health and Obesity. *Nat Immunol* (2021) 22(5):639–53. doi: 10.1038/s41590-021-00922-4
48. Jaitin DA, Adlung L, Thaiss CA, Weiner A, Li B, Descamps H, et al. Lipid-Associated Macrophages Control Metabolic Homeostasis in a Trem2-Dependent Manner. *Cell* (2019) 178(3):686–98.e14. doi: 10.1016/j.cell.2019.05.054
49. Ruggiero AD, Key CC, Kavanagh K. Adipose Tissue Macrophage Polarization in Healthy and Unhealthy Obesity. *Front Nutr* (2021) 8:625331. doi: 10.3389/fnut.2021.625331
50. Ni Y, Ni L, Zhuge F, Xu L, Fu Z, Ota T. Adipose Tissue Macrophage Phenotypes and Characteristics: The Key to Insulin Resistance in Obesity and Metabolic Disorders. *Obesity (Silver Spring)* (2020) 28(2):225–34. doi: 10.1002/oby.22674
51. Kloting N, Fasshauer M, Dietrich A, Kovacs P, Schon MR, Kern M, et al. Insulin-Sensitive Obesity. *Am J Physiol Endocrinol Metab* (2010) 299(3):E506–15. doi: 10.1152/ajpendo.00586.2009
52. Muir LA, Cho KW, Geletka LM, Baker NA, Flesher CG, Ehlers AP, et al. Human Cd206+ Macrophages Associate With Diabetes and Adipose Tissue Lymphoid Clusters. *JCI Insight* (2022) 7(3):1–16. doi: 10.1172/jci.insight.146563
53. Russo L, Lumeng CN. Properties and Functions of Adipose Tissue Macrophages in Obesity. *Immunology* (2018) 155(4):407–17. doi: 10.1111/imm.13002
54. Thomas D, Apovian C. Macrophage Functions in Lean and Obese Adipose Tissue. *Metabolism* (2017) 72:120–43. doi: 10.1016/j.metabol.2017.04.005
55. Nahrendorf M, Swirski FK. Abandoning M1/M2 for a Network Model of Macrophage Function. *Circ Res* (2016) 119(3):414–7. doi: 10.1161/CIRCRESAHA.116.309194
56. Lacasa D, Taleb S, Keophiphath M, Miranville A, Clement K. Macrophage-Secreted Factors Impair Human Adipogenesis: Involvement of Proinflammatory State in Preadipocytes. *Endocrinology* (2007) 148(2):868–77. doi: 10.1210/en.2006-0687
57. Maumus M, Sengenes C, Decaunes P, Zakaroff-Girard A, Bourlier V, Lafontan M, et al. Evidence of *in Situ* Proliferation of Adult Adipose Tissue-Derived Progenitor Cells: Influence of Fat Mass Microenvironment and Growth. *J Clin Endocrinol Metab* (2008) 93(10):4098–106. doi: 10.1210/jc.2008-0044
58. Constant VA, Gagnon A, Yarmo M, Sorisky A. The Antiadipogenic Effect of Macrophage-Conditioned Medium Depends on Erk1/2 Activation. *Metabolism* (2008) 57(4):465–72. doi: 10.1016/j.metabol.2007.11.005
59. Constant VA, Gagnon A, Landry A, Sorisky A. Macrophage-Conditioned Medium Inhibits the Differentiation of 3t3-L1 and Human Abdominal Preadipocytes. *Diabetologia* (2006) 49(6):1402–11. doi: 10.1007/s00125-006-0253-0
60. Yarmo MN, Gagnon A, Sorisky A. The Anti-Adipogenic Effect of Macrophage-Conditioned Medium Requires the Ikkbeta/Nf-Kappab Pathway. *Horm Metab Res* (2010) 42(12):831–6. doi: 10.1055/s-0030-1263124
61. Liu LF, Craig CM, Tolentino LL, Choi O, Morton J, Rivas H, et al. Adipose Tissue Macrophages Impair Preadipocyte Differentiation in Humans. *PloS One* (2017) 12(2):e0170728. doi: 10.1371/journal.pone.0170728
62. Ide J, Gagnon A, Molgat AS, Landry A, Foster C, Sorisky A. Macrophage-Conditioned Medium Inhibits the Activation of Cyclin-Dependent Kinase 2 by Adipogenic Inducers in 3t3-L1 Preadipocytes. *J Cell Physiol* (2011) 226(9):2297–306. doi: 10.1002/jcp.22566
63. Yarmo MN, Landry A, Molgat AS, Gagnon A, Sorisky A. Macrophage-Conditioned Medium Inhibits Differentiation-Induced Rb Phosphorylation

in 3t3-L1 Preadipocytes. *Exp Cell Res* (2009) 315(3):411–8. doi: 10.1016/j.yexcr.2008.10.036
64. Kang X, Liang H, Luo Y, Li Z, He F, Han X, et al. Streptococcus Thermophilus Mn-Zlw-002 Can Inhibit Pre-Adipocyte Differentiation Through Macrophage Activation. *Biol Pharm Bull* (2021) 44(3):316–24. doi: 10.1248/bpb.b20-00335
65. Gagnon A, Yarmo MN, Landry A, Sorisky A. Macrophages Alter the Differentiation-Dependent Decreases in Fibronectin and Collagen I/Iii Protein Levels in Human Preadipocytes. *Lipids* (2012) 47(9):873–80. doi: 10.1007/s11745-012-3696-8
66. Keophiphath M, Achard V, Henegar C, Rouault C, Clement K, Lacasa D. Macrophage-Secreted Factors Promote a Profibrotic Phenotype in Human Preadipocytes. *Mol Endocrinol* (2009) 23(1):11–24. doi: 10.1210/me.2008-0183
67. Lu C, Kumar PA, Fan Y, Sperling MA, Menon RK. A Novel Effect of Growth Hormone on Macrophage Modulates Macrophage-Dependent Adipocyte Differentiation. *Endocrinology* (2010) 151(5):2189–99. doi: 10.1210/en.2009-1194
68. Jang JE, Ko MS, Yun JY, Kim MO, Kim JH, Park HS, et al. Nitric Oxide Produced by Macrophages Inhibits Adipocyte Differentiation and Promotes Profibrogenic Responses in Preadipocytes to Induce Adipose Tissue Fibrosis. *Diabetes* (2016) 65(9):2516–28. doi: 10.2337/db15-1624
69. Kurokawa J, Arai S, Nakashima K, Nagano H, Nishijima A, Miyata K, et al. Macrophage-Derived Aim Is Endocytosed Into Adipocytes and Decreases Lipid Droplets *Via* Inhibition of Fatty Acid Synthase Activity. *Cell Metab* (2010) 11(6):479–92. doi: 10.1016/j.cmet.2010.04.013
70. Molgat AS, Gagnon A, Sorisky A. Macrophage-Induced Preadipocyte Survival Depends on Signaling Through Akt, Erk1/2, and Reactive Oxygen Species. *Exp Cell Res* (2011) 317(4):521–30. doi: 10.1016/j.yexcr.2010.10.024
71. Molgat AS, Gagnon A, Sorisky A. Preadipocyte Apoptosis Is Prevented by Macrophage-Conditioned Medium in a Pdgf-Dependent Manner. *Am J Physiol Cell Physiol* (2009) 296(4):C757–65. doi: 10.1152/ajpcell.00617.2008
72. Molgat AS, Gagnon A, Foster C, Sorisky A. The Activation State of Macrophages Alters Their Ability to Suppress Preadipocyte Apoptosis. *J Endocrinol* (2012) 214(1):21–9. doi: 10.1530/JOE-12-0114
73. Altintas MM, Azad A, Nayer B, Contreras G, Zaias J, Faul C, et al. Mast Cells, Macrophages, and Crown-Like Structures Distinguish Subcutaneous From Visceral Fat in Mice. *J Lipid Res* (2011) 52(3):480–8. doi: 10.1194/jlr.M011338
74. Elieh Ali Komi D, Shafaghat F, Christian M. Crosstalk Between Mast Cells and Adipocytes in Physiologic and Pathologic Conditions. *Clin Rev Allergy Immunol* (2020) 58(3):388–400. doi: 10.1007/s12016-020-08785-7
75. Liu J, Divoux A, Sun J, Zhang J, Clement K, Glickman JN, et al. Genetic Deficiency and Pharmacological Stabilization of Mast Cells Reduce Diet-Induced Obesity and Diabetes in Mice. *Nat Med* (2009) 15(8):940–5. doi: 10.1038/nm.1994
76. Zhou Y, Yu X, Chen H, Sjoberg S, Roux J, Zhang L, et al. Leptin Deficiency Shifts Mast Cells Toward Anti-Inflammatory Actions and Protects Mice From Obesity and Diabetes by Polarizing M2 Macrophages. *Cell Metab* (2015) 22(6):1045–58. doi: 10.1016/j.cmet.2015.09.013
77. Hirai S, Ohyane C, Kim YI, Lin S, Goto T, Takahashi N, et al. Involvement of Mast Cells in Adipose Tissue Fibrosis. *Am J Physiol Endocrinol Metab* (2014) 306(3):E247–55. doi: 10.1152/ajpendo.00056.2013
78. Ishijima Y, Ohmori S, Ohneda K. Mast Cell Deficiency Results in the Accumulation of Preadipocytes in Adipose Tissue in Both Obese and Non-Obese Mice. *FEBS Open Bio* (2013) 4:18–24. doi: 10.1016/j.fob.2013.11.004
79. Zhang X, Wang X, Yin H, Zhang L, Feng A, Zhang QX, et al. Functional Inactivation of Mast Cells Enhances Subcutaneous Adipose Tissue Browning in Mice. *Cell Rep* (2019) 28(3):792–803.e4. doi: 10.1016/j.celrep.2019.06.044
80. Tanaka A, Nomura Y, Matsuda A, Ohmori K, Matsuda H. Mast Cells Function as an Alternative Modulator of Adipogenesis Through 15-Deoxy-Delta-12, 14-Prostaglandin J2. *Am J Physiol Cell Physiol* (2011) 301(6):C1360–7. doi: 10.1152/ajpcell.00514.2010
81. Chen T, Zhang Y, Dong Y, Zhang D, Xia L, Sun X, et al. Mast Cell and Heparin Promote Adipogenesis in Superficial Fascia of Rats. *Biochim Biophys Acta Mol Cell Biol Lipids* (2021) 1866(11):159024. doi: 10.1016/j.bbalip.2021.159024
82. McKenzie ANJ, Spits H, Eberl G. Innate Lymphoid Cells in Inflammation and Immunity. *Immunity* (2014) 41(3):366–74. doi: 10.1016/j.immuni.2014.09.006
83. Koyasu S, Moro K. Th2-Type Innate Immune Responses Mediated by Natural Helper Cells. *Ann N Y Acad Sci* (2013) 1283:43–9. doi: 10.1111/nyas.12106
84. Walker JA, Barlow JL, McKenzie AN. Innate Lymphoid Cells–How Did We Miss Them? *Nat Rev Immunol* (2013) 13(2):75–87. doi: 10.1038/nri3349
85. Price AE, Liang HE, Sullivan BM, Reinhardt RL, Eisley CJ, Erle DJ, et al. Systemically Dispersed Innate Il-13-Expressing Cells in Type 2 Immunity. *Proc Natl Acad Sci USA* (2010) 107(25):11489–94. doi: 10.1073/pnas.1003988107
86. Neill DR, Wong SH, Bellosi A, Flynn RJ, Daly M, Langford TK, et al. Nuocytes Represent a New Innate Effector Leukocyte That Mediates Type-2 Immunity. *Nature* (2010) 464(7293):1367–70. doi: 10.1038/nature08900
87. Moro K, Yamada T, Tanabe M, Takeuchi T, Ikawa T, Kawamoto H, et al. Innate Production of T(H)2 Cytokines by Adipose Tissue-Associated C-Kit (+)Sca-1(+) Lymphoid Cells. *Nature* (2010) 463(7280):540–4. doi: 10.1038/nature08636
88. Molofsky AB, Nussbaum JC, Liang HE, Van Dyken SJ, Cheng LE, Mohapatra A, et al. Innate Lymphoid Type 2 Cells Sustain Visceral Adipose Tissue Eosinophils and Alternatively Activated Macrophages. *J Exp Med* (2013) 210(3):535–49. doi: 10.1084/jem.20121964
89. Brestoff JR, Kim BS, Saenz SA, Stine RR, Monticelli LA, Sonnenberg GF, et al. Group 2 Innate Lymphoid Cells Promote Beiging of White Adipose Tissue and Limit Obesity. *Nature* (2015) 519(7542):242–6. doi: 10.1038/nature14115
90. Lee MW, Odegaard JI, Mukundan L, Qiu Y, Molofsky AB, Nussbaum JC, et al. Activated Type 2 Innate Lymphoid Cells Regulate Beige Fat Biogenesis. *Cell* (2015) 160(1-2):74–87. doi: 10.1016/j.cell.2014.12.011
91. Miyajima Y, Ealey KN, Motomura Y, Mochizuki M, Takeno N, Yanagita M, et al. Effects of Bmp7 Produced by Group 2 Innate Lymphoid Cells on Adipogenesis. *Int Immunol* (2020) 32(6):407–19. doi: 10.1093/intimm/dxaa013
92. Boulenouar S, Michelet X, Duquette D, Alvarez D, Hogan AE, Dold C, et al. Adipose Type One Innate Lymphoid Cells Regulate Macrophage Homeostasis Through Targeted Cytotoxicity. *Immunity* (2017) 46(2):273–86. doi: 10.1016/j.immuni.2017.01.008
93. Wang H, Shen L, Sun X, Liu F, Feng W, Jiang C, et al. Adipose Group 1 Innate Lymphoid Cells Promote Adipose Tissue Fibrosis and Diabetes in Obesity. *Nat Commun* (2019) 10(1):3254. doi: 10.1038/s41467-019-11270-1
94. O'Sullivan TE, Rapp M, Fan X, Weizman OE, Bhardwaj P, Adams NM, et al. Adipose-Resident Group 1 Innate Lymphoid Cells Promote Obesity-Associated Insulin Resistance. *Immunity* (2016) 45(2):428–41. doi: 10.1016/j.immuni.2016.06.016
95. Wensveen FM, Jelencic V, Valentic S, Sestan M, Wensveen TT, Theurich S, et al. Nk Cells Link Obesity-Induced Adipose Stress to Inflammation and Insulin Resistance. *Nat Immunol* (2015) 16(4):376–85. doi: 10.1038/ni.3120
96. O'Rourke RW, Metcalf MD, White AE, Madala A, Winters BR, Maizlin II, et al. Depot-Specific Differences in Inflammatory Mediators and a Role for Nk Cells and Ifn-Gamma in Inflammation in Human Adipose Tissue. *Int J Obes (Lond)* (2009) 33(9):978–90. doi: 10.1038/ijo.2009.133
97. Pan XX, Yao KL, Yang YF, Ge Q, Zhang R, Gao PJ, et al. Senescent T Cell Induces Brown Adipose Tissue "Whitening" *Via* Secreting Ifn-Gamma. *Front Cell Dev Biol* (2021) 9:637424. doi: 10.3389/fcell.2021.637424
98. Wu H, Ghosh S, Perrard XD, Feng L, Garcia GE, Perrard JL, et al. T-Cell Accumulation and Regulated on Activation, Normal T Cell Expressed and Secreted Upregulation in Adipose Tissue in Obesity. *Circulation* (2007) 115(8):1029–38. doi: 10.1161/CIRCULATIONAHA.106.638379
99. Winer S, Chan Y, Paltser G, Truong D, Tsui H, Bahrami J, et al. Normalization of Obesity-Associated Insulin Resistance Through Immunotherapy. *Nat Med* (2009) 15(8):921–9. doi: 10.1038/nm.2001
100. Sbierski-Kind J, Goldeck D, Buchmann N, Spranger J, Volk HD, Steinhagen-Thiessen E, et al. T Cell Phenotypes Associated With Insulin Resistance:

Results From the Berlin Aging Study Ii. *Immun Ageing* (2020) 17(1):40. doi: 10.1186/s12979-020-00211-y

Conflict of Interest: The authors declare that the research was conducted in the absence of any commercial or financial relationships that could be construed as a potential conflict of interest.

Publisher's Note: All claims expressed in this article are solely those of the authors and do not necessarily represent those of their affiliated organizations, or those of the publisher, the editors and the reviewers. Any product that may be evaluated in this article, or claim that may be made by its manufacturer, is not guaranteed or endorsed by the publisher.

frontiers in Endocrinology

ORIGINAL RESEARCH
published: 30 March 2022
doi: 10.3389/fendo.2022.820023

Magnetic Resonance Imaging Assessment of Abdominal Ectopic Fat Deposition in Correlation With Cardiometabolic Risk Factors

*Qin-He Zhang[1], Lu-Han Xie[2], Hao-Nan Zhang[1], Jing-Hong Liu[1], Ying Zhao[1], Li-Hua Chen[1], Ye Ju[1], An-Liang Chen[1], Nan Wang[1], Qing-Wei Song[1], Li-Zhi Xie[3] and Ai-Lian Liu[1]**

[1] Department of Radiology, The First Affiliated Hospital of Dalian Medical University, Dalian, China, [2] Department of Pathology and Forensics, Dalian Medical University, Dalian, China, [3] MR Research, GE Healthcare, Beijing, China

OPEN ACCESS

Edited by:
Matthias Blüher,
Leipzig University, Germany

Reviewed by:
Yuyan Liu,
China Medical University, China
Xinli Li,
Nanjing Medical University, China
Jane Dagmar Renner,
Universidade de Santa Cruz do Sul, Brazil
Maricarmen Chacín,
Simón Bolívar University, Colombia

***Correspondence:**
Ai-Lian Liu
liuailian@dmu.edu.cn

Specialty section:
This article was submitted to Obesity, a section of the journal Frontiers in Endocrinology

Received: 22 November 2021
Accepted: 01 March 2022
Published: 30 March 2022

Citation:
Zhang Q-H, Xie L-H, Zhang H-N, Liu J-H, Zhao Y, Chen L-H, Ju Y, Chen A-L, Wang N, Song Q-W, Xie L-Z and Liu A-L (2022) Magnetic Resonance Imaging Assessment of Abdominal Ectopic Fat Deposition in Correlation With Cardiometabolic Risk Factors. Front. Endocrinol. 13:820023. doi: 10.3389/fendo.2022.820023

Purpose: Ectopic fat accumulation and abdominal fat distribution may have different cardiometabolic risk profiles. This study aimed to assess the associations between various magnetic resonance imaging (MRI)-acquired fat depots and cardiometabolic risk factors.

Methods: A total of 320 subjects with median age of 59 years, 148 men and 172 women, were enrolled in the study. Visceral adipose tissue (VAT) area and fat fraction (FF), subcutaneous adipose tissue (SAT) area and FF at the L1–L2 levels, preperitoneal adipose tissue (pPAT) area and FF, hepatic FF, pancreatic FF, and intramuscular FF were assessed by MRI FF maps. The associations of various MRI-acquired fat depots with blood pressure, glucose, and lipid were examined using sex-stratified linear regression. Logistic regression stratified by sex was used to analyze the association of various MRI-acquired fat depots with the risk of hypertension, T2DM, and dyslipidemia.

Results: The intraclass correlation coefficient (ICC) values were >0.9, which suggested good interobserver and intraobserver agreement. VAT area, V/S, hepatic fat, pancreatic fat, and pPAT rather than SAT area were significantly associated with multiple cardiometabolic risk factors (all $p < 0.05$). However, the patterns of these correlations varied by sex and specific risk factors. Also, VAT and SAT FF were only significantly associated with multiple cardiometabolic risk factors in women (all $p < 0.05$).

Conclusions: VAT, hepatic fat, pancreatic fat, and pPAT were associated with cardiovascular metabolic risk factors independent of BMI. The patterns of these correlations were related to gender. These findings further the understanding of the association between ectopic fat deposition and cardiometabolic risk factors and help to better understand the obesity heterogeneity.

Keywords: ectopic fat deposition, cardiometabolic risk factors, abdominal fat distribution, magnetic resonance imaging, obesity

1 INTRODUCTION

Obesity is becoming one of the most significant public health problems and a leading cause of preventable death. Fatty acids produced in the human body are predominantly stored in adipose tissue in the form of triglycerides (TG). As the primary site of excessive TG storage, subcutaneous adipose tissue (SAT) capacity is limited. When SAT cannot store excessive amounts of energy, excessive TG leads to the accumulation of triglycerides in visceral adipose tissue (VAT), preperitoneal adipose tissue (pPAT), and nonadipose tissues, such as the heart, liver, pancreas, and skeletal muscles. These fat depots are described as "ectopic fat depots" (1, 2), which have been identified as an essential diagnostic and prognostic marker for the onset, progression, and mortality risk of cardiometabolic disease (1, 3–9). Obesity is a heterogeneous condition, and some obese individuals can be metabolically healthy (10). Thus, specific patterns of body fat deposition may confer different cardiometabolic risks (11).

Previously, the assessment of abdominal fat distribution mainly relied on several anthropometric measures, e.g., body mass index (BMI), waist-to-hip ratio (WHR), or waist circumference (WC), and/or broadly available clinical tools, such as dual-energy x-ray absorptiometry (DXA) and bioelectrical impedance analysis (BIA) (12–15). Still, none of these approaches mentioned above can evaluate the regional fat distribution and ectopic fat deposition. By contrast, computed tomography (CT) and magnetic resonance imaging (MRI) can be used to visually evaluate the abdominal fat distribution and ectopic fat deposition. Particularly, they are noninvasive, fast, and accurate, making them an ideal clinical indicator for fat quantification and monitoring changes in visceral and ectopic fat over time. The MRI protocol for the iterative decomposition of water and fat with echo asymmetry and least-squares estimation-iron quantification (IDEAL-IQ) sequence is a new method to fat quantification and can lead to a more accurate measurement of fat content because of a low flip angle for suppressing the longitudinal relaxation effects, and multiecho acquisition permit correction of the transverse relaxation effects. It has also been widely used to assess the fat quantification of different tissues (16).

Cardiometabolic risk factors included hypertension, type 2 diabetes mellitus (T2DM), dyslipidemia, and others. The simultaneous coexistence of two or more risk factors in a person at the same time has been recognized as clustering of cardiometabolic risk factors (CCRFs) (17), while the synergy of CCRFs can increase the risk of cardiovascular disease. In the early stages of cardiometabolic risk factors, deleterious and progressive changes in each organ are often asymptomatic and possibly reversible. Thus, a lifestyle modification can reduce morbidity and mortality of cardiometabolic risk factor-related diseases (18, 19). Defining imaging markers of high-risk fat accumulation might have important implications for prediction of cardiometabolic risk factors and early prevention or therapeutic intervention. Currently, studies that performed a direct comparison between various MRI-acquired fat depots accumulated in six abdominal regions (VAT, SAT, pPAT, liver, pancreas, and muscle) and multiple cardiometabolic risk factors are lacking. Accordingly, it remains unknown which MRI-acquired fat depots contribute the most to the individual cardiometabolic risk factors.

The aim of the present study was to assess the association between the various MRI-acquired fat depots and cardiometabolic risk factors. We hypothesized that the association between each fat content and cardiometabolic risk factors varies with the type of fat depots; there are fat depots that are more strongly associated with cardiometabolic risk factors than others, and they may therefore serve as imaging biomarkers in prediction, early prevention, or therapeutic intervention of cardiometabolic risk factors.

Abbreviations: BIA, bioelectrical impedance analysis; BMI, body mass index; BP, blood pressure; CCRFs, clustering of cardiometabolic risk factors; CT, computed tomography; DXA, dual-energy x-ray absorptiometry; FF, fat fraction; FPG, fasting plasma glucose; HDL-C, high-density lipoprotein cholesterol; ICC, intraclass correlation coefficient; IDEAL-IQ, iterative decomposition of water and fat with echo asymmetry and least-squares estimation-iron quantification; LDL-C, low-density lipoprotein cholesterol; MRI, magnetic resonance imaging; ORs, odds ratios; pPAT, preperitoneal adipose tissue; ROI, region of interest; SAT, subcutaneous adipose tissue; TC, total cholesterol; TG, triglycerides; T2DM, type 2 diabetes mellitus; VAT, visceral adipose tissue; WC, waist circumference; WHR, waist-to-hip ratio; V/S, visceral/subcutaneous adipose tissue area ratio.

2 MATERIALS AND METHODS

2.1 Study Population

This single-center, retrospective study included 4,718 patients who underwent upper abdominal MRI examination between January 2017 and August 2020. The target population was the general population. Of these participants, those who met at least one of the following criteria were excluded: age <18 years (n = 9); a history of heavy drinking (alcohol consumption ≥30 g/week in men or ≥20 g/week in women in the last 10 years) (n = 78); evidence of cirrhosis, malignant liver tumor, large benign liver tumor, liver posthepatectomy, and decompensated liver diseases (n = 992); evidence of other liver diseases (n = 171), including viral hepatitis, autoimmune liver diseases, drug-induced liver injury, etc.; evidence of pancreas diseases (n = 840), including acute or chronic pancreatitis, autoimmune pancreas diseases, pancreas tumor, pancreas postpancreatectomy, pancreatic trauma; intrahepatic bile, or pancreatic duct dilation (n = 126); thyroid diseases (n = 62); evidence of ascites, mesenteric injuries, huge abdominal mass, abdominal wall edema, and postostomy (n = 31); radiotherapy, chemotherapy, immunosuppressive therapy, antiviral therapy, and endocrine therapy (n = 1213); pregnancy (n = 3); suspected secondary hypertension and other types of diabetes except T2DM (n = 11); missing cardiometabolic risk factors (n = 858); missing IDEAL-IQ sequence (n = 130); missing covariates (n = 2); weight change by more than 5% (within 1 month) (n = 185); poor image quality (poor signal-to-noise ratio or motion artifacts) (n = 8). Finally, a total of 320 subjects (148 men and 172 women) were included in the analysis.

This retrospective study was approved by review board of the First Affiliated Hospital of Dalian Medical University, and a waiver of informed consent was remitted.

2.2 MRI Examinations

In this study, the MRI scanner (GE Medical Systems, Inc., Waukesha, WI, USA) with an eight-channel phased-array body coil was used. The patients fasted for 4–6 h and were trained to exhale and hold their breath for more than 20 s before scanning. The subjects were placed in the supine position during examination. A three-plane localization imaging gradient-echo sequence was performed at the beginning of acquisition.

IDEAL-IQ sequence and routine MRI Ax T1 FSPGR, Ax T2 FSE, DWI sequence, and Dual echo sequence were acquired. MRI parameters were as follows: 3.0 T MRI IDEAL-IQ sequence: TR/TE = 6.9 ms/3.0 ms, slice thickness of 10 mm, 200 kHZ bandwidth, FOV = 36 cm × 36 cm, matrix = 256 × 160, flip angle = 3°, NEX = 1, breath holding for less than 24 s. 1.5 T MRI IDEAL-IQ sequence: TR/TE = 13.4 ms/4.8 ms, slice thickness of 10 mm, 125 kHZ bandwidth, FOV = 36 cm × 36 cm, matrix = 256 × 160, flip angle = 5°, NEX = 1, breath holding for less than 24 s. T1WI sequence: TR/TE = 210 ms/2.4 ms. T2WI: TR/TE = 8,571 ms/100 ms. Dual-echo sequence: TR = 190 ms, TE = 2, 4.3 ms. DWI sequence: TR/TE = 7,500 ms/58 ms, NEX = 4, *b*-value = 0, 600 s/mm^2, FOV = 42 cm × 42 cm. The images were processed using IDEAL Research software provided by the manufacturer to generate water-phase, fat-phase, in-phase, out-phase, along with R2* and fat fraction (FF) maps.

2.3 MRI-Acquired Fat Measurements

2.3.1 Measurement of VAT and SAT

VAT and SAT were semiautomatically measured on the axial FF images by Image J (National Institutes of Health, USA), as previously described (23–25). The abdominal fat was determined at the L1–L2 level and did not include intestinal loops.

VAT was defined as intraabdominal fat (including intraperitoneal and retroperitoneal fat) bound by parietal peritoneum or transversalis fascia, excluding the vertebral column and the paraspinal muscles (23). The SAT was defined as fat superficial to the abdominal and back muscles (24). Area (cm^2) and FF (%) of VAT and SAT were assessed. Meanwhile, visceral/subcutaneous adipose tissue area ratio (V/S) was also calculated.

In this study, the abdominal fat was measured at the L1/L2 level according to Kuk et al. (25). Most studies used the L4/L5 lumbar vertebra level for intraabdominal fat measurements to capture the highest percentage of body fat (7, 26). However, studies have shown that the cross-sectional areas of VAT and SAT measured at each level of T12-L5 are highly correlated with the volume of overall VAT and SAT (r = 0.89–0.98) (27). In addition, VAT significantly associated with metabolic syndrome regardless of measurement site (25, 28). Importantly, it was found that the VAT measured at L1–L2 level may predict the overall VAT more than L4/L5 level (28).

The MRI fat fraction map calculated from IDEAI-IQ was the most practical method to accurately assess ectopic fat deposition (29). In addition, several ROI sampling methods to assess ectopic fat deposition have been used in previous studies (1, 4, 24). Due to spatial heterogeneity in ectopic fat deposition, differences in the ROI sampling method can lead to fat quantification variability. To avoid such occurrences, a 3D semiautomatic segmentation method was used to assess the whole-hepatic FF, whole-pancreatic FF, and intramuscular FF in scan ranging.

2.3.2 Measurement of Hepatic FF

On the postprocessing platform (Intellispace Portal, ISP, Philips, Holland), the software algorithm defined the margins of the liver in three dimensions, and the whole liver was semiautomatically traced on FF maps. If the margins needed tweaking, the operator made corrections; if margins were included within the contours of liver segmentation, the main portal vein, inferior vena cava, and the gallbladder were manually removed. Liver was then segmented, and the whole hepatic FF was automatically calculated (**Figure 1A**).

2.3.3 Measurement of Intramuscular FF

The same methodology was used to measure intramuscular FF, which referred to the arithmetic mean FF of bilateral paraspinal muscles (including erector spinae and multifidus muscles) in the scanning range (30) (**Figure 1B**).

2.3.4 Measurement of Pancreatic FF

The whole pancreatic FF was calculated using the same method avoiding extrapancreatic adipose tissue and vessel (**Figure 1C**).

2.3.5 Measurement of pPAT

pPAT was defined as the fat depot anteriorly seen from the anterior surface of the left lobe of the liver to the linea alba (31). pPAT area and FF were measured using the spline contour region of interest (ROI) method (**Figure 1D**).

2.4 Inter- and Intraobserver Variability

The intra- and interobserver variability of the MRI-acquired fat measurements was determined by repeated analysis of 30 randomly selected patients more than 4 weeks apart by the same observer and by the MRI-acquired fat measurements of the same patient by a second independent observer. Two radiologists were blinded to the grouping.

2.5 Cardiometabolic Risk Factors

Trained examiners measured systolic and diastolic blood pressure (BP) twice with 1–2 min intervals in the left arm after participants were seated and rested for 5 min; the mean values of the last two readings were used for analysis. Hypertension was indicated by systolic blood pressure ≥140 mmHg, diastolic blood pressure ≥90 mmHg, or on current antihypertensive drug treatment. Blood samples were collected in the morning from patients who fasted for ≥12 h prior to the blood draw. Fasting plasma glucose (FPG), TG, total cholesterol (TC), high-density lipoprotein cholesterol (HDL-C), and low-density lipoprotein cholesterol (LDL-C) were evaluated from the blood samples. FPG ≥7.0 mmol/L or current use of insulin or an oral hypoglycemic agent were classified as T2DM (32). High TG was defined as triglycerides ≥2.3 mmol/L (200 mg/dl) or on drug treatment to reduce lipid concentrations. High TC was defined as total cholesterol ≥6.2 mmol/L (240 mg/dl) or on drug treatment

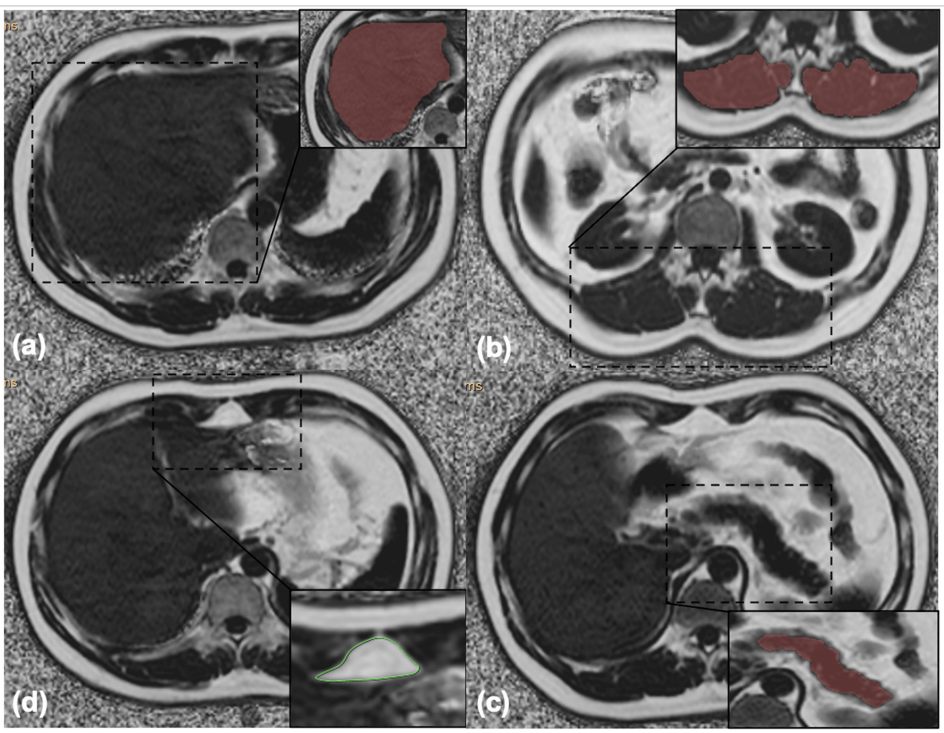

FIGURE 1 | **(A)** Liver segmentation: the whole hepatic fat fraction was calculated using the 3D semiautomatic segmentation method. **(B)** Muscle segmentation: the arithmetic mean fat fraction of bilateral paraspinal muscles (including erector spinae and multifidus muscles) in the scanning range was calculated as the intramuscular fat fraction using the 3D semiautomatic segmentation method. **(C)** Pancreas segmentation: the whole pancreatic fat fraction was calculated using the 3D semiautomatic segmentation method. **(D)** Preperitoneal adipose tissue measurement: the area and the fat fraction of preperitoneal adipose tissue were measured using spline contour region of interest (ROI) method.

to reduce lipid concentrations. The cutoff point of HDL-cholesterol concentrations for defining low HDL-C was less than 1.0 mmol/L (40 mg/dl) or on drug treatment to elevate HDL-C. The cutoff point of LDL-C concentrations for defining high LDL-C was more than but equal to 4.1 mmol/L (160 mg/dl) or on drug treatment to decrease LDL-C. CCRFs were defined as the presence of two or more of these risk factors.

2.6 Covariates

Weight was measured in kilograms and height in meters that were then used to calculate BMI (weight divided by the square of height). Data on smoking status, alcohol intake, and family history of cardiometabolic risk factors were collected by an on-site physician-administered medical and through physical history interview during the regular clinical examination. For women, information on postmenopausal status was also collected.

2.7 Statistical Analysis

All data were analyzed using SPSS Ver.25.0 (SPSS Inc., Chicago, IL, USA). The Kolmogorow–Smironov test was used to test the normality of the variables in overall subjects. Normally distributed data were expressed as means ± standard deviations, and nonnormally distributed data were expressed as medians and ranges (25th and 75th percentiles). Nominal data were expressed as the frequency with percentage.

The comparisons between men and women were determined using two-sided *t*-tests or the nonparametric Mann–Whitney *U*-test for normally or nonnormally distributed data for continuous variables and the chi-square test for categorical variables.

The intraclass correlation coefficient (ICC) is defined as the ratio of the between-group variance to the total variance and is used to check the consistency or reliability of data measured multiple times on the same subject. The closer the ICC value is to 1, the closer the multiple measurement data of the same research object is, the higher the consistency of measurement results is. The generally accepted ICC evaluation criteria are as follows (33), when it is below 0.40, the consistency is poor; when it is between 0.40 and 0.59, the consistency is fair; when it is between 0.60 and 0.74, the consistency is good; and when it is between 0.75 and 1.00, the consistency is excellent.

To assess the associations between fat measurements, age and sex-adjusted correlation coefficients (r) among various MRI-acquired fat depots were computed. Correlation coefficients were interpreted as follows: weak, 0–0.4; moderate, 0.4–0.7; and strong, 0.7–1.0. This method was also performed to evaluate correlations of MRI-acquired fat depots and each cardiometabolic risk factor. Age-adjusted correlation analyses stratified by sex were also conducted.

Multivariable logistic and linear regression models were performed for the dichotomous and continuous outcomes, respectively. Odds ratios (ORs) from the logistic regression models and β-coefficients from the linear regression models, and their 95% CIs were used to assess the associations of the cardiometabolic risk factors per 1-SD increase in various MRI-acquired fat depots. Multivariable adjustments included age, sex, smoking status, current alcohol use, postmenopausal status (women only), and family history of cardiometabolic risk factors. Furthermore, an additional model-specific adjustment was applied for models as follows: antihypertensive treatment for the systolic and diastolic blood pressure models; diabetes treatment for the FPG model; lipid-lowering treatment for the TG, TC, HDL-C, and LDL-C models.

Additional models evaluated the associations between MRI-acquired fat depots and cardiometabolic risk factors after further adjustment for BMI to explore whether the associations persisted after adjusting for generalized obesity. Sex-specific multivariable-adjusted regression models were also performed.

A two-tailed $p < 0.05$ was considered to be statistically significant.

3 RESULTS

3.1 Study Sample Characteristics

A total of 320 patients (148 men and 172 women) with a median age of 59 years (range from 19 to 90 years) and a mean BMI of 24.68 kg/m^2 were finally included in the study. The patients' demographic, clinical, lifestyle characteristics, and family history of cardiometabolic risk factors are shown in **Table 1**. Hypertension had the highest prevalence rate (40.94%), while high LDL-C was the least prevalent (9.38%). The prevalence rate of CCRFs was 33.75%. For fat measurements, men had higher BMI, higher SAT area, higher VAT area, higher VAT FF, higher V/S, higher pancreatic FF, higher intramuscular FF, and higher pPAT area, but lower SAT FF compared with women (all $p < 0.05$). For cardiometabolic risk factors, men had a higher prevalence of hypertension, T2DM, high TC, and low HDL-C than women (all $p < 0.05$).

3.2 Consistency Analysis

The data consistency is shown in **Table S1**. The ICC values were more than 0.9, which suggested good inter-observer and intra-observer agreement.

3.3 Correlations Among Fat Measurements

Age- and sex-adjusted correlation coefficients among fat measurements are shown in **Table 2**. Most of the fat measurements were associated with each other ($p < 0.05$), but the strengths of these associations greatly varied. Both hepatic FF and pancreatic FF had the strongest correlations with VAT area (correlation coefficients (r) = 0.313 and 0.367, respectively), but intramuscular FF had the strongest correlation with SAT area (r-value = 0.226). Different from other MRI-acquired fat depots, VAT FF, V/S, and pPAT area were not correlated with BMI ($p > 0.05$). However, the patterns of the correlations slightly varied in both men and women **(Table S2).**

3.4 Correlations Between the MRI-Acquired Fat Measurements and Cardiometabolic Risk Factors

The age- and sex-adjusted correlations between MRI-acquired fat measurements and continuous cardiometabolic risk factors are described in **Table 3**. For all patients, SAT area was significantly correlated with most continuous cardiometabolic risk factors (r-value ranging 0.124 to −0.203), except for TC and LDL-C, and had the strongest correlations with HDL-C (r-value = −0.203). SAT FF was only significantly correlated with HDL-C (r-value = −0.120). VAT area was significantly correlated with all continuous cardiometabolic risk factors (r-values ranging from 0.124 to 0.285) and had the strongest correlations with FPG (r-value = 0.285). V/S was only significantly correlated with FPG (r-value = 0.205). Hepatic FF was significantly correlated with most continuous cardiometabolic risk factors (r-value ranging from 0.140 to 0.306), except for systolic BP and HDL-C, and had the strongest correlations with TG (r-value = 0.306). Pancreatic FF was significantly correlated with FPG, TG, and HDL-C (r-value = 0.245, 0.183, and −0.193, respectively). VAT FF, intramuscular FF, and pPAT area were not significantly correlated with any continuous cardiometabolic risk factors (all $p > 0.05$). Preperitoneal FF was significantly correlated with diastolic BP, FPG, and TG (r-value = 0.118, 0.122, and 0.174, respectively).

The results of correlations between the MRI-acquired fat measurements and cardiometabolic risk factors in the sex-stratified analyses are described in **Supplementary Material I**.

3.5 MRI-Acquired Fat Measurements as Factor Correlate With Continuous Cardiometabolic Risk Factors

Results of linear regression analyses for various MRI-acquired fat measurements for continuous cardiometabolic risk factors are shown in **Table 4**. For all patients, higher VAT area was associated with higher systolic BP, higher diastolic BP, higher FPG, higher TG, lower HDL-C, and higher LDL-C (β = 0.025, 0.018, 0.005, 0.003, −0.001, and 0.001, respectively). After further adjustment for BMI, these correlations continued to exist, except for systolic and diastolic BP (**Figures 2A, B**). Higher V/S was associated with higher systolic BP and higher FPG (β = 1.823 and 0.178, respectively), but the correlation was no longer significant after further adjustment for BMI. Higher hepatic FF was associated with higher FPG, higher TG, higher TC, lower HDL-C, and higher LDL-C (β = 0.080, 0.080, 0.038, −0.014, and 0.033, respectively), and after further adjustment for BMI, these correlations were still significant, except for HDL-C (**Figures 2C, D**). Although higher SAT area, higher SAT FF, higher pancreatic FF, and higher pPAT FF have a greater risk of multiple continuous cardiometabolic risk factors, after further adjustment for BMI, most of the correlations were not significant. Also, higher VAT FF, higher intramuscular FF, and higher pPAT area were not associated with any continuous cardiometabolic risk factors. The significant relationships between various MRI-acquired fat measurements and continuous cardiometabolic risk factors independent of BMI are shown in **Figure 3**.

TABLE 1 | Clinical characteristics of the study subjects.

Characteristics	Overall patients (*n* = 320)	Men (*n* = 148)	Women (*n* = 172)	*p*-value (men vs. women)
Demographics				
Age (years)	59 (50, 65)	58 (48, 65)	60 (52, 66)	0.577
Height (m)	1.67 (1.61, 1.74)	1.74 (1.70, 1.77)	1.62 (1.60, 1.65)	<0.001
Weight (kg)	68 (60, 77)	75 (70, 82)	62.25 (58.5, 69.00)	<0.001
BMI (kg/m^2)	24.68 ± 3.04	25.18 ± 2.80	24.25 ± 3.16	0.006
MRI-acquired fat measurements				
SAT area (cm^2)	121.68 (94.60, 158.95)	106.19 (79.99, 126.74)	145.00 (114.65, 187.11)	<0.001
SAT FF (%)	81.73 (77.95, 84.45)	79.02 (75.62, 82.10)	83.80 (80.97, 85.67)	<0.001
VAT area (cm^2)	141.98 (100.77, 190.36)	176.63 (128.86, 222.26)	125.22 (86.50, 162.68)	<0.001
VAT FF (%)	77.77 (74.22, 80.54)	78.37 (74.85, 80.94)	77.25 (73.69, 79.88)	0.045
V/S	1.04 (0.71, 1.62)	1.65 (1.16, 2.27)	0.76 (0.61, 1.00)	<0.001
Hepatic FF (%)	3.70 (2.70, 6.40)	3.90 (2.90, 6.60)	3.55 (2.60, 6.25)	0.415
Pancreatic FF (%)	8.10 (5.00, 12.30)	8.50 (5.60, 13.50)	7.35 (4.40, 11.65)	0.010
Intramuscular FF (%)	5.15 (3.80, 7.45)	6.00 (4.45, 8.15)	4.20 (3.30, 5.65)	<0.001
pPAT FF (%)	85.10 (80.25, 89.00)	85.20 (80.25, 88.95)	85.00 (80.15, 89.00)	0.662
pPAT area (cm^2)	2.79 (1.97, 4.00)	3.35 (2.38, 4.71)	2.44 (1.73, 3.41)	<0.001
Cardiometabolic risk factors				
Systolic BP (mmHg)	121 (120, 140)	130 (120,140)	120 (110, 130)	0.001
Diastolic BP (mmHg)	80 (70, 80)	80 (74, 86)	80 (70, 80)	<0.001
FPG (mmol/L)	5.16 (4.73, 5.86)	5.33 (4.80, 6.29)	5.06 (4.68, 5.55)	0.014
TG (mmol/L)	1.24 (0.89, 1.88)	1.25 (0.93, 1.92)	1.22 (0.85, 1.83)	0.357
TC (mmol/L)	4.88 (4.24, 5.59)	4.62 (3.95, 5.26)	5.12 (4.44, 5.88)	<0.001
HDL-C (mmol/L)	1.27 (0.97, 1.47)	1.10 (0.91, 1.38)	1.39 (1.17, 1.61)	<0.001
LDL-C (mmol/L)	2.66 (2.20, 3.21)	2.58 (2.14, 3.10)	2.79 (2.36, 3.35)	0.008
Hypertension (*n* (%))	131 (40.94)	70 (47.29)	61 (35.47)	0.032
T2DM (*n* (%))	66 (20.63)	38 (25.68)	28 (16.28)	0.038
High TG (*n* (%))	71 (22.19)	31 (20.95)	40 (22.47)	0.620
High TC (*n* (%))	55 (17.19)	16 (10.81)	39 (21.91)	0.004
Low HDL-C (*n* (%))	104 (32.50)	63 (42.57)	41 (23.84)	<0.001
High LDL-C (*n* (%))	30 (9.38)	11 (7.43)	19 (10.67)	0.265
CCRFs (*n* (%))	108 (33.75)	61 (41.22)	47 (27.33)	0.171
Lifestyle factors				
Smoking status				<0.001
Current smoker (*n* (%))	30 (9.38)	29 (19.59)	1 (0.58)	–
Former smoker (*n* (%))	8 (2.50)	8 (5.41)	0 (0)	–
Never smoker (*n* (%))	282 (88.13)	111 (75.00)	171 (99.42)	–
Current alcohol use (*n* (%))	14 (4.38)	13 (8.78)	1 (0.58)	< 0.001
Antihypertensive treatment (*n* (%))	107 (33.44)	56 (37.84)	51 (29.65)	0.620
Diabetes treatment (*n* (%))	45 (14.16)	27 (18.24)	18 (10.47)	0.238
Lipid-lowering treatment (*n* (%))	27 (8.44)	13 (2.03)	14 (8.14)	0.836
Postmenopausal status (*n* (%))	–	–	138 (80.23)	–
Family history of cardiometabolic risk factors (*n* (%))	25 (7.81)	11 (7.43)	14 (8.14)	0.814

Data were expressed as mean ± SD, median (25th and 75th percentiles) (due to nonnormal distribution), or n (%).

BMI, body mass index; SAT, subcutaneous adipose tissue; FF, fat fraction; VAT, visceral adipose tissue; V/S, visceral/subcutaneous adipose tissue area ratio; pPAT, preperitoneal adipose tissue; BP, blood pressure; FPG, fasting plasma glucose; TG, triglycerides; TC, total cholesterol; HDL-C, high-density lipoprotein cholesterol; LDL-C, low-density lipoprotein cholesterol; T2DM, type 2 diabetes mellitus; CCRFs, clustering of cardiometabolic risk factors.

The results of MRI-acquired fat measurements as factor correlate with continuous cardiometabolic risk factors in the sex-stratified analyses are described in **Supplementary Material II**.

3.6 MRI-Acquired Fat Measurements as Factor Correlate With Dichotomous Cardiometabolic Risk Factors

Results of sex-specific logistic regression analyses for various MRI-acquired fat measurements for dichotomous cardiometabolic risk factors are shown in **Table 5**. For all patients, VAT area was significantly associated with increased risk of hypertension, T2DM, high TG, low HDL-C, and CCRFs, with ORs of 1.009, 1.005, 1.007, 1.007, 1.007, and 1.011, respectively. After further adjustment for BMI, these correlations continued to be significant (**Figures 4A, B**). V/S was significantly associated with increased risk of hypertension, T2DM, low HDL-C, and CCRFs, with ORs of 1.597, 1.780, 1.519, and 1.865, respectively. After further adjustment for BMI, these correlations continued to be significant (**Figure 4C, D**). Hepatic FF was significantly associated with increased risk of hypertension, T2DM, high TG, high TC, low HDL-C, high LDL-C, and CCRFs, with ORs of 1.063, 1.072, 1.144, 1.102, 1.094, 1.136, and 1.144, respectively. After further adjustment for BMI, these correlations continued to be significant, except for hypertension, T2DM, and low HDL-C (**Figures 4E, F**).

TABLE 2 | The age- and sex-adjusted correlations among MRI-acquired fat measurements in all patients.

MRI-acquired fat measurements	SAT area	SAT FF	VAT area	VAT FF	V/S	Hepatic FF	Pancreatic FF	Intramuscular FF	pPAT area	pPAT FF
SAT area	–	0.644**	0.380**	–0.072	–0.140*	0.300**	0.293*	0.226**	0.118*	0.155*
SAT FF	0.644**	–	0.313**	–0.128*	–0.123*	0.250**	0.205*	0.099	0.086	0.280**
VAT area	0.380*	0.313**	–	–0.059	0.762**	0.313**	0.367**	0.118*	0.091	0.186*
VAT FF	–0.072	–0.128*	–0.059	–	0.046	–0.041	–0.052	–0.042	0.003	0.026
V/S	–0.140**	–0.123*	0.762**	0.046	–	0.075	0.136*	–0.019	0.007	0.058
Hepatic FF	0.300**	0.250**	0.313**	–0.041	0.075	–	0.205**	0.097	0.044	0.186**
Pancreatic FF	0.293**	0.205*	0.367**	–0.052	0.136*	0.205**	–	0.169*	0.069	0.154**
Intramuscular FF	0.226**	0.099	0.118*	–0.042	–0.019	0.097	0.169*	–	0.043	0.048
pPAT area	0.118*	0.086	0.091	0.003	0.007	0.044	0.069	0.043	–	0.010
pPAT FF	0.155*	0.280**	0.186*	0.026	0.058	0.186**	0.154**	0.048	0.010	–

*$p < 0.05$; **$p < 0.001$.

BMI, body mass index; SAT, subcutaneous adipose tissue; FF, fat fraction; VAT, visceral adipose tissue; V/S, visceral/subcutaneous adipose tissue area ratio; pPAT, preperitoneal adipose tissue.

TABLE 3 | The age- and sex-adjusted correlations between MRI-acquired fat measurements and continuous cardiometabolic risk factors.

MRI-acquired fat measurements	Continuous cardiometabolic risk factors						
	Systolic BP	Diastolic BP	FPG	TG	TC	HDL-C	LDL-C
SAT area	0.126*	0.128*	0.124*	0.177*	0.042	–0.203**	0.060
SAT FF	–0.010	0.087	0.083	0.106	0.027	–0.120*	0.052
VAT area	0.150*	0.207**	0.285**	0.210**	0.124*	–0.185*	0.154*
VAT FF	0.019	0.001	–0.038	–0.027	–0.100	–0.064	–0.079
V/S	0.088	0.081	0.205**	0.064	0.050	–0.081	0.068
Hepatic FF	0.099	0.140*	0.168*	0.306**	0.148*	–0.104	0.156*
Pancreatic FF	0.081	0.097	0.245**	0.183*	0.045	–0.193*	0.071
Intramuscular FF	0.108	0.086	–0.021	0.030	0.020	–0.068	0.031
pPAT area	0.048	0.043	0.099	0.071	0.013	0.020	0.022
pPAT FF	0.096	0.118*	0.122*	0.174*	0.045	–0.101	0.032

*$p < 0.05$; **$p < 0.001$.

BMI, body mass index; SAT, subcutaneous adipose tissue; FF, fat fraction; VAT, visceral adipose tissue; V/S, visceral/subcutaneous adipose tissue area ratio; pPAT, preperitoneal adipose tissue; BP, blood pressure; FPG, fasting plasma glucose; TG, triglycerides; TC, total cholesterol; HDL-C, high-density lipoprotein cholesterol; LDL-C, low-density lipoprotein cholesterol.

Pancreatic FF was significantly associated with increased risk of hypertension, T2DM, high TG, low HDL-C, and CCRFs, with ORs of 1.066, 1.088, 1.062, 1.056, and 1.100, respectively. After further adjustment for BMI, these correlations continued to be significant (**Figures 4G, H**). pPAT FF was significantly associated with increased risk of high TG, high TC, low HDL-C, and CCRFs, with ORs of 1.075, 1.052, 1.062, and 1.075, respectively. After further adjustment for BMI, these correlations continued to be significant, except for high TG (**Figures 4I, J**). Although SAT area and SAT FF were significantly associated with increased risk of multiple dichotomous cardiometabolic risk factors, after further adjustment for BMI, most of the correlations were not significant. In addition, VAT FF, intramuscular FF, and pPAT area were not significantly associated with any dichotomous cardiometabolic risk factors. The significant relationships between various MRI-acquired fat measurements and dichotomous cardiometabolic risk factors independent of BMI were shown in **Figure 5**.

The results of MRI-acquired fat measurements as factor correlate with dichotomous cardiometabolic risk factors in the sex-stratified analyses are described in **Supplementary Material II**.

4 DISCUSSION

In this study, the main observations can be summarized as follows: firstly, most fat measurements were associated with each other, but the strength of these associations greatly varied. Both hepatic FF and pancreatic FF had the strongest correlations with the VAT area, but intramuscular FF had the strongest correlation with SAT area. Secondly, we found VAT area, V/S, hepatic fat, and pancreatic fat rather than SAT area were significantly associated with multiple cardiometabolic risk factors. However, the patterns of these correlations varied by sex and specific risk factors. In addition, VAT and SAT FF were only significantly associated with multiple cardiometabolic risk factors in women. Finally, we also identified differential correlations between pPAT and cardiometabolic risk factors, especially in men.

4.1 SAT, VAT, and Cardiometabolic Risk Factors

It is well documented that SAT and VAT are associated with different cardiometabolic risk factors; in particular, a more adverse effect may be attributed to VAT (8, 23, 32). Similarly, in this study, we found that VAT area and V/S were significantly

TABLE 4 | Correlations between continuous cardiometabolic risk factors and MRI-acquired fat measurements.

Risk factors	Model type[a]	Effect size	SAT area	SAT FF	VAT area	VAT FF	V/S	Hepatic FF	Pancreatic FF	Intramuscular FF	pPAT area	pPAT FF
Systolic BP[b]	MV	*β* (95% CI)	–	–	0.025 (0.003, 0.046)	–	1.823 (0.245, 3.401)	–	–	–	–	–
		p-value	–	–	0.023	–	0.024	–	–	–	–	–
	MV+BMI	*β* (95% CI)	–	–	–	–	–	–	–	–	–	–
		p-value	–	–	–	–	–	–	–	–	–	–
Diastolic BP[b]	MV	*β* (95% CI)	–	–	0.018 (0.005, 0.030)	–	–	–	–	–	–	–
		p-value	–	–	0.006	–	–	–	–	–	–	–
	MV+BMI	*β* (95% CI)	–	–	–	–	–	–	–	–	–	–
		p-value	–	–	–	–	–	–	–	–	–	–
FPG[c]	MV	*β* (95% CI)	0.004 (0.001, 0.007)	–	0.005 (0.003, 0.007)	–	0.178 (0.022, 0.333)	0.080 (0.037, 0.122)	0.033 (0.011, 0.055)	–	–	0.016 (0.000, 0.032)
		p-value	0.017	–	<0.001	–	0.025	<0.001	0.003	–	–	0.048
	MV+BMI	*β* (95% CI)	–	–	0.003 (0.001, 0.006)	–	–	0.048 (0.003, 0.093)	–	–	–	–
		p-value	–	–	0.006	–	–	0.036	–	–	–	–
TG[d]	MV	*β* (95% CI)	0.004 (0.001, 0.006)	–	0.003 (0.001, 0.004)	–	–	0.090 (0.053, 0.108)	0.020 (0.007, 0.033)	–	–	0.017 (0.007, 0.028)
		p-value	0.002	–	<0.001	–	–	<0.001	0.002	–	–	0.002
	MV+BMI	*β* (95% CI)	–	–	0.002 (0.000, 0.003)	–	–	0.068 (0.038, 0.098)	–	–	–	0.013 (0.002, 0.024)
		p-value	–	–	0.031	–	–	<0.001	–	–	–	0.016
TC[d]	MV	*β* (95% CI)	–	–	–	–	–	0.038 (0.006,0.070)	–	–	–	–
		p-value	–	–	–	–	–	0.020	–	–	–	–
	MV+BMI	*β* (95% CI)	–	–	–	–	–	0.038 (0.006,0.070)	–	–	–	–
		p-value	–	–	–	–	–	0.020	–	–	–	–
HDL-C[d]	MV	*β* (95% CI)	−0.002 (−0.003, −0.001)	−0.009 (−0.018, −0.001)	−0.001 (−0.002 −0.001)	–	–	−0.014 (−0.164, −0.018)	−0.009 (−0.014, −0.0014	–	–	–
		p-value	<0.001	0.037	<0.001	–	–	0.015	0.001	–	–	–
	MV+BMI	*β* (95% CI)	−0.002 (−0.003, −0.001)	–	−0.001 (−0.002 −0.001)	–	–	–	–	–	–	–
		p-value	<0.001	–	<0.001	–	–	–	–	–	–	–
LDL-C[d]	MV	*β* (95% CI)	–	–	0.001 (0.000, 0.003)	–	–	0.033 (0.008, 0.058)	–	–	–	–
		p-value	–	–	0.018	–	–	0.009	–	–	–	–
	MV+BMI	*β* (95% CI)	–	–	0.001 (0.000, 0.003)	–	–	0.033 (0.008, 0.058)	–	–	–	–
		p-value	–	–	0.018	–	–	0.009	–	–	–	–

Blank cells indicate that the MRI-acquired fat depots were not selected using the forward selection regression procedure.
[a]MV model included the following covariates: age, sex, smoking status, current alcohol use, family history of cardiometabolic risk factors, and postmenopausal status (women only). BMI was additionally adjusted for in the models labeled "MV+BMI model."
[b]Antihypertensive treatment was included as a covariate for systolic and diastolic blood pressure models.
[c]Diabetes treatment was included as a covariate for the fasting plasma glucose model.
[d]Lipid-lowering treatment was included as a covariate for TG, TC, HDL-C, and LDL-C models.
BMI, body mass index; SAT, subcutaneous adipose tissue; FF, fat fraction; VAT, visceral adipose tissue; V/S, visceral/subcutaneous adipose tissue area ratio; pPAT, preperitoneal adipose tissue; BP, blood pressure; FPG, fasting plasma glucose; TG, triglycerides; TC, total cholesterol; HDL-C, high-density lipoprotein cholesterol; LDL-C, low-density lipoprotein cholesterol.

associated with multiple cardiometabolic risk factors and these correlations remained after adjustment for BMI. SAT area was significantly associated with multiple cardiometabolic risk factors, but these correlations were no longer statistically significant after adjustment for BMI. Thus, the VAT area has a pathological role in developing cardiometabolic risk factors, whereas SAT area does not contribute to cardiometabolic risk factors beyond a measure of generalized adiposity. This could be due to several reasons: first, VAT has metabolic properties that are distinct from SAT (34); second, VAT is constantly releasing free fatty acids into portal circulation. Excessive intake of free fatty acids by hepatocytes can lead to insulin resistance and systemic hyperinsulinemia (35); third, excess VAT can lead to leptin resistance and increased leptin secretion (36); and fourth, VAT is a marker of ectopic fat deposition (24, 37). Our result suggests that VAT may be a better indicator for the risk of cardiometabolic risk factors. Thus, reduced VAT deposition risk may have beneficial influences in cardiometabolic risk factor control.

Interestingly, our results revealed that SAT FF and VAT FF were associated with multiple cardiometabolic risk factors independent of BMI in women. Adipose tissue with higher lipid content and lipolytic activity can increase systemic free fatty acids (38) and can also induce whole-body insulin resistance (39) and endothelial dysfunction (40). Thus, an increased fat fraction of adipose tissue may reflect worsening fat quality, which may concur with adipocyte hyperplasia and hypertrophy (41), eventually leading to an increased risk of cardiometabolic risk factors. To the best of our knowledge, this is the first study that assessed fat quality in VAT and SAT FF *via* MRI fat fraction maps to explore the association between VAT and SAT FF and cardiometabolic risk factors. Nevertheless, this finding was only observed in women in the present study. It may be explained by sexual dimorphism in the process of adipose tissue remodeling (41) and cardioprotective effects of estrogen before and after menopause (42). The precise mechanism for these sex differences is not clear and remains to be elucidated in future studies.

4.2 Hepatic Fat and Cardiometabolic Risk Factors

Several studies have reported that hepatic fat was associated with hypertension, T2DM, and dyslipidemia (32, 43). This may be explained by the joint role of VAT and hepatic fat in glucose and lipid metabolism (44). Because the portal vein drains most VAT, the hyperlipolytic state of adipocytes associated with VAT exposes the liver to high concentrations of free fatty acids and glycerol, leading to several impairments in liver metabolism, such as increased production of triglyceride-rich lipoproteins, as well as increased production of hepatic glucose (45). In the presence of hepatic steatosis, various intermediate lipid moieties generated during triglyceride synthesis (e.g., diacylglycerols and ceramide) have been shown to promote lipotoxicity and enhance hepatic insulin resistance (46, 47), likely by inhibiting insulin signaling pathways (48, 49). In addition, hepatic steatosis can accelerate the lipolysis and the secretion of very low-density lipoprotein, leading to dyslipidemia (50). Decreased insulin

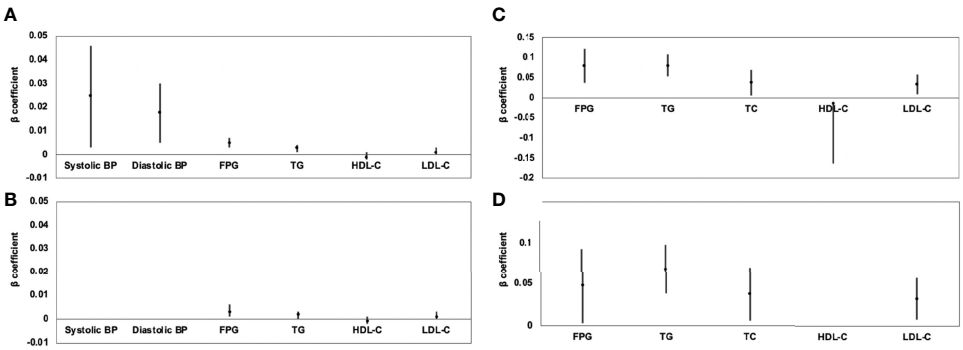

FIGURE 2 | Association of VAT area **(A)** and hepatic FF **(C)** with continuous cardiometabolic risk factors and further adjustment for BMI **(B, D)** expressed by β-coefficients and 95% confidence intervals. For all patients, higher VAT area was associated with higher systolic BP, higher diastolic BP, higher FPG, higher TG, lower HDL-C, and higher LDL-C **(A)**; after further adjustment for BMI, these correlations continued to exist, except for systolic and diastolic BP **(B)**. Higher hepatic FF was associated with higher FPG, higher TG, higher TC, lower HDL-C, and higher LDL-C **(C)**; after further adjustment for BMI, these correlations were still significant, except for HDL-C **(D)**.

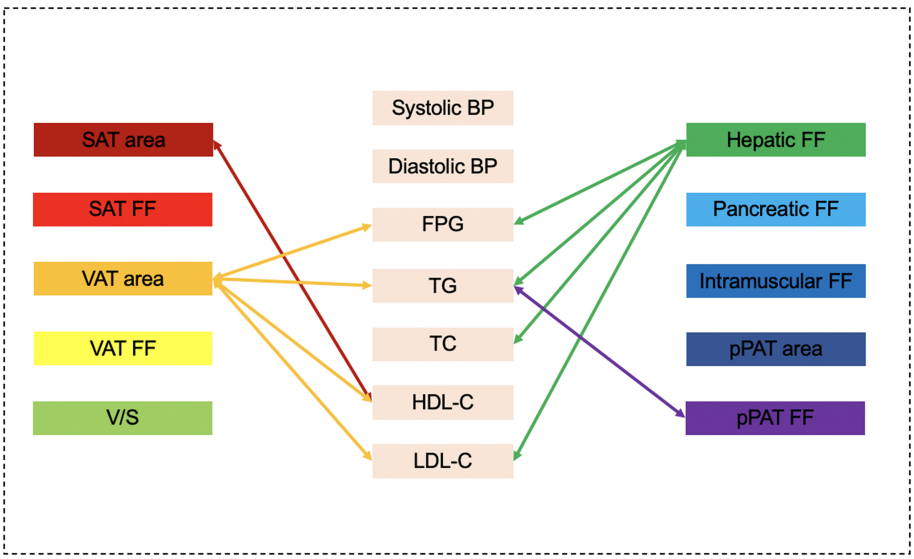

FIGURE 3 | Graphical summary of the important correlates between various MRI-acquired fat measurements and continuous cardiometabolic risk factors independent of BMI shown in the present study. VAT area and hepatic fat were significantly associated with multiple continuous cardiometabolic risk factors.

sensitivity and increased glucose production lead to decreased islet cell function and hyperglycemia (51), as well as increased release of inflammatory factors (such as IL-6, TNF-α, and C-reactive protein) (52, 53). Similarly, our study showed that hepatic FF was mainly associated with multiple cardiometabolic risk factors related to dyslipidemia traits, including high TG, high TC, high LDL-C, as well as measures of FPG, TG, TC, and LDL-C independent of BMI. This finding supports that hepatic fat may be associated with glycolipid regulation and metabolism. Thus, hepatic fat may be useful to identify those with higher risk of cardiometabolic risk factors.

4.3 Pancreatic Fat and Cardiometabolic Risk Factors

It was found that pancreatic fat bears adverse effects on the cardiometabolic health. In agreement with findings from previous studies, we found that pancreatic FF was significantly associated with multiple cardiometabolic risk factors, including hypertension, T2DM, high TG, low HDL-C, and CCRFs, and the correlations remained after adjustment for BMI. Zhou et al. (54) reported similarly a significant correlation of pancreatic steatosis with abdominal obesity, hypertension, hyperglycemia, and hypertriglyceridemia in a Chinese population. Bi et al. (55)

TABLE 5 | Correlations between dichotomous cardiometabolic risk factors and MRI-acquired fat measurements.

Risk factors	Model type[a]	Effect size	SAT area	SAT FF	VAT area	VAT FF	V/S	Hepatic FF	Pancreatic FF	Intramuscular FF	pPAT area	pPAT FF
Hypertension	MV	OR (95% CI)	1.009 (1.004, 1.015)	–	1.009 (1.005, 1.013)	0.999 (0.997, 1.001)	1.597 (1.142, 2.232)	1.063 (1.000, 1.130)	1.066 (1.028, 1.106)	–	1.041 (0.992, 1.092)	–
		p-value	0.001	–	<0.001	0.430	0.006	0.049	0.001	–	0.103	–
	MV+BMI	OR (95% CI)	–	–	1.005 (1.002, 1.009)	–	1.413 (1.027 1.945)	–	1.046 (1.009, 1.083)	–	–	–
		p-value	–	–	0.006	–	0.034	–	0.013	–	–	–
T2DM	MV	OR (95% CI)	–	–	1.007 (1.003, 1.011)	–	1.780 (1.247, 2.541)	1.072 (1.003, 1.147)	1.088 (1.049, 1.128)	–	–	–
		p-value	–	–	<0.001	–	0.001	0.041	<0.001	–	–	–
	MV+BMI	OR (95% CI)	–	–	1.007 (1.003, 1.011)	–	1.693 (1.185, 2.420	–	1.088 (1.049, 1.128)	–	–	–
		p-value	–	–	<0.001	–	0.004	–	<0.001	–	–	–
High TG	MV	OR (95% CI)	1.006 (1.001, 1.011)	–	1.007 (1.003, 1.010)	–	–	1.144 (1.073, 1.221)	1.062 (1.029, 1.095)	–	–	1.075 (1.027, 1.126)
		p-value	0.025	–	0.001	–	–	<0.001	<0.001	–	–	0.002
	MV+BMI	OR (95% CI)	–	–	1.005 (1.001, 1.008)	–	–	1.113 (1.040, 1.191)	1.051 (1.018, 1.084)	–	–	–
		p-value	–	–	0.017	–	–	0.002	0.002	–	–	–
High TC	MV	OR (95% CI)	–	–	–	–	–	1.102 (1.031, 1.177)	–	–	–	1.052 (1.003, 1.104)
		p-value	–	–	–	–	–	0.004	–	–	–	0.036
	MV+BMI	OR (95% CI)	–	–	–	–	–	1.102 (1.031, 1.177)	–	–	–	1.052 (1.003, 1.104)
		p-value	–	–	–	–	–	0.004	–	–	–	0.036
Low HDL-C	MV	OR (95% CI)	1.009 (1.003, 1.014)	1.073 (1.016, 1.133)	1.007 (1.003, 1.011)	–	1.519 (1.076, 2.144)	1.094 (1.027, 1.165)	1.056 (1.025, 1.089)	–	–	1.062 (1.020, 1.105)
		p-value	0.002	0.012	<0.001	–	0.018	0.005	<0.001	–	–	0.003
	MV+BMI	OR (95% CI)	1.009 (1.003, 1.014)	–	1.007 (1.003, 1.011)	–	1.420 (1.006, 2.004)	–	1.046 (1.015, 1.079)	–	–	1.044 (1.003, 1.087)
		p-value	0.002	–	<0.001	–	0.046	–	0.004	–	–	0.036
High LDL-C	MV	OR (95% CI)	–	–	–	–	–	1.136 (1.052, 1.227)	–	–	–	–
		p-value	–	–	–	–	–	0.001	–	–	–	–
	MV+BMI	OR (95% CI)	–	–	–	–	–	1.136 (1.052, 1.227)	–	–	–	–
		p-value	–	–	–	–	–	0.001	–	–	–	–
CCRFs	MV	OR (95% CI)	1.008 (1.003, 1.013)	–	1.011 (1.007, 1.015)	–	1.865 (1.330, 2.614)	1.144 (1.073, 1.221)	1.100 (1.061, 1.140)	–	–	1.075 (1.034, 1.118)
		p-value	0.003	–	<0.001	–	<0.001	<0.001	<0.001	–	–	<0.001
	MV+BMI	OR (95% CI)	–	–	1.011 (1.007, 1.015)	–	1.675 (1.191, 2.356)	1.102 (1.030, 1.179)	1.084 (1.038, 1.238)	–	–	1.050 (1.009, 1.092)
		p-value	–	–	<0.001	–	0.003	0.005	0.005	–	–	0.016

Blank cells indicate that the MRI-acquired fat depots were not selected via the forward LR selection regression procedure.

[a]MV model included the following covariates: age, sex, smoking status, current alcohol use, family history of cardiometabolic risk factors, and postmenopausal status (women only); BMI was additionally adjusted for in the models labeled "MV+BMI model."

BMI, body mass index; SAT, subcutaneous adipose tissue; FF, fat fraction; VAT, visceral adipose tissue; V/S, visceral/subcutaneous adipose tissue area ratio; pPAT, prepentoneal adipose tissue; BP, blood pressure; FPG, fasting plasma glucose; TG, triglycerides; TC, total cholesterol; HDL-C, high-density lipoprotein cholesterol; LDL-C, low-density lipoprotein cholesterol; T2DM, type 2 diabetes mellitus; CCRFs, clustering of cardiometabolic risk factors.

systematically reviewed the association between pancreatic steatosis and metabolic comorbidities and indicated that pancreatic steatosis was significantly associated with an increased risk of metabolic syndrome and its components. However, the results in the literature showing correlations between pancreatic FF and cardiometabolic risk factors are often inconsistent, as previous studies found no significant differences in pancreatic fat fraction among subjects with normal glucose tolerance, prediabetes, and T2DM (56). These inconsistencies may be related to the small sample size, heterogeneous distribution of pancreatic fat, and genetic factors. Different from previous studies, pancreatic fat was more accurately evaluated using the 3D semiautomatic segmentation method in MRI fat fraction map in our study because of avoiding the effects of the heterogeneous distribution of pancreatic fat. Our results further confirm that assessment and monitoring of pancreatic fat may be used in the prediction of cardiometabolic risk factors and their early prevention.

4.4 Intramuscular Fat and Cardiometabolic Risk Factors

As with other ectopic fat depots, ectopic muscle fat has the potential of impairing insulin action through the inhibition of insulin signaling by lipotoxic diacylglycerols and ceramide and cause insulin resistance (57). Also, secretions of skeletal muscle adipocytes are able to impair insulin action and signaling of muscle fibers (58). In addition, T cells and macrophages accumulate in skeletal muscle fat of mice with diet-induced obesity. T cells and macrophages further impair metabolic functions of skeletal muscle cells through a paracrine mechanism (59). Yet, we found that it was not significantly correlated with any cardiometabolic risk factors (except for diastolic BP in women) in our study, which may be because diet and exercise can individually affect intramuscular FF (60). Further studies are required to address the role of intramuscular FF on cardiometabolic risk factors.

4.5 pPAT and Cardiometabolic Risk Factors

pPAT is a less-explored abdominal depot, and its nature has been debated. Although pPAT has sometimes been defined as VAT, it is actually SAT that is not located intraperitoneally and is connected to the systemic circulation rather than the portal circulation. Compared with VAT and SAT, adipose-derived stem/stromal cells derived from pPAT revealed highest capacity to generate new adipocytes by adipogenesis and low proinflammatory profile (61). Nevertheless, pPAT behaves like VAT and is correlated positively with hypertension, dyslipidemia, insulin resistance, cardiovascular disease risks, and obesity (5, 31). Compared with previous research, we found that pPAT area was significantly associated with hypertension, T2DM, high TG, low-HDL-C, CCRFs, and measures of TG and HDL-C independent of BMI in men rather than women. pPAT FF was significantly associated with low HDL-C and a measure of TG in women and CCRFs in men. Yet, the precise mechanism for this sex difference for pPAT is not clear. pPAT may play an important role in the occurrence and

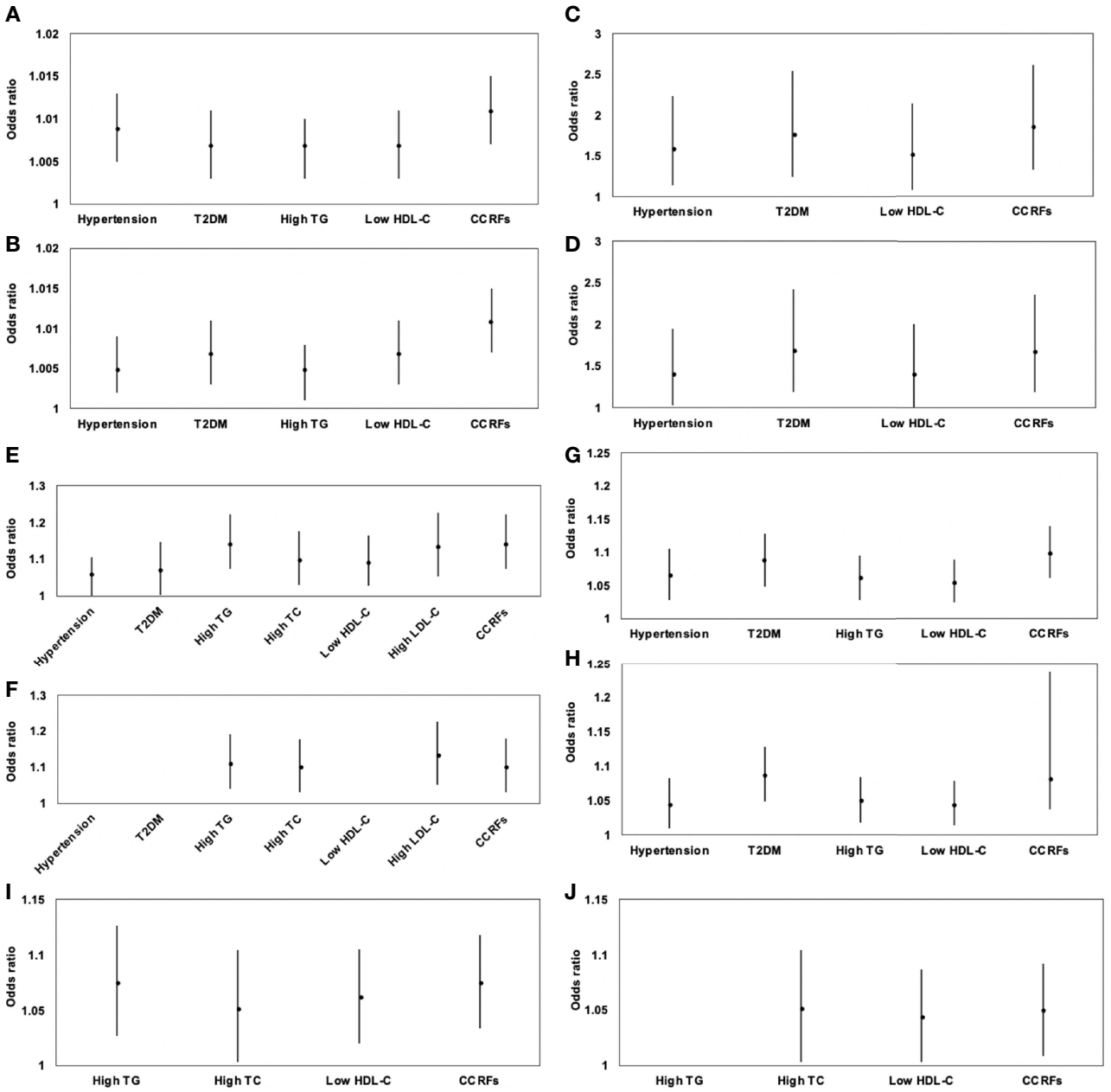

FIGURE 4 | Association of VAT area **(A)**, V/S **(C)**, hepatic FF **(E)**, pancreatic FF **(G)**, and pPAT FF **(I)** with dichotomous cardiometabolic risk factors and further adjustment for BMI **(B**, **D**, **F**, **H**, **J)** expressed by odds ratios and 95% confidence intervals. VAT area was significantly associated with increased risk of hypertension, T2DM, high TG, low HDL-C, and CCRFs **(A)**; after further adjustment for BMI, these correlations continued to be significant **(B)**. V/S was significantly associated with increased risk of hypertension, T2DM, low HDL-C, and CCRFs **(C)**. After further adjustment for BMI, these correlations continued to be significant **(D)**. Hepatic FF was significantly associated with increased risk of hypertension, T2DM, high TG, high TC, low HDL-C, high LDL-C, and CCRFs **(E)**; after further adjustment for BMI, these correlations continued to be significant, except for hypertension, T2DM, and low HDL-C **(F)**. Pancreatic FF was significantly associated with increased risk of hypertension, T2DM, high TG, low HDL-C, and CCRFs **(G)**; after further adjustment for BMI, these correlations continued to be significant **(H)**. pPAT FF was significantly associated with increased risk of high TG, high TC, low HDL-C, and CCRFs **(I)**; after further adjustment for BMI, these correlations continued to be significant, except for high TG **(J)**.

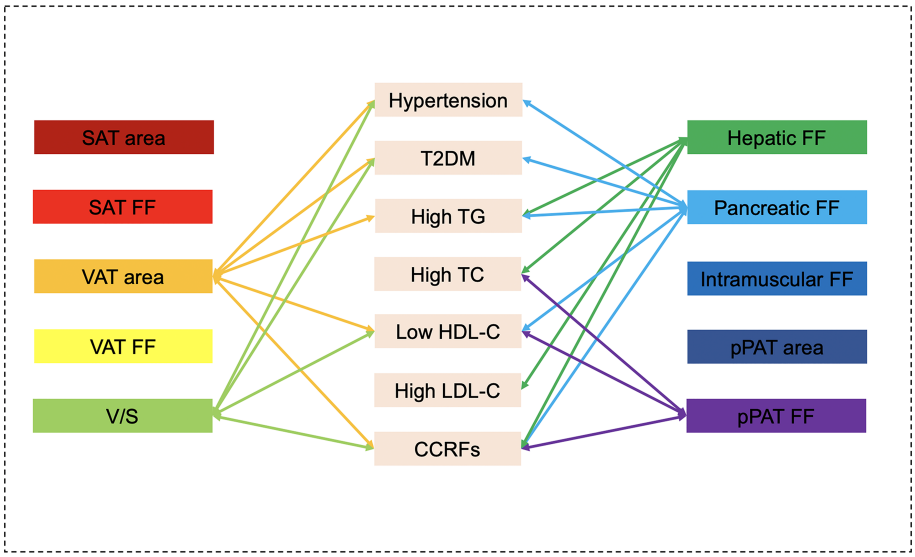

FIGURE 5 | Graphical summary of the important correlates between various MR-acquired fat measurements and dichotomous cardiometabolic risk factors independent of BMI shown in the present study. VAT area, V/S, hepatic fat, pancreatic fat, and pPAT were significantly associated with multiple dichotomous cardiometabolic risk factors.

development of cardiovascular metabolic risk factors and the underlying mechanism remains to be elucidated in the future studies.

Our results showed that there was a BMI-independent association between ectopic fat depots and cardiometabolic risk factors, suggesting that ectopic fat depots might be more adequate indicators for the evaluation of cardiometabolic risk factors because BMI can neither reflect the regional body fat distribution nor distinguish between muscle and adipose tissue. Importantly, obesity is heterogeneity. Between 10% and 30% of obese individuals (defined by BMI) have been characterized as metabolically healthy obese. Yet, some nonobese individuals show evidence of metabolic complications typical for obesity (62). Thus, the use of BMI is only an approximation of the evaluation of the amount of fat mass and is inadequate to reflect the association between the obesity and cardiometabolic risk factors. However, the results about the strength of associations of fat depots and BMI with cardiometabolic risk factors are still inconsistent. Previous studies found that associations between fat depots and cardiometabolic risk factors were not independent of BMI and BMI seemed stronger associated with some indicators of cardiometabolic risk factors (63–65). Several potential factors may have contributed to this inconsistency. First, sex-related differences: some studies showed that BMI may adequately capture cardiometabolic risk in men but not in women (63, 64). The exact mechanism underlying the sex difference is not known but may be related to the greater effect of free fatty acid mobilization from VAT into the hepatic portal circulation in women than in men (66). Second, racial/ethnic disparities: for each 1-unit increase in BMI, Asians had higher risk of hypertension and T2DM compared with non-Hispanic whites, Hispanics, and non-Hispanic blacks, indicating incremental weight gain in Asians is more detrimental (67). In addition, there are also racial/ethnic differences in prevalence of obesity, VAT, and NAFLD (68, 69). Due to genetic differences, NAFLD occurs not only in people with high BMI but also in people with low BMI. It was found that the G allele of PNPLA3 rs738409 was associated with increased risk of NAFLD in Asians (70) as well as in nonobese or lean individuals (71). Previous study showed that PNPLA3 polymorphism was associated with the rate of T2DM in Japanese population (72).

4.6 Strengths and Limitations

This study has some strengths. Initially, MRI fat fraction map was used to accurately evaluate the ectopic fat deposition in different parts of the abdomen, including VAT, SAT, pPAT, whole hepatic fat, whole pancreatic fat, and bilateral paraspinous muscle fat. Furthermore, it was the first paper to evaluate the VAT FF and SAT FF by MRI fat fraction map to explore the associations between VAT FF, SAT FF and cardiovascular metabolic risk factors. Finally, the subgroup analysis of gender stratification was performed to explore the gender differences in the association between various ectopic fat deposition and cardiovascular metabolic risk factors.

This study has several limitations. First, this was a cross-sectional study; thus, the causal relationship of MRI-acquired fat depots with cardiometabolic risk factors cannot be inferred. Well-designed prospective cohort studies are needed to elaborate the causality in the future. Second, selection bias was a major limitation of this study. Third, the sample size was small because of high cost of MRI measurements as well as strict exclusion criteria. Fourth, the intramuscular FFs in most previous studies were measured at L3 level (1, 3); however, we measured it using 3D semiautomatic segmentation ranging from

T4 to T12. Fifth, data on mortality and exercise factors were unavailable in the current study; thus, we cannot evaluate these factors" influences on the observed associations. Sixth, compared with Asians, other ethnicities could have different types of ectopic fat deposition; therefore, the associations with cardiometabolic risk factors may be different, which limits the generalization of the presented findings beyond Asian populations. Sixth, FPG ≥7.0 mmol/L was used as a single diagnostic criterion for T2DM (32), which may have an impact on the results. Finally, those should be considered preliminary results. We will continue to conduct combined analysis of significant various MRI-acquired fat depots according to sex and specific risk factors, and then obtain personalized models in prediction, early prevention or therapeutic intervention of cardiometabolic risk factors in the further study.

4.7 Clinical Implications

This study adds an important facet to the obesity study spectrum in which, within the heterogeneity of abdominal fat distribution, VAT, hepatic fat, pancreatic fat, and pPAT were associated with cardiovascular metabolic risk factors independently of BMI. Regarding the preventive significance of this study, our findings support that only making recommendations based on BMI may lead to misclassification of high-risk individuals as "metabolically healthy obesity." Those who are "metabolically unhealthy nonobese" and "metabolically unhealthy normal weight" will be misclassified as people with lower risk. Our study also demonstrated the patterns of these correlations varied by gender, supporting that gender should be considered an important point in classifying individuals at the high risk of cardiometabolic abnormalities. In addition, the result showed that pPAT should not be overlooked as pathologic fat depots contributing to cardiometabolic risk factors. It is necessary to explore the biology of various ectopic fat storage to precisely decipher the pathogenicity of excess adiposity in future studies.

5 CONCLUSION

VAT area, V/S, hepatic fat, pancreatic fat, and pPAT rather than SAT area were significantly associated with multiple cardiometabolic risk factors. However, the patterns of these correlations varied by sex and specific risk factors. In addition, VAT and SAT FF were only significantly associated with multiple cardiometabolic risk factors in women. These findings broaden the understanding of the association between ectopic fat deposition and cardiometabolic risk factors, thus further clarifying the heterogeneity of obesity.

DATA AVAILABILITY STATEMENT

The original contributions presented in the study are included in the article/**Supplementary Material**. Further inquiries can be directed to the corresponding author.

ETHICS STATEMENT

The studies involving human participants were reviewed and approved by the First Affiliated Hospital of Dalian Medical University. Written informed consent for participation was not required for this study in accordance with the national legislation and the institutional requirements. Written informed consent was not obtained from the individual(s) for the publication of any potentially identifiable images or data included in this article.

AUTHOR CONTRIBUTIONS

Data analysis and interpretation, study design, manuscript writing, and manuscript approval were performed by Q-HZ, L-HX, L-HC, YZ, H-NZ, and A-LL, and they are accountable for all aspects of the work. MRI data and clinical data analysis and interpretation, statistical analysis, and manuscript approval were performed by J-HL, A-LC, YJ, and NW. MRI data analysis and manuscript approval were performed by Q-WS and A-LL. Statistical analysis and manuscript approval were performed by L-ZX. All authors read and approved the final manuscript.

SUPPLEMENTARY MATERIAL

The Supplementary Material for this article can be found online at: https://www.frontiersin.org/articles/10.3389/fendo.2022.820023/full#supplementary-material

REFERENCES

1. Pieńkowska J, Brzeska B, Kaszubowski M, Kozak O, Jankowska A, Szurowska E. MRI Assessment of Ectopic Fat Accumulation in Pancreas, Liver and Skeletal Muscle in Patients With Obesity, Overweight and Normal BMI in Correlation With the Presence of Central Obesity and Metabolic Syndrome. *Diabetes Metab Syndr Obes* (2019) 12:623–36. doi: 10.2147/DMSO.S194690
2. Yeoh AJ, Pedley A, Rosenquist KJ, Hoffmann U, Fox CS. The Association Between Subcutaneous Fat Density and the Propensity to Store Fat Viscerally. *J Clin Endocrinol Metab* (2015) 100:E1056–64. doi: 10.1210/jc.2014-4032
3. Granados A, Gebremariam A, Gidding SS, Terry JG, Carr JJ, Steffen LM, et al. Association of Abdominal Muscle Composition With Prediabetes and Diabetes: The CARDIA Study. *Diabetes Obes Metab* (2019) 21:267–75. doi: 10.1111/dom.13513
4. Chen J, Duan S, Ma J, Wang R, Chen J, Liu X, et al. MRI-Determined Liver Fat Correlates With Risk of Metabolic Syndrome in Patients With Nonalcoholic Fatty Liver Disease. *Eur J Gastroenterol Hepatol* (2020) 32:754–61. doi: 10.1097/MEG.0000000000001688
5. Bi X, Loo YT, Henry CJ. Ultrasound Measurement of Intraabdominal Fat Thickness as a Predictor of Insulin Resistance and Low HDL Cholesterol in Asians. *Nutrition* (2018) 55-56:99–103. doi: 10.1016/j.nut.2018.04.003
6. Tu AW, Humphries KH, Lear SA. Longitudinal Changes in Visceral and Subcutaneous Adipose Tissue and Metabolic Syndrome: Results From the

Multicultural Community Health Assessment Trial (M-CHAT). *Diabetes Metab Syndr* (2017) 2:S957–61. doi: 10.1016/j.dsx.2017.07.022
7. Chen P, Hou X, Hu G, Wei L, Jiao L, Wang H, et al. Abdominal Subcutaneous Adipose Tissue: A Favorable Adipose Depot for Diabetes? *Cardiovasc Diabetol* (2018) 17:93. doi: 10.1186/s12933-018-0734-8
8. Hou X, Chen P, Hu G, Wei L, Jiao L, Wang H, et al. Abdominal Subcutaneous Fat: A Favorable or Nonfunctional Fat Depot for Glucose Metabolism in Chinese Adults? *Obes (Silver Spring)* (2018) 26:1078–87. doi: 10.1002/oby.22183
9. Lorbeer R, Rospleszcz S, Schlett CL, Heber SD, Machann J, Thorand B, et al. Correlation of MRI-Derived Adipose Tissue Measurements and Anthropometric Markers With Prevalent Hypertension in the Community. *J Hypertens* (2018) 36:1555–62. doi: 10.1097/HJH.0000000000001741
10. Blüher M. Metabolically Healthy Obesity. *Endocr Rev* (2020) 41:405–20. doi: 10.1210/endrev/bnaa004
11. Ferrara D, Montecucco F, Dallegri F, Carbone F. Impact of Different Ectopic Fat Depots on Cardiovascular and Metabolic Diseases. *J Cell Physiol* (2019) 234:21630–41. doi: 10.1002/jcp.28821
12. Omura-Ohata Y, Son C, Makino H, Koezuka R, Tochiya M, Tamanaha T, et al. Efficacy of Visceral Fat Estimation by Dual Bioelectrical Impedance Analysis in Detecting Cardiovascular Risk Factors in Patients With Type 2 Diabetes. *Cardiovasc Diabetol* (2019) 18:137. doi: 10.1186/s12933-019-0941-y
13. Froelich MF, Fugmann M, Daldrup CL, Hetterich H, Coppenrath E, Saam T, et al. Measurement of Total and Visceral Fat Mass in Young Adult Women: A Comparison of MRI With Anthropometric Measurements With and Without Bioelectrical Impedance Analysis. *Br J Radiol* (2020) 93:20190874. doi: 10.1259/bjr.20190874
14. Nyangasa MA, Buck C, Kelm S, Sheikh MA, Brackmann KL, Hebestreit A. Association Between Cardiometabolic Risk Factors and Body Mass Index, Waist Circumferences and Body Fat in a Zanzibari Cross-Sectional Study. *BMJ Open* (2019) 9:e025397. doi: 10.1136/bmjopen-2018-025397
15. Yan Y, Liu J, Zhao X, Cheng H, Huang G, Mi J. Abdominal Visceral and Subcutaneous Adipose Tissues in Association With Cardiometabolic Risk in Children and Adolescents: The China Child and Adolescent Cardiovascular Health (CCACH) Study. *BMJ Open Diabetes Res Care* (2019) 7:e000824. doi: 10.1136/bmjdrc-2019-000824
16. Wang M, Luo Y, Cai H, Xu L, Huang M, Li C, et al. Prediction of Type 2 Diabetes Mellitus Using Noninvasive MRI Quantitation of Visceral Abdominal Adiposity Tissue Volume. *Quant Imaging Med Surg* (2019) 9:1076–86. doi: 10.21037/qims.2019.06.01
17. Wang LS, Zhang B, Wang HJ, Guo CL, Zhang YP, Zhang JG, et al. Analysis on Cardio-Metabolic Related Risk Factors in Farmers of 15 Provinces in China. *Zhonghua Liu Xing Bing Xue Za Zhi* (2018) 39:1239–43. doi: 10.3760/cma.j.issn.0254-6450.2018.09.018
18. Catanzaro R, Cuffari B, Italia A, Marotta F. Exploring the Metabolic Syndrome: Nonalcoholic Fatty Pancreas Disease. *World J Gastroenterol* (2016) 22:7660–75. doi: 10.3748/wjg.v22.i34.7660
19. Kim SR, Lerman LO. Diagnostic Imaging in the Management of Patients With Metabolic Syndrome. *Transl Res* (2018) 194:1–18. doi: 10.1016/j.trsl.2017.10.009
20. Hu X, Xiong Q, Xu Y, Zhang X, Xiao Y, Ma X, et al. Contribution of Maternal Diabetes to Visceral Fat Accumulation in Offspring. *Obes Res Clin Pract* (2018) 12:426–31. doi: 10.1016/j.orcp.2018.07.005
21. Bao Y, Ma X, Yang R, Wang F, Hao Y, Dou J, et al. Inverse Relationship Between Serum Osteocalcin Levels and Visceral Fat Area in Chinese Men. *J Clin Endocrinol Metab* (2013) 98:345–51. doi: 10.1210/jc.2012-2906
22. van Vugt JL, Levolger S, Gharbharan A, Koek M, Niessen WJ, Burger JW, et al. A Comparative Study of Software Programmes for Cross-Sectional Skeletal Muscle and Adipose Tissue Measurements on Abdominal Computed Tomography Scans of Rectal Cancer Patients. *J Cachexia Sarcopenia Muscle* (2017) 8:285–97. doi: 10.1002/jcsm.12158
23. Tang L, Zhang F, Tong N. The Association of Visceral Adipose Tissue and Subcutaneous Adipose Tissue With Metabolic Risk Factors in a Large Population of Chinese Adults. *Clin Endocrinol (Oxf)* (2016) 85:46–53. doi: 10.1111/cen.13013
24. Tirkes T, Jeon CY, Li L, Joon AY, Seltman TA, Sankar M, et al. Association of Pancreatic Steatosis With Chronic Pancreatitis, Obesity, and Type 2 Diabetes Mellitus. *Pancreas* (2019) 48:420–6. doi: 10.1097/MPA.0000000000001252
25. Kuk JL, Church TS, Blair SN, Ross R. Does Measurement Site for Visceral and Abdominal Subcutaneous Adipose Tissue Alter Associations With the Metabolic Syndrome? *Diabetes Care* (2006) 29:679–84. doi: 10.2337/diacare.29.03.06.dc05-1500
26. Onishi Y, Hayashi T, Sato KK, Leonetti DL, Kahn SE, Fujimoto WY, et al. Natural History of Impaired Glucose Tolerance in Japanese Americans: Change in Visceral Adiposity is Associated With Remission From Impaired Glucose Tolerance to Normal Glucose Tolerance. *Diabetes Res Clin Pract* (2018) 142:303–11. doi: 10.1016/j.diabres.2018.05.045
27. Cheng X, Zhang Y, Wang C, Deng W, Wang L, Duanmu Y, et al. The Optimal Anatomic Site for a Single Slice to Estimate the Total Volume of Visceral Adipose Tissue by Using the Quantitative Computed Tomography (QCT) in Chinese Population. *Eur J Clin Nutr* (2018) 72:1567–75. doi: 10.1038/s41430-018-0122-1
28. Kuk JL, Church TS, Blair SN, Ross R. Measurement Site and the Association Between Visceral and Abdominal Subcutaneous Adipose Tissue With Metabolic Risk in Women. *Obes (Silver Spring)* (2010) 18:1336–40. doi: 10.1038/oby.2009.414
29. Reeder SB, Hu HH, Sirlin CB. Proton Density Fat-Fraction: A Standardized MR-Based Biomarker of Tissue Fat Concentration. *J Magn Reson Imaging* (2012) 36:1011–4. doi: 10.1002/jmri.23741
30. Oguz SH, İdilman I, Helvaci N, Guzelce EC, Eyupoglu D, Karcaaltincaba M, et al. Tissue Fat Quantification by Magnetic Resonance Imaging: Proton Density Fat Fraction in Polycystic Ovary Syndrome. *Reprod BioMed Online* (2020) 41:329–34. doi: 10.1016/j.rbmo.2020.04.024
31. Parente DB, Oliveira Neto JA, Brasil PEAA, Paiva FF, Ravani JPR, Gomes MB, et al. Preperitoneal Fat as a non-Invasive Marker of Increased Risk of Severe non-Alcoholic Fatty Liver Disease in Patients With Type 2 Diabetes. *J Gastroenterol Hepatol* (2018) 33:511–7. doi: 10.1111/jgh.13903
32. Lee JJ, Pedley A, Hoffmann U, Massaro JM, Levy D, Long MT. Visceral and Intrahepatic Fat Are Associated With Cardiometabolic Risk Factors Above Other Ectopic Fat Depots: The Framingham Heart Study. *Am J Med* (2018) 131:684–92.e12. doi: 10.1016/j.amjmed.2018.02.002
33. Cicchetti, Domenic V. Guidelines, Criteria, and Rules of Thumb for Evaluating Normed and Standardized Assessment Instruments in Psychology. *psychol Assess* (1994) 6:284–90. doi: 10.1037/1040-3590.6.4.284
34. Neeland IJ, Ross R, Després JP, Matsuzawa Y, Yamashita S, Shai I, et al. Visceral and Ectopic Fat, Atherosclerosis, and Cardiometabolic Disease: A Position Statement. *Lancet Diabetes Endocrinol* (2019) 7:715–25. doi: 10.1016/S2213-8587(19)30084-1
35. Odegaard JI, Chawla A. Pleiotropic Actions of Insulin Resistance and Inflammation in Metabolic Homeostasis. *Science* (2013) 339:172–7. doi: 10.1126/science.1230721
36. Ouchi N, Parker JL, Lugus JJ, Walsh K. Adipokines in Inflammation and Metabolic Disease. *Nat Rev Immunol* (2011) 11:85–97. doi: 10.1038/nri2921
37. Lee JJ, Pedley A, Hoffmann U, Massaro JM, Fox CS. Association of Changes in Abdominal Fat Quantity and Quality With Incident Cardiovascular Disease Risk Factors. *J Am Coll Cardiol* (2016) 68:1509–21. doi: 10.1016/j.jacc.2016.06.067
38. Koutsari C, Jensen MD. Thematic Review Series: Patient-Oriented Research. Free Fatty Acid Metabolism in Human Obesity. *J Lipid Res* (2006) 47:1643–50. doi: 10.1194/jlr.R600011-JLR200
39. Verboven K, Wouters K, Gaens K, Hansen D, Bijnen M, Wetzels S, et al. Abdominal Subcutaneous and Visceral Adipocyte Size, Lipolysis and Inflammation Relate to Insulin Resistance in Male Obese Humans. *Sci Rep* (2018) 8:4677. doi: 10.1038/s41598-018-22962-x
40. Antonio-Villa NE, Bello-Chavolla OY, Vargas-Vázquez A, Mehta R, Fermín-Martínez CA, Martagón-Rosado AJ, et al. Increased Visceral Fat Accumulation Modifies the Effect of Insulin Resistance on Arterial Stiffness and Hypertension Risk. *Nutr Metab Cardiovasc Dis* (2021) 31:506–17. doi: 10.1016/j.numecd.2020.09.031
41. Tchoukalova YD, Koutsari C, Karpyak MV, Votruba SB, Wendland E, Jensen MD. Subcutaneous Adipocyte Size and Body Fat Distribution. *Am J Clin Nutr* (2008) 87:56–63. doi: 10.1093/ajcn/87.1.56
42. Wells GL. Cardiovascular Risk Factors: Does Sex Matter? *Curr Vasc Pharmacol* (2016) 14:452–7. doi: 10.2174/1570161114666160722113116
43. Du T, Sun X, Yuan G, Zhou X, Lu H, Lin X, et al. Sex Differences in the Impact of Nonalcoholic Fatty Liver Disease on Cardiovascular Risk Factors. *Nutr Metab Cardiovasc Dis* (2017) 27(1):63–9. doi: 10.1016/j.numecd.2016.10.004

44. Abraham TM, Pedley A, Massaro JM, Hoffmann U, Fox CS. Association Between Visceral and Subcutaneous Adipose Depots and Incident Cardiovascular Disease Risk Factors. *Circulation* (2015) 132:1639–47. doi: 10.1161/CIRCULATIONAHA.114.015000
45. Neeland IJ, Hughes C, Ayers CR, Malloy CR, Jin ES. Effects of Visceral Adiposity on Glycerol Pathways in Gluconeogenesis. *Metabolism* (2017) 67:80–9. doi: 10.1016/j.metabol.2016.11.008
46. Perry RJ, Samuel VT, Petersen KF, Shulman GI. The Role of Hepatic Lipids in Hepatic Insulin Resistance and Type 2 Diabetes. *Nature* (2014) 510:84–91. doi: 10.1038/nature13478
47. Choromańska B, Myśliwiec P, Razak Hady H, Dadan J, Myśliwiec H, Chabowski A, et al. Metabolic Syndrome is Associated With Ceramide Accumulation in Visceral Adipose Tissue of Women With Morbid Obesity. *Obes (Silver Spring)* (2019) 27:444–53. doi: 10.1002/oby.22405
48. Luukkonen PK, Zhou Y, Sädevirta S, Leivonen M, Arola J, Orešič M, et al. Hepatic Ceramides Dissociate Steatosis and Insulin Resistance in Patients With non-Alcoholic Fatty Liver Disease. *J Hepatol* (2016) 64:1167–75. doi: 10.1016/j.jhep.2016.01.002
49. Chavez JA, Summers SA. A Ceramide-Centric View of Insulin Resistance. *Cell Metab* (2012) 15:585–94. doi: 10.1016/j.cmet.2012.04.002
50. Yazıcı D, Sezer H. Insulin Resistance, Obesity and Lipotoxicity. *Adv Exp Med Biol* (2017) 960:277–304. doi: 10.1007/978-3-319-48382-5_12
51. Valenti L, Bugianesi E, Pajvani U, Targher G. Nonalcoholic Fatty Liver Disease: Cause or Consequence of Type 2 Diabetes? *Liver Int* (2016) 36:1563–79. doi: 10.1111/liv.13185
52. Uemura H, Katsuura-Kamano S, Yamaguchi M, Bahari T, Ishizu M, Fujioka M, et al. Relationships of Serum High-Sensitivity C-Reactive Protein and Body Size With Insulin Resistance in a Japanese Cohort. *PloS One* (2017) 12: e0178672. doi: 10.1371/journal.pone.0178672
53. Petersen MC, Shulman GI. Mechanisms of Insulin Action and Insulin Resistance. *Physiol Rev* (2018) 98:2133–223. doi: 10.1152/physrev.00063.2017
54. Zhou J, Li ML, Zhang DD, Lin HY, Dai XH, Sun XL, et al. The Correlation Between Pancreatic Steatosis and Metabolic Syndrome in a Chinese Population. *Pancreatology* (2016) 16:578–83. doi: 10.1016/j.pan.2016.03.008
55. Bi Y, Wang JL, Li ML, Zhou J, Sun XL. The Association Between Pancreas Steatosis and Metabolic Syndrome: A Systematic Review and Meta-Analysis. *Diabetes Metab Res Rev* (2019) 35:e3142. doi: 10.1002/dmrr.3142
56. Kühn JP, Berthold F, Mayerle J, Völzke H, Reeder SB, Rathmann W, et al. Pancreatic Steatosis Demonstrated at MR Imaging in the General Population: Clinical Relevance. *Radiology* (2015) 276:129–36. doi: 10.1148/radiol.15140446
57. Sachs S, Zarini S, Kahn DE, Harrison KA, Perreault L, Phang T, et al. Intermuscular Adipose Tissue Directly Modulates Skeletal Muscle Insulin Sensitivity in Humans. *Am J Physiol Endocrinol Metab* (2019) 316:E866–79. doi: 10.1152/ajpendo.00243.2018
58. Laurens C, Louche K, Sengenes C, Coué M, Langin D, Moro C, et al. Adipogenic Progenitors From Obese Human Skeletal Muscle Give Rise to Functional White Adipocytes That Contribute to Insulin Resistance. *Int J Obes (Lond)* (2016) 40:497–506. doi: 10.1038/ijo.2015.193
59. Khan IM, Perrard XY, Brunner G, Lui H, Sparks LM, Smith SR, et al. Intermuscular and Perimuscular Fat Expansion in Obesity Correlates With Skeletal Muscle T Cell and Macrophage Infiltration and Insulin Resistance. *Int J Obes (Lond)* (2015) 39:1607–18. doi: 10.1038/ijo.2015.104
60. Kawanishi N, Takagi K, Lee HC, Nakano D, Okuno T, Yokomizo T, et al. Endurance Exercise Training and High-Fat Diet Differentially Affect Composition of Diacylglycerol Molecular Species in Rat Skeletal Muscle. *Am J Physiol Regul Integr Comp Physiol* (2018) 314:R892–901. doi: 10.1152/ajpregu.00371.2017
61. Silva KR, Côrtes I, Liechocki S, Carneiro JR, Souza AA, Borojevic R, et al. Characterization of Stromal Vascular Fraction and Adipose Stem Cells From Subcutaneous, Preperitoneal and Visceral Morbidly Obese Human Adipose Tissue Depots. *PloS One* (2017) 12:e0174115. doi: 10.1371/journal.pone.0174115
62. Gustafson B, Smith U. Regulation of White Adipogenesis and its Relation to Ectopic Fat Accumulation and Cardiovascular Risk. *Atherosclerosis* (2015) 241:27–35. doi: 10.1016/j.atherosclerosis.2015.04.812
63. Kammerlander A, Lyass A, Mahoney T, Massaro J, Long M, Vasan R, et al. Sex Differences in the Associations of Visceral Adipose Tissue and Cardiometabolic and Cardiovascular Disease Risk: The Framingham Heart Study. *J Am Heart Assoc* (2021) 10:e019968. doi: 10.1161/JAHA.120.019968
64. Lv X, Zhou W, Sun J, Lin R, Ding L, Xu M, et al. Visceral Adiposity is Significantly Associated With Type 2 Diabetes in Middle-Aged and Elderly Chinese Women: A Cross-Sectional Study. *J Diabetes* (2017) 9:920–8. doi: 10.1111/1753-0407.12499
65. Therkelsen K, Pedley A, Speliotes E, Massaro J, Murabito J, Hoffmann U, et al. Intramuscular Fat and Associations With Metabolic Risk Factors in the Framingham Heart Study. *Arterioscler Thromb Vasc Biol* (2013) 33:863–70. doi: 10.1161/ATVBAHA.112.301009
66. Nielsen S, Guo Z, Johnson C, Hensrud D, Jensen M. Splanchnic Lipolysis in Human Obesity. *J Clin Invest* (2004) 113:1582–8. doi: 10.1172/JCI21047
67. Wong R, Chou C, Sinha S, Kamal A, Ahmed A. Ethnic Disparities in the Association of Body Mass Index With the Risk of Hypertension and Diabetes. *J Community Health* (2014) 39:437–45. doi: 10.1007/s10900-013-9792-8
68. Agbim U, Carr R, Pickett-Blakely O, Dagogo-Jack S. Ethnic Disparities in Adiposity: Focus on Non-Alcoholic Fatty Liver Disease, Visceral, and Generalized Obesity. *Curr Obes Rep* (2019) 8:243–54. doi: 10.1007/s13679-019-00349-x
69. Katzmarzyk P, Bray G, Greenway F, Johnson W, Newton R, Ravussin E, et al. Racial Differences in Abdominal Depot-Specific Adiposity in White and African American Adults. *Am J Clin Nutr* (2010) 91:7–15. doi: 10.3945/ajcn.2009.28136
70. Shen J, Wong G, Chan H, Chan H, Yeung D, Chan R, et al. PNPLA3 Gene Polymorphism Accounts for Fatty Liver in Community Subjects Without Metabolic Syndrome. *Aliment Pharmacol Ther* (2014) 39:532–9. doi: 10.1111/apt.12609
71. Wei J, Leung J, Loong T, Wong G, Yeung D, Chan R, et al. Prevalence and Severity of Nonalcoholic Fatty Liver Disease in Non-Obese Patients: A Population Study Using Proton-Magnetic Resonance Spectroscopy. *Am J Gastroenterol* (2015) 110:1306–14. doi: 10.1038/ajg.2015.235 quiz 15.
72. Suzuki K, Akiyama M, Ishigaki K, Kanai M, Hosoe J, Shojima N, et al. Identification of 28 New Susceptibility Loci for Type 2 Diabetes in the Japanese Population. *Nat Genet* (2019) 51:379–86. doi: 10.1038/s41588-018-0332-4

Conflict of Interest: Author L-ZX was employed by GE Healthcare, Beijing, China.

The remaining authors declare that the research was conducted in the absence of any commercial or financial relationships that could be construed as a potential conflict of interest.

Publisher's Note: All claims expressed in this article are solely those of the authors and do not necessarily represent those of their affiliated organizations, or those of the publisher, the editors and the reviewers. Any product that may be evaluated in this article, or claim that may be made by its manufacturer, is not guaranteed or endorsed by the publisher.

frontiers in Endocrinology

REVIEW
published: 31 March 2022
doi: 10.3389/fendo.2022.739882

New Insights Into the Interplay Among Autophagy, the NLRP3 Inflammasome and Inflammation in Adipose Tissue

Liyuan Zhu[1,2,3,4] *and Ling Liu*[1,2,3,4]*

[1] Department of Cardiovascular Medicine, The Second Xiangya Hospital, Central South University, Changsha, China, [2] Research Institute of Blood Lipid and Atherosclerosis, Central South University, Changsha, China, [3] Modern Cardiovascular Disease Clinical Technology Research Center of Hunan Province, Changsha, China, [4] Cardiovascular Disease Research Center of Hunan Province, Changsha, China

Obesity is a feature of metabolic syndrome with chronic inflammation in obese subjects, characterized by adipose tissue (AT) expansion, proinflammatory factor overexpression, and macrophage infiltration. Autophagy modulates inflammation in the enlargement of AT as an essential step for maintaining the balance in energy metabolism and waste elimination. Signaling originating from dysfunctional AT, such as AT containing hypertrophic adipocytes and surrounding macrophages, activates NOD-like receptor family 3 (NLRP3) inflammasome. There are interactions about altered autophagy and NLRP3 inflammasome activation during the progress in obesity. We summarize the current studies and potential mechanisms associated with autophagy and NLRP3 inflammasome in AT inflammation and aim to provide further evidence for research on obesity and obesity-related complications.

Keywords: inflammation, autophagy, inflammasome, NLRP3, adipose tissue

OPEN ACCESS

Edited by:
Matthias Blüher,
Leipzig University, Germany

Reviewed by:
Jin Young Huh,
Seoul National University, South Korea
Jun Ren,
University of Washington, United States

***Correspondence:**
Ling Liu
feliuling@csu.edu.cn

Specialty section:
This article was submitted to Obesity, a section of the journal Frontiers in Endocrinology

Received: *12 July 2021*
Accepted: *09 March 2022*
Published: *31 March 2022*

Citation:
Zhu L and Liu L (2022) New Insights Into the Interplay Among Autophagy, the NLRP3 Inflammasome and Inflammation in Adipose Tissue. Front. Endocrinol. 13:739882. doi: 10.3389/fendo.2022.739882

1 INTRODUCTION

Owing to the rapid socioeconomic development and increasingly obesogenic environments, obesity has become prevalent worldwide in recent decades (1, 2). Obesity is a serious health issue. According to the latest national surveys based on Chinese criteria of obesity, the number of obese (body mass index (BMI) ≥ 28 kg/m^2) adults has more than quadrupled and the number of overweight (BMI 24-27.9 kg/m^2) has more than doubled in China (3–5). Data also showed that 16.4% of Chinese adults were obese and another 34.3% were overweight (6).

Obesity increases the risk of several inflammation-related complications, including type 2 diabetes and insulin resistance, cardiovascular diseases, hepatic steatosis and several types of cancer. Obesity and its complications involve plenty of etiological mechanisms, including disproportionate or unbalanced food intake and energy expenditure, and a complex interplay between genetic and environmental factors that have effects on hemodynamic, neurohormonal, and metabolic regulation, leading to oxidative stress, inflammation, apoptosis and lipotoxicity (7). The pathogenic progression of obesity-related complications is exacerbated by persistent adipose tissue (AT) inflammation (8, 9). Current approaches to obesity management are mainly containing

lifestyle interventions (physical exercise and dietary modification) and non-lifestyle interventions (weight-loss medications or surgery). One recent review summarizes that natural and pharmaceutical agents display promise in alleviating endoplasmic reticulum stress and maladaptive unfolded protein response which improves obesity pathogenesis and management (10). How to effectively reduce AT inflammation is a challenging task in obesity management.

Recent research support altered (enhanced or inhibited) autophagy is major process regulating cellular metabolism and energy homeostasis, which has integrated into AT inflammation (11, 12). Obese individuals exhibited elevated release of inflammatory cytokines and raised infiltration of macrophages in WAT (white adipose tissue), including visceral white adipose tissue (vWAT) and subcutaneous white adipose tissue (sWAT) (13). The NOD-like receptor protein 3 (NLRP3) inflammasome has recently been demonstrated to detect nonmicrobial danger signals in dysfunctional AT and involved in obesity-related inflammation (14, 15). Moreover, WAT resists obesity-related inflammation through compensatory enhancement of autophagy. Thus, WAT from obese individuals presented increased levels of autophagic markers, autophagy-related genes (ATGs), microtubule-associated protein 1A/1B-light chain 3 (LC3), p62, and Beclin-1, at either gene and/or protein levels (11, 16, 17). Here, we focus on the mutual regulation and cellular mechanism between NLRP3 inflammasome and autophagy in AT during obesity.

2 ADIPOSE TISSUE COMPOSITION AND INFLAMMATION

To store extra energy and prevent ectopic lipid accumulation, AT mass expanses in two ways: hypertrophy (increasing the size of existing adipocytes) or hyperplasia (the differentiation of preadipocytes into adipocytes) (18). The quantity of adipocytes in AT is determined early in infancy and remains constant throughout maturity. The balance between hypertrophy and hyperplasia in adipocytes has a significant impact on energy metabolism in AT (19). AT is composed of various cell types in adult mammals, including adipocytes, macrophages, vascular endothelial cells, fibroblasts, preadipocytes, and other immune cells (20).

Preadipocytes develop into new adipocytes in response to sustained caloric excess, contributing to AT enlargement. For example, adipocytes with smaller lipid droplets can store lipids, convert excess free fatty acids (FFA) to triglycerides, and maintain an insulin-sensitive state. AT expansion by increasing adipogenesis can decrease cellular inflammatory cytokines and the number of hypertrophic adipocytes (21). Newly differentiated adipocytes have the potential of hypertrophy, which can grow to hundreds of microns in diameter (18). Larger adipocytes expand to the oxygen diffusion limit, resulting in cellular hypoxia. The small adipocytes gradually increase in size and contact surrounding cells, resulting in the increased extracellular matrix and mechanical pressure. When hypoxia is combined with mechanical and metabolic stress, small adipocytes enhance adipogenesis, lowering hypoxic stress and consequent inflammation in AT. It revealed that adipogenic capacity from preadipocytes enabled WAT in obese individuals to perform normal physiological functions (22).

As an endocrine organ, AT produces various proinflammatory cytokines and integrates immune signaling in dysfunctional metabolic status (23). Some cytokines, including tumor necrosis factor (TNF)-α, interleukin (IL)-1β, IL-6, IL-8, and monocyte chemotactic protein-1 (MCP-1), also indicated metabolic dysfunction of AT (24). Individuals with more hypertrophic adipocytes typically had higher levels of proinflammatory cytokines and lower levels of adiponectin and IL-10 (25, 26). Hypertrophic adipocytes drove collagen deposition and fibrosis, resulting in AT remodeling and insulin resistance (27–30). It has been suggested that FFA promotes inflammation mediated by Toll-like receptors (TLRs) in adipocytes and macrophages. FFA activated TLR 4/TLR 2, stimulated nuclear factor kappa B (NF-κB) and Jun amino-terminal kinase (JNK) signaling, induced the expression of inflammatory cytokine genes, such as TNF-α and IL-6, and aggravated insulin resistance in adipocytes and macrophages (31, 32). P38 mitogen-activated protein kinase (MARK) and Jnk were upregulated and activated in vWAT with increased numbers of hypertrophic adipocytes. The extent to which p38 MARK and Jnk were phosphorylated, particularly in vWAT, corresponded with fasting levels of triglycerides, insulin, and glucose (33). Another study confirmed that mice with AT-specific *Jnk1* deletion were protected against diet-induced insulin resistance and inflammation (34). These results indicated that TLRs were connected to cytokine activation *via* NF-κB and JNK in adipocytes and macrophages.

Crosstalk between adipocytes and adipose tissue macrophages (ATMs) leads to chronic inflammation and accelerates the inflammatory process in AT (35). First, increased FFA and chemotactic factors, for example MCP-1, derived from adipocytes can enhance the accumulation and transition of proinflammatory M1 macrophage subsets rather than anti-inflammatory M2 macrophage subsets in the expanded AT (36). For example, AT from obese mice with high-fat diet (HFD) represented increased F4/80 and *CD11b*+ macrophages and elevated IL-6 and MCP-1 levels. The high double-positive *CD11b*+ and F4/80 macrophages and inflammatory cytokines were reduced in mice through docosahexaenoic acid supplement (37). Another study showed that n-3 PUFAs added to mice with HFD prevented macrophage chemotaxis, stimulated M2 polarization, and suppressed M1 polarization in AT from *in vitro* and vivo experiments (38). Second, with increased volume and number of adipocytes, hypertrophic adipocytes have to face heavier mechanical stress and hypoxia, which further exacerbated ATMs-related inflammation (39, 40). Selective *Jnk* insufficiency in macrophages decreased ATM infiltration and maintained insulin sensitivity in mice fed HFD. Hypertrophic adipocytes triggered the release of proinflammatory cytokines and then attracted more macrophages to AT through increasing the productions of reactive oxidative species (ROS) and endogenous redox stress (41–44).

Notably, ATMs delivered proinflammatory signals to other organs, indicating a link between obesity and secondary organ damage, such as that in the liver, skeletal muscle, and pancreas (45).*In vivo* imaging studies showed that ATM migrated from the periphery of apoptotic adipocytes, such as crown-like structures, and resided in the cellular interstitium of other tissues (46) (**Figure 1**).

3 OBESITY AND AUTOPHAGY

Autophagy is an evolutionarily conserved process in all eukaryotes that transports damaged proteins and organelles to the lysosome for degradation. Autophagy is intimately involved in the development of obesity and obesity-related metabolism (47, 48) (**Figure 1**). Excessive autophagy is hypothesized to be another form of cell death known as autophagy-related cell death (49).

3.1 Autophagy and WAT Inflammation

Autophagy is associated with innate and adaptive immunity, the elimination of pathogens and intracellular waste, and the regulation of immune functions in immune and nonimmune cells, such as antigen presentation and cytokine synthesis and secretion (50, 51) (**Figure 1**). The outcome of autophagy is determined by the type of stimulus, the microenvironment, cell types, and other biological factors (52). Consistent with its role in pathogen degradation, the activation of pattern recognition receptors such as TLRs or nucleotide oligomerization domain-like receptors (NLRs) initiated autophagy by endogenously recognizing and binding microbial components, such as pathogen-associated molecular patterns (PAMPs) or damage-associated molecular patterns (DAMPs) (53). Once activated, autophagy suppresses inflammation by blocking the generation and secretion of proinflammatory molecules, including IL-1β degradation *via* autophagosomes and the direct inhibition of inflammasomes (53–56) (**Figure 1**).

The variations in autophagy between vWAT and sWAT must be investigated independently in obesity (57, 58). Kovsan et al. discovered that patients with vWAT accumulation had significantly higher mRNA levels of ATG5, LC3-I, and LC3-II than those with peripheral obesity. The researchers concluded that autophagic genes and proteins were expressed more abundantly in vWAT than in sWAT, independent of BMI or glycemic status (17). Numerous studies have examined the link between autophagy in WAT and adipocyte size in obesity (16, 17, 59). Adipocyte size was strongly correlated with ATG expression (16, 17). However, not all research has demonstrated a clear correlation between adipocyte size and adipocyte autophagic flux (16, 17, 59). Different methodologies may account for these discrepancies. The link between autophagy flux and hypertrophy in adipocytes should be further examined.

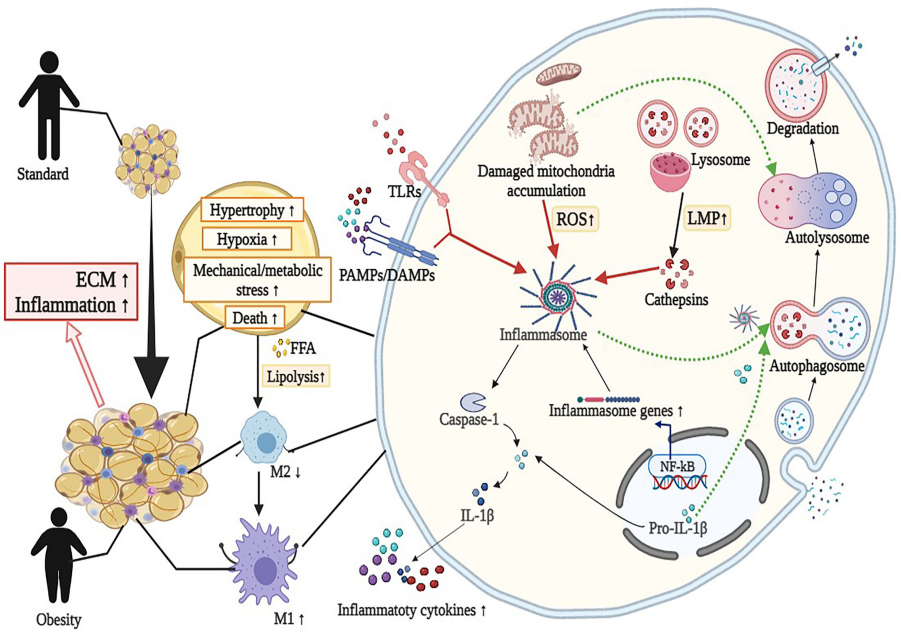

FIGURE 1 | Overview of the interaction between autophagy and NLRP3 inflammasome in adipose tissue inflammation (mainly adipocytes and macrophages). Activation of NLRP3 inflammasome by diverse metabolic stimuli (such as LPS, cathepsins, and mitochondrial dysfunction) *via* TLRs or PAMPs/DAMPs leads to metabolic and immune dysregulation, including insulin resistance, macrophage polarization (M2 to M1), hypoxia, impaired adipogenesis and increased fibrosis in adipose tissue. Detailed descriptions and explanations for each alteration can be found in Section 2 and Section 3. DAMPs, damage-associated molecular patterns; ECM, extracellular matrix; FFA, free fatty acids; IL-1β, interleukin 1β; LMP, lysosomal membrane permeabilization; LPS, lipopolysaccharide; ROS, reactive oxidative species; PAMPs, pathogen-associated molecular patterns; TLRs, Toll-like receptors. Image created with BioRender.com.

Compared to normoglycemic and lean individuals, AT from obese ones was characterized by increased autophagy, proinflammatory cytokines, and macrophage infiltration (13). *In vitro*, hypertrophic 3T3L1 adipocytes had decreased autophagy and increased inflammation. 3-Methyladenine, an autophagy inhibitor and lysosomal blocker, increased inflammatory cytokine expression (12). The outcome validated the connection in the opposite direction. The specific mechanism by which WAT alleviates nutritional stress at the molecular and cellular levels has not been determined.

3.2 Autophagy Flux Detection of WAT Fraction

Evaluating alterations of autophagy requires analyzing the autophagy flux of different cell types in WAT. Several studies have examined autophagy in mature adipocytes and stromal vascular fractions (SVFs) (11, 17, 60). Expressions of ATGs have been shown in mature adipocytes. The difference between the SVF and adipocytes depended on the analyzed ATGs, although it was unclear which component of AT influenced the overall autophagy level. Kovsan et al. discovered that visceral adipocytes had much higher gene and protein expressions of ATG5 and LC3 than subcutaneous adipocytes (17). Jansen et al. demonstrated that ATG5 and ATG7 expression levels were reduced in the SVF and adipocytes of the vWAT and sWAT of healthy individuals. However, the researchers discovered that ATG1 and ATG16L expression levels were lower in mature adipocytes than in the SVF, indicating the opposite of previously observed (11). On the contrary, Rodriguez et al. showed no significant change in Beclin-1, ATG5, or ATG7 expression between visceral adipocytes and the SVF in obese patients. Although not statistically significant, ATG7 expression tended to be higher in the SVF than in adipocytes (60). Increased autophagy in WAT was related to the metabolic state. Clinical studies have shown that the gene and protein levels of autophagic markers in sWAT and vWAT are favorably linked with plasma triglycerides, cholesterol, FFA, and the insulin resistance index but negatively correlated with adiponectin (11, 17). It was difficult to identify special cell clusters of WAT engaged in autophagy when confronted with various stress or metabolic signaling in obesity. Further study of autophagic activity should focus on cells directly isolated from AT in different metabolic states.

The polarization of macrophages and function-related autophagy in macrophages are critical for WAT immunological homeostasis. WAT of *Atg7* mutant mice fed HFD had increased the infiltration and proportion of proinflammatory M1 macrophages and impaired systemic insulin sensitivity. Inhibition autophagy *in vitro* experiment was similarly characterized by increased ROS and IL-1β in macrophages (61–63). Recent research showed that *Lc3* levels of macrophages in WAT from genetically modified obese mice were much higher than that of diet-induced obesity (DIO) animals. Additionally, the data indicated that the microenvironment of WAT could influence local ATMs by increasing autophagic flux (64). However, given that autophagy is considered to inhibit the inflammatory response (39), increased inflammation in WAT in genetically modified obese mice is perplexing.

3.3 WAT Autophagy: Animal Models

Due to the convenience and availability of animal models, systemic metabolic changes related to autophagy in WAT come from mice studies (**Table 1**). Genetic deletion of *Atg7* or *Atg5*, which were essential autophagy genes in adipocytes, resulted in the impaired differentiation of white adipocytes. *Atg7* or *Atg5* knockout mice exhibited decreased diet-induced weight gain, increased WAT volume, and improved insulin sensitivity (65, 66). Additional studies indicated that *p62* affects energy metabolism in AT by regulating the activity of mitochondria. *P62* deficiency in adipocytes resulted in decreased mitochondrial activity. The activation of *p38* targets was reduced by silencing *p62*, impacting signaling molecules that governed mitochondrial activity (67). *Bif-1* is a protein that induces membrane curvature and is involved in controlling autophagy. Bax-interacting factor 1(*Bif-1*) deficiency increases the volume of AT and contributes to the development of insulin resistance. Obesity caused by *Bif-1* deficiency decreased the expression of proteins involved in the autophagy-lysosomal pathway in adipose tissue, including *Atg9a* and *Lamp1* (68). If adipogenesis was viewed as a mechanism for the healthy expansion of WAT, *Atg*-knockout mice with favorable metabolic profiles appear contradictory. These findings indicated that *Atg5* or *Atg7* deletion in mice enhanced oxidation during metabolic activity and reduced browning and fibrosis in WAT (65, 66, 71). The capacity of increased heat production and oxygen consumption may help to explain animals remaining in an insulin-sensitive state, even when WAT adipogenesis is decreased. The aforementioned findings indicated that autophagy was required for hyperplasia. Autophagy activation in AT may be necessary for adipogenesis and healthy expansion in obesity. Although data from autophagic gene knockout animal models have been acquired, the specific regulation of autophagic processes in obesity and related metabolic disorders is unclear.

Research needs to explore the WAT autophagy state to elucidate the mechanisms of WAT dysfunction in obesity. There was impaired autophagy in WAT in DIO mice (12, 69). It reported that *Lc3-II* and *p62* protein levels were increased in the vWAT of DIO mice, while *Atg5* or *Beclin-1* levels remained unchanged. Autophagic flux and autophagosome formation were enhanced in vWAT, and vWAT lysosomal function was impaired in DIO mice (69). Another study reported that DIO mice presented inhibited autophagy, but *Lc3-II* immunofluorescence analysis was not performed (12). In addition, Nuñez et al. described decreased levels of phosphorylated mTOR and increased *Beclin-1* and *p62* in DIO mice compared to lean mice (70), and there were reduced numbers of autophagosomes in AT of calorie-restricted obese mice compared with calorie-restricted lean mice. It was concluded that obesity and caloric overfeeding are associated with the defective regulation of autophagy in AT.

Another related issue was the exact step that regulated the autophagic process and was affected by DIO. Yoshizaki et al. showed that autophagy is impaired at an early stage of autophagosome formation in DIO mice and that lysosomal inhibition led to LC3-II accumulation (12). In contrast,

TABLE 1 | Animal studies about autophagy and inflammation in obese models.

Reference	Groupings	Diet types/Intervention	Samples	Results (compared to the control group)
Zhang Y et al. (65, 66)	*ATG7*$^{-/-}$ transgenic C57BL/6 mice	HFD (60 kcal% fat) for 8 w beginning at 8 w of age	Gonadal WAT	β-oxidation, basal physical activity, LC3-I, P62 ↑; Lipolysis, leptin, triglyceride, cholesterol ↓; Absence of LC3-II
Yoshizaki et al. (12)	GFP-LC3 transgenic C57BL/6 mice	NCD (13.5% fat) or HFD (60% fat) for 16 w beginning at 8 w of age	Epididymal AT	LAMP1, LAMP2, and ATG5 ↓; LC3-II, MCP-1, IL-6, and IL-1β ↑
Mueller et al. (67)	*P62*$^{-/-}$ transgenic C57BL/6 mice	NCD (5.6% fat) or HFD (58% kcal fat)	BAT	Impaired mitochondrial function; Activation of p38 targets ↓
Liu Y et al. (68)	Bif-1$^{-/-}$ and wildtype transgenic C57BL/6 mice	NCD (18% kcal from fat) or HFD (55% kcal from fat;) at 6 w of age	WAT	P62, LC3-II/LC3 ↑; Bif-1, ATG9a, LAMP1 ↓
Mizunoe Y et al. (69)	*Ob/ob* and wild-type C57BL/6 mice	NCD (10% kcal from fat) or HFD (60% kcal from fat;) for 4 w beginning at 6 w of age	Epididymal AT	Obese AT: CTSB, LC3-I/LC3-II, P62 ↑;CTSL ↓; ATG5 and Beclin1 unchanged
Nunez CE et al. (70)	Male Swiss mice	NCD (10% kcal from fat) or HFD (60% kcal from fat;) for 8 w beginning at 4 w of age	Epididymal AT	Beclin1, P62, CHOP, phospho-JNK ↑; Phospho-mTOR ↓

AT, adipose tissue; WAT, white adipose tissue; BAT, brown adipose tissue; NCD, normal chow diet; HFD, high fat diet; T2D, type 2 diabetic; TNF, tumor necrosis factor; IL, interleukin; CTSB, cathepsin B; CTSL, cathepsin L; LAMP, lysosomal associated membrane protein.

Mizunoe et al. reported an increase in diet-induced autophagosome formation, an increase in *Lc3-II* and *p62* after lysosomal inhibition, and the dysregulation of protease lysosomes, suggesting that the autophagic process may be gradually attenuated in DIO animals (69). Similar to other studies, these differences might result from different experimental approaches and uniform criteria were required to determine the autophagic status (52). Another problem was differences in the timing of diets from study to study, and the effects on autophagy may differ (12, 69, 70). Notably, there were inconsistent interpretations of the autophagic state in different studies. For example, it has been suggested that elevated *p62* attenuates autophagy (69). It has also been suggested that elevated *p62* enhances autophagy (70). It is difficult to draw a definite conclusion in these cases.

3.4 WAT Autophagy: Human Clinical Study

The convenience of obtaining AT compared to that of liver or muscle from humans has ensured research in obese individuals (**Table 2**). Regarding human studies, the overall trend was that WAT autophagy was increased in obese individuals (11, 13, 16, 17, 70, 72). Autophagy markers (Beclin-1, ATG5, ATG12, ATG7, LC3-I, LC3-II, and p62) in obese patients had higher mRNA or protein levels than those in lean individuals, and mammalian target of rapamycin (mTOR) expression was decreased, along with sWAT or vWAT (11, 13, 16, 17, 70, 72). Notably, not all studies analyzed the same autophagy markers, and the expression of these autophagy markers was analyzed independently in each study. Given the inconsistent conclusions on autophagic status in the WAT of DIO mice and obese subjects, it is necessary to confirm whether autophagic flux is accompanied by increased expression of autophagic proteins related to substrate recognition and autophagosome formation, such as LC3 or p62. There are two opposing situations: increased autophagic flux and impaired lysosomal degradation, leading to autophagosome accumulation. Autophagic flux assays could distinguish between these two conditions (52). Thus, *in vitro* experiments under lysosomal inhibitor conditions revealed enhanced autophagic flux in sWAT and vWAT from obese patients and DIO mice, and the findings suggested consistent WAT autophagic gene or protein expression in obesity (17, 69).

Studies on WAT autophagy have also been performed in humans with weight-loss operations, confirming that autophagy levels were elevated in obese states (70, 72). Nuñez et al. showed decreased Beclin-1 and autophagosomes in the sWAT of obese patients after bariatric surgery with or without diabetes (70). Some investigators have suggested that metabolic improvements after bariatric surgery are associated with sWAT autophagy. Soussi et al. indicated that autophagic flux in adipocytes was impaired in obese patients, while autophagic flux was restored after bariatric surgery (16). The study only compared the levels of LC3-II before and after surgery in response to lysosomal inhibition. Autophagic flux was not detected in the presence of lysosomal inhibition. In this context, autophagy plays a protective role against nutrient metabolism-related stress. However, the specific expression of ATGs in response to

TABLE 2 | Clinical studies about autophagy and inflammation in obese individuals.

Reference	Groupings	Diet types/Intervention	Samples	Results (compared to the control group)
Nunez CE et al. (70)	9 obese-nondiabetic and 6 obese-diabetic subjects	Bariatric surgery	Subcutaneous AT	Body mass, Beclin1, autophagosomes, TNF-1a, IL6, IL-1β ↓
Camargo A et al. (72)	39 obese subjects with metabolic syndrome	Four dieting models: HSFAD, HMUFAD, LFHCCD with longchain n-3 polyunsaturated fatty acids (n-3) or placebo (LFHCCD) for 12w	Subcutaneous AT	HMUFA diet: Beclin1 and ATG7 ↑; LFHCC and LFHCC n-3 diet: Caspase-3, Caspase7, HOMA-IR ↑
Soussi H et al. (16)	Middle-aged obese or overweight subjects	Bariatric surgery	Subcutaneous AT	Obese adipocytes: P62 ↑; barely detected LC3-II with lysosome inhibitor; Nonobese adipocytes: LC3-II accumulation with lysosome inhibitors ↑
Jansen HJ et al. (11)	Healthy lean and obese subjects at age of 30-70 years old	–	Visceral and subcutaneous AT	LC3-II ↑; positively correlated with systemic insulin resistance and morphological characteristics of AT inflammation; Obesity with 3-methylalanine: proinflammatory gene expression, IL-1β, IL-6, IL-8 ↑
Kosacka J et al. (13)	60 lean and obese subjects with (n = 20) or without T2D (n = 20)	Open abdominal surgery (cholecystectomy, abdominal hernia, gastric sleeve, Roux-enY gastric bypass surgery or explorative laparotomy)	Visceral and subcutaneous AT	Obesity with T2D: autophagy, apoptosis, LC3 ratio, TNF-α, IL-1β, IL-6, IL-10 ↑; IL-10 ↓; Lean and nondiabetic: LC3 cannot detect in AT
Kovsan, J et al. (17)	Obese and nonobese subjects	Elective abdominal surgery (bariatric surgery or cholecystectomy)	Omental and subcutaneous AT	ATG5, LC3-I and LC3-II were higher in Omental AT than subcutaneous AT among obese subjects, with intraabdominal fat accumulation; Obesity with lysosome inhibitors: autophagy genes, autophagosomes, autophagic flux ↑

AT, adipose tissue; WAT, white adipose tissue; T2D, type 2 diabetic; TNF, tumor necrosis factor; IL, interleukin; HSFAD, high-saturated fatty acid diet; HMUFAD, high-monounsaturated fatty acid diet; LFHCCD, low-fat, high-complex carbohydrate diets; HOMA-IR, homeostatic model assessment for insulin resistance; CTSB, cathepsin B; CTSL, cathepsin L; LAMP, lysosomal associated membrane protein.

metabolic changes caused by surgery has not been investigated, and the function of operation-induced vWAT autophagy in systemic responses is unclear.

4 OBESITY AND NLRP3 INFLAMMASOME

Unhealthy expansion of AT referred to the accumulation of inflammatory factors and destruction of cellular homeostasis. The canonical NLRP3 inflammasome consists of the NLRP3 receptor, the adaptor molecule apoptosis-associated speck-like protein with a CARD (ASC), and Caspase-1. NLRP3 inflammasome interacted with the adaptor protein ASC and then recruited inflammatory Caspase-1 to the complex, subsequently oligomerized into pentameric inflammasomes. Caspase-1 was a common effector molecule that cleaved the inactive precursors of IL-1β and IL-18 into their mature forms, and these factors are then secreted from cells. Transcription factor NF-κB was the most crucial signal in the activation of NLRP3 inflammasome. One study investigated mice fed HFD and found increased activity of *NF-κB* and systemic inflammation. Inflammasome-induced pyroptosis was alleviated by blocking *NF-κB/Gsdmd* signaling in AT of mice (73). In contrast to other inflammasomes, NLRP3 inflammasome may be activated in response to various stimuli (74). Evidence showed that ROS, lysosomal membrane permeabilization (LMP), and mitochondrial dysfunction were involved in NLRP3 inflammasome activation (75–77) (**Figure 1**).

A recent systematic review revealed increased NLRP3 and IL-1β in the sWAT and vWAT of obese individuals or mouse models (78). For example, increased gene expression of NLRP3 and its products IL-1β and IL-18 was found in the vWAT of metabolically unhealthy obese individuals compared to lean or metabolically healthy obese individuals or healthy controls (79). Alternatively, obese individuals with increased visceral fat ratios or increased vWAT and sWAT had elevated IL-1β, Caspase-1, and NLRP3 gene expression (80). A study in mice showed that *Nlrp3* inflammasome recognized lipotoxicity-associated elevations in intracellular ceramide to trigger Caspase-1 cleavage in macrophages and AT, and the expression of inflammasome components in sWAT was positively linked with ceramide levels. In obese mice, knocking down *Nlrp3* decreased *Il-18* expression and effector T cells and increased naïve T cells in AT (81). Adipocytes but not SVF showed an increase in NLRP3 and IL-1β expression in the sWAT of obese females (82). Obese and type 2 diabetic patients exhibited decreased gene expressions of IL-1β and NLRP3 in sWAT and increased insulin sensitivity after diet intervention or exercise (81). Likewise, weight loss by bariatric surgery also reduced gene expression and secretion of IL-1β in the AT of humans and animals (81, 83–85). Other studies showed that inflammasome activators were decreased, and inflammasome inhibitors were increased after bariatric surgery (86–88). It was unclear whether these changes directly caused NLRP3 inflammasome declines in AT.

4.1 NLRP3 Inflammasome Regulation in WAT

The senescent WAT was associated with an inappropriate expansion of adipocytes, insulin resistance, and dyslipidemia (89).

Inflammasomes in senescent WAT, each of which had its priming and stimulus, such as gut-derived endotoxin, adipocytokines, lipid metabolites, and mitochondrial dysfunction, played an essential role in chronic inflammation and insulin resistance (90–95). Adipocytes differentiate, hypertrophy, and die in response to nutritional status or environmental variables. Caspase-1 and IL-1β were expressed dynamically during the differentiation of adipocytes (96). Stienstra et al. found that Caspase-1 inhibition increased genes expression of adipogenesis in adipocytes, including adiponectin and peroxisome proliferator-activated receptor γ, and inhibited IL-1β but not IL-18 production *in vitro*. *Caspase-1-* or *Nlrp3-* promoted adipogenesis and improved AT function and insulin sensitivity in mice (96). A recent study showed that NLRP3 inflammasome was activated by LPS and palmitic acid, which contributed to adipogenesis and, conversely, inhibited the osteogenesis of stem cells *in vitro* (97). The reason for these differences may be the different activators of NLRP3 inflammasome or cell types. NLRP3 inflammasome was implicated in the downregulation of adipogenesis in the sWAT of obese adolescents (80). Impaired adipogenesis may affect *de novo* adipocyte recruitment and lead to preexisting hypertrophy of adipocytes. Studies showed that *Nlrp3-* or *Caspase-1* prevented hypertrophy of adipocytes in DIO mice (81, 98). However, the mechanism of energy consumption requires a detailed examination of inflammasomes in the process of adipogenesis and lipolysis.

Autophagy is a conserved, lysosome-mediated catabolic mechanism that is responsible for degradation and recycling. Cysteine cathepsins in the lysosome are a cluster of compensatory proteases involved in various cellular processes such as proteolytic degradation through crossing or overlapping signaling pathways. Lysosomal cysteine cathepsins include cathepsins B (CTSB), C, F, H, K, L, O, S, V, and Z (99). Some researchers showed that the mRNA and serum levels of CTSS were positively correlated with BMI and were decreased by weight loss (100). Others demonstrated that CTSK, CTSB, and CTSL were expressed in AT and were elevated in obese humans and mice models (69, 101–103). CTSB has been implicated as a modulator of NLRP3 inflammasome activation through the release of the lysosomal enzyme due to LMP (77). According to one study, the overexpression of *Ctsb* in obese mice increased Caspase-1 *in vivo* and *in vitro* (69). Mizunoe et al. discovered that *Ctsb* overexpression inhibited the expression of Perilipin-1 in 3T3L1 adipocytes. *Ctsb* overexpression resulted in lipolysis and metabolic dysfunction in 3T3L1 adipocytes (104). Enhanced autophagy in *db/db* mice fed HFD showed the accumulation of autophagosomes and an increased ratio of *Lc3-II* to *Lc3-I* with low-grade systemic inflammation (105). Reduced protein expression of Perilipin-1 was related to the activation of inflammatory responses in obese individuals (106). Understanding the specific inflammasome pathways activated by cysteine cathepsins will be important for obesity-related metabolic diseases.

4.2 NLRP3 Inflammasome and AT Remodeling

Chronic and systemic inflammation underlined immune activation during obesity. Dysfunctional AT exhibits impaired angiogenesis, altered extracellular matrix (ECM) remodeling and fibrosis (43). One study showed that blocking the expression of NLRP3 inflammasome reduced AT inflammation and significantly attenuated fibrosis by decreasing the production of IL-1β (107). In addition, researchers have revealed that NLRP3 inflammasome in visceral adipocytes is regulated by exogenous (LPS, aluminum or TNF-α) and endogenous (ATP or TNF-α) factors and hypoxia. NLRP3 gene silencing reduced the expression and release of inflammatory markers, such as IL-1β and IL-6, IL-8, and TNF-α (107). NLRP3 inhibition in AT attenuated the expression of essential molecules involved in ECM deposition and fibrosis, including different collagens and proteases, such as collagen type I alpha 1 chain 1 (COL1A1), COL4A3, COL6A3, MMP2, and MMP9 (107, 107).

In addition, activation of NLRP3 inflammasome in AT exacerbated fibrosis, restricted the healthy expansion of adipocytes and increased circulating levels of FFA during obesity (28, 107). Such as palmitate decreased active AMP-activated protein kinase, blocked the unc-51–like kinase-1 autophagy signaling cascade, and reduced glucose tolerance and insulin sensitivity in HFD mouse models (108). Genes knockdown of *Nlrp3* and *Tlr4* prevented diet-induced AT fibrosis in mice by modulating upstream factors of the inflammatory response in immune cells (109). There had been few studies on inflammation in brown AT, but there was evidence that inflammation could impair thermogenesis and exacerbate the whitening of BAT (40). Mice with *Atgl* knockout exhibited increased whitening of BAT and the induction of *Nlrp3* inflammasome expression (109). These results provided a helpful framework to understand the pathogenesis of obesity-associated diseases. A better understanding of the involvement of NLRP3 inflammasome pathway will inspire the development of therapeutics for reducing collagen deposition and fibrosis in AT.

4.3 NLRP3 Inflammasome and Obesity-Associated Liver Disease

Inflammasome activation also has been recently recognized to play a critical role in the development of obesity-associated liver disease. The histological evidence of hepatic steatosis from 9-month-old DIO *Nlrp3-* mice suggests that compared to WT mice, the ablation of NLRP3 resulted in reduction in hepatic steatosis. Obesity-related inflammasome activation in AT and liver was prevented, and insulin signaling was improved in *Nlrp3-* mice (81). Another study generated global and myeloid cell-specific conditional mutant *Nlrp3* knockin mice, resulting in a hyperactive *Nlrp3*. It demonstrated that global and myeloid-specific NLRP3 inflammasome activation resulted in severe liver inflammation and fibrosis while identifying a novel mechanism of NLRP3-mediated liver damage (110).

5 INTERACTION BETWEEN AUTOPHAGY AND NLRP3 INFLAMMASOME

There is a reciprocal regulatory relationship between autophagy and inflammasome activation. Not only does autophagy or mitophagy affect NLRP3 inflammasome activation, but NLRP3 inflammasome

activation also dictates autophagy or mitophagy status. Appropriate inflammasome activation helps the organism cope with external metabolic stress. Excessive activation of NLRP3 inflammasome intensified the development of inflammatory products (95, 111). Autophagy is an essential process for the recycling and removal of damaged proteins and organelles. Autophagy-mediated degradation relies on lysosomes to remove double-membraned organelles. The acidic environment and proteases in the lysosome ensure normal autophagy. Autophagy can remove NLRP3 inflammasome activators (ROS and damaged mitochondria) and degrade NLRP3 inflammasome components, reducing inflammasome activation and the inflammatory response. Moreover, NLRP3 inflammasome signaling pathways can regulate the autophagic processes necessary to balance the required inflammatory response and prevent excessive and detrimental inflammation (112–114). Defective mitochondrial function is among the upstream signals that activate NLRP3 inflammasome. Myoung et al. found that global or brown adipocyte-specific deletion of *Pink1*, a Parkinson disease-related gene involved in mitophagy, induced BAT dysfunction, and obesity in mice (115). However, Zhang et al. suggested that *Nlrp3* may also serve as an upstream regulator for *Parkin*-mediated mitophagy in cardiomyocytes and is regulated by *iNOS* but unlikely mitochondrial ROS in $Akt2^{-/-}$ insulin resistance model (116). These data suggest that mitophagy and NLRP3 activation go both ways in regulating whole-body energy metabolism that might depend on certain cells or organs. Understanding the interrelation between these two essential biological processes is essential to comprehend the biological mechanisms and alleviate inflammation in obesity.

5.1 Autophagy Inhibits NLRP3 Inflammasome Activation

Recent studies have shown that autophagy mediates the activation of NLRP3 inflammasome. Activators of NLRP3 inflammasome can be removed by autophagy. Giordano et al. found that the increase in cholesterol crystals and accumulation of calcium and ROS in hypertrophic adipocytes in obesity triggered NLRP3 inflammasome with subsequent massive activation of Caspase-1 in sWAT and vWAT (117). Zhou et al. demonstrated that mitochondrial ROS was associated with NLRP3-dependent Caspase-1 activation and IL-1β release in monocytes and macrophages (118). 3-Methyladenine inhibited autophagy, which led to mitochondrial accumulation, generated ROS, and activated NLRP3 while enhancing inflammasomes. These inflammatory responses were reversed by ROS scavengers (118). Consistently, rapamycin (sirolimus) induced autophagy and suppressed the production of IL-1β and Caspase-1 activation (119). Disruption of autophagy could lead to the accumulation of damaged mitochondria. Autophagy maintained mitochondrial homeostasis by removing ROS produced by damaged mitochondria (118, 120). One study showed that deficiencies in mitochondrial clearance led to an increase in *Nlrp3* inflammasome and brown AT dysfunction, which could be reversed through *Nlpr3* deletion in $Pink1^{-/-}$ mice (115).

Inflammation in AT was improved by an interaction between adipocytes and macrophages with enhanced autophagy. Sirtuin 3 (SIRT3), an NAD+-dependent deacetylase, played an essential role in regulating macroautophagy and lipid metabolism. Sirtuin 3 regulated the 3T3-L1-mediated differentiation of adipocytes and activated the AMP-activated protein kinase-unc-51-like kinase 1 pathway in mature adipocytes by macroautophagy (121). The overexpression of *Sirt3* inhibited *Nlrp3* inflammasome by reversing mitochondrial dysfunction and activating AMPK in macrophages of vWAT. Moreover, activated autophagy attenuated inflammatory responses induced by the conditioned medium from macrophage in adipocytes and blocked the migration of macrophages toward adipocytes. This evidence suggested that autophagy regulated the activation of inflammasomes in a positive way.

5.2 Autophagy Targets NLRP3 Inflammasome Components

P62 was a ubiquitinated degradation substrate associated with autophagy. LPS induced NF-κB-dependent p62 expression in macrophages. P62 was recruited to the damaged mitochondria upon NLRP3 activation. P62 bound damaged mitochondria that underwent *Parkin*-dependent clearance and reduced *Nlrp3* inflammasome activation in macrophages (122) (**Figure 2**). The possible mechanism was that inflammasome activation prevented p62-dependent degradation of inflammasome components. p62 recognized the adaptor protein ASC, an NLRP3 inflammasome component, which colocalized with autophagosomes. This result indicated that *Nlrp3* inflammasome could be engulfed and degraded by autophagosomes. Autophagy inhibition and targeted p62 inhibition markedly enhanced NLRP3 inflammasome activation (123). Recently, it was proposed that phosphorylation of NLRP3 is inactivated in an autophagy-dependent manner (124). Phosphorylated NLRP3 interacted with p62 in an ASC-dependent way and then was sequestered in phagosomes for degradation (124) (**Figure 2**). Modification of NLRP3 inflammasome (e.g., phosphorylation and ubiquitination) and subsequent autophagic encapsulation prevented excessive inflammatory responses (123, 124).

In addition, autophagy controlled the production of IL-1β by targeting pro-IL-1β for lysosomal degradation (**Figure 1**). Harris et al. reported that rapamycin enhanced autophagy, induced the degradation of pro-IL-1β and blocked the secretion of mature cytokines in macrophages. Inhibition of autophagy promoted the processing and secretion of IL-1β (114). Zhang et al. observed that autophagy could degrade IL-1β during the maturation of autophagosomes (125). Similarly, inhibiting autophagy in THP-1 cells reduced IL-1β secretion and increased intracellular IL-1β levels following LPS stimulation (126). The regulation of IL-1β release by autophagic mechanisms is complex and requires further investigation, depending on conditions such as cell type, inflammasome activators, autophagy inducers, or autophagy inhibitors.

5.3 NLRP3 Inflammasome Regulates Autophagy in AT

The status of autophagy or mitophagy may depend on inflammasomes. It was discovered that NLRP3 inflammasome

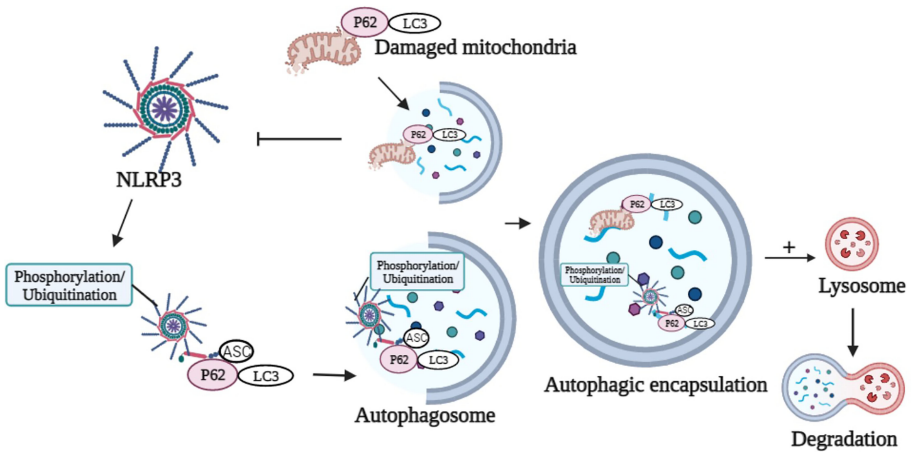

FIGURE 2 | Graphical representation of p62 in the modulation of NLRP3 activation and degradation. p62 binds damaged mitochondria to reduce NLRP3 inflammasome activation. Phosphorylation or ubiquitination of NLRP3 interacts with p62 in an ASC-dependent manner and sequesters in phagosomes for degradation. Image created with BioRender.com.

enhanced autophagy initiation by interacting with Beclin-1 (127). NLRP3 acted as a regulator of autophagy. In THP-1 cells, overexpression of NLRP3 inflammasome enhanced autophagy and expression of the LC3-II protein (128). Similarly, silencing NLRP3 decreased autophagy and decreased the conversion of LC3-I to LC3-II (129). In addition to NLRP3, Caspase-1 has been shown to control the autophagic process *via* substrate cleavage (130, 131). Yu et al. found that activating NLRP3 inflammasome resulted in Caspase-1-dependent mitochondrial arrest in macrophages, resulting in the buildup of mitochondrial DNA and defective mitochondria. *Caspase-1*-mediated *Parkin* cleavage enhanced Caspase-1-dependent mitochondrial clearance from macrophages during inflammasome activation (132). Overall, inflammasome activation of mature adipocytes are rarely studied. It is worth investigating whether activating NLRP3 inflammasome affects autophagy initiation in mature adipocytes.

6 CONCLUSIONS AND REMARKS

The review summarized the current studies and potential mechanisms associated with autophagy and NLRP3 inflammasome in AT inflammation. Although hyperplasia and hypertrophy of adipocytes in AT are vital determinants in the progress of obesity, proinflammatory cytokine secretion and immune cell migration are the driving forces for systemic inflammation and insulin resistance, promoting alterations in (suppressed or enhanced) autophagy and NLRP3 inflam masome. Although clinical trials and animal models evaluated autophagy and inflammatory levels in isolated AT components, challenges still need to be overcome before targeted therapeutics will be clinically helpful for controlling obesity. First, it is relatively difficult to evaluate autophagic activity at a specific stage of growth and development in humans. At present, the ATG-knockout model and the evaluation of overall autophagic activity mainly come from animal research. Second, there are differences in insulin resistance, basic metabolic rates and antioxidant capacity among obese individuals in different metabolic states, resulting in inconsistent levels of basic inflammation. A unified evaluation of the relevant indicators of the level of inflammation is needed. Third, the body is in a state of dynamic equilibrium. Moderate autophagy and inflammation reflect AT adjustment to external energy, which is beneficial for reducing ectopic lipotoxicity. When studying autophagy modulators and inhibitors of NLRP3 inflammasome activation, the effects on the total metabolic capacity of the organism should be considered.

In conclusion, targeting autophagy and NLRP3 inflam masome as therapeutic strategies is beneficial in managing AT inflammation and obesity-related complications. Further studies should manipulate the exact pathways associated with altered autophagy and activated inflammasomes, leading to possible treatments for patients suffering from obesity.

AUTHOR CONTRIBUTIONS

LZ wrote the manuscript. LL designed the topic and critically revised the work. All authors contributed to the article and approved the submitted version.

FUNDING

This study was funded by the National Natural Science Foundation of China [grant numbers 81270956 and 81470577].

REFERENCES

1. Nyberg ST, Batty GD, Pentti J, Virtanen M, Alfredsson L, Fransson EI, et al. Obesity and Loss of Disease-Free Years Owing to Major non-Communicable Diseases: A Multicohort Study. *Lancet Public Health* (2018) 3(10):e490–e7. doi: 10.1016/s2468-2667(18)30139-7
2. Afshin A, Forouzanfar MH, Reitsma MB, Sur P, Estep K, Lee A, et al. Health Effects of Overweight and Obesity in 195 Countries Over 25 Years. *N Engl J Med* (2017) 377(1):13–27. doi: 10.1056/NEJMoa1614362
3. Zhang J, Wang H, Wang Z, Huang F, Zhang X, Du W, et al. Trajectories of Dietary Patterns and Their Associations With Overweight/Obesity Among Chinese Adults: China Health and Nutrition Survey 1991-2018. *Nutrients* (2021) 13(8):2835. doi: 10.3390/nu13082835
4. Wang L, Zhou B, Zhao Z, Yang L, Zhang M, Jiang Y, et al. Body-Mass Index and Obesity in Urban and Rural China: Findings From Consecutive Nationally Representative Surveys During 2004-18. *Lancet* (2021) 398 (10294):53–63. doi: 10.1016/s0140-6736(21)00798-4
5. Huang L, Wang Z, Wang H, Zhao L, Jiang H, Zhang B, et al. Nutrition Transition and Related Health Challenges Over Decades in China. *Eur J Clin Nutr* (2021) 75(2):247–52. doi: 10.1038/s41430-020-0674-8
6. Zeng Q, Li N, Pan X-F, Chen L, Pan A. Clinical Management and Treatment of Obesity in China. *Lancet Diabetes Endocrinol* (2021) 9(6):393–405. doi: 10.1016/s2213-8587(21)00047-4
7. Zhang Y, Sowers JR, Ren J. Targeting Autophagy in Obesity: From Pathophysiology to Management. *Nat Rev Endocrinol* (2018) 14(6):356–76. doi: 10.1038/s41574-018-0009-1
8. Carobbio S, Pellegrinelli V, Vidal-Puig A. Adipose Tissue Function and Expandability as Determinants of Lipotoxicity and the Metabolic Syndrome. *Adv Exp Med Biol* (2017) 960:161–96. doi: 10.1007/978-3-319-48382-5_7
9. Pellegrinelli V, Carobbio S, Vidal-Puig A. Adipose Tissue Plasticity: How Fat Depots Respond Differently to Pathophysiological Cues. *Diabetologia* (2016) 59(6):1075–88. doi: 10.1007/s00125-016-3933-4
10. Ajoolabady A, Liu S, Klionsky DJ, Lip GYH, Tuomilehto J, Kavalakatt S, et al. ER Stress in Obesity Pathogenesis and Management. *Trends Pharmacol Sci* (2022) 43(2):97–109. doi: 10.1016/j.tips.2021.11.011
11. Jansen HJ, van Essen P, Koenen T, Joosten LA, Netea MG, Tack CJ, et al. Autophagy Activity is Up-Regulated in Adipose Tissue of Obese Individuals and Modulates Proinflammatory Cytokine Expression. *Endocrinology* (2012) 153(12):5866–74. doi: 10.1210/en.2012-1625
12. Yoshizaki T, Kusunoki C, Kondo M, Yasuda M, Kume S, Morino K, et al. Autophagy Regulates Inflammation in Adipocytes. *Biochem Biophys Res Commun* (2012) 417(1):352–7. doi: 10.1016/j.bbrc.2011.11.114
13. Kosacka J, Kern M, Kloting N, Paeschke S, Rudich A, Haim Y, et al. Autophagy in Adipose Tissue of Patients With Obesity and Type 2 Diabetes. *Mol Cell Endocrinol* (2015) 409(C):21–32. doi: 10.1016/j.mce.2015.03.015
14. Pahwa R, Singh A, Adams-Huet B, Devaraj S, Jialal I. Increased Inflammasome Activity in Subcutaneous Adipose Tissue of Patients With Metabolic Syndrome. *Diabetes Metab Res Rev* (2021) 37(3):e3383. doi: 10.1002/dmrr.3383
15. ZhuGe DL, Javaid HMA, Sahar NE, Zhao YZ, Huh JY. Fibroblast Growth Factor 2 Exacerbates Inflammation in Adipocytes Through NLRP3 Inflammasome Activation. *Arch Pharm Res* (2020) 43(12):1311–24. doi: 10.1007/s12272-020-01295-2
16. Soussi H, Reggio S, Alili R, Prado C, Mutel S, Pini M, et al. DAPK2 Downregulation Associates With Attenuated Adipocyte Autophagic Clearance in Human Obesity. *Diabetes* (2015) 64(10):3452–63. doi: 10.2337/db14-1933
17. Kovsan J, Bluher M, Tarnovscki T, Kloting N, Kirshtein B, Madar L, et al. Altered Autophagy in Human Adipose Tissues in Obesity. *J Clin Endocrinol Metab* (2011) 96(2):E268–77. doi: 10.1210/jc.2010-1681
18. Spalding KL, Arner E, Westermark PO, Bernard S, Buchholz BA, Bergmann O, et al. Dynamics of Fat Cell Turnover in Humans. *Nature* (2008) 453 (7196):783–7. doi: 10.1038/nature06902
19. Wang QA, Tao C, Gupta RK, Scherer PE. Tracking Adipogenesis During White Adipose Tissue Development, Expansion and Regeneration. *Nat Med* (2013) 19(10):1338–44. doi: 10.1038/nm.3324
20. Rosenwald M, Wolfrum C. The Origin and Definition of Brite Versus White and Classical Brown Adipocytes. *Adipocyte* (2014) 3(1):4–9. doi: 10.4161/adip.26232
21. Halberg N, Khan T, Trujillo ME, Wernstedt-Asterholm I, Attie AD, Sherwani S, et al. Hypoxia-Inducible Factor 1alpha Induces Fibrosis and Insulin Resistance in White Adipose Tissue. *Mol Cell Biol* (2009) 29 (16):4467–83. doi: 10.1128/MCB.00192-09
22. Sun K, Wernstedt Asterholm I, Kusminski CM, Bueno AC, Wang ZV, Pollard JW, et al. Dichotomous Effects of VEGF-A on Adipose Tissue Dysfunction. *Proc Natl Acad Sci USA* (2012) 109(15):5874–9. doi: 10.1073/pnas.1200447109
23. Zhang Y, Proenca R, Maffei M, Barone M, Leopold L, Friedman JM. Positional Cloning of the Mouse Obese Gene and its Human Homologue. *Nature* (1994) 372(6505):425–32. doi: 10.1038/372425a0
24. Fasshauer M, Bluher M. Adipokines in Health and Disease. *Trends Pharmacol Sci* (2015) 36(7):461–70. doi: 10.1016/j.tips.2015.04.014
25. Bluher M. Are There Still Healthy Obese Patients? *Curr Opin Endocrinol Diabetes Obes* (2012) 19(5):341–6. doi: 10.1097/MED.0b013e328357f0a3
26. Skurk T, Alberti-Huber C, Herder C, Hauner H. Relationship Between Adipocyte Size and Adipokine Expression and Secretion. *J Clin Endocrinol Metab* (2007) 92(3):1023–33. doi: 10.1210/jc.2006-1055
27. McLaughlin T, Sherman A, Tsao P, Gonzalez O, Yee G, Lamendola C, et al. Enhanced Proportion of Small Adipose Cells in Insulin-Resistant vs Insulin-Sensitive Obese Individuals Implicates Impaired Adipogenesis. *Diabetologia* (2007) 50(8):1707–15. doi: 10.1007/s00125-007-0708-y
28. Khan T, Muise ES, Iyengar P, Wang ZV, Chandalia M, Abate N, et al. Metabolic Dysregulation and Adipose Tissue Fibrosis: Role of Collagen VI. *Mol Cell Biol* (2009) 29(6):1575–91. doi: 10.1128/MCB.01300-08
29. Salans LB, Knittle JL, Hirsch J. The Role of Adipose Cell Size and Adipose Tissue Insulin Sensitivity in the Carbohydrate Intolerance of Human Obesity. *J Clin Invest* (1968) 47(1):153–65. doi: 10.1172/JCI105705
30. Yang J, Eliasson B, Smith U, Cushman SW, Sherman AS. The Size of Large Adipose Cells is a Predictor of Insulin Resistance in First-Degree Relatives of Type 2 Diabetic Patients. *Obes (Silver Spring)* (2012) 20(5):932–8. doi: 10.1038/oby.2011.371
31. Song MJ, Kim KH, Yoon JM, Kim JB. Activation of Toll-Like Receptor 4 is Associated With Insulin Resistance in Adipocytes. *Biochem Biophys Res Commun* (2006) 346(3):739–45. doi: 10.1016/j.bbrc.2006.05.170
32. Nguyen MT, Favelyukis S, Nguyen AK, Reichart D, Scott PA, Jenn A, et al. A Subpopulation of Macrophages Infiltrates Hypertrophic Adipose Tissue and is Activated by Free Fatty Acids *via* Toll-Like Receptors 2 and 4 and JNK-Dependent Pathways. *J Biol Chem* (2007) 282(48):35279–92. doi: 10.1074/jbc.M706762200
33. Bashan N, Dorfman K, Tarnovscki T, Harman-Boehm I, Liberty IF, Bluher M, et al. Mitogen-Activated Protein Kinases, inhibitory-kappaB Kinase, and Insulin Signaling in Human Omental Versus Subcutaneous Adipose Tissue in Obesity. *Endocrinology* (2007) 148(6):2955–62. doi: 10.1210/en.2006-1369
34. Sabio G, Das M, Mora A, Zhang Z, Jun JY, Ko HJ, et al. A Stress Signaling Pathway in Adipose Tissue Regulates Hepatic Insulin Resistance. *Science* (2008) 322(5907):1539–43. doi: 10.1126/science.1160794
35. Hotamisligil GS. Inflammation and Metabolic Disorders. *Nature* (2006) 444 (7121):860–7. doi: 10.1038/nature05485
36. Lumeng CN, Bodzin JL, Saltiel AR. Obesity Induces a Phenotypic Switch in Adipose Tissue Macrophage Polarization. *J Clin Invest* (2007) 117(1):175–84. doi: 10.1172/jci29881
37. Titos E, Rius B, González-Périz A, López-Vicario C, Morán-Salvador E, Martínez-Clemente M, et al. Resolvin D1 and its Precursor Docosahexaenoic Acid Promote Resolution of Adipose Tissue Inflammation by Eliciting Macrophage Polarization Toward an M2-Like Phenotype. *J Immunol (Baltimore Md: 1950)* (2011) 187(10):5408–18. doi: 10.4049/jimmunol.1100225
38. Song MY, Wang J, Lee Y, Lee J, Kwon KS, Bae EJ, et al. Enhanced M2 Macrophage Polarization in High N-3 Polyunsaturated Fatty Acid Transgenic Mice Fed a High-Fat Diet. *Mol Nutr Food Res* (2016) 60 (11):2481–92. doi: 10.1002/mnfr.201600014
39. Thomas D, Apovian C. Macrophage Functions in Lean and Obese Adipose Tissue. *Metabol: Clin Exp* (2017) 72:120–43. doi: 10.1016/j.metabol.2017.04.005

40. Villarroya F, Cereijo R, Gavalda-Navarro A, Villarroya J, Giralt M. Inflammation of Brown/Beige Adipose Tissues in Obesity and Metabolic Disease. *J Intern Med* (2018) 284(5):492–504. doi: 10.1111/joim.12803
41. Rodriguez A, Ezquerro S, Mendez-Gimenez L, Becerril S, Fruhbeck G. Revisiting the Adipocyte: A Model for Integration of Cytokine Signaling in the Regulation of Energy Metabolism. *Am J Physiol Endocrinol Metab* (2015) 309(8):E691–714. doi: 10.1152/ajpendo.00297.2015
42. Malagon MM, Diaz-Ruiz A, Guzman-Ruiz R, Jimenez-Gomez Y, Moreno NR, Garcia-Navarro S, et al. Adipobiology for Novel Therapeutic Approaches in Metabolic Syndrome. *Curr Vasc Pharmacol* (2013) 11 (6):954–67. doi: 10.2174/15701611113116660170
43. Sun K, Tordjman J, Clement K, Scherer PE. Fibrosis and Adipose Tissue Dysfunction. *Cell Metab* (2013) 18(4):470–7. doi: 10.1016/j.cmet.2013.06.016
44. Zmora N, Bashiardes S, Levy M, Elinav E. The Role of the Immune System in Metabolic Health and Disease. *Cell Metab* (2017) 25(3):506–21. doi: 10.1016/j.cmet.2017.02.006
45. Lee J. Adipose Tissue Macrophages in the Development of Obesity-Induced Inflammation, Insulin Resistance and Type 2 Diabetes. *Arch Pharm Res* (2013) 36(2):208–22. doi: 10.1007/s12272-013-0023-8
46. Haase J, Weyer U, Immig K, Kloting N, Bluher M, Eilers J, et al. Local Proliferation of Macrophages in Adipose Tissue During Obesity-Induced Inflammation. *Diabetologia* (2014) 57(3):562–71. doi: 10.1007/s00125-013-3139-y
47. Behl T, Sehgal A, Bala R, Chadha S. Understanding the Molecular Mechanisms and Role of Autophagy in Obesity. *Mol Biol Rep* (2021) 48 (3):2881–95. doi: 10.1007/s11033-021-06298-w
48. Ferhat M, Funai K, Boudina S. Autophagy in Adipose Tissue Physiology and Pathophysiology. *Antioxid Redox Signal* (2019) 31(6):487–501. doi: 10.1089/ars.2018.7626
49. Yan X, Zhou R, Ma Z. Autophagy-Cell Survival and Death. *Adv Exp Med Biol* (2019) 1206:667–96. doi: 10.1007/978-981-15-0602-4_29
50. Jang YJ, Kim JH, Byun S. Modulation of Autophagy for Controlling Immunity. *Cells* (2019) 8(2):138. doi: 10.3390/cells8020138
51. Qian M, Fang X, Wang X. Autophagy and Inflammation. *Clin Transl Med* (2017) 6(1):24. doi: 10.1186/s40169-017-0154-5
52. Klionsky DJ, Abdelmohsen K, Abe A, Abedin MJ, Abeliovich H, Acevedo Arozena A, et al. Guidelines for the Use and Interpretation of Assays for Monitoring Autophagy (3rd Edition). *Autophagy* (2016) 12(1):1–222. doi: 10.1080/15548627.2015.1100356
53. Joven J, Guirro M, Marine-Casado R, Rodriguez-Gallego E, Menendez JA. Autophagy Is an Inflammation-Related Defensive Mechanism Against Disease. *Adv Exp Med Biol* (2014) 824:43–59. doi: 10.1007/978-3-319-07320-0_6
54. Shibutani ST, Saitoh T, Nowag H, Munz C, Yoshimori T. Autophagy and Autophagy-Related Proteins in the Immune System. *Nat Immunol* (2015) 16 (10):1014–24. doi: 10.1038/ni.3273
55. Matsuzawa-Ishimoto Y, Hwang S, Cadwell K. Autophagy and Inflammation. *Ann Rev Immunol* (2018) 36:73–101. doi: 10.1146/annurevimmunol-042617-053253
56. Saitoh T, Fujita N, Jang MH, Uematsu S, Yang BG, Satoh T, et al. Loss of the Autophagy Protein Atg16L1 Enhances Endotoxin-Induced IL-1beta Production. *Nature* (2008) 456(7219):264–8. doi: 10.1038/nature07383
57. Ghaben AL, Scherer PE. Adipogenesis and Metabolic Health. *Nat Rev Mol Cell Biol* (2019) 20(4):242–58. doi: 10.1038/s41580-018-0093-z
58. Pachon-Pena G, Serena C, Ejarque M, Petriz J, Duran X, Oliva-Olivera W, et al. Obesity Determines the Immunophenotypic Profile and Functional Characteristics of Human Mesenchymal Stem Cells From Adipose Tissue. *Stem Cells Transl Med* (2016) 5(4):464–75. doi: 10.5966/sctm.2015-0161
59. Xu Q, Mariman ECM, Roumans NJT, Vink RG, Goossens GH, Blaak EE, et al. Adipose Tissue Autophagy Related Gene Expression is Associated With Glucometabolic Status in Human Obesity. *Adipocyte* (2018) 7(1):12–9. doi: 10.1080/21623945.2017.1394537
60. Rodriguez A, Gomez-Ambrosi J, Catalan V, Rotellar F, Valenti V, Silva C, et al. The Ghrelin O-Acyltransferase-Ghrelin System Reduces TNF-Alpha-Induced Apoptosis and Autophagy in Human Visceral Adipocytes. *Diabetologia* (2012) 55(11):3038–50. doi: 10.1007/s00125-012-2671-5
61. Kang YH, Cho MH, Kim JY, Kwon MS, Peak JJ, Kang SW, et al. Impaired Macrophage Autophagy Induces Systemic Insulin Resistance in Obesity. *Oncotarget* (2016) 7(24):35577–91. doi: 10.18632/oncotarget.9590
62. Liu K, Zhao E, Ilyas G, Lalazar G, Lin Y, Haseeb M, et al. Impaired Macrophage Autophagy Increases the Immune Response in Obese Mice by Promoting Proinflammatory Macrophage Polarization. *Autophagy* (2015) 11(2):271–84. doi: 10.1080/15548627.2015.1009787
63. Litwinoff EMS, Gold MY, Singh K, Hu J, Li H, Cadwell K, et al. Myeloid ATG16L1 Does Not Affect Adipose Tissue Inflammation or Body Mass in Mice Fed High Fat Diet. *Obes Res Clin Pract* (2018) 12(2):174–86. doi: 10.1016/j.orcp.2017.10.006
64. Grijalva A, Xu X, Ferrante AW Jr. Autophagy Is Dispensable for Macrophage-Mediated Lipid Homeostasis in Adipose Tissue. *Diabetes* (2016) 65(4):967–80. doi: 10.2337/db15-1219
65. Zhang Y, Goldman S, Baerga R, Zhao Y, Komatsu M, Jin S. Adipose-Specific Deletion of Autophagy-Related Gene 7 (Atg7) in Mice Reveals a Role in Adipogenesis. *Proc Natl Acad Sci USA* (2009) 106(47):19860–5. doi: 10.1073/pnas.0906048106
66. Baerga R, Zhang Y, Chen PH, Goldman S, Jin S. Targeted Deletion of Autophagy-Related 5 (Atg5) Impairs Adipogenesis in a Cellular Model and in Mice. *Autophagy* (2009) 5(8):1118–30. doi: 10.4161/auto.5.8.9991
67. Muller TD, Lee SJ, Jastroch M, Kabra D, Stemmer K, Aichler M, et al. P62 Links Beta-Adrenergic Input to Mitochondrial Function and Thermogenesis. *J Clin Invest* (2013) 123(1):469–78. doi: 10.1172/JCI64209
68. Liu Y, Takahashi Y, Desai N, Zhang J, Serfass JM, Shi YG, et al. Bif-1 Deficiency Impairs Lipid Homeostasis and Causes Obesity Accompanied by Insulin Resistance. *Sci Rep* (2016) 6:20453. doi: 10.1038/srep20453
69. Mizunoe Y, Sudo Y, Okita N, Hiraoka H, Mikami K, Narahara T, et al. Involvement of Lysosomal Dysfunction in Autophagosome Accumulation and Early Pathologies in Adipose Tissue of Obese Mice. *Autophagy* (2017) 13(4):642–53. doi: 10.1080/15548627.2016.1274850
70. Nunez CE, Rodrigues VS, Gomes FS, Moura RF, Victorio SC, Bombassaro B, et al. Defective Regulation of Adipose Tissue Autophagy in Obesity. *Int J Obes (2005)* (2013) 37(11):1473–80. doi: 10.1038/ijo.2013.27
71. Marcelin G, Da Cunha C, Gamblin C, Suffee N, Rouault C, Leclerc A, et al. Autophagy Inhibition Blunts PDGFRA Adipose Progenitors' Cell-Autonomous Fibrogenic Response to High-Fat Diet. *Autophagy* (2020) 16 (12):2156–66. doi: 10.1080/15548627.2020.1717129
72. Camargo A, Rangel-Zuniga OA, Alcala-Diaz J, Gomez-Delgado F, Delgado-Lista J, Garcia-Carpintero S, et al. Dietary Fat may Modulate Adipose Tissue Homeostasis Through the Processes of Autophagy and Apoptosis. *Eur J Nutr* (2017) 56(4):1621–8. doi: 10.1007/s00394-016-1208-y
73. Liu Z, Gan L, Xu Y, Luo D, Ren Q, Wu S, et al. Melatonin Alleviates Inflammasome-Induced Pyroptosis Through Inhibiting NF-κb/GSDMD Signal in Mice Adipose Tissue. *J Pineal Res* (2017) 63(1):e12414. doi: 10.1111/jpi.12414
74. He Y, Hara H, Núñez G. Mechanism and Regulation of NLRP3 Inflammasome Activation. *Trends Biochem Sci* (2016) 41(12):1012–21. doi: 10.1016/j.tibs.2016.09.002
75. Guicciardi ME, Gores GJ. Complete Lysosomal Disruption: A Route to Necrosis, Not to the Inflammasome. *Cell Cycle* (2013) 12(13):1995. doi: 10.4161/cc.25317
76. Abais JM, Xia M, Zhang Y, Boini KM, Li PL. Redox Regulation of NLRP3 Inflammasomes: ROS as Trigger or Effector? *Antioxid Redox Signal* (2015) 22(13):1111–29. doi: 10.1089/ars.2014.5994
77. Elliott EI, Sutterwala FS. Initiation and Perpetuation of NLRP3 Inflammasome Activation and Assembly. *Immunol Rev* (2015) 265(1):35–52. doi: 10.1111/imr.12286
78. Rheinheimer J, de Souza BM, Cardoso NS, Bauer AC, Crispim D. Current Role of the NLRP3 Inflammasome on Obesity and Insulin Resistance: A Systematic Review. *Metabol: Clin Exp* (2017) 74:1–9. doi: 10.1016/j.metabol.2017.06.002
79. Esser N, L'Homme L, De Roover A, Kohnen L, Scheen AJ, Moutschen M, et al. Obesity Phenotype is Related to NLRP3 Inflammasome Activity and Immunological Profile of Visceral Adipose Tissue. *Diabetologia* (2013) 56 (11):2487–97. doi: 10.1007/s00125-013-3023-9
80. Kursawe R, Dixit VD, Scherer PE, Santoro N, Narayan D, Gordillo R, et al. A Role of the Inflammasome in the Low Storage Capacity of the Abdominal

Subcutaneous Adipose Tissue in Obese Adolescents. *Diabetes* (2016) 65 (3):610–8. doi: 10.2337/db15-1478
81. Vandanmagsar B, Youm YH, Ravussin A, Galgani JE, Stadler K, Mynatt RL, et al. The NLRP3 Inflammasome Instigates Obesity-Induced Inflammation and Insulin Resistance. *Nat Med* (2011) 17(2):179–88. doi: 10.1038/nm.2279
82. Yin Z, Deng T, Peterson LE, Yu R, Lin J, Hamilton DJ, et al. Transcriptome Analysis of Human Adipocytes Implicates the NOD-Like Receptor Pathway in Obesity-Induced Adipose Inflammation. *Mol Cell Endocrinol* (2014) 394 (1-2):80–7. doi: 10.1016/j.mce.2014.06.018
83. Moschen AR, Molnar C, Enrich B, Geiger S, Ebenbichler CF, Tilg H. Adipose and Liver Expression of Interleukin (IL)-1 Family Members in Morbid Obesity and Effects of Weight Loss. *Mol Med* (2011) 17(7-8):840–5. doi: 10.2119/molmed.2010.00108
84. Dalmas E, Venteclef N, Caer C, Poitou C, Cremer I, Aron-Wisnewsky J, et al. T Cell-Derived IL-22 Amplifies IL-1beta-Driven Inflammation in Human Adipose Tissue: Relevance to Obesity and Type 2 Diabetes. *Diabetes* (2014) 63(6):1966–77. doi: 10.2337/db13-1511
85. Mocanu AO, Mulya A, Huang H, Dan O, Shimizu H, Batayyah E, et al. Effect of Roux-En-Y Gastric Bypass on the NLRP3 Inflammasome in Adipose Tissue From Obese Rats. *PloS One* (2015) 10(10):e0139764. doi: 10.1371/journal.pone.0139764
86. Hoffstedt J, Andersson DP, Eriksson Hogling D, Theorell J, Naslund E, Thorell A, et al. Long-Term Protective Changes in Adipose Tissue After Gastric Bypass. *Diabetes Care* (2017) 40(1):77–84. doi: 10.2337/dc16-1072
87. Li Y, Guan W, Ma S, Lin S, Yang N, Liu R, et al. Lipopolysaccharide and Inflammatory Cytokines Levels Decreased After Sleeve Gastrectomy in Chinese Adults With Obesity. *Endocr J* (2019) 66(4):337–47. doi: 10.1507/endocrj.EJ18-0446
88. Frikke-Schmidt H, O'Rourke RW, Lumeng CN, Sandoval DA, Seeley RJ. Does Bariatric Surgery Improve Adipose Tissue Function? *Obes Rev* (2016) 17(9):795–809. doi: 10.1111/obr.12429
89. Smith U, Li Q, Rydén M, Spalding KL. Cellular Senescence and its Role in White Adipose Tissue. *Int J Obes (2005)* (2021) 45(5):934–43. doi: 10.1038/s41366-021-00757-x
90. Dasu MR, Devaraj S, Jialal I. High Glucose Induces IL-1beta Expression in Human Monocytes: Mechanistic Insights. *Am J Physiol Endocrinol Metab* (2007) 293(1):E337–46. doi: 10.1152/ajpendo.00718.2006
91. Tannahill GM, Curtis AM, Adamik J, Palsson-McDermott EM, McGettrick AF, Goel G, et al. Succinate is an Inflammatory Signal That Induces IL-1beta Through HIF-1alpha. *Nature* (2013) 496(7444):238–42. doi: 10.1038/nature11986
92. Xia M, Boini KM, Abais JM, Xu M, Zhang Y, Li PL. Endothelial NLRP3 Inflammasome Activation and Enhanced Neointima Formation in Mice by Adipokine Visfatin. *Am J Pathol* (2014) 184(5):1617–28. doi: 10.1016/j.ajpath.2014.01.032
93. Camell C, Goldberg E, Dixit VD. Regulation of Nlrp3 Inflammasome by Dietary Metabolites. *Semin Immunol* (2015) 27(5):334–42. doi: 10.1016/j.smim.2015.10.004
94. Bauernfeind F, Niepmann S, Knolle PA, Hornung V. Aging-Associated TNF Production Primes Inflammasome Activation and NLRP3-Related Metabolic Disturbances. *J Immunol (Baltimore Md: 1950)* (2016) 197 (7):2900–8. doi: 10.4049/jimmunol.1501336
95. Dror E, Dalmas E, Meier DT, Wueest S, Thevenet J, Thienel C, et al. Postprandial Macrophage-Derived IL-1beta Stimulates Insulin, and Both Synergistically Promote Glucose Disposal and Inflammation. *Nat Immunol* (2017) 18(3):283–92. doi: 10.1038/ni.3659
96. Stienstra R, Joosten LA, Koenen T, van Tits B, van Diepen JA, van den Berg SA, et al. The Inflammasome-Mediated Caspase-1 Activation Controls Adipocyte Differentiation and Insulin Sensitivity. *Cell Metab* (2010) 12 (6):593–605. doi: 10.1016/j.cmet.2010.11.011
97. Wang L, Chen K, Wan X, Wang F, Guo Z, Mo Z. NLRP3 Inflammasome Activation in Mesenchymal Stem Cells Inhibits Osteogenic Differentiation and Enhances Adipogenic Differentiation. *Biochem Biophys Res Commun* (2017) 484(4):871–7. doi: 10.1016/j.bbrc.2017.02.007
98. Koenen TB, Stienstra R, van Tits LJ, de Graaf J, Stalenhoef AF, Joosten LA, et al. Hyperglycemia Activates Caspase-1 and TXNIP-Mediated IL-1beta Transcription in Human Adipose Tissue. *Diabetes* (2011) 60(2):517–24. doi: 10.2337/db10-0266
99. Campden RI, Zhang Y. The Role of Lysosomal Cysteine Cathepsins in NLRP3 Inflammasome Activation. *Arch Biochem Biophys* (2019) 670:32–42. doi: 10.1016/j.abb.2019.02.015
100. Kitamoto S, Sukhova GK, Sun J, Yang M, Libby P, Love V, et al. Cathepsin L Deficiency Reduces Diet-Induced Atherosclerosis in Low-Density Lipoprotein Receptor-Knockout Mice. *Circulation* (2007) 115(15):2065–75. doi: 10.1161/circulationaha.107.688523
101. Xiao Y, Junfeng H, Tianhong L, Lu W, Shulin C, Yu Z, et al. Cathepsin K in Adipocyte Differentiation and its Potential Role in the Pathogenesis of Obesity. *J Clin Endocrinol Metab* (2006) 91(11):4520–7. doi: 10.1210/jc.2005-2486
102. Chiellini C, Costa M, Novelli SE, Amri EZ, Benzi L, Bertacca A, et al. Identification of Cathepsin K as a Novel Marker of Adiposity in White Adipose Tissue. *J Cell Physiol* (2003) 195(2):309–21. doi: 10.1002/jcp.10253
103. Yang M, Zhang Y, Pan J, Sun J, Liu J, Libby P, et al. Cathepsin L Activity Controls Adipogenesis and Glucose Tolerance. *Nat Cell Biol* (2007) 9 (8):970–7. doi: 10.1038/ncb1623
104. Mizunoe Y, Kobayashi M, Hoshino S, Tagawa R, Itagawa R, Hoshino A, et al. Cathepsin B Overexpression Induces Degradation of Perilipin 1 to Cause Lipid Metabolism Dysfunction in Adipocytes. *Sci Rep* (2020) 10(1):634. doi: 10.1038/s41598-020-57428-6
105. Ebato C, Uchida T, Arakawa M, Komatsu M, Ueno T, Komiya K, et al. Autophagy is Important in Islet Homeostasis and Compensatory Increase of Beta Cell Mass in Response to High-Fat Diet. *Cell Metab* (2008) 8(4):325–32. doi: 10.1016/j.cmet.2008.08.009
106. Sohn JH, Lee YK, Han JS, Jeon YG, Kim JI, Choe SS, et al. Perilipin 1 (Plin1) Deficiency Promotes Inflammatory Responses in Lean Adipose Tissue Through Lipid Dysregulation. *J Biol Chem* (2018) 293(36):13974–88. doi: 10.1074/jbc.RA118.003541
107. Unamuno X, Gómez-Ambrosi J, Ramírez B, Rodríguez A, Becerril S, Valentí V, et al. NLRP3 Inflammasome Blockade Reduces Adipose Tissue Inflammation and Extracellular Matrix Remodeling. *Cell Mol Immunol* (2021) 18(4):1045–57. doi: 10.1038/s41423-019-0296-z
108. Wen H, Gris D, Lei Y, Jha S, Zhang L, Huang MT, et al. Fatty Acid-Induced NLRP3-ASC Inflammasome Activation Interferes With Insulin Signaling. *Nat Immunol* (2011) 12(5):408–15. doi: 10.1038/ni.2022
109. Kotzbeck P, Giordano A, Mondini E, Murano I, Severi I, Venema W, et al. Brown Adipose Tissue Whitening Leads to Brown Adipocyte Death and Adipose Tissue Inflammation. *J Lipid Res* (2018) 59(5):784–94. doi: 10.1194/jlr.M079665
110. Wree A, Eguchi A, McGeough MD, Pena CA, Johnson CD, Canbay A, et al. NLRP3 Inflammasome Activation Results in Hepatocyte Pyroptosis, Liver Inflammation, and Fibrosis in Mice. *Hepatology* (2014) 59(3):898–910. doi: 10.1002/hep.26592
111. Stienstra R, van Diepen JA, Tack CJ, Zaki MH, van de Veerdonk FL, Perera D, et al. Inflammasome is a Central Player in the Induction of Obesity and Insulin Resistance. *Proc Natl Acad Sci USA* (2011) 108(37):15324–9. doi: 10.1073/pnas.1100255108
112. Wu KK, Cheung SW, Cheng KK. NLRP3 Inflammasome Activation in Adipose Tissues and Its Implications on Metabolic Diseases. *Int J Mol Sci* (2020) 21(11):4184. doi: 10.3390/ijms21114184
113. Harris J, Lang T, Thomas JPW, Sukkar MB, Nabar NR, Kehrl JH. Autophagy and Inflammasomes. *Mol Immunol* (2017) 86:10–5. doi: 10.1016/j.molimm.2017.02.013
114. Harris J, Hartman M, Roche C, Zeng SG, O'Shea A, Sharp FA, et al. Autophagy Controls IL-1beta Secretion by Targeting Pro-IL-1beta for Degradation. *J Biol Chem* (2011) 286(11):9587–97. doi: 10.1074/jbc.M110.202911
115. Ko MS, Yun JY, Baek IJ, Jang JE, Hwang JJ, Lee SE, et al. Mitophagy Deficiency Increases NLRP3 to Induce Brown Fat Dysfunction in Mice. *Autophagy* (2021) 17(5):1205–21. doi: 10.1080/15548627.2020.1753002
116. Ren J, Pei Z, Chen X, Berg MJ, Matrougui K, Zhang QH, et al. Inhibition of CYP2E1 Attenuates Myocardial Dysfunction in a Murine Model of Insulin Resistance Through NLRP3-Mediated Regulation of Mitophagy. *Biochim Biophys Acta Mol Basis Dis* (2019) 1865(1):206–17. doi: 10.1016/j.bbadis.2018.08.017
117. Giordano A, Murano I, Mondini E, Perugini J, Smorlesi A, Severi I, et al. Obese Adipocytes Show Ultrastructural Features of Stressed Cells and Die of Pyroptosis. *J Lipid Res* (2013) 54(9):2423–36. doi: 10.1194/jlr.M038638
118. Zhou R, Yazdi AS, Menu P, Tschopp J. A Role for Mitochondria in NLRP3 Inflammasome Activation. *Nature* (2011) 469(7329):221–5. doi: 10.1038/nature09663

119. Ko JH, Yoon SO, Lee HJ, Oh JY. Rapamycin Regulates Macrophage Activation by Inhibiting NLRP3 Inflammasome-P38 MAPK-Nfκb Pathways in Autophagy- and P62-Dependent Manners. *Oncotarget* (2017) 8(25):40817–31. doi: 10.18632/oncotarget.17256
120. Nakahira K, Haspel JA, Rathinam VA, Lee SJ, Dolinay T, Lam HC, et al. Autophagy Proteins Regulate Innate Immune Responses by Inhibiting the Release of Mitochondrial DNA Mediated by the NALP3 Inflammasome. *Nat Immunol* (2011) 12(3):222–30. doi: 10.1038/ni.1980
121. Zhang T, Liu J, Tong Q, Lin L. SIRT3 Acts as a Positive Autophagy Regulator to Promote Lipid Mobilization in Adipocytes via Activating AMPK. *Int J Mol Sci* (2020) 21(2):372. doi: 10.3390/ijms21020372
122. Zhong Z, Umemura A, Sanchez-Lopez E, Liang S, Shalapour S, Wong J, et al. NF-kappaB Restricts Inflammasome Activation *via* Elimination of Damaged Mitochondria. *Cell* (2016) 164(5):896–910. doi: 10.1016/j.cell.2015.12.057
123. Shi C-S, Shenderov K, Huang N-N, Kabat J, Abu-Asab M, Fitzgerald KA, et al. Activation of Autophagy by Inflammatory Signals Limits IL-1 Beta Production by Targeting Ubiquitinated Inflammasomes for Destruction. *Nat Immunol* (2012) 13(3):255–U74. doi: 10.1038/ni.2215
124. Spalinger MR, Lang S, Gottier C, Dai X, Rawlings DJ, Chan AC, et al. PTPN22 Regulates NLRP3-Mediated IL1B Secretion in an Autophagy-Dependent Manner. *Autophagy* (2017) 13(9):1590–601. doi: 10.1080/15548627.2017.1341453
125. Zhang M, Kenny SJ, Ge L, Xu K, Schekman R. Translocation of Interleukin-1beta Into a Vesicle Intermediate in Autophagy-Mediated Secretion. *Elife* (2015) 4:e11205. doi: 10.7554/eLife.11205
126. Iula L, Keitelman IA, Sabbione F, Fuentes F, Guzman M, Galletti JG, et al. Autophagy Mediates Interleukin-1beta Secretion in Human Neutrophils. *Front Immunol* (2018) 9:269. doi: 10.3389/fimmu.2018.00269
127. Jounai N, Kobiyama K, Shiina M, Ogata K, Ishii KJ, Takeshita F. NLRP4 Negatively Regulates Autophagic Processes Through an Association With Beclin1. *J Immunol (Baltimore Md: 1950)* (2011) 186(3):1646–55. doi: 10.4049/jimmunol.1001654
128. Deng Q, Wang Y, Zhang Y, Li M, Li D, Huang X, et al. Pseudomonas Aeruginosa Triggers Macrophage Autophagy To Escape Intracellular Killing by Activation of the NLRP3 Inflammasome. *Infect Immun* (2016) 84(1):56–66. doi: 10.1128/IAI.00945-15
129. Allaeys I, Marceau F, Poubelle PE. NLRP3 Promotes Autophagy of Urate Crystals Phagocytized by Human Osteoblasts. *Arthritis Res Ther* (2013) 15(6):R176. doi: 10.1186/ar4365
130. Yu J, Nagasu H, Murakami T, Hoang H, Broderick L, Hoffman HM, et al. Inflammasome Activation Leads to Caspase-1-Dependent Mitochondrial Damage and Block of Mitophagy. *Proc Natl Acad Sci USA* (2014) 111(43):15514–9. doi: 10.1073/pnas.1414859111
131. Jabir MS, Ritchie ND, Li D, Bayes HK, Tourlomousis P, Puleston D, et al. Caspase-1 Cleavage of the TLR Adaptor TRIF Inhibits Autophagy and Beta-Interferon Production During Pseudomonas Aeruginosa Infection. *Cell Host Microbe* (2014) 15(2):214–27. doi: 10.1016/j.chom.2014.01.010
132. Yu EPK, Reinhold J, Yu H, Starks L, Uryga AK, Foote K, et al. Mitochondrial Respiration Is Reduced in Atherosclerosis, Promoting Necrotic Core Formation and Reducing Relative Fibrous Cap Thickness. *Arterioscler Thromb Vasc Biol* (2017) 37(12):2322–32. doi: 10.1161/atvbaha.117.310042

Conflict of Interest: The authors declare that the research was conducted in the absence of any commercial or financial relationships that could be construed as a potential conflict of interest.

frontiers | Frontiers in Endocrinology

ORIGINAL RESEARCH
published: 11 April 2022
doi: 10.3389/fendo.2022.856530

Subtype-Specific Surface Proteins on Adipose Tissue Macrophages and Their Association to Obesity-Induced Insulin Resistance

Kristina Strand[1,2], Natalie Stiglund[3], Martha Eimstad Haugstøyl[1,2], Zahra Kamyab[1,2], Victoria Langhelle[1,2], Laurence Lawrence-Archer[1,2], Christian Busch[4], Martin Cornillet[3], Iren Drange Hjellestad[1,5], Hans Jørgen Nielsen[6], Pål Rasmus Njølstad[7,8], Gunnar Mellgren[1,2], Niklas K. Björkström[3] and Johan Fernø[1,2†]*

[1] Hormone Laboratory, Department of Medical Biochemistry and Pharmacology, Haukeland University Hospital, Bergen, Norway, [2] Mohn Nutrition Research Laboratory, Department of Clinical Science, University of Bergen, Bergen, Norway, [3] Center for Infectious Medicine, Department of Medicine Huddinge, Karolinska Institutet, Karolinska University Hospital, Stockholm, Sweden, [4] Plastikkirurg1, Bergen, Norway, [5] Department of Medicine, Haukeland University Hospital, Bergen, Norway, [6] Department of Surgery, Voss Hospital, Haukeland University Hospital, Bergen, Norway, [7] Center for Diabetes Research, Department of Clinical Science, University of Bergen, Bergen, Norway, [8] Department of Pediatrics and Adolescents, Haukeland University Hospital, Bergen, Norway

OPEN ACCESS

Edited by:
Katherine Samaras, St Vincent's Hospital Sydney, Australia

Reviewed by:
Alexander Bartelt, Ludwig Maximilian University of Munich, Germany
Isabel Casimiro, The University of Chicago, United States

***Correspondence:**
Johan Fernø
johan.ferno@uib.no

†Lead Contact

Specialty section:
This article was submitted to Obesity, a section of the journal Frontiers in Endocrinology

Received: *17 January 2022*
Accepted: *15 March 2022*
Published: *11 April 2022*

Citation:
Strand K, Stiglund N, Haugstøyl ME, Kamyab Z, Langhelle V, Lawrence-Archer L, Busch C, Cornillet M, Hjellestad ID, Nielsen HJ, Njølstad PR, Mellgren G, Björkström NK and Fernø J (2022) Subtype-Specific Surface Proteins on Adipose Tissue Macrophages and Their Association to Obesity-Induced Insulin Resistance. Front. Endocrinol. 13:856530. doi: 10.3389/fendo.2022.856530

A chronic low-grade inflammation, originating in the adipose tissue, is considered a driver of obesity-associated insulin resistance. Macrophage composition in white adipose tissue is believed to contribute to the pathogenesis of metabolic diseases, but a detailed characterization of pro- and anti-inflammatory adipose tissue macrophages (ATMs) in human obesity and how they are distributed in visceral- and subcutaneous adipose depots is lacking. In this study, we performed a surface proteome screening of pro- and anti-inflammatory ATMs in both subcutaneous- (SAT) and visceral adipose tissue (VAT) and evaluated their relationship with systemic insulin resistance. From the proteomics screen we found novel surface proteins specific to M1-like- and M2-like macrophages, and we identified depot-specific immunophenotypes in SAT and VAT. Furthermore, we found that insulin resistance, assessed by HOMA-IR, was positively associated with a relative increase in pro-inflammatory M1-like macrophages in both SAT and VAT.

Keywords: surface proteomics, adipose tissue macrophage, obesity, insulin resistance, flow cytometry

INTRODUCTION

Obesity is a major global health problem associated with high risk of developing co-morbidities, such as insulin resistance and type 2 diabetes (T2D) (1). Obesity-induced inflammation, which is typically chronic and low-grade, is considered to be a mechanistic link between obesity and insulin resistance (2, 3). The inflammation is manifested by accumulation of immune cells in the adipose tissue (AT), and elevated levels of pro-inflammatory cytokines such as tumor necrosis factor (TNF), C-C motif chemokine ligand (CCL) 2, and interleukin (IL)-6 that can block insulin signaling through various mechanisms (4).

Obesity-related adipose tissue inflammation is in large driven by infiltration of monocytes from the circulation that differentiates into pro-inflammatory macrophages (5, 6). Pro-inflammatory macrophages may also be derived from anti-inflammatory macrophages already present in the tissue that undergo a phenotypic switch in response to the stressed adipose tissue microenvironment (7, 8). Pro-inflammatory M1 macrophages are normally involved in clearing pathogens during infections while the anti-inflammatory M2 macrophages have functions in tissue repair. These subsets of macrophages can be identified by different surface receptors, such as CD80, CD86, CD206, and CD163 (9, 10). However, the pro- and anti-inflammatory macrophages located in the adipose tissue express somewhat different surface receptors, and they are therefore normally referred to as "M1-like" and "M2-like" macrophages (11, 12). In humans, the M1-like macrophages are typically characterized by co-expression of CD11c and CD206, and tend to gather around necrotic adipocytes, forming syncytial aggregates known as crown-like structures (CLS) (11). Indeed, the CLS have been demonstrated to be associated with insulin resistance in human obesity (13). The M2-like macrophages, on the other hand, express CD206 but not CD11c, and are normally dispersed throughout the tissue (11).

Individuals with central obesity that accumulate fat in the visceral adipose tissue (VAT) rather than in subcutaneous adipose tissue (SAT) generally have an increased risk for obesity-related metabolic disease (14–16). These individuals typically display higher levels of inflammation and infiltration of macrophages in their VAT (17, 18). However, other studies report that insulin resistance is associated with elevated amounts of macrophages in SAT instead of VAT (11, 13). Thus, the exact role of pro- and anti-inflammatory macrophages in SAT compared to VAT with respect to metabolic disease remains controversial. Furthermore, in recent years the M1-like/M2-like paradigm has been challenged by the identification of other pro-inflammatory adipose tissue macrophages (ATMs), the so-called metabolically activated macrophages (Mme's), identified in adipose tissue of both rodents and humans (19, 20). These macrophages are activated by nutritional signals including glucose, insulin, and fatty acids and express surface receptors such as CD36, ABCA1, and PLIN2 that differ from the ones expressed by M1- and M2-like macrophages (19). Thus, the immunological landscape of adipose tissue and the difference between various adipose tissue depots is still not fully understood, and there is currently no established consensus regarding which surface receptors best define pro- and anti-inflammatory M1- and M2-like ATMs or the novel MMe's in humans.

To better characterize the adipose tissue M1- and M2-like macrophages in humans and investigate their role in obesity-induced insulin resistance, we here analyzed M1- and M2-like macrophages in SAT and VAT in a sizeable cohort of individuals with obesity. We then performed a surface proteome characterization of M1- and M2-like macrophages and AT monocytes from human SAT in comparison to blood monocytes and validated key findings in another cohort of individuals with obesity. Next, we investigated how the levels of M1- and M2-like macrophages related to the degree of insulin resistance. Lastly, we explore how the macrophages related to other inflammatory features, such as the formation of CLS and AT pro-inflammatory gene expression. The results are discussed in relation to current knowledge about the links between inflammation and obesity-induced insulin resistance.

MATERIAL AND METHODS

Clinical Cohorts and Study Subject Details

The patient cohorts used in this study was approved by the Regional Committees for medical and health research ethics (REK 2015/2343 and REK 2010/502) and written informed consent was obtained from all participants. This study included two clinical cohorts consisting of individuals with obesity undergoing bariatric surgery at Voss Regional Hospital and with patients undergoing plastic surgery. The first cohort consisted of 57 individuals and was used for flow cytometry characterization of ATMs, gene expression and immunohistochemistry analysis. The second cohort contained 23 individuals and was used for verification of surface protein expression by flow cytometry. Clinical characteristics and biochemical measurements of the patients are presented in **Tables 1** and **2**. HOMA-IR was calculated with the HOMA2 calculator using fasting glucose and insulin levels (21). Liposuction aspirates from individuals undergoing plastic surgery were used for the surface proteome screening of ATMs. Buffy coats from anonymous donors were used both as controls and as blood samples for the surface proteome screening. The buffy coats were obtained from the Blood bank services as Haukeland University Hospital.

Isolation of PBMC From Blood Samples

PBMC were isolated from heparin blood samples or buffy coats using density gradient centrifugation. The blood sample was diluted in PBS (Sigma Aldrich), carefully layered on top of Lymphoprep (Stemcell Technologies) and centrifuged at 2000 rpm for 20 minutes with brake and acceleration set to 1. The leukocyte layer was isolated and washed in PBS and the cells were counted before staining for flow cytometry.

Isolation of Stromal Vascular Cells From Adipose Tissue Biopsies or Liposuction Aspirates

Stromal vascular cells (SVCs) were isolated from adipose tissue biopsies or liposuction aspirates. Adipose tissue biopsies from the subcutaneous and the visceral adipose tissue were collected during bariatric surgery and kept in Krebs Ringer Phosphate (KRP) buffer until further processing. Biopsies were cut into smaller pieces before enzymatic digestion with collagenase type I (Life Technologies, 0.66 mg/ml). Liposuction aspirates were washed in NaCl to get rid of excess blood and diluted in the same volume of Krebs Ringer Phosphate (KRP) buffer as the volume of the fat, before enzymatic digestion by Liberase (Roche, final concentration 0,078 Wünsch units/ml). Digestion was carried out for about 1 h with shaking at 37°C. The digested tissue samples were then filtered, and the stromal vascular cells

TABLE 1 | Individuals with obesity – cohort 1.

Subjects	57
T2D	10/57
Gender	70.2% females (40/57)
Age	44.0 (22 – 70)
BMI (kg/m^2)	41.5 (31.1 – 57.4)
Glucose (mmol/L)	5.70 (4.70 – 8.10)
Insulin (mIU/L)	15.1 (3.20 – 50.5)
C-peptide (nmol/L)	1.31 (0.480 – 2.74)
HbA1c (mmol/mol)	37.0 (26.0 – 54.0)
HOMA-IR	1.98 (0.415 – 6.62)
Total cholesterol (mmol/L)	4.70 (2.50 – 6.40)
HDL-C (mmol/L)	1.10 (0.500 – 2.80)
LDL-C (mmol/L)	3.10 (1.10 – 4.30)
Triglycerides (mmol/L)	1.32 (0.530 – 5.94)
CRP (mg/L)	4.00 (0.240 – 25.0)

Data are given as median (range), T2D, type 2 diabetes; BMI, body mass index; HOMA-IR, homeostatic model assessment of insulin resistance index; LDL-C, low-density lipoprotein cholesterol; HDL-C, high-density lipoprotein cholesterol; CRP, C-reactive protein

were removed from underneath the floating layer of mature adipocytes. The SVCs were washed in PBS and centrifuged at 300 x *g* for 5 minutes to pellet the stromal vascular cells. The SVCs isolated from the liposuction aspirates were treated with red blood cell lysis buffer. The cells were counted, and freshly isolated SVCs were stained immediately for flow cytometry analysis.

Flow Cytometry

Macrophage surface protein characterization and verification of surface protein expression was performed on freshly isolated PBMC and SVC samples. Antibodies used are listed in **Table S1** LIVE/DEAD Fixable Aqua Dead Cell Stain kit (Invitrogen, 1:100 dilution) was used to distinguish between live and dead cells during analysis. Staining was performed in FACS buffer (PBS with 2 mM EDTA and 2% FBS) for 20 min at RT in the dark. Following staining, the cells were washed twice in FACS buffer before the cells were fixed in 2% formaldehyde for 15 minutes. After washing twice, the cells were resuspended in FACS buffer and kept at 4°C in the dark.

Surface proteome screening was performed using the LEGENDScreen™ Human PE Kit (Biolegend, Cat# 700007).

TABLE 2 | Individuals with obesity– cohort 2.

Subjects	23
Gender	78.2% females (18/23)
Age	35.0 (22 – 64)
BMI (kg/m^2)	42.1 (29.3 – 54.0)
Glucose (mmol/L)	5.50 (4.40 – 10.9)
Insulin (mIU/L)	13.5 (3.50 – 36.2)
C-peptide (nmol/L)	0.95 (0.040 – 1.58)
HbA1c (mmol/mol)	34.0 (27.0 – 62.0)
HOMA-IR	1.74 (0.531 – 4.57)
Total cholesterol (mmol/L)	4.20 (3.00 – 7.40)
HDL-C (mmol/L)	1.20 (0.800 – 1.60)
LDL-C (mmol/L)	2.70 (1.50 – 5.30)
Triglycerides (mmol/L)	1.19 (0.650 – 2.03)
CRP (mg/L)	6.00 (1.00 – 34.0)

Data are given as median (range), T2D, type 2 diabetes; BMI, body mass index; HOMA-IR, homeostatic model assessment of insulin resistance index; LDL-C, low-density lipoprotein cholesterol; HDL-C, high-density lipoprotein cholesterol; CRP, C-reactive protein.

First, barcoding was performed to be able to separate PBMCs and SVC in the analysis. PBMCs were thawed and stained with CD45 BV650 (Cat# 304044), while the freshly isolated SVC were stained with CD45 AF700 (Cat# 304024). The PBMC and SVC were mixed and stained with a backbone panel containing the following antibodies: BB515 CD206 (Cat# 564668) from BD Biosciences, APC-Cy7 HLA-DR (Cat# 307617) and BV605 CD14 (Cat# 301834) from Biolegend and PE-Cy5.5 CD11c (Cat# MHCD11c18) from Life Technologies. The backbone staining was performed for 20 min at room temperature (RT) in the dark before washing. The cells were then added to the plates provided in the LEGENDScreen™ kit and the rest of the experiment was performed according to the manufacturer's protocol.

All samples were run on an 18-color LSR Fortessa (BD Biosciences) with 407, 488, 561 and 640 lasers using the BD FACSDiva™ Software (BD Biosciences). Flow cytometry data was analyzed using FlowJo version 10 (Treestar, USA) with the DownSample and Uniform Manifold Approximation and Projection (UMAP) plugins. Acquired data was compensated in FlowJo using a compensation matrix generated based on antibody-stained control beads. For UMAP analysis, the different myeloid populations from blood, SAT or VAT were concatenated, generating 8 files. These files were then downsampled so that all samples contained the same number of events. The files were then concatenated for analysis. UMAP was run using all parameters from the verification panel.

Gene Expression Analysis

Total RNA was isolated from frozen adipose tissue using the RNA/DNA/Protein Purification Plus kit (Norgen Biotek Corp.). Briefly, approximately 100 mg of adipose tissue was cut, and the tissue was lysed in Buffer SKP (from the kit) using cold stainless-steel beads in a Tissuelyser (Qiagen) for 3 x 2 minutes at 25 Hz. RNA was then purified according to the protocol provided in the kit. cDNA was synthesized using 350 ng RNA input with the High-Capacity cDNA Reverse Transcription Kit (Applied Biosystems) and diluted 1:2 in PCR-grade water. Real-time qPCR was performed using SYBR Green I Master (Roche) on a Lightcycler ® 480 II (Applied Biosystems). Primers were purchased from Sigma (see **Table S2**). Gene expression was calculated relative to the expression of importin 8 (IPO8).

Immunohistochemistry and Determination of Adipocyte Cell Size

Adipose tissue biopsies collected during bariatric surgery were kept in Histocon transport solution (Histolab) before the tissue was fixed in 4% formalin (in PBS) for approximately 24 h. The tissue was then transferred to 70% EtOH before paraffin embedment, sectioning and staining with CD68. Antigen unmasking and deparaffinization were performed simultaneously using a PTLink machine (Dako, Denmark) containing Target Retrieval Solution, Low pH (Dako, Denmark). The sections were heated at 98°C for 24 minutes and cooled down to 58°C. The sections were then washed in PBS and incubated with 3% H_2O_2 (in H_2O) for 10 minutes to block endogenous peroxidase activity, before washing again. The sections were then incubated with 2-3 drops of INNOVEX Background Buster (Biosciences, #NB306) for

20 minutes in a moisture chamber at RT. Following washing, the sections were stained with the primary antibody mouse-anti human CD68 (Thermo Fisher Scientific Cat# 14-0688-82) at a concentration of 0.05 mg/ml diluted in Normal Horse Serum 2.5% (ImmPRESS kit, Vector, MP-7402) over night at 4°C. Mouse anti-human IgG1 antibody (Abcam, ab18443) was used as isotype control. Following primary antibody staining, the sections were washed and incubated with 2-3 drops of the secondary antibody, horse anti-mouse IgG conjugated with HRP (ImmPress kit, Vector MP-7402) for 30 minutes at room temperature. After washing, the sections were incubated with DAB substrate (Vector, SK-4105) diluted in ImmPACT DAB diluent (Vector, SK-4105) for 10 minutes at RT before washing again. The sections were then counterstained with hematoxylin for 3 minutes before they were rehydrated in increasing concentrations of EtOH (70, 96 and 100%) and xylene. Lastly, the sections were mounted with cover glass using Pertex glue (Histolab. The slides were imaged using an Olympus BX61VS microscope with the imaging system Olympus VS120 S6 slide scanner. CD68+ macrophages in crown-like structures around adipocytes were identified. Crown-like structures were defined three or more macrophages surrounding an adipocyte (11). The images were processed in Image J (Fiji) with the plugin Adiposoft to measure adipocyte diameter (22). The median diameter was calculated for each sample.

Statistical Analysis

Data was analyzed using Prism version 9 (GraphPad). Correlation analyses were performed using SPSS (IBM) or R (https://www.r-project.org). D'Agostino & Pearson omnibus normality test was used to determine normality of the data. For normally distributed data, the t-test or one-way ANOVA with Tukey's multiple comparisons test was used. When data was not normally distributed, the Mann-Whitney t-test or Kruskal-Wallis test with Dunn's multiple comparisons test was used. Correlation analyses in SPSS were performed on log-transformed data using bootstrapped (bias-corrected and accelerated, BCa) confidence intervals. Details on statistical analysis are given in figure legends together with the number of subjects included in each analysis. A p-value of < 0.05 was considered statistically significant.

RESULTS

Visceral Adipose Tissue Contains More M1-Like Macrophages Than Subcutaneous Adipose Tissue

We first set out to compare macrophage levels in SAT and VAT and to characterize adipose tissue M1- and M2-like macrophage composition in a depot-specific manner. Using flow cytometry, we analyzed stromal vascular cells from both SAT and VAT as well as peripheral blood mononuclear cells (PBMC) from a cohort of 57 individuals with obesity. The clinical characteristics of this cohort is summarized in **Table 1**. Macrophages and monocytes were identified based on their positive expression of CD45 and HLA-DR and lack of CD3, CD19, and CD56 expression (**Figure 1A**). Further, the macrophage population was divided into M1-(CD11c+CD206+) and M2-like (CD11c-CD206+) macrophages whereas monocytes were defined as CD11c+CD206- cells (**Figure 1B**). The total macrophage/monocyte population was larger in SAT compared to VAT (**Figure 1C**). However, the pro-inflammatory M1-like macrophage population was higher in VAT, whereas no differences were found in the amount ofM2-like macrophages between the two adipose tissue depots (**Figure 1D**). As expected, peripheral blood contained almost exclusively CD11c-positive monocytes, with a small, yet a detectable populations of CD11c+CD206+ myeloid cells (**Figure 1D**). Taken together, these data suggests that although SAT has the largest population of total monocytes and macrophages, pro-inflammatory M1-like macrophages are more abundant in VAT in individuals with obesity.

Confirming the Pro- and Anti-Inflammatory Characteristics of M1-Like and M2-Like ATMs

Currently, there is a lack of consensus regarding which surface receptors best define M1- and M2-like macrophages in adipose tissue. We therefore investigated whether the stratification of macrophages into pro- and anti-inflammatory subsets based on expression of CD11c and CD206 could be further refined by assessing expression of other, known macrophage/monocyte surface receptors, such as CCR2, CD16, CD163, CD44, CD14, CD40, and HLA-DR (**Figure 1E**). Indeed, the M1-like macrophages (CD11c+ CD206+) expressed high levels of CCR2, an established pro-inflammatory, chemotactic marker (23), whereas CCR2-expression on the M2-like macrophages (CD11c-CD206+) was low (**Figure 1F**). CCR2 expression was also high on monocytes both in blood and adipose tissue. CD44 is another pro-inflammatory receptor (12) that displayed a similar pattern to CCR2, although with somewhat higher expression on M2-like macrophages compared to CCR2 (**Figure 1G**). CD14 and CD16 have also been described as pro-inflammatory ATM surface receptors (24). In line with this, we found CD16 expression on more of the M1-like macrophages than the M2-like macrophages. However, about 80% of the M1-like macrophages did not express CD16 (**Figure 1H**), suggesting the existence of CD16+/- M1-like macrophage subpopulations in both SAT and VAT. CD14 was more highly expressed on macrophages than on monocytes, but there was no difference in CD14 expression between the M1- and M2-like macrophage populations (**Figure 1I**). In agreement with their high capacity for antigen presentation, M1-like macrophages expressed the highest levels of HLA-DR in both fat depots and in the blood (**Figure 1J**). The same pattern was observed for CD40 (**Figure 1K**), which is expressed at higher levels on activated macrophages and is known to be expressed on recruited ATMs (24). CD163 has been described as an anti-inflammatory macrophage marker (25). Accordingly, CD163 was expressed on a higher percentage of the M2-like macrophages relative to the M1-like macrophages in VAT. However, this was not the case in SAT,

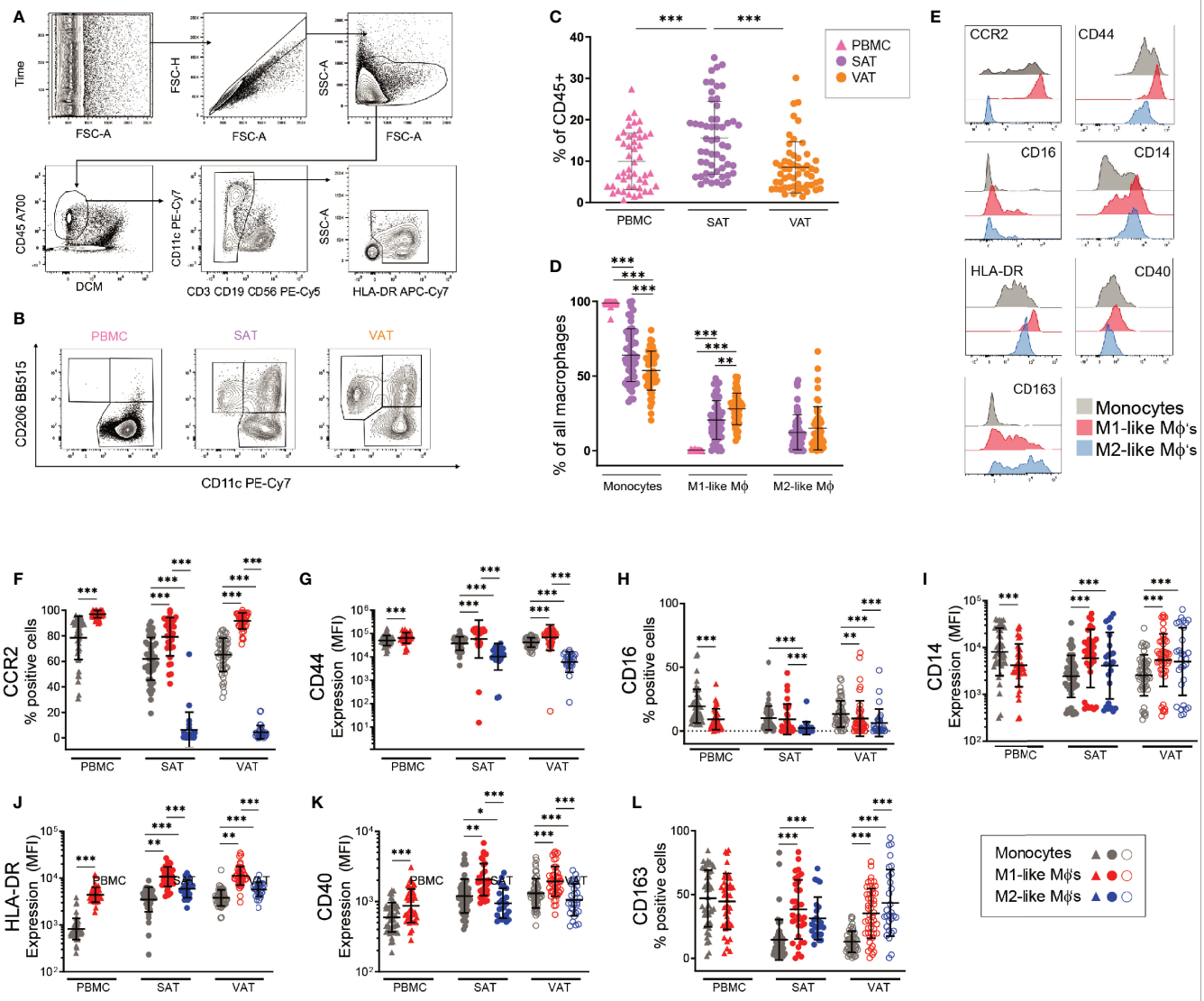

FIGURE 1 | Identification and characterization of macrophage populations in blood and adipose tissue of humans with obesity. **(A)** Flow cytometry gating scheme used to identify monocytes and macrophages. Arrows indicate the sequence of gating. **(B)** Representative flow cytometry plots showing CD206 and CD11c expression on monocytes (CD11c+CD206-), M1-(CD11c+CD206+) and M2-like (CD206+CD11c-) macrophages from PBMC, SAT, and VAT samples from one patient. **(C)** The total monocyte and macrophage population as a fraction of total CD45+ cells in PBMC (n=47), SAT (n=54), and VAT (n=54). **(D)** Monocytes, M1- and M2-like macrophages (MΦ) as a fraction of the total monocyte and macrophage population in PBMC (n=47), SAT (n=54), and VAT (n=54). **(E)** Representative stainings for the surface proteins shown in **(F-L)**. **(F-L)** Scatter plots showing expression of surface proteins **(F)** CCR2, **(G)** CD44, **(H)** CD16, **(I)** CD14, **(J)** HLA-DR, **(K)** CD40, and **(L)** CD163 on monocytes (grey), M1 (red)-, and M2 (blue)-like macrophages (MΦ's) from PBMC (n=47), SAT, and VAT (n=54). For **(F, H, L)** scatter plots showing percentage of cells expressing the proteins. For **(G, I-K)** scatter plots showing expression (mean fluorescence intensity, MFI) of surface proteins. For **(C, D, F-L)** line and error bars represent mean and SD. For **(C, D)**, the Mann-Whitney *U*-test was used for comparison between groups. **p< 0.01, ***p<0.001. For **(E-L)**, the Wilcoxon matched pair signed rank test was used for comparison between groups, *p < 0.05, **p < 0.001, ***p < 0.001.

and it should be noted that expression of CD163 varied considerably within both the M1- and M2-like cell populations (**Figure 1L**).

Taken together, the positive expression of CD44, HLA-DR, CD40, and in particular CCR2, support the pro-inflammatory identity of M1-like macrophages. M2-like macrophages displayed low levels of CCR2 and at the same time expressed somewhat higher levels of CD163 than M1-like macrophages, supporting their anti-inflammatory nature. The large variation in the expression of several surface receptors on both the M1- and the M2-like macrophages suggest that subpopulations within both pro- and anti-inflammatory ATMs exist, potentially with different functional patterns.

Identification of Novel Adipose Tissue Macrophages Surface Proteins Using a Proteome Screen

With the aim to identify novel surface receptor expression for detailed characterization of macrophages and monocytes in the adipose tissue, we performed a flow cytometry-based surface proteome screening using the LEGENDScreen™ kit. SVF isolated from SAT and PBMCs isolated from blood donors were pre-stained with a backbone panel allowing for the identification of myeloid cells from the AT as well as blood monocytes ($CD45^+CD14^+HLA\text{-}DR^+$ cells), and then evaluated for surface expression of 315 distinct proteins. The experimental overview is presented in **Figure 2A**.

Among the commonly expressed surface markers by AT- and blood monocytes, the blood monocytes generally expressed higher levels of many of the analyzed markers (**Figure 2B**). Also, a number of surface proteins seemed to be unique for blood monocytes, including CD99, CD87, CD102, CD13, CD93 and CD61, whereas only three markers, CD274, CD83, and CXCL16, were unique to the AT monocytes (**Figure 2B**). It is worth noting that the blood and AT samples were not obtained from the same donors.

We further compared the expression of the surface proteins on AT monocytes ($CD11c^+CD206^-$), M1- ($CD11c^+CD206^+$), and M2-like ($CD11c^-CD206^+$) macrophages (**Figure 2C**). A substantial overlap was observed between the surface proteome of macrophages and monocytes and when comparing M1- and M2-like macrophages, but we also identified distinct M1- and M2-like macrophage and monocyte/macrophage proteins (**Figure 2C**). M1-like macrophages expressed the surface proteins CCR2, CD48, CD371, CD85a, CD49d, CX3CR1, and CD52 at higher levels than the M2-like macrophages, while CD116, CD51, CD26, and integrin α9β1 were expressed at higher levels on the M2-like macrophages. AT monocytes displayed a surface receptor expression pattern similar to the M1-like macrophages, still, several surface proteins were expressed on M1-like macrophages but not on AT monocytes, such as CD40, CD74, FcεRIα, integrin β5, and CD276. The last two were also expressed on M2-like macrophages, indicating that these receptors separate ATMs from AT monocytes.

Verification of Identified ATM Surface Proteins and Comparing Their Expression in SAT and in VAT

Based on degree of differential expression and novelty, we next selected some surface proteins for a more detailed characterization of macrophages from both subcutaneous and visceral adipose tissue in a new cohort of individuals with obesity (N=23). This allowed for validation of the protein expression on ATMs obtained from the proteomic screen as well as exploring the expression of these surface proteins on ATMs from individuals with obesity. We analyzed expression of the surface proteins CCR2/CD192, CD85a, CD48, and CD371, which were found to be highly expressed on M1-like macrophages and the proteins CD26, CD116, CD51 and integrin α9β1 that were expressed at higher levels on the M2-like macrophages. We confirmed that expression of CCR2 was high on M1-like macrophages and AT monocytes and low on M2-like macrophages (**Figure 3A**) and this protein was expressed at higher levels on M1-like macrophages from VAT compared to SAT. CD85a was also highly expressed on M1-like compared to M2-like macrophages, however, this protein was also expressed on a smaller population of M2-like macrophages (**Figure 3A**). CD48 and CD371, known to be involved in regulation and initiation of immune responses (26), were also expressed more highly on M1-like compared to M2-like macrophages (**Figure 3A**). However, on average only around 50% of M1-like macrophages expressed these proteins, and with expression varying from low (around 10%) to higher (around 80%), which could be indicative of subtypes of M1-like macrophages.

CD26, also known as dipeptidyl peptidase-4 (DPP-4), was expressed on around 70% of M2-like macrophages and 50% of M1-like macrophages from the screening. However, the validation showed that this protein was expressed at low levels on both M1- and M2-like macrophages, and expression was not different between the two ATM populations (**Figure 3A**). CD116, also identified as a M2-like specific marker from the screening, was expressed at higher levels on M1-like macrophages and was quite lowly expressed on M2-like macrophages, suggesting that this might be an M1-like rather than a M2-like macrophage marker (**Figure 3A**). Another surface protein found to be more highly expressed on M2-like macrophages in the screening was CD51 and this protein was expressed on higher levels on M2-like macrophages compared to M1-like macrophages, but only in VAT (**Figure 3A**). Integrin α9β1 was found to be highly expressed on M2-like macrophages, and a higher expression on M2-like compared to M1-like macrophages was confirmed in both SAT and VAT in the validation cohort (**Figure 3A**). However, the overall expression was found to be low on both M1- and M2-like macrophages in contrast to what was observed in the screening.

The single-parameter flow cytometry shown in **Figure 3A** gives an overall representation of each surface marker expression on the different cell types; however, it does not provide information about the combination of different surface proteins on each cell. Thus, we performed UMAP analysis to investigate multivariate relationships between the phenotypic markers (**Figure 3B**). To this end, monocytes, M1-, and M2-like macrophages from peripheral blood, SAT and VAT were electronically barcoded, concatenated, and analyzed. We observed that myeloid cells from peripheral blood (pink) clustered separately from the adipose tissue myeloid cells (purple and orange), indicating tissue-specific expression patterns. Also, separate clusters were observed for monocytes (grey) and M1-like macrophages (red) from the peripheral blood, which was also true for monocytes, M1- and M2-like macrophages in the adipose tissue. Here, the monocyte and M1-like macrophage clusters were closer together compared to the M2-like macrophages, indicating their similarities. Interestingly, the M2-like macrophages from SAT and VAT seemed to localize in two clusters, indicating that these cells might be phenotypically different depending on the adipose depot where they reside.

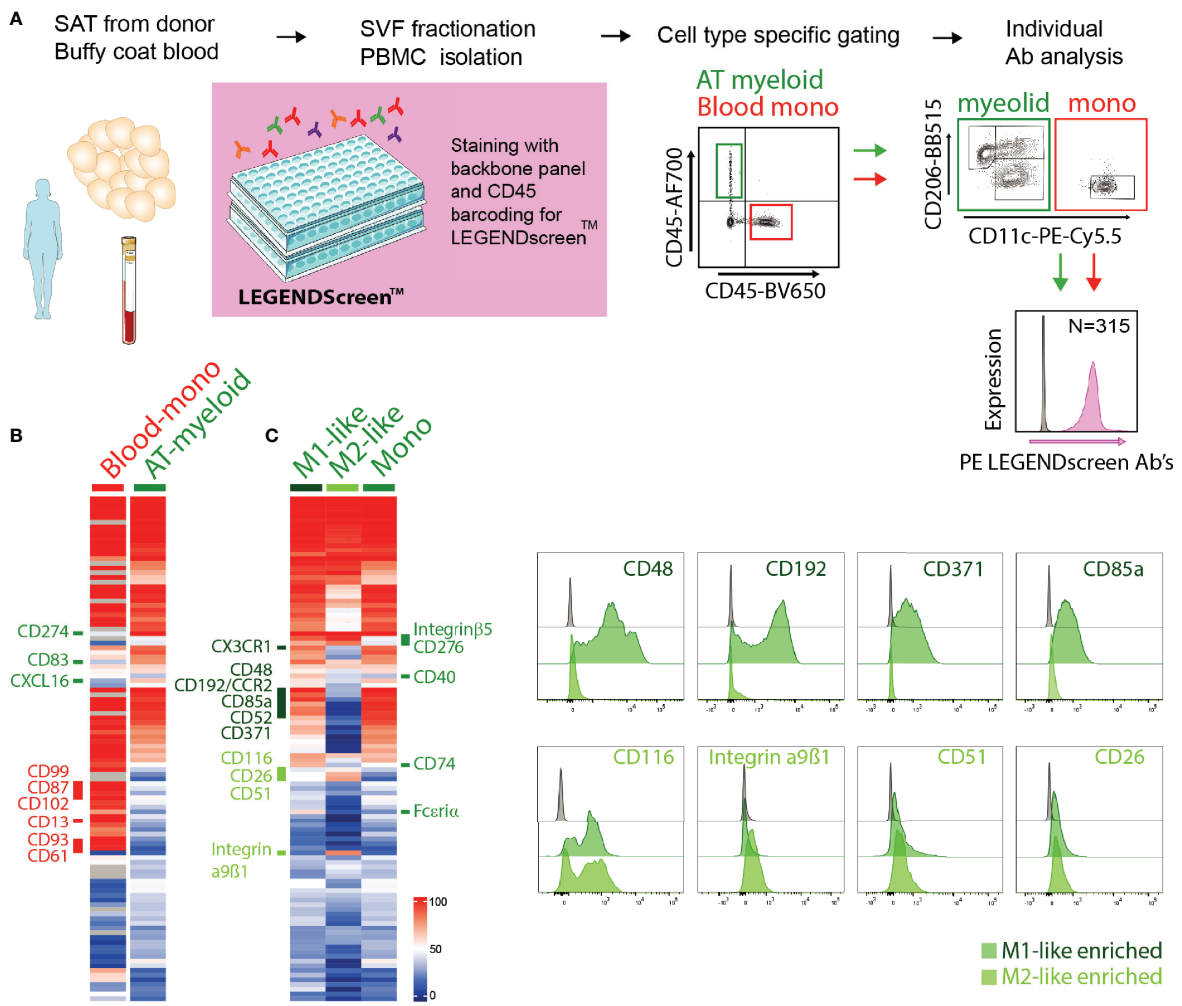

FIGURE 2 | Surface proteome analysis of adipose tissue macrophages. **(A)** Experimental overview of the surface proteome screening using the LEGENDscreen™ kit. **(B)** Expression of surface proteins on blood monocytes (Blood-mono) and AT myeloid cells. Heatmap based on the percentage of cells expressing each surface protein, with a cut-off of minimum 20% expression by at least one of the populations. **(C)** Expression of surface proteins on AT M1- and M2-like macrophages and monocytes (mono). Heatmap based on the percentage of cells expressing each surface protein, with a cut-off of minimum 20% expression by at least one of the populations. Representative staining of a selection of surface proteins expressed on M1-like (dark green) or M2-like (light green) ATMs.

The high-dimensional UMAP analysis confirmed that CCR2 and CD116 were highly expressed on monocytes and M1-like macrophages and lowly expressed on M2-like macrophages. The expression patterns of CD48 and CD371 were similar, but highly expressed only in a subgroup of the M1-macrophages. The VAT M2-like macrophages displayed a higher expression of both integrin α9β1 and CD51, and there was a separate population of SAT M2-like macrophages that expressed higher levels of CD26, CD116, and CD51. The UMAP analysis also confirmed overall low expression of CD26. However, this protein seemed to be differentially expressed between distinct myeloid populations, including a group of monocytes that expressed high levels of CD116, CD26, and CD85a and low levels of CD48, further supporting the existence of monocyte/macrophage subsets.

Taken together, we verified CCR2, CD85a, CD48 and CD371 as proteins expressed at M1-like macrophages. Additionally, CD116 was found to be highly expressed on M1- compared to M2-like macrophages. Expression of CD26 was overall low but enriched in some clusters, whereas CD51 and integrin α9β1 seems to be distinctly expressed on M2-like macrophages.

Adipose Tissue Macrophages Associate With Insulin Resistance and Circulating Lipids

Next, we wanted to investigate how the M1- and M2-like macrophage composition in the adipose tissue of individuals with obesity was related to systemic insulin resistance and other

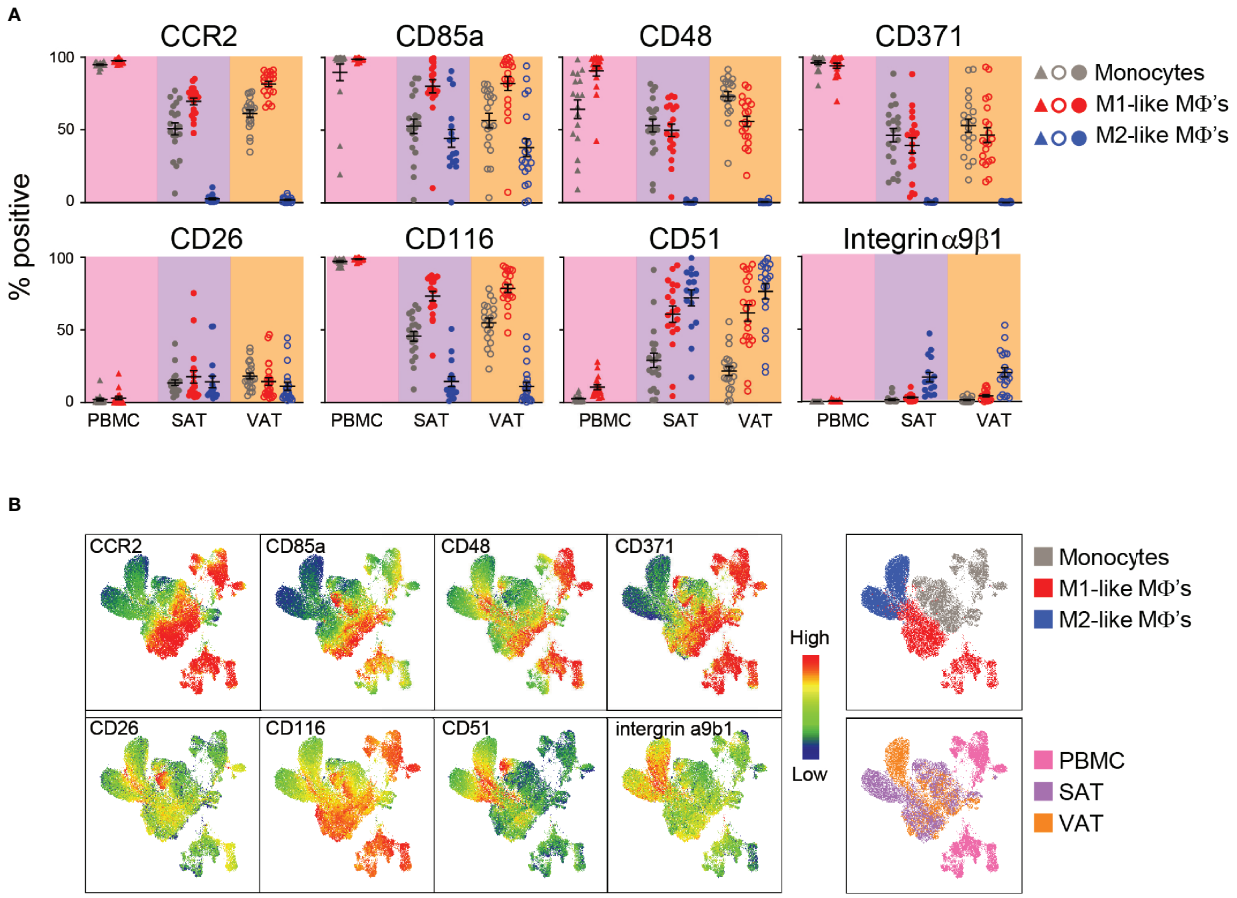

FIGURE 3 | Verification of surface protein expression on M1- and M2-like adipose tissue macrophages from humans with obesity. **(A)** Scatter plots showing expression of surface proteins CCR2, CD85a, CD48, CD371, CD26, CD116, CD51, and integrin α9β1 on monocytes (grey), M1 (red)-, and M2 (blue)-like macrophages (MΦ's) from PBMC (n=17), SAT (N=23), and VAT (n=23). **(B)** UMAP plots showing expression of the surface proteins analyzed in **(A)** with blue indicating low and red indicating high expression as well as UMAP plots colored according to cell origin (top) and tissue origin (bottom).

parameters relevant for metabolic function in the total patient cohort (Cohort 1 and 2, N=80). Insulin resistance, assessed by homeostatic model assessment for insulin resistance (HOMA-IR), was positively correlated with M1-like macrophages (*r=0.319, p=0.014*) and negatively correlated with M2-like macrophages (*r= –0.325, p=0.012*) in VAT, but not in SAT. Additionally, HOMA-IR was correlated with the pro-inflammatory M1/M2 ratio in VAT (*r=0.331, p=0.011*). Because BMI is a potential confounder for associations with metabolic parameters, we performed a partial correlation analysis (**Figure 4A**). The correlation between HOMA-IR and M1-like macrophages, M2-like macrophages and the M1/M2 ratio in VAT was still statistically significant after correcting for BMI. Additionally, the M1/M2 ratio in SAT now displayed a positive correlation with HOMA-IR. Further, serum triglyceride levels correlated negatively with M2-like macrophages and positively with the M1/M2 ratio in both adipose tissue depots, whereas HDL levels were positively correlated with M2-like macrophages in VAT. Interestingly, there were no significant correlations between ATMs and circulating CRP levels.

Taken together, these results indicate that, independently of BMI, insulin resistance is associated with an elevated ratio of M1- to M2-like macrophages in both SAT and VAT. M1/M2 ratio in both adipose tissue depots correlated positively with triglycerides, and this seemed to be driven by a negative correlation between M2-like macrophages and triglycerides.

Insulin Resistance, CLS and Transcriptional Inflammatory Markers in SAT and VAT

In the first cohort of 57 individuals with obesity we next compared adipose tissue inflammation in SAT and VAT of individuals with obesity by measuring inflammatory gene expression and performing immunohistochemistry analyses of crown-like structures (CLS). The gene expression level of the general macrophage marker *CD68* was higher in SAT than in VAT (**Figure 4B**), in agreement with the flow cytometry data of elevated macrophage/monocyte levels in SAT (**Figure 1C**). The same was the case for *CCL-2*, encoding the cytokine MCP-1, which

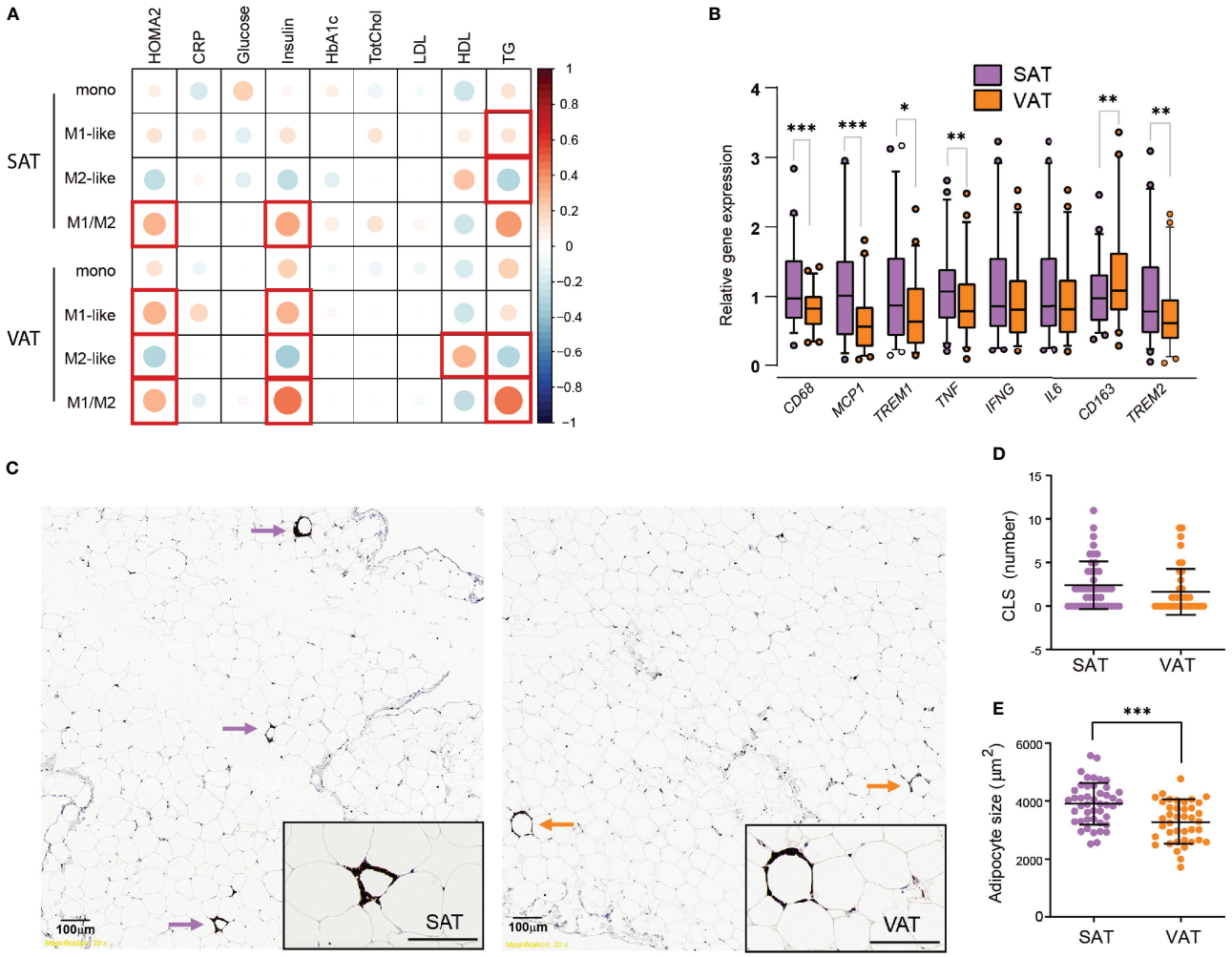

FIGURE 4 | Insulin resistance, dyslipidemia, and inflammatory markers in SAT and VAT. **(A)** Pearson correlations between monocytes, M1-, and M2-like macrophages and M1/M2 ratio in SAT and VAT and biochemical parameters, corrected for BMI (n=80). Size and color intensities of circles indicate correlation coefficients. Red squares indicate significant ($p<0.05$) correlations. **(B)** Relative gene expression of *CD68*, *MCP1*, *TREM1*, *TNF*, *IFNG*, *IL6*, *CD163*, and *TREM2* for n = 46 (39 matched) SAT and VAT samples. Results are presented as fold changes ($2^{-\Delta\Delta CT}$) of target gene and normalized to *IPO8*. Expression levels of the SAT samples were set to 100%. **(C)** Representative pictures showing from SAT and VAT samples stained with CD68 antibody identifying crown-like structures (CLS) defined as three or more macrophages surrounding an adipocyte. **(D)** Graph showing numbers of CLS in SAT and VAT for n = 46 (39 matched) SAT and VAT samples. **(E)** Graph showing median adipocyte size in μm^2 in SAT and VAT for n = 53 SAT and VAT samples. Bars in **(B)** represent mean and error bars represent SD. For **(D, E)** line represents the mean and error bars represents SD. The Wilcoxon matched pairs signed rank test was used for comparison between SAT and VAT in **(B, D)**. The paired t-test was used for comparison between SAT and VAT in **(E)**. *$p < 0.05$, **$p < 0.01$, ***$p < 0.001$.

is associated with infiltration of monocytes (23). The pro-inflammatory genes *TNF* and *TREM1* were also expressed at higher levels in SAT compared to VAT. However, no differences between SAT and VAT were found in the expression of two other pro-inflammatory genes, *IL6* and *interferon* (*IFN*)-*γ*. The two anti-inflammatory genes analyzed showed opposite expression patterns to each other, with *TREM2* being elevated in SAT, whereas *CD163* expression was higher in VAT. Thus, these gene expression data did not reveal clear differences in inflammation between the AT depots.

Furthermore, we found that CLS, made up of CD68-positive macrophages surrounding adipocytes, were present in both SAT and in VAT (**Figure 4C**), similar to what has been observed by others (27). However, there were in general very few CLS observed in our cohort, and we found no significant differences in the amount of CLS between SAT and VAT (**Figure 4D**). CLS are expected to form around large, dying adipocytes, and we therefore performed histological measurements of adipocyte size. We found a higher median adipocyte size in SAT compared to VAT (**Figure 4E**), however, when investigating the association between gene expression, numbers of CLS, adipocyte size, and insulin resistance or circulating lipid parameters, we found only weak, non-significant correlations (data not shown).

Taken together, these data support larger adipocytes and somewhat higher expression of macrophage-related genes in

SAT as compared to VAT. However, the lack of depot-specific differences in the number of CLS and the measured transcriptional inflammatory markers suggest that any difference in inflammatory tone between SAT and VAT in our cohort of individuals with obesity is moderate. Moreover, we found no clear associations between these markers of adipose tissue inflammation and circulating biochemical markers for metabolic dysregulation.

DISCUSSION

Recent investigations, including single-cell transcriptional studies, have revealed that adipose tissue harbor various macrophage subpopulations, including metabolically activated macrophages, and antioxidant macrophages (Mox) (19, 28, 29). Similar to the M1- and M2-like ATMs, these cells respond to changes in adipose tissue microenvironment during obesity, also displaying pro- and anti-inflammatory properties (19). However, the literature regarding which combination of surface proteins that define the different ATM subtypes in humans is still ambiguous. Here, we used a surface proteomics approach to identify novel proteins for a more detailed characterization of human M1- and M2-like ATMs, defined as myeloid cells that co-express CD11c and CD206 or CD206 only, respectively (11).

The pro-inflammatory nature of M1-like ATMs was first confirmed by their elevated expression of CCR2, CD44, HLA-DR and CD40 relative to M2-like cells. The proteomics screen and subsequent verification analysis, further identified CD85a, CD48, CD371, CX3CR1 and CD116 as additional M1-like macrophages-specific markers. To our knowledge, CD85a, CD48, and CD371 have not previously been reported to be expressed on ATMs. CD48 and CD371 are involved in regulation and initiation of immune responses (26, 30), and CD85a and CX3CR1 are known to be expressed on various myeloid cell types (31, 32). Indeed, all these markers were also expressed on monocytes, which is in agreement with known functional similarities between AT monocytes and M1-like macrophages, such as their ability to infiltrate into the AT (24, 31). Interestingly, the surface proteome screening demonstrated generally low expression of proteins on the tissue-resident M2 macrophages, and only the expression levels of the two integrins CD51 and integrin $\alpha 9\beta 1$ were confirmed to be expressed at higher levels on the M2-compared to M1-like macrophages. Nevertheless, an UMAP analysis, which includes signals from all the surface markers in the panel simultaneously, revealed two distinct M2-like populations in SAT and VAT, respectively, possibly with functional differences. This emphasizes the potential of using multiple markers to characterize ATM composition with high resolution.

The literature concerning depot-specific differences in adipose tissue macrophage subtypes is contradictory. While some studies claim that infiltrating pro-inflammatory macrophages are most abundant in VAT (14, 17), others report higher levels of M1-like macrophages in SAT (11). In our study, the flow cytometry data indicated a higher relative abundance of total macrophages and monocytes in SAT, but still the pro-inflammatory M1 macrophages were more abundant in VAT, supporting previous findings that AT inflammation in splanchnic areas is of clinical relevance in obesity (15).

The pro-inflammatory M1/M2 ratio in both SAT and VAT correlated positively with HOMA-IR and circulating markers of dyslipidemia in our study, in agreement with the notion that inflammation in both these adipose tissue depots may contribute to metabolic dysfunction (33). These correlations were for most parts intact when correcting for BMI, suggesting that BMI variation among individuals with obesity is of minor importance for these associations. Interestingly, the significant correlations between adipose tissue M1/M2 ratio and circulating triglyceride levels seemed to be mainly driven by the inverse association with M2-like macrophages levels, suggesting a protective role for M2 macrophages in the development of dyslipidemia. This is in line with recent findings of accumulating anti-inflammatory, lipid-metabolizing macrophages in the adipose tissue, acting to prevent metabolic derangements during overnutrition (29). In fact, these lipid-associated macrophages (LAMs) formed CLS for lipid transfer into the macrophages in order to prevent adipocyte hypertrophy and loss of systemic lipid homeostasis under obesity conditions, a process that was dependent on Trem2 expression (29). Accordingly, others have shown that CLS contain anti-inflammatory Mox macrophages, characterized by expression of HO1 and Txnrd1 (31). In this sense, CLS occurrence in adipose tissue is not necessarily a measure of inflammation, and the low levels of CLS macrophages found in our study may thus represent a weakened protective mechanisms rather than low inflammation, although a more detailed characterized of these CLS will be necessary before making firm conclusions about their role in obesity-related adipose tissue inflammation.

Interestingly, a very recent study found that pro-inflammatory ATMs were not related to adipose tissue insulin resistance in humans (34). In that study, adipose tissue insulin resistance was elegantly measured, using state-of the-art tracer methods to determine the insulin concentration necessary to suppresses adipose tissue lipolysis by 50% (IC_{50}). It was found that adipocyte size is the major driver for adipose tissue insulin resistance, and that any positive associations between adipose tissue inflammation and adipose tissue insulin resistance could be explained by the confounding effect of adipocyte hypertrophy (34). This was the case both when measuring inflammatory gene expression and pro- and anti-inflammatory ATMs by immunohistochemistry, defined as CD14- and CD206-positive cells, respectively. In fact, our transcriptional data supported this notion, as we did not find any significant association between adipose tissue inflammatory gene expression levels and HOMA-IR. However, the inflammatory gene expression levels represent an average from many cell types, and is less accurate than flow cytometry data that provides a distinct, high-resolution measure of macrophages *per se*. The flow cytometry data should thus be considered a more representative measurement for ATM status than both gene expression data and low-resolution IHC single-

markers measurements (34). Of note, in our study the positive association between pro-inflammatory ATMs and HOMA-IR remained statistically significant even after correcting for adipocyte size, and our data is thus in line with the established idea that inflammatory mediators in the obese adipose tissue represent a mechanistic link that can lead to systemic insulin resistance (35). The discrepancy between the studies may, in addition to the abovementioned methodological issues, be explained by the different measures of insulin resistance; HOMA-IR reflects the balance between hepatic glucose output and insulin secretion by the β-cell (36), whereas the IC_{50} reflects lipolytic activity in the adipose tissue. Thus, further investigation of the role of ATMs in adipose tissue insulin resistance should be investigated using more high-resolution methods in future studies.

Therapeutic use of anti-inflammatory agents has been suggested for the treatment of metabolic disease (35). Indeed, targeting classical inflammatory molecules including IL-1, IL-6 and TNF have been shown to reduce the risk of diabetes and improve insulin sensitivity in some studies, although with variable effects (37–39). These treatments normally target circulating cytokines, even though interactions with paracrine/autocrine signaling within the tissue may be more relevant (40). Thus, targeting the local inflammation in the adipose tissue may be a valid treatment strategy, and ATMs are considered important targets for the treatment of chronic inflammation and obesity-related metabolic diseases (41, 42). It is, however, still not clear whether accumulation of pro-inflammatory ATMs is a cause or a consequence of insulin resistance, and to what extent immune cell infiltration and activation have beneficial or detrimental effects on adipose tissue homeostasis (29, 43, 44). Thus, interventional strategies focusing on ATMs will require a thorough understanding of the balance between beneficial versus pathological immune cell subsets and how they contribute to metabolic homeostasis. In conclusion, our study confirms a positive association between pro-inflammatory ATM ratio in both SAT and VAT and insulin resistance, measured by HOMA-IR. We also provide novel ATM surface markers that may enable detailed characterization and functional measurements, as well as act as potential targets for therapeutic manipulation of adipose tissue macrophages in the treatment of metabolic disease.

DATA AVAILABILITY STATEMENT

The original contributions presented in the study are included in the article/**Supplementary Material**. Further inquiries can be directed to the corresponding author.

ETHICS STATEMENT

The studies involving human participants were reviewed and approved by Regional Etisk komité for forskningsetikk, Vest Norge (REK Vest). The patients/participants provided their written informed consent to participate in this study.

AUTHOR CONTRIBUTIONS

KS planned and performed experiments, acquired and analyzed data and wrote the manuscript. NS designed the flow cytometry panels, planned experiments and reviewed/edited the manuscript. MH planned and performed experiments and reviewed/edited the manuscript. ZK and VL performed experiments, acquired and analyzed data. LL-A analyzed data. MC contributed to the discussion, supervised the work and reviewed/edited the manuscript. IH acquired data and reviewed/edited the manuscript. CB and HN sampled the adipose tissue biopsies. PN provided reagents and funding and reviewed/edited the manuscript. GM and NB provided funding, contributed to the discussion, supervised the work and reviewed/edited the manuscript. JF designed the study, oversaw its conduction, researched data, provided funding, contributed to the discussion, and wrote the manuscript. All authors contributed to the article and approved the submitted version.

ACKNOWLEDGMENTS

The flow cytometry was performed at the Flow Cytometry Core Facility, Department of Clinical Science, University of Bergen. The microscope imaging was performed at the Molecular Imaging Center, Dept. of Biomedicine, University of Bergen. This work was funded by the Western Norway Regional Health Authority (Helse Vest RHF), the Swedish Research Council, the Swedish Cancer Society, the Swedish Foundation for Strategic Research, the Swedish Society for Medical Research, Knut and Alice Wallenberg Foundation, the Novo Nordisk Foundation, the Center for Innovative Medicine at Karolinska Institutet, Region Stockholm, The Erling-Persson Family Foundation, SRP Diabetes Karolinska Institutet, Karolinska Institutet, Trond Mohn Stiftelse, and The Norwegian Diabetes Association.

SUPPLEMENTARY MATERIAL

The Supplementary Material for this article can be found online at: https://www.frontiersin.org/articles/10.3389/fendo.2022.856530/full#supplementary-material

REFERENCES

1. Haslam DW, James WPT. Obesity. *Lancet* (2005) 366(9492):1197–209. doi: 10.1016/S0140-6736(05)67483-1
2. Hotamisligil GS. Inflammation and Metabolic Disorders. *Nature* (2006) 444 (7121):860–7. doi: 10.1038/Nature05485
3. Lumeng CN, Saltiel AR. Inflammatory Links Between Obesity and Metabolic Disease. *J Clin Invest* (2011) 121(6):2111–7. doi: 10.1172/JCI57132
4. Kahn SE, Hull RL, Utzschneider KM. Mechanisms Linking Obesity to Insulin Resistance and Type 2 Diabetes. *Nature* (2006) 444(7121):840–6. doi: 10.1038/Nature05482
5. Xu H, Barnes GT, Yang Q, Tan G, Yang D, Chou CJ, et al. Chronic Inflammation in Fat Plays a Crucial Role in the Development of Obesity-Related Insulin Resistance. *J Clin Invest* (2003) 112(12):1821–30. doi: 10.1172/JCI19451
6. Weisberg SP, McCann D, Desai M, Rosenbaum M, Leibel RL, Ferrante AW. Obesity is Associated With Macrophage Accumulation in Adipose Tissue. *J Clin Invest* (2003) 112(12):1796–808. doi: 10.1172/JCI19246

7. Lumeng CN, Bodzin JL, Saltiel AR. Obesity Induces a Phenotypic Switch in Adipose Tissue Macrophage Polarization. *J Clin Invest* (2007) 117(1):175–84. doi: 10.1172/JCI29881
8. Fernø J, Strand K, Mellgren G, Stiglund N, Björkström NK. Natural Killer Cells as Sensors of Adipose Tissue Stress. *Trends Endocrinol Metab* (2020) 31 (1):3–12. doi: 10.1016/j.Tem.2019.08.011
9. Chávez-Galán L, Olleros ML, Vesin D, Garcia I. Much More Than M1 and M2 Macrophages, There are Also CD169+ and TCR+ Macrophages. *Front Immunol* (2015) 6:263(MAY). doi: 10.3389/Fimmu.2015.00263
10. Bertani FR, Mozetic P, Fioramonti M, Iuliani M, Ribelli G, Pantano F, et al. Classification of M1/M2-Polarized Human Macrophages by Label-Free Hyperspectral Reflectance Confocal Microscopy and Multivariate Analysis. *Sci Rep* (2017) 7(1):8965. doi: 10.1038/S41598-017-08121-8
11. Wentworth JM, Naselli G, Brown WA, Doyle L, Phipson B, Smyth GK, et al. Pro-Inflammatory CD11c+CD206+ Adipose Tissue Macrophages Are Associated With Insulin Resistance in Human Obesity. *Diabetes* (2010) 59 (7):1648–56. doi: 10.2337/Db09-0287
12. Liu LF, Kodama K, Wei K, Tolentino LL, Choi O, Engleman EG, et al. The Receptor CD44 is Associated With Systemic Insulin Resistance and Proinflammatory Macrophages in Human Adipose Tissue. *Diabetologia* (2015) 58(7):1579–86. doi: 10.1007/S00125-015-3603-Y
13. Apovian CM, Bigornia S, Mott M, Meyers MR, Ulloor J, Gagua M, et al. Adipose Macrophage Infiltration is Associated With Insulin Resistance and Vascular Endothelial Dysfunction in Obese Subjects. *Arterioscler Thromb Vasc Biol* (2008) 28(9):1654–9. doi: 10.1161/ATVBAHA.108.170316
14. Harman-Boehm I, Blher M, Redel H, Sion-Vardy N, Ovadia S, Avinoach E, et al. Macrophage Infiltration Into Omental Versus Subcutaneous Fat Across Different Populations: Effect of Regional Adiposity and the Comorbidities of Obesity. *J Clin Endocrinol Metab* (2007) 92(6):2240–7. doi: 10.1210/Jc.2006-1811
15. Klöting N, Fasshauer M, Dietrich A, Kovacs P, Schön MR, Kern M, et al. Insulin-Sensitive Obesity. *Am J Physiol Metab* (2010) 299(3):E506–15. doi: 10.1152/Ajpendo.00586.2009
16. Appleton SL, Seaborn CJ, Visvanathan R, Hill CL, Gill TK, Taylor AW, et al. Diabetes and Cardiovascular Disease Outcomes in the Metabolically Healthy Obese Phenotype. *Diabetes Care* (2013) 36(8):2388–94. doi: 10.2337/Dc12-1971
17. Cancello R, Tordjman J, Poitou C, Guilhem G, Bouillot JL, Hugol D, et al. Increased Infiltration of Macrophages in Omental Adipose Tissue Is Associated With Marked Hepatic Lesions in Morbid Human Obesity. *Diabetes* (2006) 55(6):1554–61. doi: 10.2337/Db06-0133
18. Hardy OT, Perugini RA, Nicoloro SM, Gallagher-Dorval K, Puri V, Straubhaar J, et al. Body Mass Index-Independent Inflammation in Omental Adipose Tissue Associated With Insulin Resistance in Morbid Obesity. *Surg Obes Relat Dis* (2011) 7(1):60–7. doi: 10.1016/j.Soard.2010.05.013
19. Kratz M, Coats BR, Hisert KB, Hagman D, Mutskov V, Peris E, et al. Metabolic Dysfunction Drives a Mechanistically Distinct Proinflammatory Phenotype in Adipose Tissue Macrophages. *Cell Metab* (2014) 20(4):614–25. doi: 10.1016/j.Cmet.2014.08.010
20. Hill DA, Lim H-W, Kim YH, Ho WY, Foong YH, Nelson VL, et al. Distinct Macrophage Populations Direct Inflammatory Versus Physiological Changes in Adipose Tissue. *Proc Natl Acad Sci* (2018) 115(22):E5096–105. doi: 10.1073/Pnas.1802611115
21. Levy JC, Matthews DR, Hermans MP. Correct Homeostasis Model Assessment (HOMA) Evaluation Uses the Computer Program. *Diabetes Care* (1998) 21(12):2191–2. doi: 10.2337/Diacare.21.12.2191
22. Galarraga M, Campión J, Muñoz-Barrutia A, Boqué N, Moreno H, Martínez JA, et al. Adiposoft: Automated Software for the Analysis of White Adipose Tissue Cellularity in Histological Sections. *J Lipid Res* (2012) 53(12):2791–6. doi: 10.1194/Jlr.D023788
23. Weisberg SP, Hunter D, Huber R, Lemieux J, Slaymaker S, Vaddi K, et al. CCR2 Modulates Inflammatory and Metabolic Effects of High-Fat Feeding. *J Clin Invest* (2006) 116(1):115–24. doi: 10.1172/JCI24335
24. Russo L, Lumeng CN. Properties and Functions of Adipose Tissue Macrophages in Obesity. *Immunology* (2018) 155(4):407–17. doi: 10.1111/Imm.13002
25. Zeyda M, Farmer D, Todoric J, Aszmann O, Speiser M, Györi G, et al. Human Adipose Tissue Macrophages Are of an Anti-Inflammatory Phenotype But Capable of Excessive Pro-Inflammatory Mediator Production. *Int J Obes* (2007) 31(9):1420–8. doi: 10.1038/Sj.Ijo.0803632
26. Zou C, Zhu C, Guan G, Guo Q, Liu T, Shen S, et al. CD48 is a Key Molecule of Immunomodulation Affecting Prognosis in Glioma. *Onco Targets Ther* (2019) 12:4181–93. doi: 10.2147/OTT.S198762
27. Cinti S, Mitchell G, Barbatelli G, Murano I, Ceresi E, Faloia E, et al. Adipocyte Death Defines Macrophage Localization and Function in Adipose Tissue of Obese Mice and Humans. *J Lipid Res* (2005) 46(11):2347–55. doi: 10.1194/Jlr.M500294-JLR200
28. Kadl A, Meher AK, Sharma PR, Lee MY, Doran AC, Johnstone SR, et al. Identification of a Novel Macrophage Phenotype That Develops in Response to Atherogenic Phospholipids *via* Nrf2. *Circ Res* (2010) 107(6):737–46. doi: 10.1161/CIRCRESAHA.109.215715
29. Jaitin DA, Adlung L, Thaiss CA, Weiner A, Li B, Descamps H, et al. Lipid-Associated Macrophages Control Metabolic Homeostasis in a Trem2-Dependent Manner. *Cell* (2019) 178(3):686–98.e14. doi: 10.1016/j.Cell.2019.05.054
30. Yan H, Kamiya T, Suabjakyong P, Tsuji NM. Targeting C-Type Lectin Receptors for Cancer Immunity. *Front Immunol* (2015) 6:408. doi: 10.3389/Fimmu.2015.00408
31. Serbulea V, Upchurch CM, Schappe MS, Voigt P, DeWeese DE, Desai BN, et al. Macrophage Phenotype and Bioenergetics are Controlled by Oxidized Phospholipids Identified in Lean and Obese Adipose Tissue. *Proc Natl Acad Sci* (2018) 115(27):E6254–63. doi: 10.1073/Pnas.1800544115
32. Yeboah MJ, Papagregoriou C, Jones DC, Chan HTC, Hu G, McPartlan JS, et al. LILRB3 (ILT5) Is a Myeloid Cell Checkpoint That Elicits Profound Immunomodulation. *JCI Insight* (2020) 5(18):e141593. doi: 10.1172/Jci.Insight.141593
33. Burhans MS, Hagman DK, Kuzma JN, Schmidt KA, Kratz M. Contribution of Adipose Tissue Inflammation to the Development of Type 2 Diabetes Mellitus. *Compr Physiol* (2018) 9(1):1–58. doi: 10.1002/Cphy.C170040. Wiley; Wiley.
34. Espinosa De Ycaza AE, Søndergaard E, Morgan-Bathke M, Lytle K, Delivanis DA, Ramos P, et al. Adipose Tissue Inflammation Is Not Related to Adipose Insulin Resistance in Humans. *Diabetes* (2021) 71(3):381–93. doi: 10.2337/DB21-0609
35. Hotamisligil GS. Inflammation, Metaflammation and Immunometabolic Disorders. *Nature* (2017) 542(7640):177–85. doi: 10.1038/NATURE21363
36. Wallace TM, Levy JC, Matthews DR. Use and Abuse of HOMA Modeling. *Diabetes Care* (2004) 27(6):1487–95. doi: 10.2337/Diacare.27.6.1487
37. Larsen CM, Faulenbach M, Vaag A, Vølund A, Ehses JA, Seifert B, et al. Interleukin-1-Receptor Antagonist in Type 2 Diabetes Mellitus. *N Engl J Med* (2007) 356(15):1517–26. doi: 10.1056/NEJMOA065213
38. Solomon DH, Massarotti E, Garg R, Liu J, Canning C, Schneeweiss S. Association Between Disease-Modifying Antirheumatic Drugs and Diabetes Risk in Patients With Rheumatoid Arthritis and Psoriasis. *JAMA* (2011) 305 (24):2525–31. doi: 10.1001/JAMA.2011.878
39. Burska AN, Sakthiswary R, Sattar N. Effects of Tumour Necrosis Factor Antagonists on Insulin Sensitivity/Resistance in Rheumatoid Arthritis: A Systematic Review and Meta-Analysis. *PloS One* (2015) 10:6. doi: 10.1371/JOURNAL.PONE.0128889
40. Sethi JK, Hotamisligil GS. Metabolic Messengers: Tumour Necrosis Factor. *Nat Metab* (2021) 3(10):1302–12. doi: 10.1038/S42255-021-00470-Z
41. Ma L, Liu TW, Wallig MA, Dobrucki IT, Dobrucki LW, Nelson ER, et al. Efficient Targeting of Adipose Tissue Macrophages in Obesity With Polysaccharide Nanocarriers. *ACS Nano* (2016) 10(7):6952–62. doi: 10.1021/ACSNANO.6B02878
42. Peterson KR, Cottam MA, Kennedy AJ, Hasty AH. Macrophage-Targeted Therapeutics for Metabolic Disease. *Trends Pharmacol Sci* (2018) 39(6):536–46. doi: 10.1016/J.TIPS.2018.03.001
43. Czech MP. Insulin Action and Resistance in Obesity and Type 2 Diabetes. *Nat Med* (2017) 23(7):804–14. doi: 10.1038/NM.4350
44. Shimobayashi M, Albert V, Woelnerhanssen B, Frei IC, Weissenberger D, Meyer-Gerspach AC, et al. Insulin Resistance Causes Inflammation in Adipose Tissue. *J Clin Invest* (2018) 128(4):1538–50. doi: 10.1172/JCI96139

Conflict of Interest: The authors declare that the research was conducted in the absence of any commercial or financial relationships that could be construed as a potential conflict of interest.

the publisher, the editors and the reviewers. Any product that may be evaluated in this article, or claim that may be made by its manufacturer, is not guaranteed or endorsed by the publisher.

frontiers | Frontiers in Endocrinology

REVIEW
published: 29 April 2022
doi: 10.3389/fendo.2022.860799

Assessing Obesity-Related Adipose Tissue Disease (OrAD) to Improve Precision Medicine for Patients Living With Obesity

Yair Pincu[1,2,3†], Uri Yoel[1,4†], Yulia Haim[1,5†], Nataly Makarenkov[1], Nitzan Maixner[1], Ruthy Shaco-Levy[6], Nava Bashan[1], Dror Dicker[7,8] and Assaf Rudich[1,5*]*

[1] Department of Clinical Biochemistry and Pharmacology, Faculty of Health Sciences, Ben-Gurion University, Beer-Sheva, Israel, [2] Department of Health and Exercise Science, University of Oklahoma, Norman, OK, United States, [3] Harold Hamm Diabetes Center, University of Oklahoma Health Sciences Center, Oklahoma City, OK, United States, [4] The Endocrinology Service, Soroka University Medical Center, Beer-Sheva, Israel, [5] The National Institute of Biotechnology in the Negev, Ben-Gurion University of the Negev, Beer-Sheva, Israel, [6] Institute of Pathology, Soroka University Medical Center, Ben-Gurion University of the Negev, Beer-Sheva, Israel, [7] Department of Internal Medicine D, Hasharon Hospital, Rabin Medical Center, Petah Tikva, Israel, [8] Sackler School of Medicine, Tel Aviv University, Tel-Aviv, Israel

Obesity is a heterogenous condition that affects the life and health of patients to different degrees and in different ways. Yet, most approaches to treat obesity are not currently prescribed, at least in a systematic manner, based on individual obesity sub-phenotypes or specifically-predicted health risks. Adipose tissue is one of the most evidently affected tissues in obesity. The degree of adipose tissue changes – "adiposopathy", or as we propose to relate to herein as Obesity-related Adipose tissue Disease (OrAD), correspond, at least cross-sectionally, to the extent of obesity-related complications inflicted on an individual patient. This potentially provides an opportunity to better personalize anti-obesity management by utilizing the information that can be retrieved by assessing OrAD. This review article will summarize current knowledge on histopathological OrAD features which, beyond cross-sectional analyses, had been shown to predict future obesity-related endpoints and/or the response to specific anti-obesity interventions. In particular, the review explores adipocyte cell size, adipose tissue inflammation, and fibrosis. Rather than highly-specialized methods, we emphasize standard pathology laboratory approaches to assess OrAD, which are readily-available in most clinical settings. We then discuss how OrAD assessment can be streamlined in the obesity/weight-management clinic. We propose that current studies provide sufficient evidence to inspire concerted efforts to better explore the possibility of predicting obesity related clinical endpoints and response to interventions by histological OrAD assessment, in the quest to improve precision medicine in obesity.

Keywords: adipocyte, cell size, inflammation, fibrosis, precision medicine, obesity, adipose tissue

OPEN ACCESS

Edited by:
Katherine Samaras, St Vincent's Hospital Sydney, Australia

Reviewed by:
Maximilian Zeyda, Medical University of Vienna, Austria
Xavier Prieur, U1087 L'unité de recherche de l'institut du thorax (INSERM), France

***Correspondence:**
Assaf Rudich
rudich@bgu.ac.il
Dror Dicker
daniel3@013.net

†These authors have contributed equally to this work

Specialty section:
This article was submitted to Obesity, a section of the journal Frontiers in Endocrinology

Received: *23 January 2022*
Accepted: *15 March 2022*
Published: *29 April 2022*

Citation:
Pincu Y, Yoel U, Haim Y, Makarenkov N, Maixner N, Shaco-Levy R, Bashan N, Dicker D and Rudich A (2022) Assessing Obesity-Related Adipose Tissue Disease (OrAD) to Improve Precision Medicine for Patients Living With Obesity. Front. Endocrinol. 13:860799. doi: 10.3389/fendo.2022.860799

INTRODUCTION

Recent decades had seen tremendous advances in the ability to personalize treatment to the specific patient based on numerous parameters, resulting in improved care (increased efficacy, less side-effects, etc.). In the treatment of cancer, the diseased tissue – the tumor – is routinely assessed macroscopically, microscopically, and molecularly; advanced imaging technologies are used to determine the extent/spread (or 'stage') of the disease, and liquid biopsies – cancer-related mutations that are captured in blood samples and serve as biomarkers or indicators of the tumor driving mutations – are increasingly used. These assist in determining prognosis of the patient and predicting response to different treatments, based on which the most efficacious treatment(s) is being offered, and non-efficacious or possibly harmful treatments avoided. The above personalized/precision care approach hardly reflects the situation in current obesity care (**Figure 1**). Obesity is still formally defined anthropometrically by body mass index (BMI), and although personal characteristics and preferences of the patient are taken into consideration to offer the best possible care, only limited investigations are routinely performed to predict future development of obesity-related complications or the response to different modes of therapy. This is despite the fact that with its enormous prevalence, obesity is clearly not a single entity, and its heterogeneity likely encompasses potentially definable sub-phenotypes that would respond differently to specific treatments. Indeed, debatable entities reflecting obesity sub-phenotypes, such as 'metabolically-healthy' versus 'metabolically-unhealthy' obesity had been proposed. Yet, largely, these definitions rely on whether the patient had already-developed health implications of obesity rather than attempting to predict their occurrence. Jointly, the clinical resolution at which obesity is currently defined is hardly helpful in optimizing care and intervention options to the individual patient, largely failing to provide prognosis, or predict side-effects or efficacy of available and emerging interventions.

Human adipose tissue is one of the most evidently altered tissues in obesity. Intriguingly, some of these alterations are clearly more evident – in their prevalence and/or extent – in obesity phenotypes with greater metabolic risk, as assessed mainly in cross-sectional studies. Such alterations, sometimes collectively related to as adiposopathy, and which we herein propose to name Obesity-elated Adipose tissue Disease (OrAD), include features such as adipocyte hypertrophy, adipose tissue inflammation and adipose tissue total and pericellular fibrosis.

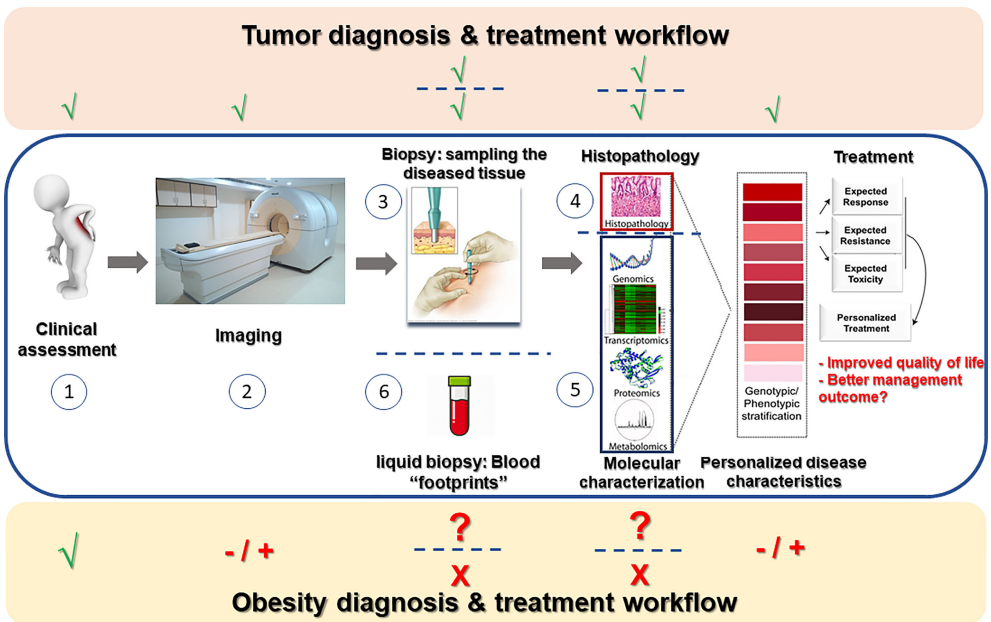

FIGURE 1 | Obesity diagnosis and treatment workflow in the mirror of cancer clinical workup. In a newly-suspected cancer patient, routine workup consists of clinical assessment of the patient (1), various imaging modalities (2) aimed at estimating the extent of tumor invasiveness and spread, sampling of the tumor (3) for microscopic (histopathological) examination (4) and frequently also molecular profiling (5), and nowadays also liquid biopsies (6) attempting to capture free tumor-related molecules (mostly cancer-DNA) secreted by the tumor into the circulation. Data from all above-mentioned procedures is gathered to assemble disease stratification- both anatomical-morphological (grading/staging) and molecular. Based on such stratification, optional treatment approaches can be considered in light of the predicted resistance/response to therapy and estimated severity of toxic effects, and precise disease-appropriate therapy may be determined. Obesity care still awaits a similar personalized approach: While clinical assessment (1) is obviously performed, imaging techniques (2) are rarely performed to estimate the extent/spread of obesity (adipose tissue distribution, adipose tissue thermogenesis, etc.). Adipose tissue sampling (3) is hardly ever performed beyond experimental/research set-ups, and thus histopathological as well as molecular assessment of the diseased tissue is not routinely performed. Overall, obesity workup is deprived of many technologically-available means that could allow to examine if such studies could be used for disease stratification and better personalization of the treatment of people living with obesity.

Many of these OrAD features can be assessed using rather basic histopathological examinations, and/or molecularly. Adipose tissue distribution and the extent of ectopic fat accumulation may be viewed as a key feature of OrAD, providing prediction of obesity-related clinical endpoints (1, 2). Indeed, high waist-to-hip ratio – an anthropometric measure of central adiposity and/or limited lower-body fat expandability (3), has been recently shown as a central component of a proposed new definition for impaired metabolic health, also among patients with obesity, and to predict all-cause and cardiovascular mortality (4). Some studies have also attempted to identify molecular patterns that could potentially help personalize obesity care (discussed briefly later) (5, 6). However, this review will focus on histopathological OrAD features that had been shown to predict subsequent clinically-relevant obesity outcomes – risk of developing obesity-related diseases, and response to intervention. We emphasize OrAD features that can be easily assessed and implemented by many centers treating obesity, and provide a practical guide approach to implement them in the obesity clinic routine. We hope to convey the message that adipose tissue retains clinically-relevant information that is readily available, and which is currently under-utilized in the quest to better personalize obesity care.

HISTOPATHOLOGICAL OrAD FEATURES THAT CAN PREDICT OBESITY OUTCOMES

The following sections will each deal with a specific OrAD histopathological feature for which we found peer-reviewed publications that provide proof-of-principle that they may predict future development of obesity endpoints and/or response to anti-obesity intervention. Available literature on each OrAD feature were divided into 4 categories, i.e., tiers, representing different "levels of linkage" between the specific OrAD feature and obesity related endpoints: Tier 1 includes examples of cross-sectional studies of a single time point, demonstrating association between an OrAD feature and an obesity phenotype. Tier 2 highlights longitudinal studies that describe a correlated *change* between an OrAD feature and a clinical characteristic based on two time-point assessment. (Note: We prioritized studies that demonstrate correlated change between both the OrAD feature and the clinical parameter over studies that merely describe a significant change (delta) in the OrAD parameter per-se). Tier 3 highlights studies describing possible mechanisms for the link between the OrAD feature and clinically-relevant endpoint(s). Tier 4, the focus of this review, are follow-up studies that demonstrate association between *baseline* OrAD feature, and *subsequent* (incident) development of obesity-related endpoint and/or response to intervention. In line with the focus of this review, studies in tiers 1-3 will be mentioned only briefly and summarized in a designated table for each OrAD feature, and tier 4 studies will be discussed in more detail.

Adipocyte Size

Adipose tissue can expand by recruiting more adipocytes – i.e., hyperplasia, likely from adipocyte progenitor cells present within the tissue, and/or by increasing adipocyte size/volume (hypertrophy) (7–9). Indeed, the adipocyte can uniquely vary in size, ranging from <20 to 300 μm in diameter (10). Cross-sectional studies, even if not unanimously, link larger adipocytes with clinical parameters consistent with greater metabolic risk [**Table 1**, tier 1, and excellently reviewed in (10, 44)]. Yet, some studies questioned whether these cross-sectional associations are superior to, or provide associations independent of, measures of total body mass and/or fat distribution (45–47). These inconsistencies in the literature possibly suggest context-specificity – i.e., differences between ethnicities, sex, BMI range, and the specific fat depot studied [(11, 44), and further discussed below]. Longitudinal studies demonstrate that decrease in adipocyte size that accompanies weight loss associates with improved obesity-related disease endpoints in some (**Table 1**, tier 2), though not all studies (48, 49), and pioglitazone treatment actually induced improved insulin sensitivity that associated with increase, not decrease, in adipocyte size (50). Mechanistically, several underlying processes were proposed to explain the link between enlarged (hypertrophic) adipocytes and metabolic dysfunction (**Table 1**, tier 3), most notable of which are: i. larger adipocytes have altered metabolic and endocrine functions compared to their smaller counterparts. In particular, they seem to be more insulin resistant, and more lipolytic (35–37). The latter feature results in greater release of non-esterified (free) fatty acids to the circulation, which in turn may contribute to metabolic dysfunction and cardiometabolic risk (51). ii. Large adipocytes are more pro-inflammatory: they secrete pro-inflammatory cytokines and chemokines that support inflammatory cell accumulation (31, 32). In addition, hypertrophied adipocytes tend to die *via* an unclear/non-classical cell-death program (necrosis, apoptosis) (33), which nevertheless seems to be pro-inflammatory, or at least contribute to macrophage recruitment to the tissue. Recently, the link between pro-inflammatory cytokine secretion by larger adipocytes was attributed to a state of premature senescence, and a senescence-associate secretory profile (SASP) (34).

Beyond association studies linking adipocyte hypertrophy with obesity phenotype (tier 1-2), prospective studies demonstrate that adipocyte size predicts subsequent, clinically-relevant, obesity-related outcomes (**Table 1**, tier 4). In Pima Indians who had normal glucose tolerance at baseline, abdominal subcutaneous adipocyte cell size predicted incident T2DM during a mean follow-up of 9.3 years (38). Although adipocyte cell size correlated with insulin resistance, the two factors contributed independently to incident T2DM risk: The risk of developing T2DM among those with abdominal subcutaneous adipocytes in the 90th size percentile was 5.8-fold greater than those in the lower 10 percent, after adjusting in the multivariate Cox regression analysis for sex, age and percent body fat (which were non-predictive of T2DM), and for insulin sensitivity and acute insulin response to a glucose load, which were also identified as independent predictors of incident T2DM (38). This finding was then corroborated by a study that followed 234 Swedish women over a 25 year period (39). A stepwise

TABLE 1 | OrAD feature - Adipocyte size.

		References
Tier 1: Cross-sectional association *Adipocyte size correlates with obesity-related diseases and/or cardiometabolic risk, *beyond other adiposity measures*	- Insulin resistance.	(11–15)
	- Dyslipidemia/particularly visceral adipocyte hypertrophy, in women.	(16, 17)/ (18, 19)
	- A subcutaneous adipocyte size threshold could be identified beyond which association with T2DM increases.	(20)
	- Non-alcoholic fatty liver disease.	(21, 22)
	- Coronary artery disease (epicardial adipocyte size).	(23, 24)
	- Polycystic ovary syndrome.	(25)
Tier 2: Longitudinal co-association *Adipocyte size changes during intervention associate with changes in obesity-related phenotype/risk*	- Glucose metabolism and/or insulin sensitivity.	(26–30)
	- Cardiovascular risk.	(29, 30)
Tier 3: Main proposed mechanisms *for the link between adipocyte size and clinical characteristics. (human studies)*	- Larger adipocytes are pro-inflammatory:	
	i. have a more proinflammatory secretome.	(31, 32)
	ii. Greater tendency for adipocyte cell death.	(33)
	iii. Display premature senescence.	(34)
	- Dysregulated lipolysis (more FFA release).	(35–37)
	- Altered adipokine profile.	(14, 31, 32)
Tier 4: Prospective/predictive studies *Baseline adipocyte size predicts subsequent progression of obesity-related conditions, and/or intervention outcome*	*Incident T2DM*	
	- Larger SC adipocyte size predicts development of obesity-related T2DM in Pima Indians *(33 cases of 108, 9 years average follow up)*.	(38)
	- Larger abdominal SC adipocytes (less so femoral) predict incident T2DM in women *(36 cases of 234, 25 year follow up)*.	(39)
	Experimental overfeeding response	
	- Larger SC adipocyte size predicts *lower* fat mass and hepatic fat gain, and a *smaller* decline in insulin sensitivity *(n=29 men, mostly non-obese; n=31 males and females, BMI 25-35 Kg/m^2).*	(40, 41)
	Obesity intervention outcome	
	- Larger SC adipocyte size predicts *lower* resolution of T2DM+insulin resistance 6 months after bariatric surgery *(2 cohorts; resolution in 61 of 79, and 13 of 33)*.	(20)
	- Smaller "adipocyte density" (indicative of larger omental adipocyte size, which in itself was not significant) predicted greater reduction in carotid intima-media thickness following metabolic surgery *(n=40).*	(42)
	- Hypertrophic SC adipocytes predicted *greater* improvement in insulin sensitivity in response to dietary intervention or bypass surgery *(n=100 and 61, respectively).*	(43)
	- Larger adipocyte morphology value predicted *greater* improvement in diastolic blood pressure after bypass surgery.	(43)

multivariate model adjusted for age, family history of T2DM and waist-to-height ratio (the strongest independent predictor in this study), demonstrated a hazard ratio of 1.54 for every standard deviation increase in abdominal subcutaneous adipocyte size. Interestingly, femoral subcutaneous adipocyte size did not remain an independent predictor of T2DM in the multivariate models, despite correlating with abdominal subcutaneous adipocyte size (39).

Prediction of obesity intervention outcome by adipocyte size assessment was proposed by a 2-center, French-German study (20). Though statistical models fell short of detecting a strong independent prediction, an association was found between subcutaneous mean adipocyte size and resolution of metabolic risk/dysfunction: Six months after bariatric surgery, women whose composite phenotype of T2DM or a high risk for developing T2DM had been resolved had smaller mean adipocyte size at baseline, compared to women whose metabolic dysfunction did not resolve postoperatively (20). A different result was obtained in a Swedish study that observed greater improvements in insulin sensitivity following weight loss among those with hypertrophic subcutaneous adipocytes at baseline (43). Two cohorts were examined to explore this relationship in response to moderate (~7%) weight loss (induced by dietary intervention, n=100), or more pronounced weight loss (33%, induced by gastric bypass surgery, n=61). Baseline adipocyte size per-se positively correlated with the subsequent improvement in insulin sensitivity (delta-HOMA-IR) only in the surgery intervention group. Yet, when adipocyte morphology value was considered – an index of adipocyte volume to total fat mass used to dichotomously classify patients to those with hyperplastic versus hypertrophic adipocytes (further discussed below) – this association was evident in both cohorts. In addition to greater improvement in insulin sensitivity, larger adipocytes predicted greater reductions in diastolic blood pressure, but not in blood lipid parameters (43). Importantly, other baseline clinical

parameters, such as anthropometric measurements, did not predict the degree of metabolic improvement in response to weight loss intervention, suggesting the potential unique clinical value in assessing this OrAD feature.

Jointly, current studies assessing the possibility to predict obesity-related outcomes by adipocyte size are promising, but seem too few to propose clear guidelines before additional studies are available. Notably, tier 4 studies (**Table 1**) suggest that larger subcutaneous adipocytes may predict different outcomes in different clinical settings: In observational prospective studies they may reflect higher risk of future metabolic deterioration; In acute, experimental weight-gain settings, larger subcutaneous adipocytes may predict less weight gain and a lower decline in insulin sensitivity; As predictors of post-bariatric/metabolic surgery, results are inconsistent, and may also require single-center assessment of adipocyte size. Finally, although subcutaneous and visceral adipocyte size are correlated, they may have differing predictivity of clinical endpoints. Since visceral fat biopsies are only available in patients undergoing abdominal surgery, current information is more limited regarding the association between visceral adipocyte size and subsequent clinical endpoints.

Additional Considerations Related to Adipocyte Size Assessment for Clinical Applications

- *Which fat depot?* Visceral (mainly studied is omental) adipose tissue is considered to be already a pathogenic/ectopic depot (2), and is therefore more intuitively connected to OrAD. Indeed, omental adipocyte size was repeatedly associated with metabolic (14, 15, 18, 19, 46, 47, 52) and cardiovascular dysfunction (42, 46). However, as described throughout this section, subcutaneous adipocyte size also correlates with these outcome measures – albeit to a lesser degree (15, 47, 52). Additionally, subcutaneous adipose tissue is clinically-accessible by a percutaneous biopsy, a minimally-invasive procedure under local anesthesia. Such procedure is reminiscent not only of percutaneous biopsy of solid tumors, but also of liver biopsy that is quite routinely preformed in the hepatology clinic. Six of the seven tier 4, predictive studies (**Table 1**) demonstrate that abdominal subcutaneous adipocyte size may also be predictive of obesity-related outcomes. Possibly, this relates to the fact that subcutaneous adipose tissue constitutes the largest fat depot in the human body, so merely by its mass, changes in this depot might exert significant impact at the whole-body level. However, even within subcutaneous adipose tissue anatomical location may impact the effect of increased adipocyte size, as abdominal subcutaneous adipocyte size was found superior to femoral adipocyte size estimation in predicting incident T2DM (39). The possible predictive value of adipocyte size in other depots such as omental adipose tissue, and even in sub-compartments of subcutaneous fat [superficial and deep subcutaneous fat, whose mass is differently associated with obesity-related morbidity (53)], require further research.

- *Method for determining adipocyte size:* Adipocyte size measured (estimated) by histological sections is likely the most available approach in most clinical settings, as it can be analyzed manually or in a semi-automated manner using image analysis software by a pathologist (**Box 1**). Yet, this clearly provides an (under)estimation of true adipocyte size, rather than an absolute size determination, and has additional biases detailed elsewhere (10, 44). Other methods include microscopic assessment of isolated adipocytes obtained by collagenase digestion of fresh tissue, osmium tetroxide-fixed isolated adipocyte size estimation, and scanning electron microscopy. Each of these approaches has its potential biases (10, 44, 55), and may be limited to centers with specialized labs that have established the technique. In general, the different methods do correlate quite well with each other, and, cross-sectionally, with adiposity measures (52). Yet, absolute size determination is crucial if one also seeks to calculate adipocyte number (55), which may be an independent parameter that associates with obesity-related endpoints.

Adipocyte size versus adipocyte morphology, and adjustment approaches - Although adipocyte size – diameter or calculated volume – has been used and shown to associate with obesity-related phenotypes, adipocyte morphology value may be a stronger predictor (43). This parameter is derived from the curvilinear association between adipocyte volume and total body fat mass (19, 44, 56), and subtracting the expected adipocyte volume from the actual measured adipocyte volume. An adipocyte morphology value above the expected denotes hypertrophy, whereas a negative value (i.e., below expected) denotes hyperplasia. Studies have also reached different conclusions on whether adipocyte size associates with clinical parameters independently of (i.e., when adjusted for) adiposity measures. This may be attributed to the adjustment for different adiposity measures (BMI, total body fat mass, regional fat, etc.). Since several studies showed that abdominal subcutaneous adiposcyte size was no longer associated with insulin resistance following adjustment for visceral fat volume, Tchernof et al. proposed that "excess visceral adipose tissue accumulation and subcutaneous fat cell hypertrophy may represent markers of a common phenomenon: limited hyperplasic capacity of adipose tissues" (44).

Which size parameter should be looked at? Adipocyte size may not be normally distributed, particularly when adipocyte volume is used (43), and bi-modal and skewed distributions have also been proposed (44, 52). This suggests that perhaps beyond mean (average, or even median) adipocyte size, other adipocyte size measures should be considered, including the maximal adipocyte size, or conversely – the percent of small adipocytes (57), large adipocytes (58), etc. Although measuring the larger and smaller range of adipocyte size may be particularly challenging methodologically (44), such measures may prove to disclose clinically useful associations with obesity and treatment related outcomes.

What do larger adipocytes mean for adipose tissue biology? Having larger mean adipocyte size, or an adipocyte morphology above the expected value, defines hypertrophic adipose tissue expansion (43). Yet, it remains controversial how this relates to the adipose expandability theory – i.e., whether it reflects decreased or rather improved capacity of adipose tissue to expand in response to excess calories, and protect from ectopic fat accumulation and insulin resistance. In fact, some studies

Box 1 Common/standard clinical laboratory methods available to assess OrAD.

Feature	Method/approach	Comments	Clinical lab	Reviewed in ref
A. Adipocyte size	Histological estimation of adipocyte size: H&E staining *- manual counting of adipocytes/field.* *- automated (software) assessment of histological images.*		Pathology	(10, 44)
	Isolated adipocytes *- manual microscopic assessment of isolated cells.* *- Automated cell size analyzer.*	requires collagenase digestion of adipose tissue	Pathology/ cytology	
B. Adipose tissue inflammation	Histopathology: *- H&E staining – assess leucocyte infiltration based on cellular overall morphology* *Immunohistochemistry using immune cell -specific antibodies:* *- anti-CD45 (common leucocyte antigen)* *- anti-CD68 staining (macrophages)* *- anti-CD117 (c-kit), tryptase (mast cells)* *- anti-CD3 (T-lymphocytes)* *- anti-CD20 (B-lymphocytes)* *- anti-CD57 (NK cells)*		Pathology	
	Flow cytometry of stromal-vascular cells (Note: adipocytes are usually unamenable for flow cytometry analysis)		Cytology; hematology	
C. Adipose tissue fibrosis	Histopathology: *- H&E staining* *- Masson Trichrome staining* *- Picrosirius red -> "FAT score"* *- Collagen immunostaining (immunohistochemistry using anti-collagen antibodies)*	May be non-standard assay	Pathology	(54)

suggest that higher mean adipocyte size but lower fraction of large adipocytes (higher percentage of small adipocytes), may actually represent impaired capacity to retain metabolic health in response to overfeeding or obesity (40, 41, 58). This was attributed to decreased lipogenic/adipogenic capacity (of the small adipocytes), and to a pro-inflammatory skeletal muscle response, possibly secondary to rapidly hypertrophying small adipocytes.

Adipose Tissue Inflammation

The link between obesity and adipose tissue inflammation had been extensively studied over the past 25 years, initially implicating obesity-associated changes in adipose tissue cytokines and later adipose tissue immune cells [references (59) and (60, 61) are considered as milestone studies that sparked research in these directions, respectively]. Excellently reviewed in recent years (62, 63), adipose tissue inflammation engages multiple arms of the immune system, with marked alterations in inflammatory gene expression and immune cell populations. Initially (and still largely) considered to offer a (causal) link between obesity and the development of adipose tissue and whole-body metabolic dysfunction and increased cardiometabolic risk, in reality this link is largely more complex, and less established in humans than in rodent models. Not only causality may be bi-directional (64), inflammation in general, and specifically in adipose tissue, cannot be simplistically viewed only as a pathological process, but as a dynamic process that is ignited in response to multiple perturbations, with the initial aim of restoring homeostasis. In established obesity, the chronic nature of low-grade adipose tissue inflammation, which in humans sometimes lasts decades, may be a major feature that is not necessarily fully captured by rodent studies. Indeed, pre-clinical and some clinical studies questioned the putative causal association between adipose tissue inflammation and metabolic dysfunction in obesity. Complementarily, adipose tissue inflammation may be in some instances a beneficial phenomenon of adipose tissue remodeling that eventually contributes to improved whole-body metabolic health and homeostasis, particularly in the early response to excessive weight loss.

Cross-sectionally, multiple human studies demonstrated activation of various inflammatory pathways in adipose tissue of patients with obesity versus people without obesity. Beyond lean-obese comparison (i.e., within the obese population), cross-sectional studies provide links between a higher pro-inflammatory state, particularly in visceral adipose tissue, and greater obesity-related cardiometabolic complications (selected studies are presented in **Table 2**, tier 1). Yet, even at this tier, some immune cells (e.g. macrophages) have been shown to positively associate with metabolic dysfunction, while others (e.g. mast cells) exhibited negative association (i.e., higher abundance of mast cells associated with better metabolic profile). Longitudinal co-association studies [Comprehensively reviewed in (82), and specifically in the response to bariatric surgery in (84), and selected publications presented in **Table 2**, tier 2], have somewhat surprisingly shown even more inconsistencies: Improvements in

TABLE 2 | OrAD feature - Adipose tissue inflammation.

		References
Tier 1: Cross-sectional association *Adipose tissue inflammation correlates with obesity-related diseases*	*Adipose tissue macrophages:* - Higher macrophage abundance in visceral adipose tissue correlates with NAFLD - Higher macrophage abundance in visceral adipose tissue correlates with insulin resistance or metabolic dysfunction. - Larger number of macrophage "crown-like structures" in subcutaneous fat in women with obesity and T2DM Vs. NGT. *Adipose tissue mast cells:* - Higher visceral adipose tissue mast cell abundance associates with better (among patients with obesity)//worse (when also compared to non-obese patients) metabolic profile. *Adipose tissue dendritic cells (DC):* - Higher abundance of CD11c+/CD1c+ DCs in subcutaneous fat correlates with insulin resistance in morbidly obese patients. *Adipose tissue T-cells:* - Higher abundance of CD4+ (Th1, Th17) and CD8+ T-cells in both subcutaneous and visceral adipose tissues in obesity associate with insulin resistance. *Expression of inflammatory genes:* - Higher expression of inflammatory genes and/or lower expression of anti-inflammatory genes associate with insulin resistance and/or high cardiometabolic risk in obesity.	(65, 66) (15, 65, 67, 68) (69) (70, 71)// (72) (73) (74) (68, 74, 75)
Tier 2: Longitudinal co-association *Adipose tissue inflammation changes during intervention associate with changes in obesity-related phenotype/risk*	<u>*Weight loss*</u> The magnitude of weight loss following bariatric surgery correlates with *decreased* adipose tissue: - macrophages; - mast cells; - expression of inflammatory cytokines Weight loss following bariatric surgery or lifestyle intervention, and consequentially improved metabolic profile, *do not associate with decreased* (and even increased): - subcutaneous adipose tissue macrophages and other leucocytes - inflammatory gene expression <u>*Experimental weight gain*</u> - Experimental acute weight gain induces insulin resistance without activating systemic or adipose tissue inflammation.	 (70, 76, 77) (70) (70, 77) (78–80) (78–80) (81)
Tier 3: Main proposed mechanisms *(human studies)*	- Contribution to systemic inflammation. - Decrease in cardiovascular-protective, adipose derived factors (e.g. adiponectin). - Adipose tissue and whole-body insulin resistance. - Source of inflammatory lipid mediators.	(82) (83) (62, 82) (82)
Tier 4: Prospective/predictive studies *Baseline adipose tissue inflammation parameters predicts subsequent intervention outcome*	Higher adipose tissue expression of mast cells -specific genes predicts greater weight-loss response to bariatric surgeries *(cohort 1: n=18, 6 months follow-up, only visceral adipose tissue; cohort 2: n=56, 1y follow-up, both visceral and subcutaneous adipose tissue)*	(70)

metabolic dysfunction following lifestyle, pharmacological or surgical interventions were associated with relatively mild, or even without any decline in adipose tissue inflammation parameters. Here, again, which inflammatory parameter was assessed, what was the intervention, and particularly follow-up duration, are likely major determinants of the results and conclusions. Overall, tier 2 studies may suggest that early improvement in metabolic dysfunction following weight loss may not require resolution of adipose tissue inflammation. In the excessive weight-loss response to bariatric surgery, some inflammatory markers (neutrophil or macrophage infiltration and related chemokines and cytokines) may even be increased up to 6 months postoperatively, followed by a gradual decline (85). An additional 'uncoupling' between adipose tissue inflammation and insulin resistance was demonstrated in the response to experimental weight gain, which induced insulin resistance without apparent stimulation of systemic or adipose tissue inflammation (81).

Nevertheless, several mechanisms have been proposed to explain the apparent link between adipose tissue inflammation and obesity-related complications, most notable of which is adipose tissues' contribution to systemic inflammation and obesity-related decline in vascular-protective adipokines (e.g. adiponectin, **Table 2**, tier 3). Yet, such mechanistic propositions are frequently indirect. Clinically, attempts to relieve obesity-related cardiometabolic complications (i.e., T2DM and related elevated cardiovascular risk) using available anti-inflammatory interventions has raised high hopes (86, 87) but was largely met with somewhat limited results. These call, again, for the need to better understand adipose tissue inflammation and its specific mediators that may link to obesity-related complications, and/or to find biomarkers that can identify humans with a defined obesity sub-phenotype, who would benefit from specific anti-inflammatory intervention(s) – i.e., predictive (tier 4) studies.

In light of this apparent need, it is surprising that while a relatively rich body of literature examines cross-sectionally or longitudinally the association between parameters of adipose tissue inflammation and obesity phenotypes, tier 4 predictive studies are surprisingly scarce (**Table 2**, tier 4). In two independent cohorts we have shown that higher expression of mast cell specific genes, which we found to be indicative of adipose tissue mast cell abundance assessed histologically, predicted the degree of subsequent weight loss induced by bariatric surgery (70). In the Israeli cohort (n=18), those who expressed mast cell -specific chymase CMA-1 above the median exhibited weight loss that was nearly 2-fold greater than those who were "CMA-1-low". CMA-1 expression in subcutaneous adipose tissue also predicted greater weight loss 1-year post surgery in an independent, German cohort (n=56). In this cohort, in omental adipose tissue, other mast cell genes [tryptase 1 (TPSB1) and c-kit (KIT)] positively correlated with the degree of weight loss. Despite extensive literature search, we could not find additional tier 4 predictive studies that explore whether baseline markers of adipose tissue inflammation correlate with future obesity-related endpoints and intervention outcomes. This surprising paucity in the literature is further discussed in the final section of this review.

Adipose Tissue Fibrosis

Fibrosis is the pathological deposition of extracellular matrix (ECM) in a tissue, such that it replaces portions of the tissue parenchyma, changes the tissue's physical properties, and impairs its function.

This elaborate process is reviewed in detail in references (54, 88, 89). Briefly, while the ECM in healthy adipose tissue is constantly being deposited and degraded as part of normal adipose tissue homeostasis, when excessively deposited, adipose tissue becomes fibrotic. As discussed in the previous sections, obesity manifests with pathological adipose tissue expansion. Adipocyte hypertrophy is associated with adipocyte cell death and inflammation, which trigger dysregulated ECM deposition and fibrosis. Moreover, increased cross-linking of ECM proteins in obesity stiffens adipose tissue and exerts mechanical pressure on hypertrophied adipocytes, resulting in further adipocyte death, lipid spillover and exacerbation of tissue and systemic inflammation.

Cross sectional association studies in humans with obesity (**Table 3**, tier 1) show that increased degree of obesity and fat mass associate with increased adipose tissue fibrosis (90) and non-alcoholic fatty liver disease (NAFLD) (96). However, conflicting evidence exist regarding how adipose tissue fibrosis associates with metabolic dysfunction in obesity. Although some studies suggest that decreased fibrosis in both subcutaneous and visceral (omental) fat depots is associated with at least some aspects of metabolic disease (98, 99), most reports provide evidence that metabolic dysfunction (e.g., insulin resistance) associates with increased adipose fibrosis, both in subcutaneous (91, 94, 106, 107) and omental (94, 95) adipose tissues.

TABLE 3 | OrAD feature - Adipose tissue fibrosis.

		References
Tier 1: Cross-sectional association *Adipoce tissue fibrosis correlates with obesity-related disease endpoints and/or cardiometabolic risk*	*Associated with increased adipose tissue fibrosis:* - Increased adiposity (obesity fat mass). - Insulin resistance. - NAFLD/Increased liver fibrosis *Associated with decreased adipose tissue fibrosis:* - Insulin resistance/Type 2 diabetes	 (90–93) (91–95) (96)/ (97) (98)/ (99)
Tier 2: Longitudinal change association *Adipose tissue fibrosis changes during intervention -/+ association with changes in obesity-related phenotype/risk*	*Decreased adipose tissue fibrosis:* - With weight loss (even as low as 5%) *No change in adipose tissue fibrosis:* - Following weight loss (bariatric surgery) despite metabolic improvement *Experimental weight-gain:* - Increased adipose tissue fibrosis following 8 weeks of overfeeding-induced weight gain	 (80, 90, 92, 100) (94, 101) (90)
Tier 3: Possible mechanisms *(human studies)*	- Increased inflammation, reduced lipid storage capacity and lipid spillover to ectopic fat deposits - Col6A3-related decreased adipose tissue oxygenation	Reviewed in (88, 102, 103) (104)
Tier 4: Prospective/predictive studies *Baseline adipose tissue fibrosis predicts intervention outcome*	- Higher baseline total and pericellular fibrosis in subcutaneous adipose tissue associated with less fat mass loss after 3, 6 and 12 months post-bariatric surgery *(n=65 persons with obesity)*. - Greater total subcutaneous adipose fibrosis adjusted for age, diabetes and circulating IL-6 was associated with a low weight loss response (i.e., <25% decrease in BMI). *(n=243 persons with obesity, OR [95% CI] = 1.58 [1.10-2.28]).* - Histological adipose fibrosis score (FAT) predicts weight loss following RYGB bariatric surgery: Pre-operative FAT score ≥2 was associated with 3-fold increased risk of reduced weight loss 12 months following the surgery *(n=183 persons with obesity)*.	(98) (97) (105)

Longitudinal studies in humans (**Table 3**, tier 2) show that fibrotic markers increase post experimental weight gain (90), and decrease with weight loss (80, 92, 100). Interestingly, even moderate 5% weight loss induced by lifestyle modification was sufficient to reduce the expression of several ECM genes in adipose tissue, whereas inflammatory gene expression did not change (80). This suggests that during moderate weight fluctuations, metabolic changes may be more closely associated with changes in fibrotic gene expression in adipose tissue than with markers of adipose tissue inflammation. Nevertheless, in response to more pronounced weight loss, such as following bariatric surgery, adipose tissue fibrosis was not reduced despite improvements in metabolic outcome measures (i.e., decrease insulin resistance) (94, 101, 108). Possibly, this is reminiscent of the effect reported by some studies in response to bariatric surgery on adipose tissue inflammation in the first 6 month (**Table 2**, tier 2).

Proposed mechanisms (**Table 3**, tier 3) implicate hypoxia and/or activation of hypoxia inducible factor 1 (HIF-1) as central mediators between adipose tissue fibrosis and metabolic complictions of obesity [reviewed in (88, 102, 103)]. Of particular interest is adipose tissue Collagen 6A3 (Col6A3), which correlates with adiposity (BMI and fat mass) (90, 91), metabolic dysfunction (91), and with reduced PPARϒ expression. Evidence suggests that Col6A3 acts to propagate a fibro-inflammatory phenotype by promoting reduction in tissue oxygenation and inducing HIF-1α expression (104), while PPARγ activation inhibits Col6A3 expression (69, 73) and promotes adipogenic differentiation, adipose tissue vascularization and suppression of HIF-1α (73).

Beyond association studies, several human studies demonstrate that assessing the degree of adipose tissue fibrosis predicts subsequent clinically-relevant outcomes of intervention in persons with obesity (**Table 3**, tier 4). In a comprehensive effort to accurately characterize fibrosis in different adipose depots and define its clinical relevance, 9 healthy-weight controls and 65 patients with obesity, who met the criteria for bariatric surgery (BMI >40 or >35 kg/m^2 with at least one comorbidity), were recruited. Participants were analyzed before, and 3, 6 and 12 months postoperatively. Preoperative total and pericellular fibrosis in subcutaneous adipose tissue, measured by picrosirius red staining, correlated with percent fat loss at 3, 6 and 12 months postoperatively (Total fibrosis: 3 months, R=-0.39, p<0.005; 6 months, R=-0.31, p<0.05; and 12 months, R=-0.30, p<0.05. Pericellular fibrosis: 3 months, R=-0.23, p<0.05; 6 months, R=-0.32, p<0.05; and 12 months, R=-0.30, p<0.05) (98). After clustering the participants into 3 groups based on the percent fat loss (using a k-means algorithm), baseline pericellular fibrosis was significantly higher in cluster C, in which participants lost the least weight postoperatively. A later study by the same group, examined a sub-cohort of 243 out of 404 bariatric surgery patients at baseline, and 3, 6, and 12 months postoperatively (97). Biopsies were collected during surgery, and used to assess fibrosis in liver, subcutaneous and omental adipose tissues by picrosirius red staining. Adipose tissue fibrosis in both subcutaneous or omental depots were associated with liver fibrosis and measures of adiposity (body weight, percent fat and BMI). Participants were further divided into 'good responders' (GR), who lost >34.8% of baseline BMI 12 months after surgery, and 'less responsive' (LR), who lost <25%. In a multivariate analysis, higher total subcutaneous adipose tissue fibrosis adjusted for age, diabetes and circulating IL-6 characterized the LR group (OR [95% CI] = 1.58 [1.10-2.28]) (97). These data suggest that subcutaneous adipose fibrosis can be used to predict weight loss outcome of bariatric surgery. This can assist in improving the preoperative expectation from the surgery, and if bariatric surgery is performed, to consider intensified postoperative intervention to optimize the weight-loss response to the surgery (as further discussed in subsequent section of this review). Indeed, for such clinical purposes, histology-based tool to grade the degree of adipose tissue fibrosis from surgical biopsies was established, and exhibited successful prediction of weight loss following bariatric surgery in 183 patients with severe obesity (105): Fibrosis score of Adipose Tissue (FAT score) is a semiquantitative tool that uses subcutaneous adipose surgical biopsies to evaluate adipose tissue fibrosis following picrosirius red staining. It utilizes a 4-stage fibrosis rating scale where Stage 0=no apparent perilobular (PLF) or pericellular (PCF) fibrosis; Stage 1= moderate PLF and/or PCF; Stage 2= severe PLF or severe PCF; and Stage 3 = severe PLF and severe PCF. FAT score was associated with adipose tissue fibrosis and with increased M2 macrophage infiltration, but not with adipocyte size. Importantly, higher FAT score was correlated with lower weight loss 12 months following bariatric surgery, and a baseline FAT score ≥2 was associated with a 3-fold increased risk of reduced weight loss response to bariatric surgery (OR [95% CI] = 3.2 [1.7 – 6.1]). When testing the ability of the FAT score to predict weight loss post bariatric surgery, the authors compared 3 prediction models and concluded that there is merit and added value in incorporating assessment of subcutaneous adipose pathology in prediction of weight loss response to bariatric surgery (105).

It is noteworthy that all 3 tier 4 studies (97, 98, 105) were by K. Clément and co-workers, representing the development and experience of a single center. Clearly, given the possible impact of the findings, it is imperative that these results are replicated and reported by additional centers, so that analysis of adipose tissue fibrosis could be considered as part of the routine clinical toolkit in the treatment of obesity.

Additional Considerations Related to Adipose Fibrosis Assessment for Clinical Applications

- *Which fat depot(s)?* The few studies that assessed fibrosis in both subcutaneous and omental adipose tissue reached conflicting conclusions: While Muir et al., report no differences in adipose fibrosis assessed using both picrosirius red staining and fibrotic gene expression between subcutaneous and omental depots (99), Divoux and colleagues demonstrate different collagen patterns between the 2 tissues (98). Moreover, these authors report increased total fibrosis percent (picrosirius red staining) in participants with obesity compared to non-obese controls in subcutaneous, but not omental fat.

- *Method for obtaining adipose tissue biopsy:* The two most common techniques to obtain adipose tissue samples are surgical

biopsies and needle-aspirated biopsies – each has its own pros and cons. A recent study compared the two techniques side by side and found that the biopsy technique affects adipose tissue gene expression profile. Specifically, needle-aspirated core biopsies were more fragmented due to the mechanical shear stress applied while the tissue is forced through the needle. As a result, needle-aspirated biopsies do not effectively aspirate the fibrotic fraction of subcutaneous adipose tissue, contain an unrepresentative smaller stroma-vascular fraction and thus misrepresent adipose tissue fibrosis (109).

- *Emerging imaging approaches to assess adipose tissue fibrosis:* A few non-invasive approaches have been proposed for assessing adipose tissue fibrosis. Transient Elastography provides assessment of adipose tissue stiffness by measuring the shear wave velocity of the tissue's response to vibration, correlating with the degree of fibrosis assessed histologically (98, 110). Recently, a new MRI application was validated against adipose tissue histology, successfully quantifying fibrosis in subcutaneous adipose tissue (111). Potentially, by creating a 3D fibrosis assessment of the subcutaneous adipose tissue, this approach may be less prone to sampling biases, which is common in histological assessment, particularly of biopsies obtained by needle aspiration.

- *How fibrosis is quantified:* Percent pericellular and percent peri-lobular fibrosis might be more sensitive measurements compared to total percent fibrosis, and may therefore prove to provide more clinically relevant information. For example, when comparing fibrosis in subcutaneous and omental adipose tissues from participants with obesity and non-obese controls, percent pericellular fibrosis, but not percent total fibrosis, differed between the groups in both depots (98).

- *Patients' characteristics might impact adipose tissue fibrosis:* Differences in adipose tissue fibrotic response to obesity and weight loss exist between different ethnic groups, for example Caucasian vs Asian-Americans (112) or Asian-Indian (113). Some studies show sex differences in adipose fibrosis (90), and aged individuals exhibit increased adipose tissue fibrosis [reviewed in (114)].

INCORPORATING OrAD ASSESSMENT IN THE OBESITY CLINIC

There is a growing "need to go beyond BMI" notion in clinical obesity medicine in the quest for better personalizing the treatment of people with obesity, and assessment of the health of the adipose tissue is certainly a potential avenue. Hence, in previous sections we provided examples for clinically-valuable information obtainable from mostly standard pathology assessment of adipose tissue biopsies in order to use such information as a decision-making tool. We hereby describe how adipose tissue biopsies and OrAD assessment could be incorporated into the obesity clinic, with relevance to patients undergoing bariatric/metabolic surgery, those offered non-surgical interventions, and even as part of the decision-making process between these two options. We consider both primary and secondary prevention concepts related to obesity and its related complications.

Adipose tissue biopsies during bariatric/metabolic surgery – When a person with obesity undergoes bariatric surgery (or for that matter, any elective intra-abdominal surgical procedure), sampling abdominal subcutaneous and omental adipose tissue could easily be incorporated as a standard care procedure. This is because, first and foremost, adding an excision of a few grams of adipose tissue is surgically simple, fast, and runs nil or very low added risk for the patient. Conceptually (medically), it is equivalent to sampling the diseased tissue in other medical circumstances, such as in oncological surgeries. As discussed above, rather standard histopathological assessment (**Box 1**) can already provide enormous amount of information, and does not require a special setting beyond that available in most operating rooms – placing the biopsies immediately in formaldehyde, and sending to the affiliated department of pathology.

Adipocyte cell size, amount of fibrosis and degree of inflammation can all be evaluated on a paraffin block section stained with standard hematoxylin & eosin (H&E). The main advantage of this method is its availability practically in all medical centers (which have a pathology department). Additionally, this technique allows examination of tissue architecture and performance of histochemical and immunohistochemical stains. A. Adipocyte size can be measured either manually or by using automated cell size analyzer on cytology specimens. Additionally, adipocyte cell size can be estimated manually on H&E-stained slides according to the average amount of adipocytes per 10 high-power fields (HPFs); one can also use software analysis for this purpose. B. Degree of Inflammation can be evaluated based on H&E-stained slides. Immunohistochemical stain for CD45 (Leukocyte Common Antigen) would highlight all inflammatory cells, making this estimation easier and possibly more accurate. In addition, identification of specific inflammatory cells can be achieved using immunohistochemical stains: CD68 for macrophages, CD3 for T-lymphocytes, CD20 for B-lymphocytes, CD57 for NK cells and CD117 (c-Kit) or tryptase for mast cells. **C.** Amount of fibrosis can be assessed based on H&E-stained sections or preferably using Masson's Trichrome stain that would highlight connective tissue fibers, staining them in a blue hue. Picrosirius red and immunohistochemical stain for specific collagens would also emphasize collagen fibers.

Subcutaneous adipose tissue needle biopsy or minimally invasive, small open surgical biopsy in the non-surgical patient with obesity – This clinical setting is more complex, as it requires subjecting patients to a procedure which is still non-standard in most clinics. Subcutaneous (usually abdominal, at the lower quadrant) adipose tissue biopsy is minimally-invasive, is performed under local anesthesia, but even if of very low risk for the patient does run added risk of local hematoma, infection, and pain. Conceptually, subcutaneous adipose tissue needle biopsy can be viewed similarly to liver biopsy in the clinical workup of patients with liver disease, and is associated with lower risks. Yet, while as discussed above in this review, such procedure can impact therapeutic options by improving the prediction of expected outcomes, it is still investigational, and requires

institutional ethical committee approval, patients' written informed consent, and careful personalized cost-benefit assessment.

Below are a few example scenarios for how might OrAD assessment inform the obesity clinician and improve precision care.

Predicting post-operative weight loss response- After bariatric/metabolic surgery, OrAD features indicative of predicted low postoperative weight-loss response to the bariatric surgery [high SC fat fibrosis score (105), low omental fat mast cell count (70), possibly adipocyte cell size (20)], may suggest the consideration of intensified post-operative intervention to ensure optimal weight loss. Possibilities may include intensifying post-operative life-style interventions and/or pharmacotherapy. Once more data are available – both on OrAD and on long-term follow-up endpoints, it would be important to determine if OrAD features can predict failure to maintain long-term weight loss induced by bariatric surgery (**Box 2**), as it is increasingly recognized that over a third of patients regain >25% of their maximal postoperative weight loss (115).

Predicting postoperative effect on cardiometabolic risk - OrAD features indicative of lower chances of reducing obesity-related cardiometabolic risk following bariatric surgery could support considering interventions aimed at secondary prevention. Although suggested to predict incident T2DM in observational studies (38, 39), the predictive value of adipocyte size assessment in the post-bariatric surgery patient is still unclear (**Table 1**, tier 4). Moreover, when attempting to predict postoperative diabetes remission, adipocyte size was not found to differ between patients with obesity and T2DM who exhibited 1y postoperative diabetes remission or not (116). Yet, a current debate is whether to discontinue all anti-diabetic medications including metformin after bariatric/metabolic surgery in the post-operatively normoglycemic patient. Possibly, a higher OrAD burden may provide a rationale for postoperative continuation of metformin.

Primary prevention in patients with "metabolically-healthy" obesity – Subcutaneous adipocyte size had been shown to predict deterioration of glycemic control even in patients with normal glucose tolerance, and beyond other risk factors (38, 39). Although further demonstration in other cohorts would be valuable, existing studies already suggest such association in diverse populations. Hence, larger adipocyte size [which may require threshold assessment in the specific clinic (20)] may indicate a need for intensified measures for primary prevention of metabolic deterioration. Collectively, in this setting, assessing OrAD in subcutaneous adipose tissue can assist in refining/sub-classifying the metabolically-healthy obese phenotype, highlighting those at greater cardiometabolic risk despite their current intact metabolic profile.

Additional outstanding questions that could inspire future studies to assess the clinical value of OrAD assessment are presented in the following section and in **Box 2**.

OUTSTANDING QUESTIONS, AND FUTURE DIRECTIONS

In modern medicine, sampling the diseased tissue in order to extract clinically-useful information that directs treatment is a common practice. We hope that this review conveys the message that adipose tissue in obesity is a potentially rich source of clinically-meaningful information that should be utilized in the hope of improving precision medicine for the care of patients with obesity. Studies that actually demonstrate that routine assessment of OrAD features could guide personalized care by providing prediction of prognosis and/or response to anti-obesity intervention are still too few to be

Box 2: Major outstanding questions

- Can OrAD features predict intervention outcomes:
  - response to emerging anti-obesity pharmacotherapy;
  - a-priori identify successful weight-loss responders to incretin receptor agonists;
  - post-bariatric/metabolic surgery weight regain.
- "Composite OrAD score" – would a composite score that integrates different OrAD features improve predictability of obesity-related endpoints and/or intervention outcomes?
- Reversibility of OrAD features in the response to intervention: Could a second, early post-intervention initiation OrAD assessment serve to predict long-term successful response?
- Could repeated OrAD assessment of the metabolically-healthy patient with obesity identify pending metabolic/health deterioration?
- Could OrAD assessment predict less-conventional obesity-related risks, such as obesity-related cancer, cognitive decline, etc?
- Is OrAD a marker or a therapeutic target on its own? Would improving OrAD features improve obesity related outcomes?

translated into clinical guidelines. But they do provide a proof of principle that is sufficient to motivate joint efforts to extract such clinically-useful information. Standard laboratory techniques available in most centers, particularly pathology labs, can already provide enormous amount of information on OrAD features, which then needs to be linked to relevant endpoints and post-intervention outcome assessment (**Box 1**). There is no doubt that predicting intervention outcome(s) will become an increasing need with newly-emerging options for anti-obesity treatments in the upcoming future.

Molecular Signatures of Adipose Tissue

This review focused on histopathological assessment of OrAD, but molecular tools should also be considered. Indeed, multiple molecular differences between people without or with obesity have been reported, and have greatly contributed to current understanding of OrAD. Yet, fewer studies assessed, even cross-sectionally, molecular differences within the heterogenous group of persons with obesity in the quest to explain obesity sub-phenotypes (15, 75). Molecular OrAD patterns associated with longitudinal changes were shown using both coding and non-coding (micro-RNA) RNAs. For example, successful maintainers of weight loss exhibited an increase in oxidative phosphorylation gene expression, and a decrease in cell-cycle and inflammatory genes in subcutaneous fat, while unsuccessful weight loss maintainers exhibited the opposite gene expression change (117). Using micro-RNAs, changes in subcutaneous adipose tissue expression of several miRNAs associated with the magnitude of decreased weight, waist circumference or fat mass loss, with no difference between different dietary intervention strategies (118). Moreover, prospectively, the viscera/subcutaneous fat expression ratio of miRNA-122 predicts the degree of weight loss 1y after bariatric surgery (n=61) (5).

Modern 'omics' technologies will clearly advance the information one would be able to extract from any biological sample, including adipose tissue biopsies. Various whole tissue 'omics' approaches hold the promise of discovering novel outcome predictors in an unbiased manner. One pioneer attempt tested the ability to *a-priori* predict the response to a 10w hypocaloric diet by a single, snap-shot assessment of global subcutaneous adipose tissue gene expression using microarrays (6). Global gene expression was able to differentiate between the groups with a maximal prediction accuracy (depending on the model used) of 61%. A stringent identification of differential gene expression between subsequent responders (who lost 8-12 kg) and non-responders (who lost up to 4 kg) using 3 statistical approaches uncovered 9 validated differentially-expressed genes among the n=53 microarrays. Yet, using these genes to predict response did not improve the maximal accuracy (of ~80%), that was obtained by using the 34 differentially-expressed genes identified when relieving the FDR criterion to 8% in the Significance Analysis of Microarray (SAM) procedure. The authors of this study concluded that the predictive performance of this approach was insufficient to be helpful in the clinical setting, and suggest that perhaps a second sample aimed at assessing the initial response to the intervention could better predict the final response to the intervention (6).

Finally, single-cell transcriptomics technologies, such as single-cell RNA-sequencing of the stromal-vascular cells of adipose tissue, or single-nucleus RNA-sequencing that can also capture adipocytes, provide new opportunities to uncover the cellular landscape, and cell-type specific gene expression changes in adipose tissue, at an unprecedented resolution (119). These will allow to determine whether specific cellular composition of adipose tissue – either specific cell types, and/or sub-populations of adipocytes - could effectively predict intervention outcome. For example, it's plausible that greater proportions of functionally-beneficial adipocytes such as adiponectin producing/insulin sensitive, and/or thermogenic adipocytes, may be expected to not only positively affect whole-body metabolic state cross-sectionally, but to also predict lower risk of developing obesity co-morbidities. If this proves to be true, single-nucleus RNA-sequencing could serve to refine the definition of metabolically-healthy obesity, and prevent un-necessary primary prevention interventions for obesity-related comorbidities in such patients.

"The Liquid Biopsy Concept" – Can OrAD be Estimated by Blood Sampling?

This review proposes histopathological OrAD assessment as a possible tool to better sub-phenotype patients by predicting obesity related clinical outcomes. A plethora of studies attempt to identify circulating biomarkers (metabolites, miRNA and other epigenetic markers) for the same purpose, related or not to OrAD. Yet, assuming that OrAD is a powerful predictor of obesity outcomes, an additional outstanding question is whether it can be estimated by sampling peripheral blood. This approach, reminiscent of the concept of liquid biopsy in oncology, may be particularly important for providing OrAD assessment of the visceral fat depot in the non-surgical patient, and has been previously attempted (120). As one example, peripheral blood monocyte sub-classes were shown to correlate with lipid storage of omental adipose tissue macrophages (121), which in turn were shown to associate (cross-sectionally) with a worse metabolic phenotype in obesity (122). Circulating blood metabolomics could uncover correlates of OrAD features such as adipocyte diameter, and associate with obesity phenotypes (123). Other circulating biomarkers indicative of OrAD and specifically of adipose tissue communication with other organs that determine obesity-related endpoints, such as fatty liver and cardiac health, should undoubtedly be further explored for clinical use. These include, among others, adipokines and circulating extracellular vesicles, which in obesity are likely significantly contributed by adipose tissue. The adipokine adiponectin is one such example: As it is produced solely by adipocytes, particularly by insulin-sensitive cells, circulating adiponectin levels may indicate improved adipose metabolic function (i.e., lower adiponectin reflecting OrAD). Indeed, although the association between circulating adiponectin and cardiovascular morbidity and mortality is complex and may greatly depend on the health status of the investigated

population (124), several studies demonstrated that low circulating adiponectin (total or high molecular weight) were independent predictors of incident metabolic syndrome or T2DM (125, 126).

CONCLUSION

Both the motivation to increase precision care in obesity medicine, and the logic of attempting to estimate OrAD to predict clinically-relevant outcomes in obesity care, are clear. Current literature provides some proof-of-principle studies for the possibility that OrAD assessment should be better utilized to enhance precision medicine of patients with obesity. Yet, in some cases (particularly adipose tissue inflammation), the scarcity of predictive studies is surprising in light of the relatively large body of association studies. In particular, longitudinal co-association studies seemingly include all the information required for testing a prediction hypothesis. Current literature remains blind to whether such hypotheses were tested and found to be negative, but remained unpublished. Notably, as an exception, it was reported that adipocyte size and morphology at baseline could not distinguish between patients who exhibited post-bariatric surgery diabetes remission (116). Alternatively, association studies that assessed at least two time-points (baseline and follow-up) may have been underpowered to provide significant predictive data. Therefore, to advance this line of research and clinical practice it would be important to: i. conduct prediction analyses on already available datasets; ii. encourage the report of negative findings, particularly of sufficiently statistically-powered studies; iii. consolidating data from different centers to enable analyses on heterogenous and larger patient databases (i.e., perform meta-analyses); iv. Using advanced approaches, such as deep learning and artificial intelligence, to detect predictive algorithms of OrAD-based clinically-important endpoints.

AUTHOR CONTRIBUTIONS

YP reviewed the literature, wrote sections of the manuscript, critically reviewed the manuscript. UY reviewed the literature, wrote sections of the manuscript, critically reviewed the manuscript. YH reviewed the literature, wrote sections of the manuscript, prepared figure, critically reviewed the manuscript. NaM reviewed the literature and critically reviewed the manuscript. NiM reviewed the literature, wrote sections of the manuscript, assisted in preparing figure. RS-L prepared **Box 1**, critically reviewed the manuscript. NB reviewed the literature, critically reviewed the manuscript. DD wrote sections of the manuscript, critically reviewed the manuscript. AR prepared the review's concept, organized writing missions between co-authors, wrote the manuscript, edited all versions. All authors contributed to the article and approved the submitted version.

FUNDING

This manuscript was funded by grants from the DFG (German Research Foundation)—Projektnummer 209933838—SFB 1052 (specific projects: B2), and the Israel Science Foundation (ISF928/14 and 2176/19 to AR).

ACKNOWLEDGMENTS

The authors wish to acknowledge additional clinical long-term research partners, including Dr. Ilana Harman-Boehm, Dr. Idit Liberty, the entire clinical research coordinators at Soroka's Diabetes Unit, Prof. Boris Kirshtein, Dr. Oleg Dukhno, Dr. Vera Polischuk, Dr. Ilia Polischuk, Dr. Aya Biderman and Dr. Ivan Kukeev. We are indebted to the devoted technical support of Ms. Tanya Tarnovscki. We also would like to apologize for colleagues whose work could not be included in the present review due to editorial limitations.

REFERENCES

1. van Woerden G, van Veldhuisen DJ, Manintveld OC, van Empel VPM, Willems TP, de Boer RA, et al. Epicardial Adipose Tissue and Outcome in Heart Failure With Mid-Range and Preserved Ejection Fraction. *Circ Heart Fail* (2021) 15(3):245–55. doi: 10.1161/CIRCHEARTFAILURE.121.009238
2. Piche ME, Tchernof A, Despres JP. Obesity Phenotypes, Diabetes, and Cardiovascular Diseases. *Circ Res* (2020) 126(11):1477–500. doi: 10.1161/CIRCRESAHA.120.316101
3. Lotta LA, Gulati P, Day FR, Payne F, Ongen H, van de Bunt M, et al. Integrative Genomic Analysis Implicates Limited Peripheral Adipose Storage Capacity in the Pathogenesis of Human Insulin Resistance. *Nat Genet* (2017) 49(1):17–26. doi: 10.1038/ng.3714
4. Zembic A, Eckel N, Stefan N, Baudry J, Schulze MB. An Empirically Derived Definition of Metabolically Healthy Obesity Based on Risk of Cardiovascular and Total Mortality. *JAMA Netw Open* (2021) 4(5):e218505. doi: 10.1001/jamanetworkopen.2021.8505
5. Liao CH, Wang CY, Liu KH, Liu YY, Wen MS, Yeh TS. Mir-122 Marks the Differences Between Subcutaneous and Visceral Adipose Tissues and Associates With the Outcome of Bariatric Surgery. *Obes Res Clin Pract* (2018) 12(6):570–7. doi: 10.1016/j.orcp.2018.06.005
6. Mutch DM, Temanni MR, Henegar C, Combes F, Pelloux V, Holst C, et al. Adipose Gene Expression Prior to Weight Loss Can Differentiate and Weakly Predict Dietary Responders. *PloS One* (2007) 2(12):e1344. doi: 10.1371/journal.pone.0001344
7. Hirsch J, Batchelor B. Adipose Tissue Cellularity in Human Obesity. *Clin Endocrinol Metab* (1976) 5(2):299–311. doi: 10.1016/s0300-595x(76)80023-0
8. Bjorntorp P. Number and Size of Adipose Tissue Fat Cells in Relation to Metabolism in Human Obesity. *Metabolism* (1971) 20(7):703–13. doi: 10.1016/0026-0495(71)90084-9
9. Salans LB, Cushman SW, Weismann RE. Studies of Human Adipose Tissue. Adipose Cell Size and Number in Nonobese and Obese Patients. *J Clin Invest* (1973) 52(4):929–41. doi: 10.1172/JCI107258
10. Stenkula KG, Erlanson-Albertsson C. Adipose Cell Size: Importance in Health and Disease. *Am J Physiol Regul Integr Comp Physiol* (2018) 315(2):R284–R95. doi: 10.1152/ajpregu.00257.2017
11. Yang J, Eliasson B, Smith U, Cushman SW, Sherman AS. The Size of Large Adipose Cells Is a Predictor of Insulin Resistance in First-Degree Relatives of Type 2 Diabetic Patients. *Obes (Silver Spring)* (2012) 20(5):932–8. doi: 10.1038/oby.2011.371
12. Ktotkiewski M, Sjostrom L, Bjorntorp P, Smith U. Regional Adipose Tissue Cellularity in Relation to Metabolism in Young and Middle-Aged Women. *Metabolism* (1975) 24(6):703–10. doi: 10.1016/0026-0495(75)90038-4

13. Roberts R, Hodson L, Dennis AL, Neville MJ, Humphreys SM, Harnden KE, et al. Markers of *De Novo* Lipogenesis in Adipose Tissue: Associations With Small Adipocytes and Insulin Sensitivity in Humans. *Diabetologia* (2009) 52 (5):882–90. doi: 10.1007/s00125-009-1300-4
14. Lundgren M, Svensson M, Lindmark S, Renstrom F, Ruge T, Eriksson JW. Fat Cell Enlargement Is an Independent Marker of Insulin Resistance and 'Hyperleptinaemia'. *Diabetologia* (2007) 50(3):625–33. doi: 10.1007/s00125-006-0572-1
15. Kloting N, Fasshauer M, Dietrich A, Kovacs P, Schon MR, Kern M, et al. Insulin-Sensitive Obesity. *Am J Physiol Endocrinol Metab* (2010) 299(3): E506–15. doi: 10.1152/ajpendo.00586.2009
16. Imbeault P, Lemieux S, Prud'homme D, Tremblay A, Nadeau A, Despres JP, et al. Relationship of Visceral Adipose Tissue to Metabolic Risk Factors for Coronary Heart Disease: Is There a Contribution of Subcutaneous Fat Cell Hypertrophy? *Metabolism* (1999) 48(3):355–62. doi: 10.1016/s0026-0495(99)90085-9
17. Heinonen S, Saarinen L, Naukkarinen J, Rodriguez A, Fruhbeck G, Hakkarainen A, et al. Adipocyte Morphology and Implications for Metabolic Derangements in Acquired Obesity. *Int J Obes (Lond)* (2014) 38(11):1423–31. doi: 10.1038/ijo.2014.31
18. Veilleux A, Caron-Jobin M, Noel S, Laberge PY, Tchernof A. Visceral Adipocyte Hypertrophy Is Associated With Dyslipidemia Independent of Body Composition and Fat Distribution in Women. *Diabetes* (2011) 60 (5):1504–11. doi: 10.2337/db10-1039
19. Hoffstedt J, Arner E, Wahrenberg H, Andersson DP, Qvisth V, Lofgren P, et al. Regional Impact of Adipose Tissue Morphology on the Metabolic Profile in Morbid Obesity. *Diabetologia* (2010) 53(12):2496–503. doi: 10.1007/s00125-010-1889-3
20. Cotillard A, Poitou C, Torcivia A, Bouillot JL, Dietrich A, Kloting N, et al. Adipocyte Size Threshold Matters: Link With Risk of Type 2 Diabetes and Improved Insulin Resistance After Gastric Bypass. *J Clin Endocrinol Metab* (2014) 99(8):E1466–70. doi: 10.1210/jc.2014-1074
21. Petaja EM, Sevastianova K, Hakkarainen A, Orho-Melander M, Lundbom N, Yki-Jarvinen H. Adipocyte Size Is Associated With Nafld Independent of Obesity, Fat Distribution, and Pnpla3 Genotype. *Obes (Silver Spring)* (2013) 21(6):1174–9. doi: 10.1002/oby.20114
22. Wree A, Schlattjan M, Bechmann LP, Claudel T, Sowa JP, Stojakovic T, et al. Adipocyte Cell Size, Free Fatty Acids and Apolipoproteins Are Associated With Non-Alcoholic Liver Injury Progression in Severely Obese Patients. *Metabolism* (2014) 63(12):1542–52. doi: 10.1016/j.metabol.2014.09.001
23. Naryzhnaya NV, Koshelskaya OA, Kologrivova IV, Kharitonova OA, Evtushenko VV, Boshchenko AA. Hypertrophy and Insulin Resistance of Epicardial Adipose Tissue Adipocytes: Association With the Coronary Artery Disease Severity. *Biomedicines* (2021) 9(1):64. doi: 10.3390/biomedicines9010064
24. Vianello E, Dozio E, Arnaboldi F, Marazzi MG, Martinelli C, Lamont J, et al. Epicardial Adipocyte Hypertrophy: Association With M1-Polarization and Toll-Like Receptor Pathways in Coronary Artery Disease Patients. *Nutr Metab Cardiovasc Dis* (2016) 26(3):246–53. doi: 10.1016/j.numecd.2015.12.005
25. Manneras-Holm L, Leonhardt H, Kullberg J, Jennische E, Oden A, Holm G, et al. Adipose Tissue Has Aberrant Morphology and Function in Pcos: Enlarged Adipocytes and Low Serum Adiponectin, But Not Circulating Sex Steroids, Are Strongly Associated With Insulin Resistance. *J Clin Endocrinol Metab* (2011) 96(2):E304–11. doi: 10.1210/jc.2010-1290
26. Salans LB, Knittle JL, Hirsch J. The Role of Adipose Cell Size and Adipose Tissue Insulin Sensitivity in the Carbohydrate Intolerance of Human Obesity. *J Clin Invest* (1968) 47(1):153–65. doi: 10.1172/JCI105705
27. Andersson DP, Eriksson Hogling D, Thorell A, Toft E, Qvisth V, Naslund E, et al. Changes in Subcutaneous Fat Cell Volume and Insulin Sensitivity After Weight Loss. *Diabetes Care* (2014) 37(7):1831–6. doi: 10.2337/dc13-2395
28. Goossens GH, Moors CC, van der Zijl NJ, Venteclef N, Alili R, Jocken JW, et al. Valsartan Improves Adipose Tissue Function in Humans With Impaired Glucose Metabolism: A Randomized Placebo-Controlled Double-Blind Trial. *PloS One* (2012) 7(6):e39930. doi: 10.1371/journal.pone.0039930
29. Rizkalla SW, Prifti E, Cotillard A, Pelloux V, Rouault C, Allouche R, et al. Differential Effects of Macronutrient Content in 2 Energy-Restricted Diets on Cardiovascular Risk Factors and Adipose Tissue Cell Size in Moderately Obese Individuals: A Randomized Controlled Trial. *Am J Clin Nutr* (2012) 95(1):49–63. doi: 10.3945/ajcn.111.017277
30. McLaughlin T, Abbasi F, Lamendola C, Yee G, Carter S, Cushman SW. Dietary Weight Loss in Insulin-Resistant Non-Obese Humans: Metabolic Benefits and Relationship to Adipose Cell Size. *Nutr Metab Cardiovasc Dis* (2019) 29(1):62–8. doi: 10.1016/j.numecd.2018.09.014
31. Skurk T, Alberti-Huber C, Herder C, Hauner H. Relationship Between Adipocyte Size and Adipokine Expression and Secretion. *J Clin Endocrinol Metab* (2007) 92(3):1023–33. doi: 10.1210/jc.2006-1055
32. Bahceci M, Gokalp D, Bahceci S, Tuzcu A, Atmaca S, Arikan S. The Correlation Between Adiposity and Adiponectin, Tumor Necrosis Factor Alpha, Interleukin-6 and High Sensitivity C-Reactive Protein Levels. Is Adipocyte Size Associated With Inflammation in Adults? *J Endocrinol Invest* (2007) 30(3):210–4. doi: 10.1007/BF03347427
33. Monteiro R, de Castro PM, Calhau C, Azevedo I. Adipocyte Size and Liability to Cell Death. *Obes Surg* (2006) 16(6):804–6. doi: 10.1381/096089206777346600
34. Li Q, Hagberg CE, Silva Cascales H, Lang S, Hyvonen MT, Salehzadeh F, et al. Obesity and Hyperinsulinemia Drive Adipocytes to Activate a Cell Cycle Program and Senesce. *Nat Med* (2021) 27(11):1941–53. doi: 10.1038/s41591-021-01501-8
35. Michaud A, Boulet MM, Veilleux A, Noel S, Paris G, Tchernof A. Abdominal Subcutaneous and Omental Adipocyte Morphology and Its Relation to Gene Expression, Lipolysis and Adipocytokine Levels in Women. *Metabolism* (2014) 63(3):372–81. doi: 10.1016/j.metabol.2013.11.007
36. Laurencikiene J, Skurk T, Kulyte A, Heden P, Astrom G, Sjolin E, et al. Regulation of Lipolysis in Small and Large Fat Cells of the Same Subject. *J Clin Endocrinol Metab* (2011) 96(12):E2045–9. doi: 10.1210/jc.2011-1702
37. Farnier C, Krief S, Blache M, Diot-Dupuy F, Mory G, Ferre P, et al. Adipocyte Functions Are Modulated by Cell Size Change: Potential Involvement of an Integrin/Erk Signalling Pathway. *Int J Obes Relat Metab Disord* (2003) 27(10):1178–86. doi: 10.1038/sj.ijo.0802399
38. Weyer C, Foley JE, Bogardus C, Tataranni PA, Pratley RE. Enlarged Subcutaneous Abdominal Adipocyte Size, But Not Obesity Itself, Predicts Type Ii Diabetes Independent of Insulin Resistance. *Diabetologia* (2000) 43 (12):1498–506. doi: 10.1007/s001250051560
39. Lonn M, Mehlig K, Bengtsson C, Lissner L. Adipocyte Size Predicts Incidence of Type 2 Diabetes in Women. *FASEB J* (2010) 24(1):326–31. doi: 10.1096/fj.09-133058
40. Johannsen DL, Tchoukalova Y, Tam CS, Covington JD, Xie W, Schwarz JM, et al. Effect of 8 Weeks of Overfeeding on Ectopic Fat Deposition and Insulin Sensitivity: Testing the "Adipose Tissue Expandability" Hypothesis. *Diabetes Care* (2014) 37(10):2789–97. doi: 10.2337/dc14-0761
41. McLaughlin T, Craig C, Liu LF, Perelman D, Allister C, Spielman D, et al. Adipose Cell Size and Regional Fat Deposition as Predictors of Metabolic Response to Overfeeding in Insulin-Resistant and Insulin-Sensitive Humans. *Diabetes* (2016) 65(5):1245–54. doi: 10.2337/db15-1213
42. Melchor-Lopez A, Suarez-Cuenca JA, Banderas-Lares DZ, Pena-Sosa G, Salamanca-Garcia M, Vera-Gomez E, et al. Identification of Adipose Tissue-Related Predictors of the Reduction in Cardiovascular Risk Induced by Metabolic Surgery. *J Int Med Res* (2021) 49(5):3000605211012569. doi: 10.1177/03000605211012569
43. Eriksson-Hogling D, Andersson DP, Backdahl J, Hoffstedt J, Rossner S, Thorell A, et al. Adipose Tissue Morphology Predicts Improved Insulin Sensitivity Following Moderate or Pronounced Weight Loss. *Int J Obes (Lond)* (2015) 39(6):893–8. doi: 10.1038/ijo.2015.18
44. Laforest S, Labrecque J, Michaud A, Cianflone K, Tchernof A. Adipocyte Size as a Determinant of Metabolic Disease and Adipose Tissue Dysfunction. *Crit Rev Clin Lab Sci* (2015) 52(6):301–13. doi: 10.3109/10408363.2015.1041582
45. Mundi MS, Karpyak MV, Koutsari C, Votruba SB, O'Brien PC, Jensen MD. Body Fat Distribution, Adipocyte Size, and Metabolic Characteristics of Nondiabetic Adults. *J Clin Endocrinol Metab* (2010) 95(1):67–73. doi: 10.1210/jc.2009-1353
46. Ledoux S, Coupaye M, Essig M, Msika S, Roy C, Queguiner I, et al. Traditional Anthropometric Parameters Still Predict Metabolic Disorders in Women With Severe Obesity. *Obes (Silver Spring)* (2010) 18(5):1026–32. doi: 10.1038/oby.2009.349

47. Meena VP, Seenu V, Sharma MC, Mallick SR, Bhalla AS, Gupta N, et al. Relationship of Adipocyte Size With Adiposity and Metabolic Risk Factors in Asian Indians. *PloS One* (2014) 9(9):e108421. doi: 10.1371/journal.pone.0108421
48. Brook CG, Lloyd JK. Adipose Cell Size and Glucose Tolerance in Obese Children and Effects of Diet. *Arch Dis Child* (1973) 48(4):301–4. doi: 10.1136/adc.48.4.301
49. Larson-Meyer DE, Heilbronn LK, Redman LM, Newcomer BR, Frisard MI, Anton S, et al. Effect of Calorie Restriction With or Without Exercise on Insulin Sensitivity, Beta-Cell Function, Fat Cell Size, and Ectopic Lipid in Overweight Subjects. *Diabetes Care* (2006) 29(6):1337–44. doi: 10.2337/dc05-2565
50. Koenen TB, Tack CJ, Kroese JM, Hermus AR, Sweep FC, van der Laak J, et al. Pioglitazone Treatment Enlarges Subcutaneous Adipocytes in Insulin-Resistant Patients. *J Clin Endocrinol Metab* (2009) 94(11):4453–7. doi: 10.1210/jc.2009-0517
51. Boden G. Obesity, Insulin Resistance and Free Fatty Acids. *Curr Opin Endocrinol Diabetes Obes* (2011) 18(2):139–43. doi: 10.1097/MED.0b013e3283444b09
52. Laforest S, Michaud A, Paris G, Pelletier M, Vidal H, Geloen A, et al. Comparative Analysis of Three Human Adipocyte Size Measurement Methods and Their Relevance for Cardiometabolic Risk. *Obes (Silver Spring)* (2017) 25(1):122–31. doi: 10.1002/oby.21697
53. Golan R, Shelef I, Rudich A, Gepner Y, Shemesh E, Chassidim Y, et al. Abdominal Superficial Subcutaneous Fat: A Putative Distinct Protective Fat Subdepot in Type 2 Diabetes. *Diabetes Care* (2012) 35(3):640–7. doi: 10.2337/dc11-1583
54. DeBari MK, Abbott RD. Adipose Tissue Fibrosis: Mechanisms, Models, and Importance. *Int J Mol Sci* (2020) 21(17):6030. doi: 10.3390/ijms21176030
55. Fried SK. Adipocyte Size Redux. *Obes (Silver Spring)* (2017) 25(1):15. doi: 10.1002/oby.21717
56. Arner E, Westermark PO, Spalding KL, Britton T, Ryden M, Frisen J, et al. Adipocyte Turnover: Relevance to Human Adipose Tissue Morphology. *Diabetes* (2010) 59(1):105–9. doi: 10.2337/db09-0942
57. McLaughlin T, Sherman A, Tsao P, Gonzalez O, Yee G, Lamendola C, et al. Enhanced Proportion of Small Adipose Cells in Insulin-Resistant Vs Insulin-Sensitive Obese Individuals Implicates Impaired Adipogenesis. *Diabetologia* (2007) 50(8):1707–15. doi: 10.1007/s00125-007-0708-y
58. Kursawe R, Eszlinger M, Narayan D, Liu T, Bazuine M, Cali AM, et al. Cellularity and Adipogenic Profile of the Abdominal Subcutaneous Adipose Tissue From Obese Adolescents: Association With Insulin Resistance and Hepatic Steatosis. *Diabetes* (2010) 59(9):2288–96. doi: 10.2337/db10-0113
59. Hotamisligil GS, Arner P, Caro JF, Atkinson RL, Spiegelman BM. Increased Adipose Tissue Expression of Tumor Necrosis Factor-Alpha in Human Obesity and Insulin Resistance. *J Clin Invest* (1995) 95(5):2409–15. doi: 10.1172/JCI117936
60. Weisberg SP, McCann D, Desai M, Rosenbaum M, Leibel RL, Ferrante AWJr. Obesity Is Associated With Macrophage Accumulation in Adipose Tissue. *J Clin Invest* (2003) 112(12):1796–808. doi: 10.1172/JCI19246
61. Xu H, Barnes GT, Yang Q, Tan G, Yang D, Chou CJ, et al. Chronic Inflammation in Fat Plays a Crucial Role in the Development of Obesity-Related Insulin Resistance. *J Clin Invest* (2003) 112(12):1821–30. doi: 10.1172/JCI19451
62. Reilly SM, Saltiel AR. Adapting to Obesity With Adipose Tissue Inflammation. *Nat Rev Endocrinol* (2017) 13(11):633–43. doi: 10.1038/nrendo.2017.90
63. Kawai T, Autieri MV, Scalia R. Adipose Tissue Inflammation and Metabolic Dysfunction in Obesity. *Am J Physiol Cell Physiol* (2021) 320(3):C375–C91. doi: 10.1152/ajpcell.00379.2020
64. Bluher M. Adipose Tissue Inflammation: A Cause or Consequence of Obesity-Related Insulin Resistance? *Clin Sci (Lond)* (2016) 130(18):1603–14. doi: 10.1042/CS20160005
65. Cancello R, Tordjman J, Poitou C, Guilhem G, Bouillot JL, Hugol D, et al. Increased Infiltration of Macrophages in Omental Adipose Tissue Is Associated With Marked Hepatic Lesions in Morbid Human Obesity. *Diabetes* (2006) 55(6):1554–61. doi: 10.2337/db06-0133
66. Tordjman J, Poitou C, Hugol D, Bouillot JL, Basdevant A, Bedossa P, et al. Association Between Omental Adipose Tissue Macrophages and Liver Histopathology in Morbid Obesity: Influence of Glycemic Status. *J Hepatol* (2009) 51(2):354–62. doi: 10.1016/j.jhep.2009.02.031
67. Harman-Boehm I, Bluher M, Redel H, Sion-Vardy N, Ovadia S, Avinoach E, et al. Macrophage Infiltration Into Omental Versus Subcutaneous Fat Across Different Populations: Effect of Regional Adiposity and the Comorbidities of Obesity. *J Clin Endocrinol Metab* (2007) 92(6):2240–7. doi: 10.1210/jc.2006-1811
68. Hardy OT, Perugini RA, Nicoloro SM, Gallagher-Dorval K, Puri V, Straubhaar J, et al. Body Mass Index-Independent Inflammation in Omental Adipose Tissue Associated With Insulin Resistance in Morbid Obesity. *Surg Obes Relat Dis* (2011) 7(1):60–7. doi: 10.1016/j.soard.2010.05.013
69. van Beek L, Lips MA, Visser A, Pijl H, Ioan-Facsinay A, Toes R, et al. Increased Systemic and Adipose Tissue Inflammation Differentiates Obese Women With T2dm From Obese Women With Normal Glucose Tolerance. *Metabolism* (2014) 63(4):492–501. doi: 10.1016/j.metabol.2013.12.002
70. Goldstein N, Kezerle Y, Gepner Y, Haim Y, Pecht T, Gazit R, et al. Higher Mast Cell Accumulation in Human Adipose Tissues Defines Clinically Favorable Obesity Sub-Phenotypes. *Cells* (2020) 9(6):1508. doi: 10.3390/cells9061508
71. Lopez-Perez D, Redruello-Romero A, Garcia-Rubio J, Arana C, Garcia-Escudero LA, Tamayo F, et al. In Patients With Obesity, the Number of Adipose Tissue Mast Cells Is Significantly Lower in Subjects With Type 2 Diabetes. *Front Immunol* (2021) 12:664576. doi: 10.3389/fimmu.2021.664576
72. Divoux A, Moutel S, Poitou C, Lacasa D, Veyrie N, Aissat A, et al. Mast Cells in Human Adipose Tissue: Link With Morbid Obesity, Inflammatory Status, and Diabetes. *J Clin Endocrinol Metab* (2012) 97(9):E1677–85. doi: 10.1210/jc.2012-1532
73. Bertola A, Ciucci T, Rousseau D, Bourlier V, Duffaut C, Bonnafous S, et al. Identification of Adipose Tissue Dendritic Cells Correlated With Obesity-Associated Insulin-Resistance and Inducing Th17 Responses in Mice and Patients. *Diabetes* (2012) 61(9):2238–47. doi: 10.2337/db11-1274
74. McLaughlin T, Liu LF, Lamendola C, Shen L, Morton J, Rivas H, et al. T-Cell Profile in Adipose Tissue Is Associated With Insulin Resistance and Systemic Inflammation in Humans. *Arterioscler Thromb Vasc Biol* (2014) 34(12):2637–43. doi: 10.1161/ATVBAHA.114.304636
75. Maixner N, Pecht T, Haim Y, Chalifa-Caspi V, Goldstein N, Tarnovscki T, et al. A Trail-Tl1a Paracrine Network Involving Adipocytes, Macrophages, and Lymphocytes Induces Adipose Tissue Dysfunction Downstream of E2f1 in Human Obesity. *Diabetes* (2020) 69(11):2310–23. doi: 10.2337/db19-1231
76. Cancello R, Henegar C, Viguerie N, Taleb S, Poitou C, Rouault C, et al. Reduction of Macrophage Infiltration and Chemoattractant Gene Expression Changes in White Adipose Tissue of Morbidly Obese Subjects After Surgery-Induced Weight Loss. *Diabetes* (2005) 54(8):2277–86. doi: 10.2337/diabetes.54.8.2277
77. Bradley D, Conte C, Mittendorfer B, Eagon JC, Varela JE, Fabbrini E, et al. Gastric Bypass and Banding Equally Improve Insulin Sensitivity and Beta Cell Function. *J Clin Invest* (2012) 122(12):4667–74. doi: 10.1172/JCI64895
78. Hagman DK, Larson I, Kuzma JN, Cromer G, Makar K, Rubinow KB, et al. The Short-Term and Long-Term Effects of Bariatric/Metabolic Surgery on Subcutaneous Adipose Tissue Inflammation in Humans. *Metabolism* (2017) 70:12–22. doi: 10.1016/j.metabol.2017.01.030
79. Kratz M, Hagman DK, Kuzma JN, Foster-Schubert KE, Chan CP, Stewart S, et al. Improvements in Glycemic Control After Gastric Bypass Occur Despite Persistent Adipose Tissue Inflammation. *Obes (Silver Spring)* (2016) 24(7):1438–45. doi: 10.1002/oby.21524
80. Magkos F, Fraterrigo G, Yoshino J, Luecking C, Kirbach K, Kelly SC, et al. Effects of Moderate and Subsequent Progressive Weight Loss on Metabolic Function and Adipose Tissue Biology in Humans With Obesity. *Cell Metab* (2016) 23(4):591–601. doi: 10.1016/j.cmet.2016.02.005
81. Boden G, Homko C, Barrero CA, Stein TP, Chen X, Cheung P, et al. Excessive Caloric Intake Acutely Causes Oxidative Stress, Glut4 Carbonylation, and Insulin Resistance in Healthy Men. *Sci Transl Med* (2015) 7(304):304re7. doi: 10.1126/scitranslmed.aac4765
82. Burhans MS, Hagman DK, Kuzma JN, Schmidt KA, Kratz M. Contribution of Adipose Tissue Inflammation to the Development of Type 2 Diabetes Mellitus. *Compr Physiol* (2018) 9(1):1–58. doi: 10.1002/cphy.c170040

83. Berg AH, Scherer PE. Adipose Tissue, Inflammation, and Cardiovascular Disease. *Circ Res* (2005) 96(9):939–49. doi: 10.1161/01.RES.0000163635.62927.34
84. Labrecque J, Laforest S, Michaud A, Biertho L, Tchernof A. Impact of Bariatric Surgery on White Adipose Tissue Inflammation. *Can J Diabetes* (2017) 41(4):407–17. doi: 10.1016/j.jcjd.2016.12.003
85. Trachta P, Dostalova I, Haluzikova D, Kasalicky M, Kavalkova P, Drapalova J, et al. Laparoscopic Sleeve Gastrectomy Ameliorates Mrna Expression of Inflammation-Related Genes in Subcutaneous Adipose Tissue But Not in Peripheral Monocytes of Obese Patients. *Mol Cell Endocrinol* (2014) 383(1-2):96–102. doi: 10.1016/j.mce.2013.11.013
86. Donath MY, Meier DT, Boni-Schnetzler M. Inflammation in the Pathophysiology and Therapy of Cardiometabolic Disease. *Endocr Rev* (2019) 40(4):1080–91. doi: 10.1210/er.2019-00002
87. Goldfine AB, Shoelson SE. Therapeutic Approaches Targeting Inflammation for Diabetes and Associated Cardiovascular Risk. *J Clin Invest* (2017) 127 (1):83–93. doi: 10.1172/JCI88884
88. Mariman EC, Wang P. Adipocyte Extracellular Matrix Composition, Dynamics and Role in Obesity. *Cell Mol Life Sci* (2010) 67(8):1277–92. doi: 10.1007/s00018-010-0263-4
89. Marcelin G, Gautier EL, Clément K. Adipose Tissue Fibrosis in Obesity: Etiology and Challenges. *Annu Rev Physiol* (2021) 84:135–55. doi: 10.1146/annurev-physiol-060721-092930
90. Pasarica M, Gowronska-Kozak B, Burk D, Remedios I, Hymel D, Gimble J, et al. Adipose Tissue Collagen Vi in Obesity. *J Clin Endocrinol Metab* (2009) 94(12):5155–62. doi: 10.1210/jc.2009-0947
91. Dankel SN, Svärd J, Matthä S, Claussnitzer M, Klöting N, Glunk V, et al. Col6a3 Expression in Adipocytes Associates With Insulin Resistance and Depends on Pparγ and Adipocyte Size. *Obes (Silver Spring)* (2014) 22 (8):1807–13. doi: 10.1002/oby.20758
92. Yoshino J, Patterson BW, Klein S. Adipose Tissue Ctgf Expression Is Associated With Adiposity and Insulin Resistance in Humans. *Obes (Silver Spring)* (2019) 27(6):957–62. doi: 10.1002/oby.22463
93. Henninger AM, Eliasson B, Jenndahl LE, Hammarstedt A. Adipocyte Hypertrophy, Inflammation and Fibrosis Characterize Subcutaneous Adipose Tissue of Healthy, Non-Obese Subjects Predisposed to Type 2 Diabetes. *PloS One* (2014) 9(8):e105262. doi: 10.1371/journal.pone.0105262
94. Chabot K, Gauthier MS, Garneau PY, Rabasa-Lhoret R. Evolution of Subcutaneous Adipose Tissue Fibrosis After Bariatric Surgery. *Diabetes Metab* (2017) 43(2):125–33. doi: 10.1016/j.diabet.2016.10.004
95. Guglielmi V, Cardellini M, Cinti F, Corgosinho F, Cardolini I, D'Adamo M, et al. Omental Adipose Tissue Fibrosis and Insulin Resistance in Severe Obesity. *Nutr Diabetes* (2015) 5(8):e175. doi: 10.1038/nutd.2015.22
96. Leven AS, Gieseler RK, Schlattjan M, Schreiter T, Niedergethmann M, Baars T, et al. Association of Cell Death Mechanisms and Fibrosis in Visceral White Adipose Tissue With Pathological Alterations in the Liver of Morbidly Obese Patients With Nafld. *Adipocyte* (2021) 10(1):558–73. doi: 10.1080/21623945.2021.1982164
97. Abdennour M, Reggio S, Le Naour G, Liu Y, Poitou C, Aron-Wisnewsky J, et al. Association of Adipose Tissue and Liver Fibrosis With Tissue Stiffness in Morbid Obesity: Links With Diabetes and Bmi Loss After Gastric Bypass. *J Clin Endocrinol Metab* (2014) 99(3):898–907. doi: 10.1210/jc.2013-3253
98. Divoux A, Tordjman J, Lacasa D, Veyrie N, Hugol D, Aissat A, et al. Fibrosis in Human Adipose Tissue: Composition, Distribution, and Link With Lipid Metabolism and Fat Mass Loss. *Diabetes* (2010) 59(11):2817–25. doi: 10.2337/db10-0585
99. Muir LA, Neeley CK, Meyer KA, Baker NA, Brosius AM, Washabaugh AR, et al. Adipose Tissue Fibrosis, Hypertrophy, and Hyperplasia: Correlations With Diabetes in Human Obesity. *Obes (Silver Spring)* (2016) 24(3):597–605. doi: 10.1002/oby.21377
100. Henegar C, Tordjman J, Achard V, Lacasa D, Cremer I, Guerre-Millo M, et al. Adipose Tissue Transcriptomic Signature Highlights the Pathological Relevance of Extracellular Matrix in Human Obesity. *Genome Biol* (2008) 9 (1):R14. doi: 10.1186/gb-2008-9-1-r14
101. Cancello R, Zulian A, Gentilini D, Mencarelli M, Della Barba A, Maffei M, et al. Permanence of Molecular Features of Obesity in Subcutaneous Adipose Tissue of Ex-Obese Subjects. *Int J Obes (Lond)* (2013) 37(6):867–73. doi: 10.1038/ijo.2013.7
102. Buechler C, Krautbauer S, Eisinger K. Adipose Tissue Fibrosis. *World J Diabetes* (2015) 6(4):548–53. doi: 10.4239/wjd.v6.i4.548
103. Hardy OT, Czech MP, Corvera S. What Causes the Insulin Resistance Underlying Obesity? *Curr Opin Endocrinol Diabetes Obes* (2012) 19(2):81–7. doi: 10.1097/MED.0b013e3283514e13
104. Pasarica M, Sereda OR, Redman LM, Albarado DC, Hymel DT, Roan LE, et al. Reduced Adipose Tissue Oxygenation in Human Obesity: Evidence for Rarefaction, Macrophage Chemotaxis, and Inflammation Without an Angiogenic Response. *Diabetes* (2009) 58(3):718–25. doi: 10.2337/db08-1098
105. Bel Lassen P, Charlotte F, Liu Y, Bedossa P, Le Naour G, Tordjman J, et al. The Fat Score, a Fibrosis Score of Adipose Tissue: Predicting Weight-Loss Outcome After Gastric Bypass. *J Clin Endocrinol Metab* (2017) 102(7):2443–53. doi: 10.1210/jc.2017-00138
106. Spencer M, Unal R, Zhu B, Rasouli N, McGehee REJr., Peterson CA, et al. Adipose Tissue Extracellular Matrix and Vascular Abnormalities in Obesity and Insulin Resistance. *J Clin Endocrinol Metab* (2011) 96(12):E1990–8. doi: 10.1210/jc.2011-1567
107. Vila Isabelle K, Badin P-M, Marques M-A, Monbrun L, Lefort C, Mir L, et al. Immune Cell Toll-Like Receptor 4 Mediates the Development of Obesity- and Endotoxemia-Associated Adipose Tissue Fibrosis. *Cell Rep* (2014) 7 (4):1116–29. doi: 10.1016/j.celrep.2014.03.062
108. Liu Y, Aron-Wisnewsky J, Marcelin G, Genser L, Le Naour G, Torcivia A, et al. Accumulation and Changes in Composition of Collagens in Subcutaneous Adipose Tissue After Bariatric Surgery. *J Clin Endocrinol Metab* (2016) 101(1):293–304. doi: 10.1210/jc.2015-3348
109. Mutch DM, Tordjman J, Pelloux V, Hanczar B, Henegar C, Poitou C, et al. Needle and Surgical Biopsy Techniques Differentially Affect Adipose Tissue Gene Expression Profiles. *Am J Clin Nutr* (2009) 89(1):51–7. doi: 10.3945/ajcn.2008.26802
110. Sasso M, Abdennour M, Liu Y, Hazrak H, Aron-Wisnewsky J, Bouillot J-L, et al. Relevance of Adipose Tissue Stiffness Evaluated by Transient Elastography (Adiposcan™) in Morbidly Obese Patients Before Bariatric Surgery. *Phys Proc* (2015) 70:1264–8. doi: 10.1016/j.phpro.2015.08.281
111. Bouazizi K, Zarai M, Marquet F, Aron-Wisnewsky J, Clément K, Redheuil A, et al. Adipose Tissue Fibrosis Assessed by High Resolution Ex Vivo Mri as a Hallmark of Tissue Alteration in Morbid Obesity. *Quant Imaging Med Surg* (2021) 11(5):2162–8. doi: 10.21037/qims-20-879
112. Alba DL, Farooq JA, Lin MYC, Schafer AL, Shepherd J, Koliwad SK. Subcutaneous Fat Fibrosis Links Obesity to Insulin Resistance in Chinese Americans. *J Clin Endocrinol Metab* (2018) 103(9):3194–204. doi: 10.1210/jc.2017-02301
113. Munoz A, Abate N, Chandalia M. Adipose Tissue Collagen and Inflammation in Nonobese Asian Indian Men. *J Clin Endocrinol Metab* (2013) 98(8):E1360–3. doi: 10.1210/jc.2012-3841
114. Von Bank H, Kirsh C, Simcox J. Aging Adipose: Depot Location Dictates Age-Associated Expansion and Dysfunction. *Ageing Res Rev* (2021) 67:101259. doi: 10.1016/j.arr.2021.101259
115. Cooper TC, Simmons EB, Webb K, Burns JL, Kushner RF. Trends in Weight Regain Following Roux-En-Y Gastric Bypass (Rygb) Bariatric Surgery. *Obes Surg* (2015) 25(8):1474–81. doi: 10.1007/s11695-014-1560-z
116. Aron-Wisnewsky J, Sokolovska N, Liu Y, Comaneshter DS, Vinker S, Pecht T, et al. The Advanced-Diarem Score Improves Prediction of Diabetes Remission 1 Year Post-Roux-En-Y Gastric Bypass. *Diabetologia* (2017) 60 (10):1892–902. doi: 10.1007/s00125-017-4371-7
117. Marquez-Quinones A, Mutch DM, Debard C, Wang P, Combes M, Roussel B, et al. Adipose Tissue Transcriptome Reflects Variations Between Subjects With Continued Weight Loss and Subjects Regaining Weight 6 Mo After Caloric Restriction Independent of Energy Intake. *Am J Clin Nutr* (2010) 92 (4):975–84. doi: 10.3945/ajcn.2010.29808
118. Giardina S, Hernandez-Alonso P, Salas-Salvado J, Rabassa-Soler A, Bullo M. Modulation of Human Subcutaneous Adipose Tissue Microrna Profile Associated With Changes in Adiposity-Related Parameters. *Mol Nutr Food Res* (2018) 62(2):1700594. doi: 10.1002/mnfr.201700594
119. Vijay J, Gauthier MF, Biswell RL, Louiselle DA, Johnston JJ, Cheung WA, et al. Single-Cell Analysis of Human Adipose Tissue Identifies Depot and Disease Specific Cell Types. *Nat Metab* (2020) 2(1):97–109. doi: 10.1038/s42255-019-0152-6
120. Pecht T, Gutman-Tirosh A, Bashan N, Rudich A. Peripheral Blood Leucocyte Subclasses as Potential Biomarkers of Adipose Tissue

Inflammation and Obesity Subphenotypes in Humans. *Obes Rev* (2014) 15 (4):322–37. doi: 10.1111/obr.12133
121. Pecht T, Haim Y, Bashan N, Shapiro H, Harman-Boehm I, Kirshtein B, et al. Circulating Blood Monocyte Subclasses and Lipid-Laden Adipose Tissue Macrophages in Human Obesity. *PloS One* (2016) 11(7):e0159350. doi: 10.1371/journal.pone.0159350
122. Shapiro H, Pecht T, Shaco-Levy R, Harman-Boehm I, Kirshtein B, Kuperman Y, et al. Adipose Tissue Foam Cells Are Present in Human Obesity. *J Clin Endocrinol Metab* (2013) 98(3):1173–81. doi: 10.1210/jc.2012-2745
123. Henninger J, Eliasson B, Smith U, Rawshani A. Identification of Markers That Distinguish Adipose Tissue and Glucose and Insulin Metabolism Using a Multi-Modal Machine Learning Approach. *Sci Rep* (2021) 11(1):17050. doi: 10.1038/s41598-021-95688-y
124. Sattar N, Wannamethee G, Sarwar N, Tchernova J, Cherry L, Wallace AM, et al. Adiponectin and Coronary Heart Disease: A Prospective Study and Meta-Analysis. *Circulation* (2006) 114(7):623–9. doi: 10.1161/CIRCULATIONAHA.106.618918
125. Lindberg S, Jensen JS, Bjerre M, Frystyk J, Flyvbjerg A, Jeppesen J, et al. Low Adiponectin Levels at Baseline and Decreasing Adiponectin Levels Over 10 Years of Follow-Up Predict Risk of the Metabolic Syndrome. *Diabetes Metab* (2017) 43(2):134–9. doi: 10.1016/j.diabet.2016.07.027
126. Kim JY, Ahn SV, Yoon JH, Koh SB, Yoon J, Yoo BS, et al. Prospective Study of Serum Adiponectin and Incident Metabolic Syndrome: The Arirang Study. *Diabetes Care* (2013) 36(6):1547–53. doi: 10.2337/dc12-0223

Conflict of Interest: The authors declare that the research was conducted in the absence of any commercial or financial relationships that could be construed as a potential conflict of interest.

frontiers | Frontiers in Endocrinology

ORIGINAL RESEARCH
published: 06 June 2022
doi: 10.3389/fendo.2022.866679

Circulating Levels of MiRNAs From 320 Family in Subjects With Lipodystrophy: Disclosing Novel Signatures of the Disease

*Alessia Dattilo[1,2], Giovanni Ceccarini[2], Gaia Scabia[2,3], Silvia Magno[2], Lara Quintino[2], Caterina Pelosini[2], Guido Salvetti[2], Roberto Cusano[4], Matteo Massidda[4], Lucia Montanelli[5], Donatella Gilio[2], Gianluca Gatti[6], Alessandro Giacomina[6], Mario Costa[7,8], Ferruccio Santini[2] and Margherita Maffei[2,3]**

[1] Institute of Life Sciences, Scuola Superiore Sant'Anna, Pisa, Italy, [2] Obesity and Lipodystrophy Center, Endocrinology Unit, Pisa University Hospital, Pisa, Italy, [3] National Research Council, Institute of Clinical Physiology, Pisa, Italy, [4] Center for Advanced Studies, Research and Development in Sardinia, Pula (CA), Italy, [5] Department of Clinical and Experimental Medicine, Endocrinology Unit, Pisa University Hospital, Pisa, Italy, [6] Plastic and Reconstructive Surgery Unit, Hospital of Pisa, Pisa, Italy, [7] National Research Council, Institute of Neuroscience, Pisa, Italy, [8] Centro Pisano Flash Radiotherapy, Center for Instrument Sharing of the University of Pisa (CPFR@CISUP), Pisa University Hospital, Pisa, Italy

OPEN ACCESS

Edited by:
Matthias Blüher,
Leipzig University, Germany

Reviewed by:
Maude Giroud,
Ludwig Maximilian University of Munich, Germany
Joan Villarroya,
University of Barcelona, Spain

***Correspondence:**
Margherita Maffei
m.maffei@ifc.cnr.it

Specialty section:
This article was submitted to Obesity, a section of the journal Frontiers in Endocrinology

Received: 31 January 2022
Accepted: 05 May 2022
Published: 06 June 2022

Citation:
Dattilo A, Ceccarini G, Scabia G, Magno S, Quintino L, Pelosini C, Salvetti G, Cusano R, Massidda M, Montanelli L, Gilio D, Gatti G, Giacomina A, Costa M, Santini F and Maffei M (2022) Circulating Levels of MiRNAs From 320 Family in Subjects With Lipodystrophy: Disclosing Novel Signatures of the Disease. Front. Endocrinol. 13:866679. doi: 10.3389/fendo.2022.866679

Lipodystrophy (LD) indicates a group of rare disorders, with generalized or partial loss of white adipose tissue (WAT) often associated with metabolic derangements. Heterogeneity/wide spectrum of the disease and lack of biomarkers make diagnosis often difficult. MicroRNAs are important to maintain a correct WAT function and WAT is a source of circulating miRNAs (cmiRs). miRNAs from 320 family were previously detected in the WAT and variably associated to the metabolic syndrome. Our aim was then to investigate if LD can result in altered abundance of cmiRs-320. We collected samples from a cohort of LD subjects of various subtypes and from age matched controls. Use of quantitative PCR determined that cmiRs- 320a-3p, 320b, 320c, 320e are upregulated, while 320d is downregulated in LD. CmiRs-320 power as classifiers was more powerful in the most extreme and defined forms of LD, including the generalized and the Dunnigan subtypes. cmiR-320a-3p showed significant inverse relationships with plasma leptin ($P < 0.0001$), typically low in LD. The hepatic enzymes gamma-glutamyl transferase (GGT), aspartate aminotransferase (AST), alanine aminotransferase (ALT) and the marker of inflammation C-reactive protein (CRP) were inversely related to cmiR 320d ($P < 0.05$, for CRP and GGT; $P < 0.01$, for AST and ALT). Gene ontology analysis revealed cell-cell adhesion as a process regulated by 320 miRNAs targets, thus disclosing a novel route to investigate origin of WAT loss/dysfunction. In conclusion, cmiRs-320 constitute novel biomarkers of LD, abundance of miR320a-3p is inversely associated to indicators related to WAT function, while downregulation of cmiR-320d predicts an altered hepatic profile and higher inflammation.

Keywords: lipodystrophy subtypes, miRNA, metabolism, gene ontology, circulating biomarker, kobberling

INTRODUCTION

Lipodystrophy (LD) designates a heterogeneous group of rare disorders, characterized by dysfunction and lack of white adipose tissue (WAT) with a prevalent loss of the subcutaneous (SAT) (1). The spectrum of the disorder is broad and the current classification scheme distinguishes 4 major categories: Congenital Generalized LD (CGL), a very rare disorder with known pathogenetic mechanism due to defects in genes involved in lipid droplet formation (1–3); Familial Partial LD (FPL), the most common form of LD in adults (4); Acquired Partial and Generalized LD (APL and AGL), with variable onset (5) and causes still to be elucidated, although an imbalance in the immune response has been hypothesized (6). Other forms include those associated with progeria, often presenting generalized fat loss (7). Besides, there is a relatively frequent form of LD occurring in human immunodeficiency virus (HIV) infected patients as a consequence of antiretroviral therapy (8), which will not be herein investigated. Metabolic and endocrine derangements, that paradoxically mimic those found in morbid obesity (9), often affect LD subjects: triglyceride overload due to overfeeding or reduced/null capacity to store energy in excess results, in fact, in dysfunctional WAT and consequent dysmetabolism including insulin resistance, dyslipidemia and hepatic steatosis (9, 10). Notwithstanding the heterogeneity of LD, there are considerations that apply to the entire spectrum of the disorder that is worth considering: 1. If we exclude CGL and some forms of FPL (11), for which we have a known cause-effect relationship between gene defects and impaired lipid droplet formation (3), the mechanisms of the other types of LD are to be defined. 2. In most LD patients, especially in the acquired forms, WAT loss is noticed and clinically evaluated when the extension of fat disappearance is advanced and metabolic health compromised, while it would be helpful to diagnose this condition as early as possible.

Among other factors, microRNAs (miRNAs) play a relevant role in the regulation of adipocyte biology (12); loss of function of the miRNA processing enzyme Dicer results in a LD and insulin resistant mouse (13) and adipose tissue-specific ablation of Dgcr8, a key regulator of miRNA biogenesis, results in dysfunctional adipose tissue (14, 15). MiRNAs bind to messenger RNAs, modulate their stability and availability to be translated, their dysregulation being implied in the onset of multiple disorders including cancer, neurodegenerative diseases, and diabetes (16). These small RNAs can be released by cells into the blood flow and reach distant tissues to act as gene expression modulators (17). Of note, WAT releases miRNAs into the circle and analyses conducted in HIV-associated LD revealed a downregulation of WAT expression of Dicer (13), and consistent alterations in the levels of both circulating and adipose tissue miRNAs (cmiRs) (18, 19).

In the present study we chose to focus our attention on 5 miRNAs belonging to the same family, i.e. 320 (from now on referred to as miRs-320), as they present features that are relevant for a better understanding of WAT dysfunction and loss: 1. they were previously reported to be present in the WAT (20) and play a pivotal role in the adipogenic versus osteogenic switch of human mesenchymal stem cells (21); 2. miRs-320 were found to be significantly associated with visceral adipose tissue levels, a depot which is overrepresented in various forms of LD at the expense of SAT loss (22); 3. miRs-320 are overexpressed in metabolically stressed 3T3-L1 murine adipocytes, where they suppress glucose uptake and lipogenesis, while inducing lipolysis *via* the insulin-phosphatidylinositol 3-kinase pathway and endoplasmic reticulum stress signaling (23, 24).

In search of novel biomarkers of LD and of molecular mechanisms underlying its pathogenesis and/or downstream targets, we characterized the circulating levels of miRs-320 (cmiRs-320) in subjects affected by the disease considered either as a single heterogeneous cohort or sub-grouped in the various subtypes; we investigated the relationship between cmiRs-320 and the clinical profile, and we finally performed gene ontology search on cmiRs-320 targets to get insights into the biological meaning of our findings. Our experimental design is represented in the flowchart of **Figure 1A**.

MATERIALS AND METHODS

Study Population

Patients attending the outpatient clinic for obesity and lipodystrophies at the University Hospital of Pisa were prospectively enrolled in the study. Medical history, clinical and laboratory data were collected and anthropometric measures were taken by standardized methods throughout the study. We recruited: patients with LD, the diagnosis of LD subtype was made based on the published criteria (2, 25); obese subjects with a BMI > 35 Kg/m2 associated to at least 2 metabolic derangements; healthy controls (HC) recruited among subjects undergoing routinary endocrinological tests with no comorbidities. Eligible were all patients between 2 and 80 years old and criteria for exclusion were presence of malignancy or diseases that may influence miRNA expression (26). A subgroup of controls, herein defined adult healthy controls (AHC), was selected for a proper age matching with FPLD1 subjects (see also **Supplementary Table 2**). Patients' recruitment and informed consent were carried out in accordance with approved guidelines from the Local Ethical Committee (CEAVNO, Protocol number D 19440).

Abbreviations: LD, Lipodystrophy/subjects with Lipodystrophy; HC, healthy controls; AHC, adult healthy controls; OB, subjects with obesity; WAT, white adipose tissue; SAT, subcutaneous adipose tissue; VAT, visceral adipose tissue; miRNAs, microRNAs; cmiRNAs, circulating microRNAs; cmiRs 320, circulating miRNAs of the 320 family; GL, generalized Lipodystrophy; AGL, acquired generalized Lipodystrophy; CGL, congenital generalized Lipodystrophy; PL, partial Lipodystrophy; FPL, familial partial Lipodystrophy; APL, acquired partial Lipodystrophy; AF, adipose fraction; SVF, stromal vascular fraction; cel-miR-39, *Caenorhabditis elegans*-miR-39; TG, triglycerides; Chol, total cholesterol; HDL-C, high density lipoprotein-cholesterol; LDL-C, low density lipoprotein-cholesterol; CRP, C-reactive protein; AST, aspartate aminotransferase; GOT, glutamic oxaloacetic transaminase; ALT, alanine aminotransferase; GPT, glutamic pyruvic transaminase; GGT, gamma-glutamyl transferase; ROC, Receiver Operating Characteristic; AUC, area under the curve; CI, confidence interval; Ct, cycle threshold; GO, gene ontology; ECM, Extra Cellular Matrix; RUNX2, RUNX family transcription Factor 2; ITG1B, integrin 1 beta.

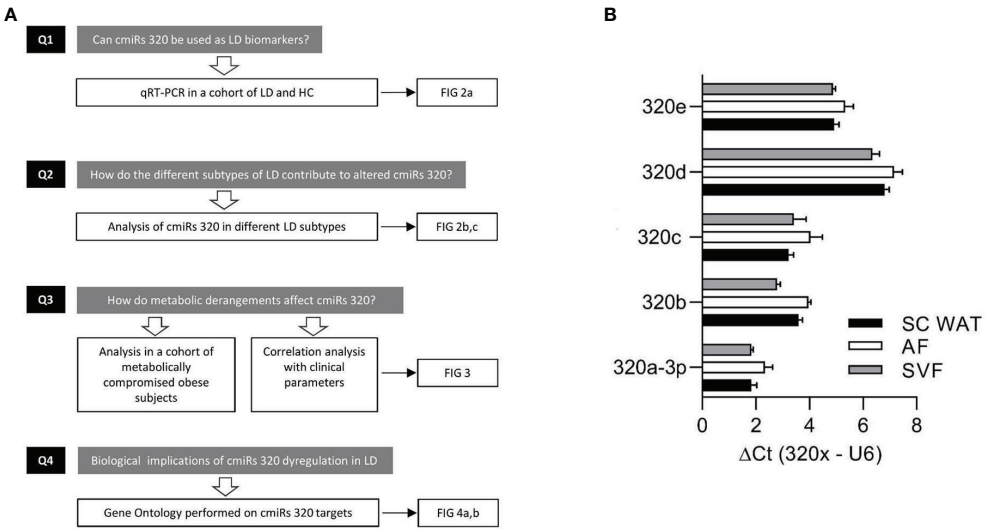

FIGURE 1 | Experimental design and discovery study. **(A)** Flowchart depicting the experimental design consisting in: quantitation of cmiRs-320 levels and further characterization steps as indicated. **(B)** Bar graphs of 320 family miRNAs in subcutaneous WAT and subfractions. Data are expressed as mean ± SEM for 3 independent samples.

Human Samples

Plasma: Whole blood was collected into EDTA tubes (BD Vacutainer, Franklin Lakes NJ, USA) and plasma obtained by centrifugation at 3000 rpm, 4°C, 15 minutes, prior to a second centrifugation at 12600 g, 4°C for 10' and storage at −80°C for subsequent analysis. Aliquots of plasma from the samples were thawed only once. We estimated cell and hemolysis contamination in our plasma samples by: 1. eye judgement checking the sample against a colorimetric scale, 2. comparing the levels of a miRNA highly expressed in red blood cells (hsa-miR-451a) and one unaffected by hemolysis (hsa-miR-23a-3p) (27). In all our samples we have found the ΔCt (miR-23a-3p - miR-451a) is smaller than five, showing the absence of hemolysis.

WAT Samples and Isolation of Adipocyte Fraction (AF) and Stromal Vascular Fraction (SVF)

Biopsies of SAT were obtained during elective surgery and one aliquot promptly frozen into liquid nitrogen and stored at -80°C. Fresh SAT was sub-fractionated into SVF and AF as previously described (28). Briefly, the subcutaneous WAT biopsy obtained during elective abdominal surgery was cut in little pieces and incubated 1 hour at 37°C with 2 mg/ml collagenase Type 1 (Sigma-Aldrich, St. Louis, MO, USA). The digestion was stopped by adding 3 volumes of DMEM completed with 10% FBS, then the homogenate was filtered through a 100 "mesh. The filtrate was then centrifuged 1,000 g for 5 min at RT in order to separate AF in the upper phase and SVF in the lower phase. The two cell fractions were separately collected in different tubes for further processing.

RNA Isolation, cDNA Synthesis and MiRNA Quantification

cmiRs were extracted from 200 µL aliquots of plasma using a miRNeasy Serum/Plasma Kit (Qiagen, Hilden, Germany), following the manufacturer's protocol. During the extraction process 3.5 µl (1.6 × 108 copies/µl) of C. elegans'miR-39 miRNA mimic spike-in control (cel-miR-39) was added to monitor the RNA isolation before purification. miRNAs were isolated from tissues using a miRNeasy micro Kit (Qiagen, Hilden, Germany) following the manufacturer's protocol. The quality and integrity of RNA samples were evaluated using a RNA 6000 Nano LabChip on an Agilent 2100 Bioanalyzer (Santa Clara, CA, USA). RNA eluted in RNase-free water was stored at −80°C until use.

3.75ul of RNA extracted from plasma and 500ng of RNA extracted from cells were reverse transcribed using Mir-X miRNA First-Strand Synthesis Kit (Takara, Mountain View, California, USA) following the manufacturer's protocol. cDNA templates were then diluted 4X and 20X respectively in nuclease free water and 1ul were used in qPCR reactions. qPCR was performed using SYBR Green-based technology.

For normalization of miRNA expression: in plasma samples the exogenous spike-in control cel-miR-39 was measured by means of cel-miR-39 miScript Primer Assays (Qiagen); in all the other samples the expression of small nuclear RNA U6 served as control of equal loading (U6 Forward and Reverse Primers from Takara).

The ΔΔCt comparative method was used for data analysis and measurements with cycles greater than 36 were considered undetectable. miRNA values were expressed using the following procedure: in each case the mean of the control group was calculated and each value was then divided by that number and multiplied by 100.

A list of forward primers used for qPCR detection and their sequence is provided below.

hsa-miR-320a-3p 5'-AAAAGCTGGGTTGAGAGGGCGA-3'
hsa-miR-320b 5'-AAAAGCTGGGTTGAGAGGGCAA-3'
hsa-miR-320c 5'-AAAAGCTGGGTTGAGAGGGT-3'
hsa-miR-320d 5'-AAAAGCTGGGTTGAGAGGA-3'
hsa-miR-320e 5'-AAAGCTGGGTTGAGAAGG-3'

The reverse primer (mRQ) was included in the Mir-X™ miRNA First-Strand Synthesis Kit (Takara, #638313) and its sequence is patent pending.

Gene Ontology Analysis

Target gene prediction for 320 miRNAs was performed using miRDB with a target score cut off set at 60. The identified proteins were ranked according to their prediction score and analyzed through Gene Ontology enrichment analysis and visualization tool GOrilla, publicly available as a web-based application at: http://cbl-gorilla.cs.technion.ac.il, which uses a statistical model that supports the discovery of GO terms enriched at the top of a ranked list, enabling a threshold to be determined in a data driven manner and providing an exact p-value for the observed event. GOrilla output is a series of GO terms associated to a P value, an FDR and an enrichment score, where p-value for the observed enrichment is calculated taking threshold multiple testing into account; FDR q-value is the correction of the above p-value for multiple testing using the Benjamini and Hochberg (1995) (29) method.

Enrichment (N, B, n, b) is defined as follows:

N - is the total number of genes

B - is the total number of genes associated with a specific GO term

n - is the number of genes in the top of the user's input list or in the target set when appropriate

b - is the number of genes in the intersection

Enrichment=(b/n)/(B/N) (30)

IPA (Qiagen, Hilden, Germany) was employed to establish the network among proteins (as identified by GOrilla) and to graphically elaborate this information.

Laboratory Tests

Venous blood samples were obtained after an overnight fasting for measurement of serum glucose, HbA1c, triglycerides, total cholesterol, LDL-C, HDL-C, CRP, ALT, AST, GGT. Serum leptin was measured by enzyme-linked immunosorbent assay (ELISA) (Mediagnost, Germany).

Statistics

Statistical analysis was performed using GraphPad Prism 8 software. Student's t-test or Mann–Whitney test were used for pair comparisons for normally or not normally distributed data, as appropriate. Parametric One-way ANOVA followed by Bonferroni *post-hoc* test or Kruskal-Wallis followed by Dunn's Multiple Comparison test were respectively used for normally or not normally distributed data. Non-parametric correlation analysis (Spearman) was performed. $P<0.05$ was considered statistically significant.

RESULTS

MiRs From 320 in LD

To substantiate the rational of our study, i.e. analysis of miRs-320 in LD, we first wanted to confirm their expression in WAT. To this end we used biopsies from 3 subjects for whom we could establish the presence of miRs-320 in intact SAT and in both the Adipocyte and Stromal Vascular Fraction (AF and SVF). As a measure of miRNA abundance for each sample we calculated the delta Ct between the miRNA of interest and U6, a small nuclear RNA, that for its stability and relatively high expression, is widely used as internal reference gene for miRNA quantification (31): as shown in **Figure 1B** delta Cts are always <8, indicating that both WAT fractions may be sources of miRs-320. We next wanted to better characterize their expression in LD.

MiRs-320 were then analyzed in the plasma of patients with or without LD. As shown in **Figure 2A** studies conducted by quantitative PCR in a cohort of healthy controls and affected patients (23 HC vs 32 LD, see clinical characteristics in **Table 1**) proved that cmiRs 320 were differentially expressed in LD versus HC. In the case of miR-320d the circulating levels were lower in LD as compared to HC; in all the other cases (miR-320a-3p, 320b, 320c, 320e) there was a significant upregulation. Corresponding delta Ct values are also reported in **Supplementary Figure 1** (**SF 1**). To evaluate the relevance of the 5 miRNAs as biomarkers of LD, we conducted an analysis of Receiver Operating Characteristic (ROC) that revealed an area under the curve (AUC) ranging from 0.71 to 0.81, with p-values between 0.0001 and 0.007 (**SF 2A**). To improve the power of the classifier, we tried several combinations of the miRNAs delta Cts (Cts miR of interest – Cts Cel-miR-39) as a possible discriminating measure between HC and LD: the sum of the measure concerning miR-320a-3p, miR-320b, miR-320c and miR-320e was the best solution providing an AUC of 0.85 ($P < 0.0001$). The optimal cut-off point of the combination was determined as being ≤24.48 (sensitivity: 75.00; specificity: 85.71) (**SF 2B**).

We then wanted to investigate if in the different subtypes included in the large cohort of LD patients the differences in cmiRs 320 were confirmed. To this end we considered 3 subtypes: CGL, FPL and APL. For all the comparisons we confirmed differences with the same sign found in whole cohort which in most cases (except 2) were significant. Within these 3 categories, the capacity of cmiRs-320 to act as disease classifier is more powerful for CGL (**Figure 2B**; **Supplementary Table 1**, **ST 1**). Multiple comparison analysis (one-way ANOVA) revealed no significant differences among LD subtypes for cmiRs-320. In the analyses presented so far we did not include subjects with Familial Partial LD, type 1 (FPLD1 or Köbberling): the reason is that they show significantly higher age and BMI compared to the rest of the LD cohort and required an *ad-hoc* group of properly matched controls (Adult Healthy Controls, AHC, clinical characteristics of FPLD1 and AHC in **ST 2**). In **Figure 2C** the analysis of cmiRs-320 in FPLD1 subjects are reported next to the analysis for FPLD2, or Dunnigan. As for FPLD1 subtype, there is no specific candidate gene and a polygenic mode of inheritance has been postulated (32)

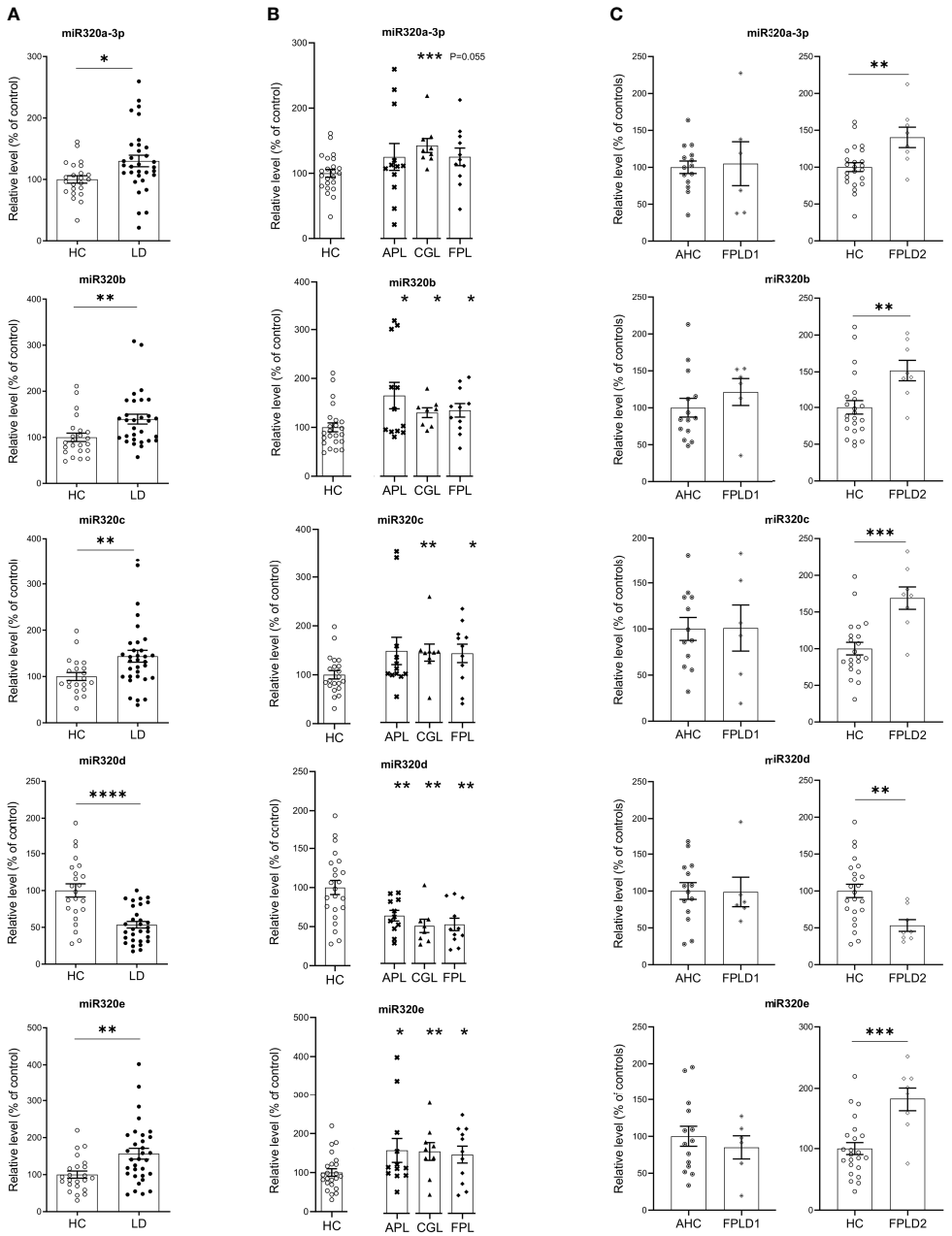

	APL (n=12)	CGL (n=9)	FPL (n=11)
Estimated prevalence	$0.5x10^{-6}$-10^{-5}	10^{-7}	$3x10^{-6}$-10^{-5}
WAT loss	partial	generalized	partia
Origin	acquired	inherited	inherited
Mode of inheritance	-	autosomal recessive	autosomal dominant (variable penetrance)
Metabolic derangements	often present	severe	present, variable severity
Age at onset	variable	birth	puberty /adulthood

	FPLD1 (n=6)	FPLD2 (n=8)
Estimated prevalence	unknown	>500 cases reported
WAT loss	partial	partial
Site of WAT loss	extremities	extremities, buttocks, hips
WAT accumulation	abdomen	Face, neck
Gene defects	unknown	LMNA
Metabolic derangements	variable	variable
Age of onset	variable.	puberty

FIGURE 2 | Relative level of cmiRs-320 in LD and HC subjects. **(A)** Scatter plots with error bar of cmiRs 320 in a) LD (n = 32) versus HC (n = 23). **(B)** in APL (n = 12), CGL (n = 9), FPL (n = 11) versus HC. Each asterisk denotes a pairwise comparison of 2 groups. **(C)** FPLD1 (*n* = 6) versus an *ad-hoc* selected group of age matched controls Adult Healthy Controls (AHC) (*n* = 14) and FPLD2 (*n* = 8) versus HC. Data, expressed as percentage of the mean of HC or AHC (in the case of FPLD1), are shown as mean ± SEM (standard error of the mean). *$P < 0.05$, **$P < 0.01$, ***$P < 0.001$, ****$P < 0.0001$, by Student's t test or Mann-Whitney as appropriate.

for a phenotype with a wide spectrum and consequent challenging diagnosis, that presents with reduction of fat in the extremities and accumulation in the central part of the body, similar to visceral obesity. FPLD2, on the other hand, collects individuals with a defect in the gene coding for *lamin A/C*, characterized by dramatic loss of fat at the extremities/trunk and typical accumulation around the neck (33). Symptoms manifestation usually starts after puberty (4), metabolic derangements are present with variable degree of severity. Of interest, all cmiRs-320 significantly discriminate FPLD2 subjects from HC; conversely FPLD1 subjects are overlapping with AHC in all cases (**Figure 2C**; **ST 1**).

Alltogether these results indicate cmiRs-320 as an additional tool to mark the LD disorder and reiterate the importance of considering each LD subtype as a different condition of WAT dysfunction.

Relationship Between CmiRs-320 and Metabolism

Our effort was then to understand the role of the metabolic derangements often affecting LD subjects in driving cmiRs-320 dysregulation. As dysmetabolism found in LD reminds that associated to obesity, we analyzed the concentration of cmiRs-320 in the plasma of a cohort of subjects with obesity (OB), displaying lipid and hepatic profiles similar to those with LD (**Table 1**), and we reasoned that if altered metabolism drives cmiRs-320 abundance, similar changes should be observed in LD and OB with respect to HC. In 3 cases (320b, c, e) the OB group shows a trend similar to LD, when compared to HC, albeit no statistically significant; in the case of miRs-320a-3p we found a change of opposite sign in LD and OB (**Figure 3A**). As a second approach we investigated the relationship between cmiRs-320 and clinical parameters relevant in defining the metabolic profile. Correlation analysis performed for the total population (LD + OB + HC) indicates that miR320a-3p shows the highest number of significant associations and it is inversely related to BMI, glucose, HbA1c, total cholesterol, low density lipoprotein-cholesterol (LDL-C) and leptin (**Figure 3B** and **Table 2**), whereas miR320d is the only member of family 320 showing significant and inverse relationships with the 3 hepatic enzymes gamma-glutamyl transferase (GGT), aspartate aminotransferase (AST), alanine aminotransferase (ALT), and with C-reactive protein (CRP). Similar analyses were performed for all the other miRNAs and the results are shown in **Table 2**.

Gene Ontology and Pathway Analysis

To search for a biological significance of these findings and investigate the involvement of specific regulatory networks, we performed the *in silico* prediction of target genes possibly modulated by miRNA 320s by integrating the use of the publicly available applications miRDB and TargetScan. Gene ontology (GO) enrichment analysis was performed on targets by using GOrilla, a web-based application, that identifies enriched GO terms for biological processes in ranked lists of genes. Highly significant GO terms associated to biological processes were identified, including: homophilic cell adhesion *via* plasma membrane adhesion molecules (P = 5.97E-10, false discovery rate, FDR, 3.93E-6); cell-cell adhesion *via* plasma membrane adhesion molecules (P = 6.31E-8, FDR 2.08E-4); nervous system development (P = 8.82E-6, FDR 1.93E-2); cell-cell adhesion (P = 1.66E-5, FDR 2.74E-2); biological adhesion (P = 2.89E-5, FDR 3.8E-2). In **Figure 4A** a graphical output of this result. A comprehensive Table showing the detail of these *in silico* results is shown as **ST 3**. **Figure 4B** shows the 320 miRNAs target proteins interaction network. The classes of proteins mostly represented are membrane and adhesion proteins: among others, gamma protocadherins constitute a substantial proportion of the protein forming the network and are highly interrelated.

In silico analysis suggests that miRs-320 target proteins which are highly aggregated in defining the capacity of cells to build contacts, and strengthen the architecture of tissues.

DISCUSSION

MiRNAs are necessary to maintain WAT homeostasis as demonstrated in experimental animal models, and LD conditions associated to HIV result in their altered production

TABLE 1 | Physical and clinical parameters of subjects enrolled in the study*.

Physical and clinical parameters	Controls (*N* = 23; F = 16)	LD (w/o FPLD1) (*N* = 32; F = 24)	Obese (*N* = 13; F = 8)	Multiple Comparisons Result
Age (years)	34.5 ± 3.9	35.0 ± 3.4	49.1 ± 3.5	ns
BMI (Kg/m^2)	21.2 ± 0.6	20.6 ± 0.7	43.5 ± 1.7	a ns; b ****; c ****
Glucose (mg/dL)	91.0 ± 2.0	94.0 ± 3.3	111.7 ± 7.3	ns
TG (mg/dL)	80.8 ± 9.2	153.6 ± 27.3	154.1 ± 13.4	a **; b ***; c ns
Chol (mg/dL)	180 ± 7.6	169.8 ± 5.7	198.8 ± 10.0	a ns; b ns; c *
HDL-C (mg/dL)	65.4 ± 3.7	45.25 ± 2.7	47.5 ± 3.2	a ***; b *; c ns
LDL-C (mg/dL)	106.3 ± 7.1	113.7 ± 5.2	137.7 ± 8.7	a ns; b *; c ns
CRP (mg/L)	0.05 ± 0.01	0.7 ± 0.2	0.88 ± 0.16	a **; b ****; c ns
AST/GOT (U/L)	18.8 ± 0.8	28.1 ± 2.1	36.4 ± 7.3	a**; b*; c ns
ALT/GPT (U/L)	13.5 ± 1.0	34.4 ± 4.6	55.9 ± 13.3	a****; b****; c ns
GGT (U/L)	11.8 ± 1.4	28.4 ± 4.1	59.3 ± 16.0	a **; b****; c ns
LD Subtype		11 FPL (of which 8 FPLD2) 12 APL 9 CGL		

*a = Controls vs. LD; b= Controls vs. Obese; c = LD vs. Obese. *P < 0.05, **P < 0.01, ***P < 0.001, ****P < 0.0001. Data are expressed as Mean ± SEM. ns, not significant.*

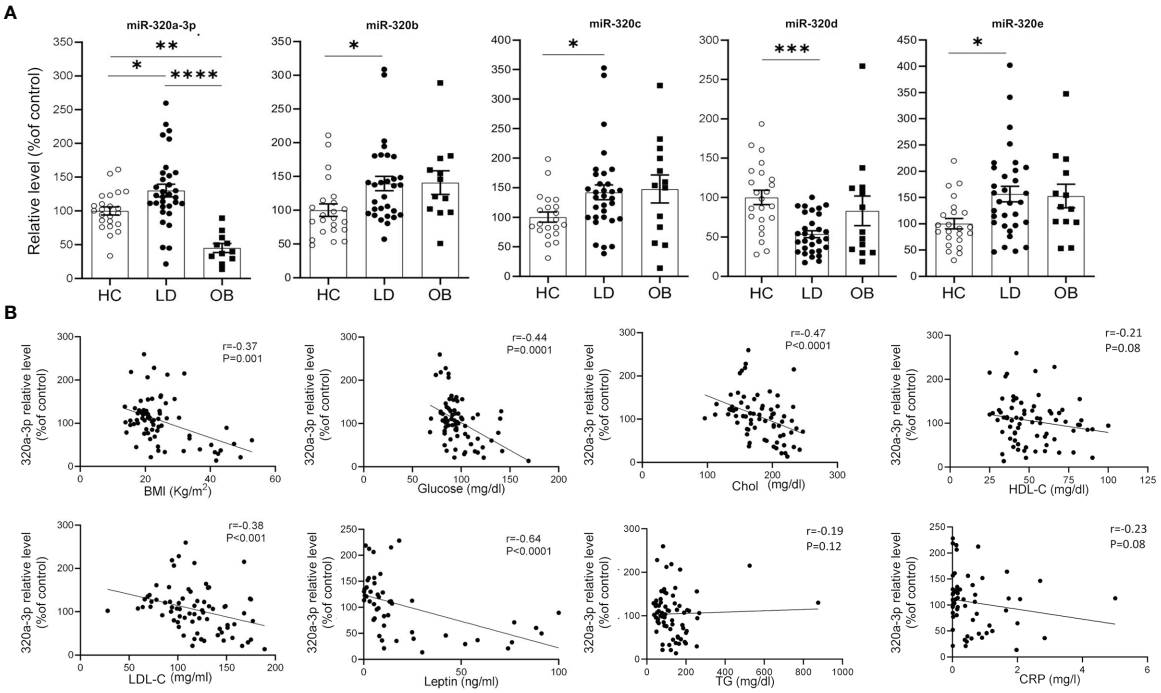

FIGURE 3 | Relationship between cmiRs-320s and metabolism. **(A)** Scatter plots with bar of circulating miRNAs from the 320 family in HC, LD and OB subjects. All data are expressed as percentage of the mean of HC and are shown as mean ± SEM. *$P < 0.05$, **$P < 0.01$, ***$P < 0.001$ and ****$P < 0.0001$ by one-way ANOVA or Kruskal-Wallis, as appropriate. **(B)** Correlation analysis between BMI, glucose, total cholesterol, HDL-C, LDL-C, plasma leptin, triglycerides, CRP and cmiRs-320a-3p in the total population (LD + OB + HC). Spearman's r and relative p-value are indicated.

and release (13, 18). Based on these lines of evidence we wanted to investigate if in different forms of human LD, of genetic or acquired origin, with partial or total loss of WAT, signatures of the disease may be tracked in the blood as variations in the level of circulating miRNAs. Indeed, we found a dysregulation of the miR-320 family, reportedly present in WAT (24) and implied as permissive for adipogenesis of human mesenchymal stem cells (34), however not previously associated to *in vivo* conditions of adipocyte dysfunction. In this regard it is worth observing that when plasma miRnome profiling was conducted in subjects with HIV-associated LD *versus* controls, cmiRs 320 were not identified as dysregulated (35). Even if both associated to fat loss the HIV-related and not related forms of LD are profoundly different; in addition, subjects enrolled in that study did not show significant metabolic alterations, differently from our cohort. Furthermore, our findings suggest that cmiRs 320 discriminate more powerfully LD subtypes with a known genetic origin and defined phenotype (i.e. CGL and FPLD2) than forms with an unknown origin and subtle phenotype: it is thus somewhat expected that in HIV-associated forms of LD, highly variable in terms of fat loss and redistribution, cmiRs 320 may not be significantly dysregulated.

Interestingly, we found that miRs-320 a3p, b, c and e are elevated, whereas d is reduced in LD. While we are not able to

TABLE 2 | Results of correlation analysis for clinical parameters with relative levels of cmiRs-320.

Names and metric units of clinical parameters	320a-3p	320b	320c	320d	320e
BMI (Kg/m^2)	-0.37**	ns	ns	ns	ns
Glucose (mg/dl)	-0.44***	ns	-0.29*	ns	-0.25*
HbA1c (mmol/mol)	-0.37*	-0.29*	ns	ns	-0.36*
TG (mg/dl)	ns	ns	ns	ns	ns
Chol (mg/dl)	-0.47****	ns	-0.24*	ns	-0.32**
HDL-C (mg/dl)	ns	-0.32**	ns	ns	-0.24*
LDL-C (mg/dl)	-0.38***	ns	ns	ns	ns
Leptin (ng/ml)	-0.64****	ns	ns	ns	ns
CRP (mg/dl)	ns	ns	ns	-0.33*	ns
GGT (U/L)	ns	ns	ns	-0.24*	ns
AST/GOT (U/L)	ns	ns	ns	-0.35**	ns
ALT/GPT (U/L)	ns	ns	ns	-0.35**	-0.25*

*Correlation analysis was assessed in the total population (LD + OB + HC). The Table reports Spearman r and *P < 0.05, **P < 0.01, ***P < 0.001, ****P < 0.0001, ns significant.*

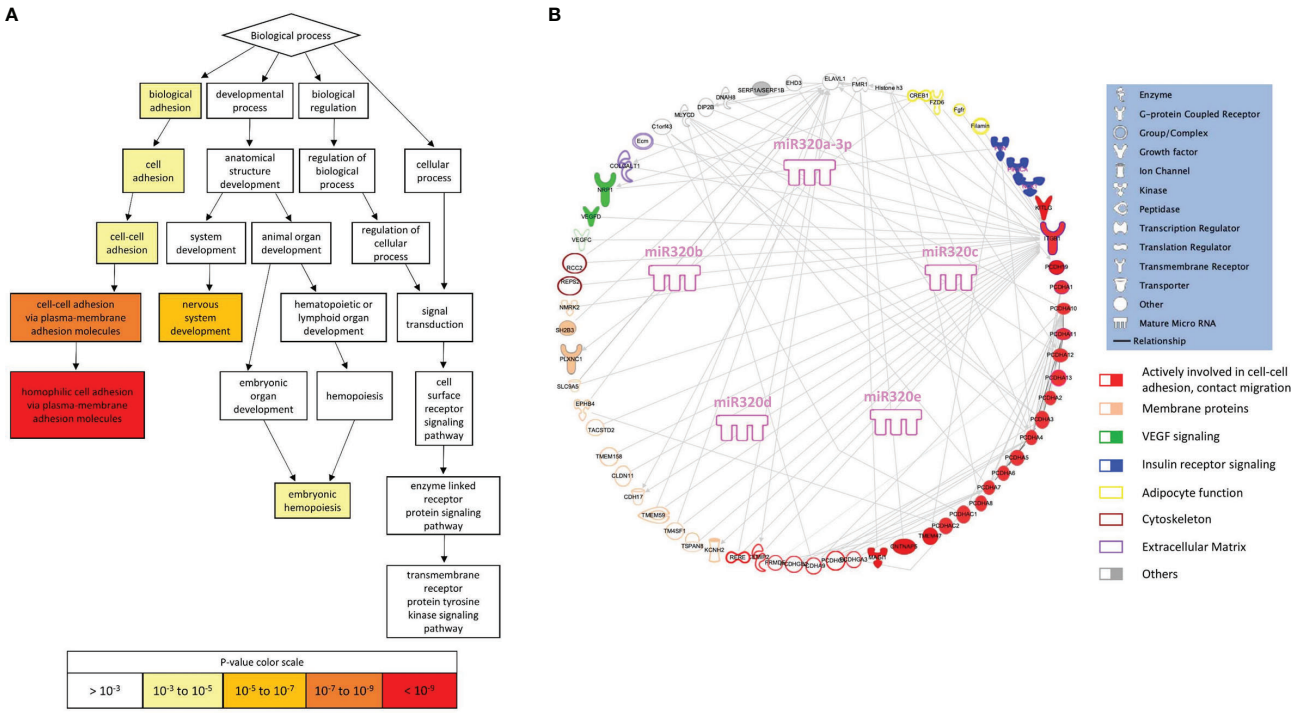

FIGURE 4 | Gene ontology and pathway analysis. **(A)** Visualization of enriched GO terms for a ranked list of 320 miRNA targets (from the publicly available platform GOrilla). The white to red scale indicates progressively increased significance of the enrichment. **(B)** Graphical representation of the network generated by the proteins included in the enriched GO terms (elaborated using IPA, Qiagen, Hilden, Germany).

predict the consequences of this opposite regulation, it is worth mentioning that in at least one case, miRNA family 200, different members have opposite effects on their target *c-JUN*, with miR-200a inhibiting its production and miR-200b acting in non-canonical way and inducing its expression (36): we cannot exclude a similar scenario for miRNAs 320. Elaborating on the same subject we also have to consider that the five 320 members (a-e), are coded by loci in different chromosomes (chr) (320a, chr8; 320b, chr1; 320c, chr18; 320d, chr13 and chrX; 320e, chr19 and therefore their transcription is under the control of 6 independent cis regulatory elements: of note miR-320d is the only coded by 2 loci in 2 different chromosomes (X and 13) (37, 38).

Despite the high degree of speculation that elaborating on altered concentrations of circulating miRNAs may involve, we will herein discuss different levels of direct and less direct implications suggested by the LD-related changes in the cmiRs-320.

The first level stems from the use of cmiRs-320 as novel biomarkers of LD. The power to discriminate between affected and not affected individuals becomes even stronger for the specific subtypes CGL and FPLD2, that, although different in terms of extension of fat loss, share the certainty of the diagnosis based on well-defined phenotypes and genetic testing. At the other extreme FPLD1, for which cmiRs-320 seem totally useless as classifier. Despite recurrent in families, a genetic cause of FPLD1 has yet to be identified and subjects described in previous studies are usually women in their mature age, characterized by peripheral LD, and one or more of the following features: central obesity and components of the metabolic syndrome, including diabetes, hypertension, and presence of hypertriglyceridemia (39). Consistent with this description the average BMI of FPLD1 subjects participating to this study defines them as overweight. Compared to the other subtypes, FPLD1 presents then with a more subtle phenotype, which in the clinical setting may partly overlap with the physiological loss of gluteofemoral fat frequent upon aging (40) and, for other aspects, with metabolically complicated obesity (32, 41). In summary, the discrepancy with the other LD subtypes emerged from the present analysis of cmiRs-320 is not a *unicum* but adds up to other features in describing FPLD1 as an atypical (less defined) form of LD.

The second question is whether cmiRs 320 differential level is downstream of metabolic derangements present in LD, that mirror obesity-associated metabolic syndrome. The fact that for 1 out of 5 miRNAs (320a-3p) the sign of the regulation with respect to control is opposite in LD and OB suggests that dysmetabolism may contribute, but is not sufficient to explain the change. One other way to elaborate on this aspect is to evaluate if metabolic syndrome signatures of LD subjects, namely, higher TG, CRP and hepatic enzymes and lower HDL-C, consistently associate to the sign of change of cmiRs-320. Given that cmiRs-320, except d, are higher in LD we would expect a positive association with metabolic/inflammatory parameters if the latter served as a trigger for their elevation. What we found, instead, is that where present, significant relationships were inverse. There are 2 cases, however, in which we could hypothesize an impact of

dysmetabolism on cmiRs. These are represented by the relationship between cmiR-320b negatively associated to HDL-C, and that between cmiR-320d, which, being downregulated in LD, is inversely associated to the concentration of hepatic enzymes and of CRP. In line with our results, lower level of serum exosomal miR-320d was found in hepatocellular carcinoma (42). Based on these evidences, dyslipidemia seems then to moderately contribute to the LD associated dysregulation of cmiR-320 b, while liver dysfunction and inflammation, abundantly interrelated conditions (43), seem to predict the downregulation of cmiR-320d.

Of note miR-320a-3p, besides showing the highest number of inverse relationships with clinical parameters, is also inversely related to BMI and plasma leptin. Notwithstanding the tight relationship between the 2 parameters (44), to consider is that both reflect WAT mass, while leptin is also tightly related to WAT function (44, 45). Circulating levels of miR-320a-3p predict therefore the salient aspects of the disease, i.e. reduced WAT mass and function.

A third interesting level of speculation emerges from gene ontology search, carried out on miRs-320 targets: there are in fact strong and highly significant indications that cell-cell adhesion and migration are modulated by proteins targeted by these miRNAs, including integrin 1 beta (ITG1B) and several protocadherins. Noteworthy, the expression of ITG1B in WAT is positively associated with body fat mass in humans (46), consistent with a putative downregulation in LD, possibly triggered by the upregulation of miRs-320. Integrins, which act also as receptors and constitute the most well studied molecules in the organization of the extra cellular matrix (ECM) (47), reside at the cell surface and require inside-out activation to reach a higher affinity for the ECM components. This activation process is facilitated by binding of intracellular adaptor proteins like Kindlin. ITG1B deletion specifically in adipocytes reduced capacity to increase WAT mass in mice exposed to high fat diet (46). Even more compelling evidences indicate *kindlin* as implied in a correct WAT function, as its deletion in the adipocyte leads to a mouse model with LD and severe metabolic alterations (48). These findings and our *in silico* data stimulate considerations on the role that an impaired cell-cell adhesion, migration and cross talk might have in the onset of human LD, a condition in which the WAT loses its architecture and undergoes a process of deaggregation and sometimes redistribution. Ground to this hypothesis is provided by the decrease in the expression of many genes involved in cell adhesion observed in 3T3-L1 adipocytes treated with ritonavir and lopinavir (49), two protease inhibitors used to treat HIV infected patients and implied in the onset of the HIV-associated form of LD (50).

This study has some limitations and questions that remain to be addressed: 1. relatively small number of recruited patients, due to the low prevalence of LD and of its subtypes; 2. no direct biological evidence to link cmiRs-320 dysregulation with LD pathogenesis and 3. The source/s of dysregulated cmiRs-320 are to be elucidated. Although they may originate from dysfunctional WAT, it is counterintuitive to reconcile increase of cmiRs-320 with dramatic fat loss, for instance in the CGL subtype. Our data, however, suggest that the stromovascular component of the adipose tissue, preserved also in the extreme generalized forms of LD (51, 52), may contribute to their release and availability of WAT biopsies from LD subjects will be essential to get insights into this matter.

In conclusion, altered abundance of circulating levels of miRNAs from 320 family constitutes a novel signature of lipodystrophy. cmiRs-320 are inversely associated with several components of the metabolic syndrome and higher abundance of cmiR-320a-3p, typical of LD, predicts lower plasma leptin. *In silico* results indicate that targets of miRs-320 influence cell-cell adhesion, thus suggesting this process as a novel direction to investigate the origin of LD.

DATA AVAILABILITY STATEMENT

The original contributions presented in the study are included in the article/**Supplementary Material**. Further inquiries can be directed to the corresponding author.

ETHICS STATEMENT

The studies involving human participants were reviewed and approved by CEAVNO, protocol number D 19440 . Written informed consent to participate in this study was provided by the participants' legal guardian/next of kin.

AUTHOR CONTRIBUTIONS

Conceptualization and study design, MMaf. Methodology, MMaf, AD, GSc, RC, MMas, and MC. Investigation, AD, GSc, LQ, and MC. Formal analysis, MMaf, AD, and GSc. Resources, MMaf, FS, AD, GC, SM, GSa, GG, AG, CP, LM, DG, and GSc. Writing original draft preparation, MMaf. Writing review and editing, AD, GSc, GC, FS, and MC. Supervision, MMaf and MC. Funding acquisition, MMaf, AD, and FS. All authors contributed to the article and approved the submitted version.

FUNDING

This research was funded by Italian Ministry of Education, University and Research, Project code 2017L8Z2EM to FS.

ACKNOWLEDGMENTS

We thank the patients and their families for their willingness to participate in this study. The Obesity and Lipodystrophy Center at the University Hospital of Pisa is part of the European Reference Networks EndoERN and MetabERNs.

SUPPLEMENTARY MATERIAL

The Supplementary Material for this article can be found online at: https://www.frontiersin.org/articles/10.3389/fendo.2022.866679/full#supplementary-material

REFERENCES

1. Brown RJ, Araujo-Vilar D, Cheung PT, Dunger D, Garg A, Jack M, et al. The Diagnosis and Management of Lipodystrophy Syndromes: A Multi-Society Practice Guideline. *J Clin Endocrinol Metab* (2016) 101(12):4500–11. doi: 10.1210/jc.2016-2466
2. Araújo-Vilar D, Santini F. Diagnosis and Treatment of Lipodystrophy: A Step-by-Step Approach. *J Endocrinol Invest* (2019) 42(1):61–73. doi: 10.1007/s40618-018-0887-z
3. Xu S, Zhang X, Liu P. Lipid Droplet Proteins and Metabolic Diseases. *Biochim Biophys Acta - Mol Basis Dis* (2018) 1864(5):1968–83. doi: 10.1016/j.bbadis.2017.07.019
4. Akinci B, Onay H, Demir T, Savas-Erdeve Ş, Gen R, Simsir IY, et al. Clinical Presentations, Metabolic Abnormalities and End-Organ Complications in Patients With Familial Partial Lipodystrophy. *Metabolism* (2017) 72:109–19. doi: 10.1016/j.metabol.2017.04.010
5. Misra A, Garg A. Clinical Features and Metabolic Derangements in Acquired Generalized Lipodystrophy. *Med (Baltimore)* (2003) 82(2):129–46. doi: 10.1097/00005792-200303000-00007
6. Garg A, Misra A. Lipodystrophies: Rare Disorders Causing Metabolic Syndrome. *Endocrinol Metab Clin North Am* (2004) 33(2):305–31. doi: 10.1016/j.ecl.2004.03.003
7. Özen S, Akıncı B, Oral EA. Current Diagnosis, Treatment and Clinical Challenges in the Management of Lipodystrophy Syndromes in Children and Young People. *J Clin Res Pediatr Endocrinol* (2020) 12(1):17–28. doi: 10.4274/jcrpe.galenos.2019.2019.0124
8. Hussain I, Garg A. Lipodystrophy Syndromes. *Endocrinol Metab Clin North Am* (2016) 45(4):783–97. doi: 10.1016/j.ecl.2016.06.012
9. Lim K, Haider A, Adams C, Sleigh A, Savage D. Lipodystrophy: A Paradigm for Understanding the Consequences of "Overloading" Adipose Tissue. *Physiol Rev* (2020) 101:907–93. doi: 10.1152/physrev.00032.2020
10. Cinti S. The Adipose Organ at a Glance. *Dis Model Mech* (2012) 5(5):588–94. doi: 10.1242/dmm.009662
11. Patni N, Li X, Adams-Huet B, Vasandani C, Gomez-Diaz RA, Garg A. Regional Body Fat Changes and Metabolic Complications in Children With Dunnigan Lipodystrophy-Causing LMNA Variants. *J Clin Endocrinol Metab* (2019) 104(4):1099–108. doi: 10.1210/jc.2018-01922
12. Sun L, Xie H, Mori MA, Alexander R, Yuan B, Hattangadi SM, et al. Mir193b-365 is Essential for Brown Fat Differentiation. *Nat Cell Biol* (2011) 13(8):958–65. doi: 10.1038/ncb2286
13. Mori MA, Thomou T, Boucher J, Lee KY, Lallukka S, Kim JK, et al. Altered miRNA Processing Disrupts Brown/White Adipocyte Determination and Associates With Lipodystrophy. *J Clin Invest* (2014) 124(8):3339–51. doi: 10.1172/JCI73468
14. Xu D, Sun L. Role of microRNA Biogenesis in Adipocyte and Lipodystrophy. *Adipocyte* (2015) 4(3):222–4. doi: 10.1080/21623945.2014.995507
15. Kim H-J, Cho H, Alexander R, Patterson HC, Gu M, Lo KA, et al. MicroRNAs Are Required for the Feature Maintenance and Differentiation of Brown Adipocytes. *Diabetes* (2014) 63(12):4045–56. doi: 10.2337/db14-0466
16. Chen X, Ba Y, Ma L, Cai X, Yin Y, Wang K, et al. Characterization of microRNAs in Serum: A Novel Class of Biomarkers for Diagnosis of Cancer and Other Diseases. *Cell Res* (2008) 18(10):997–1006. doi: 10.1038/cr.2008.282
17. Valadi H, Ekström K, Bossios A, Sjöstrand M, Lee JJ, Lötvall JO. Exosome-Mediated Transfer of mRNAs and microRNAs Is a Novel Mechanism of Genetic Exchange Between Cells. *Nat Cell Biol* (2007) 9(6):654–9. doi: 10.1038/ncb1596
18. Thomou T, Mori MA, Dreyfuss JM, Konishi M, Sakaguchi M, Wolfrum C, et al. Adipose-Derived Circulating miRNAs Regulate Gene Expression in Other Tissues. *Nature* (2017) 542(7642):450–5. doi: 10.1038/nature21365
19. Squillace N, Bresciani E, Torsello A, Bandera A, Sabbatini F, Giovannetti C, et al. Changes in Subcutaneous Adipose Tissue microRNA Expression in HIV-Infected Patients. *J Antimicrob Chemother* (2014) 69(11):3067–75. doi: 10.1093/jac/dku264
20. Jiménez-Lucena R, Rangel-Zúñiga OA, Alcalá-Díaz JF, López-Moreno J, Roncero-Ramos I, Molina-Abril H, et al. Circulating miRNAs as Predictive Biomarkers of Type 2 Diabetes Mellitus Development in Coronary Heart Disease Patients From the CORDIOPREV Study. *Mol Ther - Nucleic Acids* (2018) 12:146–57. doi: 10.1016/j.omtn.2018.05.002
21. Cho WCS. MicroRNAs: Potential Biomarkers for Cancer Diagnosis, Prognosis and Targets for Therapy. *Int J Biochem Cell Biol* (2010) 42(8):1273–81. doi: 10.1016/j.biocel.2009.12.014
22. Munetsuna E, Yamada H, Ando Y, Yamazaki M, Tsuboi Y, Kondo M, et al. Association of Subcutaneous and Visceral Fat With Circulating microRNAs in a Middle-Aged Japanese Population. *Ann Clin Biochem Int J Lab Med* (2018) 55(4):437–45. doi: 10.1177/0004563217735124
23. Ling H-Y, Ou H-S, Feng S-D, Zhang X-Y, Tuo Q-H, Chen L-X, et al. CHANGES IN microRNA (Mir) PROFILE AND EFFECTS OF miR-320 IN INSULIN-RESISTANT 3t3-L1 ADIPOCYTES. *Clin Exp Pharmacol Physiol* (2009) 36(9):e32–9. doi: 10.1111/j.1440-1681.2009.05207.x
24. Liu L, Li X. Downregulation of miR-320 Alleviates Endoplasmic Reticulum Stress and Inflammatory Response in 3T3-L1 Adipocytes. *Exp Clin Endocrinol Diabetes* (2021) 129(02):131–7. doi: 10.1055/a-1012-8420
25. von Schnurbein J, Adams C, Akinci B, Ceccarini G, D'Apice MR, Gambineri A, et al. European Lipodystrophy Registry: Background and Structure. *Orphanet J Rare Dis* (2020) 15(1):17. doi: 10.1186/s13023-020-1295-y
26. Shrestha S, Hsu S-D, Huang W-Y, Huang H-Y, Chen W, Weng S-L, et al. A Systematic Review of microRNA Expression Profiling Studies in Human Gastric Cancer. *Cancer Med* (2014) 3(4):878–88. doi: 10.1002/cam4.246
27. Blondal T, Jensby Nielsen S, Baker A, Andreasen D, Mouritzen P, Wrang Teilum M, et al. Assessing Sample and miRNA Profile Quality in Serum and Plasma or Other Biofluids. *Methods* (2013) 59(1):51–6. doi: 10.1016/j.ymeth.2012.09.015
28. Scabia G, Cancello R, Dallanoce C, Berger S, Matera C, Dattilo A, et al. ICH3, a Selective Alpha7 Nicotinic Acetylcholine Receptor Agonist, Modulates Adipocyte Inflammation Associated With Obesity. *J Endocrinol Invest* (2020) 43(7):983–93. doi: 10.1007/s40618-020-01182-z
29. Benjamini Y, Hochberg Y. Controlling the False Discovery Rate: A Practical and Powerful Approach to Multiple Testing. *J R Stat Soc Ser B* (1995) 57(1):289–300. doi: 10.1111/j.2517-6161.1995.tb02031.x
30. Eden E, Navon R, Steinfeld I, Lipson D, Yakhini Z. GOrilla: A Tool for Discovery and Visualization of Enriched GO Terms in Ranked Gene Lists. *BMC Bioinformatics* (2009) 10:48. doi: 10.1186/1471-2105-10-48
31. Duan Z-Y, Cai G-Y, Li J-J, Bu R, Wang N, Yin P, et al. *U6 can be Used as a Housekeeping Gene for Urinary Sediment miRNA Studies of IgA Nephropathy* . Available at: www.nature.com/scientificreports/.
32. Guillín-Amarelle C, Sánchez-Iglesias S, Castro-Pais A, Rodriguez-Cañete L, Ordóñez-Mayán L, Pazos M, et al. Type 1 Familial Partial Lipodystrophy: Understanding the Köbberling Syndrome. *Endocrine* (2016) 54(2):411–21. doi: 10.1007/s12020-016-1002-x
33. Varlet A-A, Helfer E, Badens C. Molecular and Mechanobiological Pathways Related to the Physiopathology of FPLD2. *Cells* (2020) 9(9). doi: 10.3390/cells9091947
34. Hamam D, Ali D, Vishnubalaji R, Hamam R, Al-Nbaheen M, Chen L, et al. microRNA-320/RUNX2 Axis Regulates Adipocytic Differentiation of Human Mesenchymal (Skeletal) Stem Cells. *Cell Death Dis* (2014) 5(10):1947. doi: 10.1038/cddis.2014.462
35. Srinivasa S, Garcia-Martin R, Torriani M, Fitch KV, Carlson AR, Kahn CR, et al. Altered Pattern of Circulating miRNAs in HIV Lipodystrophy Perturbs Key Adipose Differentiation and Inflammation Pathways. *JCI Insight* (2021) 6(18). doi: 10.1172/jci.insight.150399
36. Del Vecchio G, De Vito F, Saunders SJ, Risi A, Mannironi C, Bozzoni I, et al. RNA-Binding Protein HuR and the Members of the miR-200 Family Play an Unconventional Role in the Regulation of *C-Jun* mRNA. *RNA* (2016) 22(10):1510–21. doi: 10.1261/rna.057588.116
37. Du H, Zhao Y, Yin Z, Wang DW, Chen C. The Role of miR-320 in Glucose and Lipid Metabolism Disorder-Associated Diseases. *Int J Biol Sci* (2021) 17(2):402–16. doi: 10.7150/ijbs.53419
38. McCreight JC, Schneider SE, Wilburn DB, Swanson WJ. Evolution of microRNA in Primates. *PloS One* (2017) 12(6):e0176596. doi: 10.1371/journal.pone.0176596
39. Herbst KL, Tannock LR, Deeb SS, Purnell JQ, Brunzell JD, Chait A. Kobberling Type of Familial Partial Lipodystrophy: An Underrecognized Syndrome. *Diabetes Care* (2003) 26(6):1819–24. doi: 10.2337/diacare.26.6.1819

40. Tchkonia T, Morbeck DE, Von Zglinicki T, Van Deursen J, Lustgarten J, Scrable H, et al. Fat Tissue, Aging, and Cellular Senescence. *Aging Cell* (2010) 9(5):667–84. doi: 10.1111/j.1474-9726.2010.00608.x
41. Donato AJ, Henson GD, Hart CR, Layec G, Trinity JD, Bramwell RC, et al. The Impact of Ageing on Adipose Structure, Function and Vasculature in the B6D2F1 Mouse: Evidence of Significant Multisystem Dysfunction. *J Physiol* (2014) 592(18):4083–96. doi: 10.1113/jphysiol.2014.274175
42. Li W, Ding X, Wang S, Xu L, Yin T, Han S, et al. Downregulation of Serum Exosomal miR-320d Predicts Poor Prognosis in Hepatocellular Carcinoma. *J Clin Lab Anal* (2020) 34(6):e23239. doi: 10.1002/jcla.23239
43. Valle-Martos R, Valle M, Martos R, Cañete R, Jiménez-Reina L, Cañete MD. Liver Enzymes Correlate With Metabolic Syndrome, Inflammation, and Endothelial Dysfunction in Prepubertal Children With Obesity. *Front Pediatr* (2021) 16:9. doi: 10.3389/fped.2021.629346
44. Maffei M, Giordano A. Leptin, the Brain and Energy Homeostasis: From an Apparently Simple to a Highly Complex Neuronal System. *Rev Endocr Metab Disord* (2021) 23:87–101. doi: 10.1007/s11154-021-09636-2
45. Lim K, Haider A, Adams C, Sleigh A, Savage DB. Lipodistrophy: A Paradigm for Understanding the Consequences of "Overloading" Adipose Tissue. *Physiol Rev* (2021) 101(3):907–93. doi: 10.1152/physrev.00032.2020
46. Ruiz-Ojeda FJ, Wang J, Bäcker T, Krueger M, Zamani S, Rosowski S, et al. Active Integrins Regulate White Adipose Tissue Insulin Sensitivity and Brown Fat Thermogenesis. *Mol Metab* (2021) 45. doi: 10.1016/j.molmet.2020.101147
47. Kechagia JZ, Ivaska J, Roca-Cusachs P. Integrins as Biomechanical Sensors of the Microenvironment. *Nat Rev Mol Cell Biol* (2019) 20(8):457–73. doi: 10.1038/s41580-019-0134-2
48. Gao H, Guo Y, Yan Q, Yang W, Li R, Lin S, et al. Lipoatrophy and Metabolic Disturbance in Mice With Adipose-Specific Deletion of Kindlin-2. *JCI Insight* (2019) 4(13). doi: 10.1172/jci.insight.128405
49. Adler-Wailes DC, Guiney EL, Koo J, Yanovski JA. Effects of Ritonavir on Adipocyte Gene Expression: Evidence for a Stress-Related Response. *Obesity* (2008) 16(10):2379–87. doi: 10.1038/oby.2008.350
50. Kolta S, Flandre P, Ngo Van P, Cohen-Codar I, Valantin M-A, Pintado C, et al. Fat Tissue Distribution Changes in HIV-Infected Patients Treated With Lopinavir/Ritonavir. Results of the MONARK Trial. *Curr HIV Res* (2011) 9 (1). doi: 10.2174/157016211794582687
51. Altay C, Secil M, Demir T, Atik T, Akinci G, Ozdemir Kutbay N, et al. Determining Residual Adipose Tissue Characteristics With MRI in Patients With Various Subtypes of Lipodystrophy. *Diagn Interv Radiol* (2017) 23 (6):428–34. doi: 10.5152/dir.2017.17019
52. Lee PL, Tang Y, Li H, Guertin DA. Raptor/mTORC1 Loss in Adipocytes Causes Progressive Lipodystrophy and Fatty Liver Disease. *Mol Metab* (2016) 5(6):422–32. doi: 10.1016/j.molmet.2016.04.001

Conflict of Interest: The authors declare that the research was conducted in the absence of any commercial or financial relationships that could be construed as a potential conflict of interest.

frontiers | Frontiers in Endocrinology

ORIGINAL RESEARCH
published: 10 June 2022
doi: 10.3389/fendo.2022.835154

Adipose Tissue Insulin Resistance Is Positively Associated With Serum Uric Acid Levels and Hyperuricemia in Northern Chinese Adults

Honglin Sun[1†], *Xiaona Chang*[1†], *Nannan Bian*[1], *Yu An*[1], *Jia Liu*[1], *Song Leng*[2*] *and Guang Wang*[1*]

[1] Department of Endocrinology, Beijing Chao-yang Hospital, Capital Medical University, Beijing, China, [2] Health Management Center, The Second Hospital of Dalian Medical University, Dalian, China

OPEN ACCESS

Edited by:
Dirk Müller-Wieland,
University Hospital RWTH Aachen,
Germany

Reviewed by:
Minxue Shen,
Central South University, China
Fengying Gong,
Peking Union Medical College Hospital (CAMS), China

***Correspondence:**
Guang Wang
wangguang@bjcyh.com
Song Leng
dllengsong@126.com

[†]These authors have contributed equally to this work

Specialty section:
This article was submitted to Obesity, a section of the journal Frontiers in Endocrinology

Received: 14 December 2021
Accepted: 04 May 2022
Published: 10 June 2022

Citation:
Sun H, Chang X, Bian N, An Y, Liu J, Leng S and Wang G (2022) Adipose Tissue Insulin Resistance Is Positively Associated With Serum Uric Acid Levels and Hyperuricemia in Northern Chinese Adults. Front. Endocrinol. 13:835154. doi: 10.3389/fendo.2022.835154

Objective: Adipose tissue plays a crucial role in serum uric acid (UA) metabolism, but the relative contribution of adipose tissue insulin resistance (IR) to serum UA levels and hyperuricemia have not explicitly been illustrated. Herein, we aimed to investigate the association between the adipose tissue insulin resistance index (Adipo-IR) and hyperuricemia in this cross-sectional study. The homeostasis model assessment of insulin resistance (HOMA-IR) index, another widely applied marker to determine systemic IR, was also explored.

Methods: A total of 5821 adults were included in this study. The relationship between Adipo-IR or HOMA-IR and serum UA levels was assessed by multivariate linear regression. Binary logistic regression analyses were applied to determine the sex-specific association of the Adipo-IR tertiles and HOMA-IR tertiles with hyperuricemia. Participants were then divided into normal BMI ($18.5 \leq BMI < 24$) and elevated BMI ($BMI \geq 24$) groups for further analysis.

Results: Both Adipo-IR and HOMA-IR were positively correlated with serum UA ($P < 0.001$). Compared with the lowest tertile, the risks of hyperuricemia increased across Adipo-IR tertiles (middle tertile: OR 1.52, 95%CI 1.24-1.88; highest tertile: OR 2.10, 95% CI 1.67–2.63) in men after full adjustment (P for trend < 0.001). In women, only the highest tertile (OR 2.09, 95%CI 1.52-2.87) was significantly associated with hyperuricemia. Those associations remained significant in participants with normal BMI status. As for HOMA-IR, only the highest tertile showed positive relationships with hyperuricemia in both genders after full adjustment (P for trend < 0.001). The association between HOMA-IR and hyperuricemia disappeared in men with normal BMI status.

Conclusions: Adipo-IR was strongly associated with serum UA and hyperuricemia regardless of BMI classification. In men with normal BMI, Adipo-IR, rather than HOMA-IR, was closely associated with hyperuricemia. Altogether, our finding highlights a critical role of adipose tissue IR on serum UA metabolism and hyperuricemia.

Keywords: adipose tissue insulin resistance, Adipo-IR, HOMA-IR, uric acid, hyperuricemia

INTRODUCTION

Uric acid (UA), the final degradation metabolite of endogenous and exogenous purine, is produced from the liver, intestine, and muscles and mainly excreted through the kidney (1, 2). Hyperuricemia, a serious threat to public health, is attributable to the imbalance between UA synthesis and clearance (3). Hyperuricemia is not only the precursor of gout and kidney stones but also the obvious risk factor of metabolic syndrome, hypertension, cardiovascular disease, and chronic kidney disease (1, 3–5). Recent studies confirmed that adipose tissue was another major organ responsible for UA production (2, 6); meanwhile, the causal role of adiposity in hyperuricemia has been established in many studies, highlighting the importance of adipose tissue on UA metabolism (7, 8). Regardless, there are no existing studies specifically addressing the exact role of insulin resistance (IR) in adipose tissue played in serum UA levels and hyperuricemia.

Adipose tissue is an insulin-sensitive organ essential for glucose and lipid metabolism (9). Under normal circumstances, insulin stimulates glucose uptake and lipogenesis while suppressing the lipolysis of fat cells. Adipose tissue IR is marked with the blunted antilipolytic effect of insulin and consequently increased FFA release from adipose tissue (10). Excessive circulation FFA delivery to liver and muscles thereby results in ectopic fat storage in these organs and subsequent hepatic and muscle IR. Therefore, the assessment of adipose tissue IR is vital as it is the early metabolic defect prior to systematic IR. The determination of lipolysis fluxes by isotope-labeled tracing through the multistep pancreatic clamp and hyperinsulinemic–euglycemic clamp techniques used to be the gold-standard measurement methods for accessing adipose tissue insulin sensitivity, which is somehow expensive, time consuming, and inapplicable to large-scale populations (11, 12). Recently, a surrogate index, adipose insulin resistance (Adipo-IR) index, calculated as fasting plasma free fatty acid (FFA) (mmol/L) × fasting plasma insulin (FINS) mIU/L concentrations, has been validated to be a unique, simple and reliable predictor of adipose tissue IR in obesity-related metabolic disorders (11–15). For instance, our previous study confirmed that Adipo-IR progressively increased from overweight to class III obesity (15). In addition, Adipo-IR has been proven to be the major determent of hepatic fat content and the fibrosis degree of Nonalcoholic fatty liver disease (NAFLD) (10, 16). Adipo-IR is also correlated with abnormal glucose intolerance and metabolic syndrome (9, 13). Results from the San Antonio Metabolism Study and two other prospective studies revealed that Adipo-IR rose progressively during the development of Type 2 diabetes mellitus (17–19). A prospective study further indicated that elevated Adipo-IR was associated with a higher risk of incident dysglycemia (20). Nonetheless, the association between Adipo-IR and hyperuricemia has never been elucidated.

Different from Adipo-IR, the homeostatic model assessment of insulin resistance (HOMA-IR), calculated as fasting plasma glucose [(FBG) (mmol/L) × FINS mIU/L)]/22.5, is a widely applied parameter that focuses on glucose metabolism and mainly introduced to demonstrate systemic IR, especially the hepatic IR (21–23). Although a high correlation between the two indexes has been observed, recent studies indicated their discordance in reflecting whole-body metabolism (24, 25). Compared to HOMA-IR, Adipo-IR was more related to visceral obesity, serum TG, and liver fibrosis (24). A previous study has indicated the association of HOMA-IR with hyperuricemia (21, 26). Nevertheless, the distinct association of the two indexes with serum UA levels and hyperuricemia has not been compared and elucidated.

This study aimed to demonstrate the impact of adipocyte IR on serum UA and hyperuricemia by using the Adipo-IR index for the first time, additionally, to compare the distinct roles of Adipo-IR and HOMA-IR played in hyperuricemia in both male and female subjects with a different BMI status.

METHODS

Study Population

This cross-sectional study included 5,925 participants in Northern China who underwent routine physical examination between April 2017 and August 2021 in Beijing Chao-yang Hospital. We excluded participants under 18 years old (n = 5), with missing UA data (n = 8), missing HbA1c value (n = 10), missing blood pressure value (n = 66), and with reduced renal dysfunction (n = 15), a final number of 5,821 subjects were included in the final analysis. Ethical approval was obtained from the ethics committee of Beijing Chao-yang Hospital. All participants signed written informed consent in the study.

Anthropometric and Biochemical Measurements

Height, body weight, systolic blood pressure (SBP), and diastolic blood pressure (DBP) were measured by the same trained team using standard methods as previously described (27). The venous blood samples were collected after overnight fasting. Serum UA levels were determined using a Siemens Advia 2400 biochemical analyzer (Siemens Healthcare Diagnostics Inc., Tarrytown, New York, USA). The FFA, total cholesterol (TC), triglyceride (TG), low-density lipoprotein cholesterol (LDL-C), high-density lipoprotein cholesterol (HDL-C), and serum creatinine (Scr) were measured by colorimetric enzymatic assays using a biochemical auto-analyzer (Hitachi 7170). FBG, FINS, and glycated hemoglobin (HbA1c) levels were detected as previously described (28). The estimated glomerular filtration rate (eGFR) was calculated as previously described (29).

Definition of Variables

Hyperuricemia was defined as serum UA ≥ 420 μmol/L in men and ≥ 360 μmol/L in women. Hypertension was identified as SBP ≥ 140 mmHg, DBP ≥ 90 mmHg, or a self-reported previous diagnosis of hypertension by a physician. Diabetes was determined as FBG ≥ 7.0 mmol/L, HbA1c ≥ 6.5% or self-reported previous diagnosis of diabetes by a physician. Dyslipidemia was defined as TC ≥ 6.22 mmol/L, TG ≥ 2.26 mmol/L, LDL-C ≥ 4.14 mmol/L, HDL-C < 1.04 mmol/L, or a self-reported previous diagnosis of hyperlipidemia by a physician. Adipo-IR was calculated by the formula: Adipo-IR= FFA (mmol/L) × FINS (mIU/L). HOMA-IR was calculated by the

following formula: HOMA-IR = FBG (mmol/L) × FINS (mIU/L)/22.5. Body mass index (BMI) was calculated as weight divided by height squared (kg/m^2). Participants were divided into normal weight (18.5 ≤ BMI < 24) and elevated weight (BMI ≥ 24) subgroups as previously described (30).

Statistical Analysis

The IBM SPSS Statistics software, version 25 (IBM Corporation, Armonk, NY, United States), the Graphpad 7.0 software and the MedCalc version 17 software were used for data analysis. Basic characteristic analysis was conducted in participants with hyperuricemia and non-hyperuricemia. We performed analysis separately in men and women to avoid potential sex influences on the proportion of hyperuricemia. The Shapiro–Wilk test was used for normality test and data were expressed as mean ± standard deviation (SD) for continuous normally distributed variables, median (upper and lower quartiles) for continuous skewed distributed variables and number (%) for categorical variables in this study. The difference of normally distributed variables between two groups was calculated with unpaired Student's *t* test. The Mann–Whitney U test and Kruskal–Wallis test were applied to compare the difference of continuous skewed variables between two groups or three groups, separately. For categorical data, the chi-square test was used as appropriate for categorical variables. The linear trends of hyperuricemia proportion across the Adipo-IR and HOMA-IR tertiles were tested by the Cochran Armitage trend test.

Sex-specific linear regression analysis was accessed to explore the association of serum UA (dependent variable) with Adipo-IR and HOMA-IR (independent variable). UA was Ln-transformed for analysis due to skewed distribution. The variables without collinearity were selected for adjustment. Model 1 was without adjustment; Model 2 was adjusted for age, BMI, SBP, TC, H-DLC, TG, HbA1c, and eGFR; and Model 3 was conducted by excluding participants with diabetes and was adjusted for Model 2.

Adipo-IR and HOMA-IR were then divided into tertiles, Adipo-IR, male: lowest tertile ≤ 2.87; middle tertile 2.88–5.30; highest tertile ≥ 5.30; Female: lowest tertile ≤ 2.96; middle tertile 2.97–5.11; highest tertile ≥ 5.11; HOMA-IR, male: lowest tertile ≤ 1.44; middle tertile 1.45–2.41; highest tertile ≥ 2.41; Female: lowest tertile ≤ 1.25; middle tertile 1.26–2.01; highest tertile ≥ 2.01. The sex-specific associations of Adipo-IR tertiles or HOMA-IR tertiles with the prevalence of hyperuricemia were detected by binary logistic regression analyses, with the lowest tertile as the reference. Model 1 was crude, model 2 was adjusted for age, BMI, HbA1c, eGFR, hypertension and dyslipidemia. Model 3 was conducted by excluding participants with diabetes and was adjusted for Model 2. Further analyses were conducted in BMI subgroups (normal BMI and elevated BMI). Age, HbA1c, eGFR, hypertension, and dyslipidemia were adjusted. Additionally, the association of per SD increase of both indexes with hyperuricemia were analyzed, respectively. Data were summarized as odds ratios (ORs) and 95% confidence intervals (CIs). Furthermore, we use the receiver operating characteristic (ROC) curve analysis to compare the predictive powers of the two indexes for hyperuricemia among men and women. The comparison of the area under the curve (AUC) was analyzed by Delong's ROC test. For the above analysis, Two-tailed *P* values <0.05 were considered statistically significant.

RESULTS

Characteristics of Participants With Hyperuricemia and Non-Hyperuricemia

As presented in **Table 1**, the prevalence of hyperuricemia was 35.2% in men and 13.3% in women. The Adipo-IR and HOMA-IR and BMI levels were all higher in participants with hyperuricemia than individuals without hyperuricemia in both genders ($P < 0.001$). Female subjects with hyperuricemia were older and were more prone to have metabolic disorders such as diabetes, hypertension, and dyslipidemia than non-hyperuricemia subjects (all $P < 0.001$). Interestingly, male participants with hyperuricemia were significantly younger ($P < 0.001$) and the proportion of individuals with diabetes was smaller ($P = 0.012$) compared to non-hyperuricemia subjects. Additionally, the proportions of individuals with hypertension were comparable among male participants with and without hyperuricemia ($P = 0.232$).

Association of Serum UA Levels With Adipo-IR or HOMA-IR Index by Linear Regression Analysis

The correlation between Adipo-IR or HOMA-IR and serum uric acid by spearman analysis was presented in **Supplementary Table 1**. Both Adipo-IR and HOMA-IR showed positive correlations with UA in both genders (all $P < 0.001$). The correlations existed in both normal BMI and elevated BMI subgroups (all $P < 0.001$). Further linear regression analysis indicated that higher Adipo-IR or HOMA-IR levels were associated with higher Ln UA levels in both genders (**Table 2**) (all $P < 0.001$). The positive correlations remained in both genders after full adjustment (all $P < 0.001$). As the proportion of diabetes was distinct in men and women, we excluded participants with diabetes and found consistent positive relationships between both the indexes and Ln UA in both genders (all $P < 0.001$). Furthermore, the serum UA levels (all $P < 0.01$) as well as the ratio of hyperuricemia (P for trend < 0.001) exhibited increasing trends from the lowest to highest tertiles of the two indexes in both genders (**Figure 1** and **Supplementary Figure 1**).

Association of Adipo-IR and HOMA-IR With Hyperuricemia by Logistic Regression Analyses

The association of sex-specific Adipo-IR and HOMA-IR tertiles with the prevalence of hyperuricemia is shown in **Table 3**. The lowest tertile was used as the reference. Overall, the risk of hyperuricemia increased across Adipo-IR tertiles and HOMA-IR tertiles (all P for the trend <0.001). In the crude model, the ORs of middle and highest Adipo-IR tertiles for hyperuricemia in men were 1.71 (95% CI 1.41–2.08) and 2.82 (95% CI 2.33–3.41), respectively. After adjusting for confounders, the ORs of the

TABLE 1 | Basic characteristics of the participants with and without hyperuricemia.

Variable	men			Women		
	Normal	Hyperuricemia	*P*-value	Normal	Hyperuricemia	*P*-value
N (%)	1,950 (64.8)	1,060 (35.2)		2,436 (86.7)	375 (13.3)	
Age, years	46.76 ± 12.85	42.96 ± 12.56	< 0.001	43.39 ± 13.29	47.64 ± 15.22	<0.001
BMI, kg/m^2	25.16 ± 3.17	26.73 ± 3.45	< 0.001	22.76 ± 3.45	25.30 ± 4.50	<0.001
DBP, mmHg	126.04 ± 16.50	128.11 ± 16.79	0.001	117.54 ± 18.24	125.01 ± 21.07	<0.001
SBP, mmHg	75.49 ± 11.37	77.33 ± 12.02	< 0.001	68.63 ± 11.03	72.06 ± 11.64	<0.001
FBG, mmol/L	4.96 (4.60-5.44)	4.97 (4.58-5.43)	0.850	4.76 (4.43-5.12)	4.98 (4.59-5.45)	<0.001
HbA1c, %	5.5 (5.3-5.8)	5.5 (5.3-5.8)	0.505	5.4 (5.2-5.7)	5.6 (5.3-6.0)	<0.001
FINS, mIU/L	7.7 (5.4-10.7)	9.7 (6.7-13.7)	< 0.001	7.2 (5.3-9.9)	10.0 (6.5-14.3)	<0.001
FFA, mmol/L	0.46 (0.35-0.60)	0.50 (0.39-0.62)	< 0.001	0.52 (0.40-0.67)	0.60 (0.46-0.75)	<0.001
TG, mmol/L	1.36 (0.98-1.92)	1.74 (1.22-2.50)	< 0.001	1.01 (0.77-1.39)	1.41 (0.96-2.12)	<0.001
TC, mmol/L	4.89 (4.31-5.51)	5.09 (4.53-5.72)	< 0.001	4.86 (4.31-5.52)	5.23 (4.59-5.99)	<0.001
H-DLC, mmol/L	1.18 (1.00-1.35)	1.10 (1.00-1.30)	< 0.001	1.50 (1.27-1.71)	1.30 (1.10-1.50)	<0.001
L-DLC, mmol/L	3.00 (2.48-3.60)	3.20 (2.67-3.73)	< 0.001	2.80 (2.30-3.36)	3.14 (2.55-3.89)	<0.001
UA, μmol/L	357.0 (320.0-388.0)	468.0 (441.0-508.0)	< 0.001	273.0 (240.0-307.0)	390,0 (373.0-418.8)	<0.001
eGFR, mL/min per 1.73 m^2	111.32 (102.82-120.07)	111.26 (100.89-120.41)	0.290	116.57 (106.62-126.18)	107.97 (99.56-121.51)	<0.001
Adipo-IR	3.50 (2.23-5.52)	4.87 (3.04-7.31)	< 0.001	3.73 (2.44-5.62)	5.67 (3.48-9.18)	<0.001
HOMA-IR	1.74 (1.17-2.53)	2.19 (1.44-3.21)	< 0.001	1.53 (1.08-2.16)	2.27 (1.39-3.39)	<0.001
Hypertension, *n* (%)	430 (22.1)	254 (24.0)	0.232	316 (13.0)	90 (24.0)	<0.001
Diabetes, *n* (%)	229 (11.7)	93 (8.8)	0.012	96 (3.9)	30 (8.0)	<0.001
Dyslipidemia, *n* (%)	861 (44.2)	626 (59.1)	< 0.001	524 (21.5)	167 (44.5)	<0.001

Data were expressed as the mean ± SD or median (upper and lower quartiles) or number (proportion). BMI, body mass index; SBP, systolic blood pressure; DBP, diastolic blood pressure; FPG, fasting plasma glucose; HbA1c, glycated hemoglobin; FINS, fasting insulin level; FFA, free fatty acid; TG, triglycerides; TC, total cholesterol; HDL-C, high-density lipoprotein cholesterol; LDL-C, low-density lipoprotein cholesterol; UA, uric acid; eGFR, estimated glomerular filtration rate; Adipo-IR, adipose tissue insulin resistance; HOMA-IR, homeostasis model assessment of insulin resistance.

TABLE 2 | Linear regression analysis for association of Adipo-IR and HOMA-IR (independent variables) with LnUA (dependent variable).

Variable	Ln UA (men)			Ln UA (women)		
	B(SE)	Standardized β	*P*-value	*B*(SE)	Standardized β	*P*-value
Adipo-IR						
Model 1	0.013 (0.001)	0.235	<0.001	0.015 (0.001)	0.266	<0.001
Model 2	0.007 (0.001)	0.125	<0.001	0.009 (0.001)	0.151	<0.001
Model 3	0.008 (0.001)	0.127	<0.001	0.009 (0.001)	0.146	<0.001
HOMA-IR						
Model 1	0.016 (0.002)	0.145	<0.001	0.033 (0.003)	0.235	<0.001
Model 2	0.007 (0.002)	0.064	0.001	0.016 (0.003)	0.114	<0.001
Model 3	0.009 (0.003)	0.059	0.004	0.022 (0.004)	0.117	<0.001

Model 1: Crude model.
Model 2: Adjusted for age, BMI, SBP, TC, H-DLC, TG, HbA1c, and eGFR.
Model 3: Excluding participant with diabetes and adjusted for Model 2.

middle and highest Adipo-IR tertiles for hyperuricemia were 1.52 (95% CI 1.24–1.88) and 2.10 (95% CI 1.67–2.63), respectively. Among women, only the OR of the highest Adipo-IR tertile for hyperuricemia was statistically significant compared to the lowest tertile, either in a crude (OR 3.53, 95%CI 2.66–4.70) or fully adjusted model (OR 2.09, 95%CI 1.52–2.87) (all *P* for trend < 0.001). Similar relationships between Adipo-IR and hyperuricemia were observed in non-diabetic participants. Furthermore, we observed a 24% and 47% higher risk of hyperuricemia with each SD increment in Adipo-IR in men and women, respectively.

As for the HOMA-IR index, similar to Adipo-IR, the highest tertile of HOMA-IR showed higher hyperuricemia risk in women (Model 1: OR 3.20, 95%CI 2.42–4.23; Model 2: OR 1.74, 95%CI 1.26–2.42; Model 3: OR 1.60, 95%CI 1.15–2.24). Meanwhile, in men, different from Adipo-IR, only the highest tertile HOMA-IR (OR 1.61, 95%CI 1.28–2.03) showed a positive relationship with hyperuricemia after full adjustment.

Association of Adipo-IR Tertiles and HOMA-Tertiles With Hyperuricemia by Logistic Regression Analyses in Normal BMI and Elevated BMI Subgroups

To evaluate the association of Adipo-IR and HOMA-IR with hyperuricemia among participants with normal weight, we conducted a subgroup analysis in participants with normal BMI or elevated BMI status. The UA levels and the proportion of subjects with hyperuricemia showed an increasing trend from the bottom to top Adipo-IR and HOMA-IR tertiles even in normal BMI subgroups of both genders (**Figure 2** and

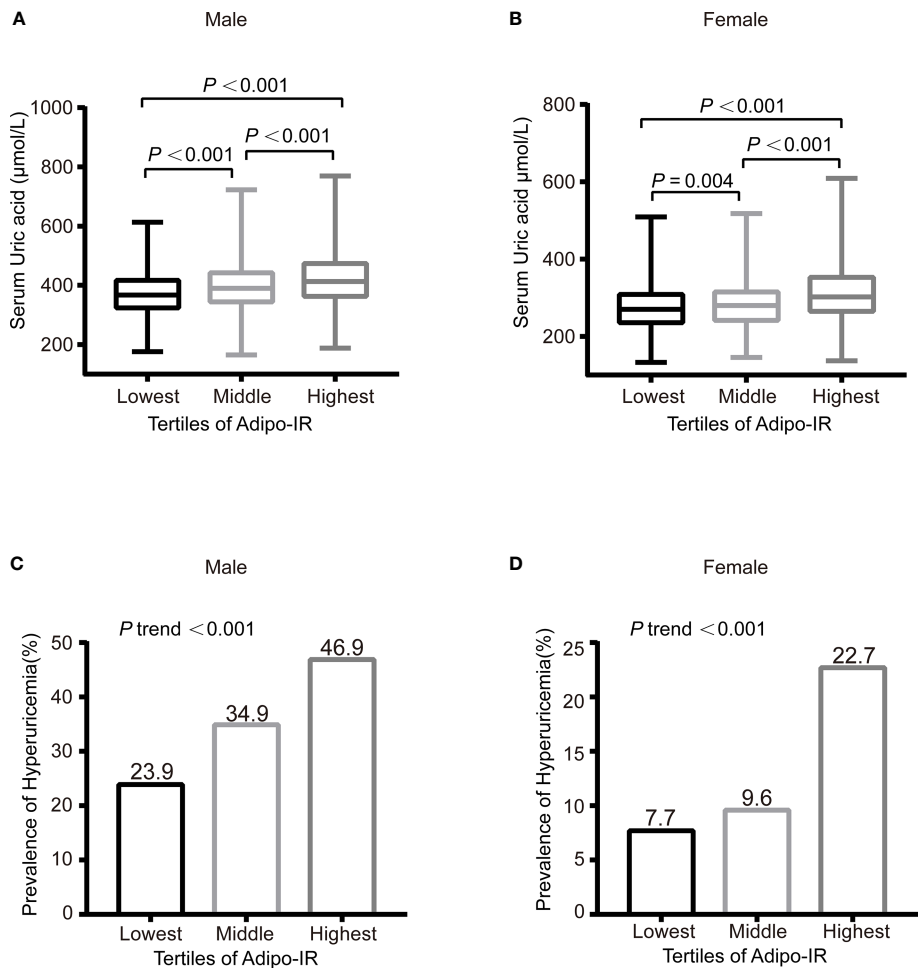

FIGURE 1 | The serum UA levels **(A**, **B)** and prevalence of hyperuricemia **(C**, **D)** across the Adipo-IR tertiles. Data were expressed as median (upper and lower quartiles) or proportion (%). *P* trend: from test for linearity.

TABLE 3 | Logistic regression analysis for association between Adipo-IR or HOMA-IR and hyperuricemia.

Variables	men			Women		
	Model 1	**Model 2**	**Model 3**	**Model 1**	**Model 2**	**Model 3**
Adipo-IR						
Lowest tertile	Ref.	Ref.	Ref.	Ref.	Ref.	Ref.
Middle tertile	**1.71(1.41,2.08)*** **	**1.52(1.24,1.88)*** **	**1.49(1.20,1.85)*** **	1.28(0.92,1.77)	1.04(0.74,1.46)	1.02(0.72,1.44)
Highest tertile	**2.82(2.33,3.41)*** **	**2.10(1.67,2.63)*** **	**2.07(1.64,2.62)*** **	**3.53(2.66,4.70)*** **	**2.09(1.52,2.87)*** **	**2.02(1.46,2.79)*** **
P for trend	<0.001	<0.001	<0.001	<0.001	<0.001	<0.001
Per SD increase	**1.45(1.34,1.57)*** **	**1.24(1.13,1.36)*** **	**1.33(1.19,1.49)*** **	**1.75(1.59,1.93)*** **	**1.47(1.31,1.64)*** **	**1.52(1.34,1.72)*** **
HOMA-IR						
Lowest tertile	Ref.	Ref.	Ref.	Ref.	Ref.	Ref.
Middle tertile	**1.41(1.17,1.71)*** **	1.14(0.92,1.40)	1.13(0.91,1.39)	1.11(0.81,1.53)	0.92(0.66,1.29)	0.85(0.61,1.20)
Highest tertile	**2.32(1.93,2.80)*** **	**1.61(1.28,2.03)*** **	**1.63(1.28,2.07)*** **	**3.20(2.42,4.23)*** **	**1.74(1.26,2.42)** **	**1.60(1.15,2.24)** **
P for trend	< 0.001	< 0.001	< 0.001	< 0.001	< 0.001	< 0.001
Per SD increase	**1.25(1.16,1.35)*** **	1.07(0.98,1.17)	**1.19(1.04,1.37)***	**1.72(1.54,1.93)*** **	**1.43(1.25,1.64)*****	**1.58(1.32,1.89)*** **

Model 1: Crude model.

Model 2: Adjusted for age, BMI, HbA1c, eGFR, hypertension, and dyslipidemia.

Model 3: Excluding participant with diabetes and adjusted for Model 2.

**P < 0.05; **P < 0.01; ***P < 0.001.*

The meaning of the bold values is the values were statistically significant.

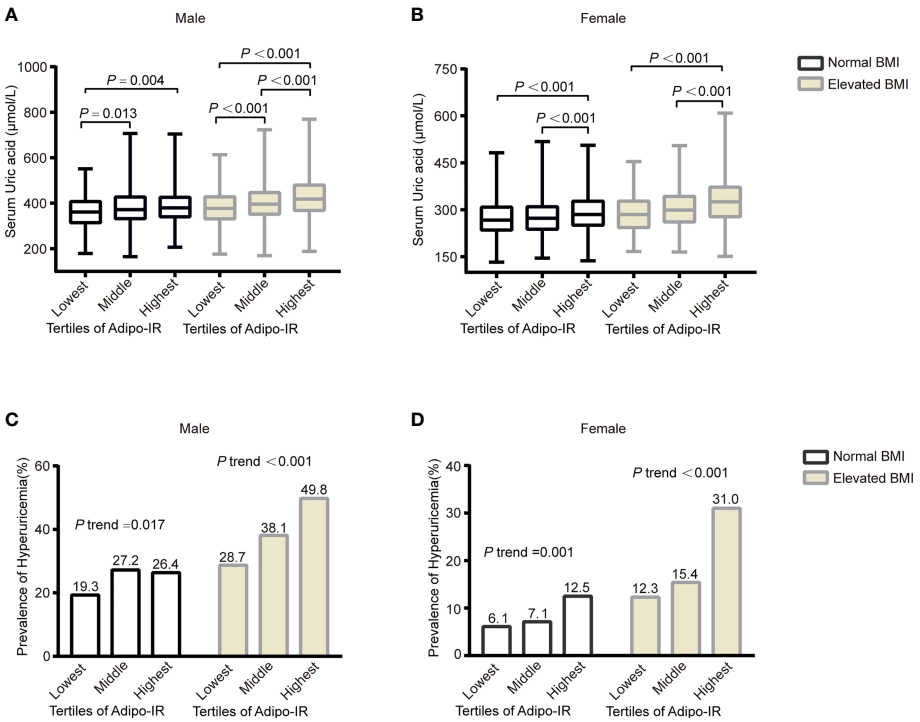

FIGURE 2 | The serum UA levels **(A, B)** and prevalence of hyperuricemia **(C, D)** across the Adipo-IR tertiles in normal BMI and elevated BMI subgroups. Data were expressed as median (upper and lower quartiles) or proportion (%). *P* trend: from test for linearity.

Supplementary Figures 2–4) (*P* for trend < 0.001). In the normal BMI subgroup, one SD increase in Adipo-IR showed 48% (*P* for trend = 0.025) and 52% (*P* for trend = 0.002) higher risks for hyperuricemia in men and women, respectively. By contrast, one SD increase in HOMA-IR was not associated with higher hyperuricemia risk in men (**Figure 3**) (**Table 4**). When Adipo-IR and HOMA-IR were entered as tertiles, both the middle and highest Adipo-IR tertiles showed significantly positive association with hyperuricemia in men irrespective of BMI classification. In contrast, no association was observed between HOMA-IR tertiles and hyperuricemia in male normal BMI subgroup (**Table 4**).

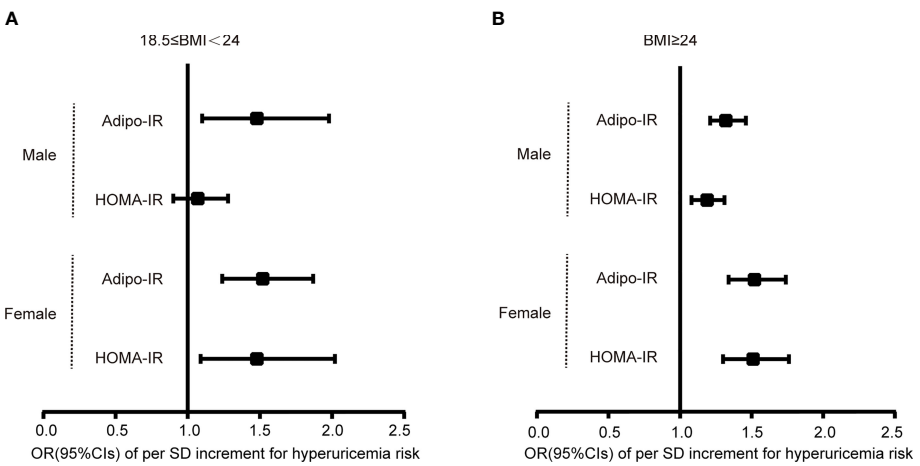

FIGURE 3 | Logistic regression analysis for the OR of per SD increment of Adipo-IR or HOMA-IR for hyperuricemia risk in normal BMI **(A)** and elevated BMI **(B)** subgroups. Models were adjusted for age, HbA1c, eGFR, hypertension, and dyslipidemia. .

TABLE 4 | Logistic regression analysis for association between Adipo-IR or HOMA-IR and hyperuricemia in both normal BMI and elevated BMI subgroups.

Variables	men		Women	
	18.5 ≤ BMI < 24	**BMI ≥ 24**	**18.5 ≤ BMI < 24**	**BMI ≥ 24**
Adipo-IR				
Lowest tertile	Ref.	Ref.	Ref.	Ref.
Middle tertile	**1.63(1.13,2.35)****	**1.59(1.23,2.06)*****	1.12(0.70,1.78)	1.23(0.70,2.15)
Highest tertile	**1.65(1.01,2.70)***	**2.63(2.03,3.40)*****	**1.99(1.25,3.17)****	**2.81(1.70,4.63)*****
P for trend	0.025	< 0.001	0.002	< 0.001
Per SD increase	**1.48(1.10,1.98)****	**1.32(1.21,1.46)*****	**1.52(1.24,1.87)*****	**1.52(1.34,1.74)*****
HOMA-IR				
Lowest tertile	Ref.	Ref.	Ref.	Ref.
Middle tertile	1.39(0.97,2.01)	1.11(0.86,1.44)	0.96(0.61,1.51)	1.00(0.56,1.81)
Highest tertile	1.58(0.91,2.76)	**1.85(1.42,2.40)*****	**1.88(1.18,3.00)****	**2.03(1.20,3.45)****
P for trend	0.020	<0.001	0.002	<0.001
Per SD increase	1.07(0.90,1.28)	**1.19(1.08,1.31)****	**1.48(1.09,2.02)***	**1.51(1.30,1.76)***

Models were adjusted for age, HbA1c, eGFR, hypertension and dyslipidemia.
**P < 0.05; **P < 0.01; ***P < 0.001.*
The meaning of the bold values is the values were statistically significant.

The AUC of Adipo-IR and HOMA-IR for Hyperuricemia

Supplementary Figure 5 displays the ROC curves related to the diagnostic ability of Adipo-IR and HOMA-IR for hyperuricemia incidence among men and women, respectively. In women, the AUC for Adipo-IR (0.667, 95%CI 0.649–0.684) and HOMA-IR (0.654, 95%CI 0.636–0.672) were comparable ($P = 0.18$), whereas in men, Adipo-IR showed larger AUC (0.624, 95%CI 0.607–0.642) than HOMA-IR (0.604, 95%CI 0.586–0.622) ($P = 0.003$), which implied a closer relationship between Adipo-IR and hyperuricemia.

DISCUSSION

This is the first study exploring the relationship between Adipo-IR and UA as well as hyperuricemia in a Northern Chinese population. Our study revealed that Adipo-IR was positively associated with serum UA levels and hyperuricemia. This relationship was independent of age, BMI, eGFR, diabetes, dyslipidemia, and hypertension. Furthermore, we found that HOMA-IR was not as good as Adipo-IR to predict hyperuricemia in men, especially in a normal BMI status, indicating a possibly closer relationship between Adipo-IR and serum UA metabolism compared to hepatic insulin resistance.

Adipose tissue is an essential endocrine organ for UA metabolism. Theoretically, xanthine oxidoreductase (XOR) is the responsible enzyme for the final step of UA production. Apart from the small intestine and liver, adipose tissue is another major organ with abundant expression and activities of XOR and is indispensable for UA production and secretion (6, 31). The causal role of obesity to elevated serum UA levels has been well established for years (7, 8). Genetically, adiposity was also considered to be positively associated with serum UA concentrations and the risk of gout (7, 8). Consistent with this, XOR was reported to be a regulator of adipogenesis and correlated positively with adipose mass. Obese adipose tissues own higher XOR activities and thereby possess a higher ability for UA secretion (31). The elevated XOR activity during obesity may be related to hypoxia and active lipid metabolism consuming nicotinamide adenine dinucleotide phosphate. Reciprocally, long-term elevated UA levels could result in a pro-inflammatory state of adipose tissue by inducing monocyte chemotactic protein 1 release and thus causing a vicious cycle (32).

IR has been suggested to be the mediator between obesity and hyperuricemia (33). The amelioration of IR decreased the serum UA level independent of weight loss, while the UA-lowering therapy did not change insulin sensitivity in hyperuricemia subjects (34, 35). By contrast, other studies indicated that hyperuricemia could be detected before hyperinsulinemia (3, 36).In a prospective study, elevated serum UA could predict IR in 15 follow-up years (4). Although current studies indicated a reciprocal causation between IR and hyperuricemia, it is doubtless that compensatory hyperinsulinemia is the bridge between IR and hyperuricemia (37). Compensated hyperinsulinemia caused by IR could decrease the renal clearance of UA, as has long been proven (26, 38, 39). Admittedly, both compensated hyperinsulinemia during hepatic IR or adipose IR could contribute to reduced UA excretion. It is noteworthy that adipose IR precedes hepatic IR or systemic IR during the course of obesity. Current evidence has revealed that visceral obesity, more closely linked to adipose dysfunction, was more responsible for hyperuricemia than overall adiposity (40, 41). Although subcutaneous fat constitutes a major proportion of total fat, visceral fat contributes more to serum UA levels. The possible explanation may be that visceral fat has a stronger lipolysis ability and attributes to adipose IR to a greater degree. Firstly, compensatory hyperinsulinemia caused by excess visceral fat IR could decrease the renal clearance of UA as described above. Secondly, a stronger lipolysis of visceral adipose tissue can increase the flow of FFA to the liver, accelerating the *de novo* lipogenesis in the liver. The increased need for nicotinamide adenine dinucleotide phosphate (NADPH) in this process is accompanied by activated PPP pathways and purine synthesis. Therefore, the above process resulted in the acceleration of hepatic UA production. Consistently, studies indicated that Adipo-IR increased proportionally with visceral fat (41). In our study, we firstly used the simple Adipo-IR index to demonstrate the role of IR in adipose tissue played in UA metabolism and found a positive

relationship between them beyond total adiposity, further implying the pathogenic effect of adipose tissue dysfunction in serum UA homeostasis.

As a simple serum index, Adipo-IR has been validated against the cumbersome isotope- tracing experiment for accurately accessing adipose insulin sensitivity. Adipo-IR was shown to be positively correlated with BMI (15, 18, 25). Additionally, previous studies indicated that the Adipo-IR index could reflect the state of adipose tissue IR only in subjects with overweight and obesity (11, 14). Recently, growing studies indicated that Adipo-IR could mirror metabolism disorders regardless of obesity. Adipo-IR showed strong correlations with both the hepatic fat and fibrosis of NAFLD patients independently of BMI and Type 2 diabetes mellitus (10, 42). Obese subjects with normal insulin-sensitive adipose tissue seldom develop ectopic fat deposition in the liver (43). In our study, Adipo-IR was shown to be an independent risk factor for hyperuricemia even in participants with normal BMI, indicating the critical role of adipose tissue function beyond fat mass on UA metabolism.

Theoretically and practically, Adipo-IR is highly correlated with HOMA-IR (25, 32, 42). However, the discordance between the two indexes for demonstrating metabolic diseases has gained great attention recently (24, 44). One study claimed that elevated Adipo-IR was more closely linked with visceral adiposity and hypertriglyceridemia, while elevated HOMA-IR was associated with a lower basic metabolic rate (24). Another study indicated that Adipo-IR was more closely associated with developing prediabetes relative to HOMA-IR (13, 18), indicating a more initial role of adipose tissue IR for glucose dysregulation. Furthermore, compared to HOMA-IR, Adipo-IR was more related to the severity of fibrosis in NAFLD and could be more critical for aortic valve calcification (10, 45). These inconsistencies are possibly due to the differential metabolic effects of adipose tissue and other metabolic organs, more importantly, the pathogenic role of adipose tissues in those diseases.

Several studies indicated a positive relationship between HOMA-IR and hyperuricemia (21). It was not equivalent to the exact role of adipose tissue IR on hyperuricemia. In addition, the present study revealed that Adipo-IR was more closely related with hyperuricemia than HOMA-IR, verifying a more essential role of adipose tissue IR on serum UA metabolism, at least in men. One explanation may be that FFA outweighs glucose for the initiation of hyperuricemia. Another factor that cannot be ignored is sex hormones. Consistent with our results, L.-K. Chen et al. claimed a positive association between serum UA and HOMA-IR in older women but not in men among a Taiwan population (46). Another study revealed a sex-difference association between metabolically healthy obese status and hyperuricemia (47). Further studies are warranted to explore the sex-related roles of IR in hyperuricemia.

Previous studies indicated a bell-shaped relationship between HbA1c, FBG, and serum UA levels (1, 2, 48, 49). UA was positively correlated with FBG and HbA1c before the onset of diabetes (2). However, in individuals with diabetes, UA would be decreased as urine glucose facilitated the excretion of UA (49). Therefore, we also evaluated the relationship between Adipo-IR and uric acid in the non-diabetes participants. We got the conclusion that Adipo-IR correlated well with serum UA levels irrespective of the blood glucose status.

There are some limitations to this study. First of all, the direct causal relationship between Adipo-IR and hyperuricemia cannot be inferred from the observational association in this research. Secondly, the serum UA level is also affected by other confounding factors, such as alcohol consumption, purine-rich diets, diuretic therapy, and genetic risk (4, 7, 50), which we did not collect in this study. Furthermore, the variables that reflect the content of visceral fat, such as waist circumference or the percentage of the body fat, were not collected in this study. Finally, all the participants were of yellow race. This may limit the generalizability of our results to other races. Consequently, more studies are needed to demonstrate the causality, and to extend our findings in different ethnicities and regions.

CONCLUSION

To summarize, this is the first study to explore the association of Adipo-IR and serum UA as well as hyperuricemia. Our study indicated a critical role of adipose tissue IR on serum UA metabolism in both normal weight and overweight/obesity participants.

DATA AVAILABILITY STATEMENT

The raw data supporting the conclusions of this article will not be made publicly available because the ethical approval obtained for this study prevents the human data being shared publicly to protect patients' privacy. Requests to access the datasets should be directed to GW, wangguang@bjcyh.com.

ETHICS STATEMENT

The studies involving human participants were reviewed and approved by the Ethics Committee of Beijing Chao-yang Hospital affiliated with Capital Medical University. The patients/participants provided their written informed consent to participate in this study.

AUTHOR CONTRIBUTIONS

GW and SL designed the study. HS, XC, NB, YA, and JL conducted the research. HS, XC, and NB analyzed the data. HS and XC wrote the manuscript. The final manuscript was read and approved by all authors.

FUNDING

This study was not supported by any sources of funding.

SUPPLEMENTARY MATERIAL

The Supplementary Material for this article can be found online at: https://www.frontiersin.org/articles/10.3389/fendo.2022.835154/full#supplementary-material

REFERENCES

1. Lima WG, Martins-Santos ME, Chaves VE. Uric Acid as a Modulator of Glucose and Lipid Metabolism. *Biochimie* (2015) 116: 17–23. doi: 10.1016/j.biochi.2015.06.025
2. Choi HK, Ford ES. Haemoglobin A1c, Fasting Glucose, Serum C-Peptide and Insulin Resistance in Relation to Serum Uric Acid Levels–the Third National Health and Nutrition Examination Survey. *Rheumatol (Oxford)* (2008) 47 (5):713–7. doi: 10.1093/rheumatology/ken066
3. Li C, Hsieh MC, Chang SJ. Metabolic Syndrome, Diabetes, and Hyperuricemia. *Curr Opin Rheumatol* (2013) 25(2):210–6. doi: 10.1097/BOR.0b013e32835d951e
4. Sharaf El Din UAA, Salem MM, Abdulazim DO. Uric Acid in the Pathogenesis of Metabolic, Renal, and Cardiovascular Diseases: A Review. *J Adv Res* (2017) 8(5):537–48. doi: 10.1016/j.jare.2016.11.004
5. Ponticelli C, Podesta MA, Moroni G. Hyperuricemia as a Trigger of Immune Response in Hypertension and Chronic Kidney Disease. *Kidney Int* (2020) 98 (5):1149–59. doi: 10.1016/j.kint.2020.05.056
6. Cheung KJ, Tzameli I, Pissios P, Rovira I, Gavrilova O, Ohtsubo T, et al. Xanthine Oxidoreductase is a Regulator of Adipogenesis and PPARgamma Activity. *Cell Metab* (2007) 5(2):115–28. doi: 10.1016/j.cmet.2007.01.005
7. Lyngdoh T, Vuistiner P, Marques-Vidal P, Rousson V, Waeber G, Vollenweider P, et al. Serum Uric Acid and Adiposity: Deciphering Causality Using a Bidirectional Mendelian Randomization Approach. *PLos One* (2012) 7(6):e39321. doi: 10.1371/journal.pone.0039321
8. Li X, Meng X, He Y, Spiliopoulou A, Timofeeva M, Wei WQ, et al. Genetically Determined Serum Urate Levels and Cardiovascular and Other Diseases in UK Biobank Cohort: A Phenome-Wide Mendelian Randomization Study. *PloS Med* (2019) 16(10):e1002937. doi: 10.1371/journal.pmed.1002937
9. Zhang K, Pan H, Wang L, Yang H, Zhu H, Gong F. Adipose Tissue Insulin Resistance is Closely Associated With Metabolic Syndrome in Northern Chinese Populations. *Diabetes Metab Syndr Obes* (2021) 14:1117–28. doi: 10.2147/DMSO.S291350
10. Rosso C, Kazankov K, Younes R, Esmaili S, Marietti M, Sacco M, et al. Crosstalk Between Adipose Tissue Insulin Resistance and Liver Macrophages in non-Alcoholic Fatty Liver Disease. *J Hepatol* (2019) 71(5):1012–21. doi: 10.1016/j.jhep.2019.06.031
11. Sondergaard E, Espinosa De Ycaza AE, Morgan-Bathke M, Jensen MD. How to Measure Adipose Tissue Insulin Sensitivity. *J Clin Endocrinol Metab* (2017) 102(4):1193–9. doi: 10.1210/jc.2017-00047
12. Fabbrini E, Magkos F, Conte C, Mittendorfer B, Patterson BW, Okunade AL, et al. Validation of a Novel Index to Assess Insulin Resistance of Adipose Tissue Lipolytic Activity in Obese Subjects. *J Lipid Res* (2012) 53(2):321–4. doi: 10.1194/jlr.D020321
13. Cai X, Xia L, Pan Y, He D, Zhu H, Wei T, et al. Differential Role of Insulin Resistance and Beta-Cell Function in the Development of Prediabetes and Diabetes in Middle-Aged and Elderly Chinese Population. *Diabetol Metab Syndr* (2019) 11:24. doi: 10.1186/s13098-019-0418-x
14. Ter Horst KW, van Galen KA, Gilijamse PW, Hartstra AV, de Groot PF, van der Valk FM, et al. Methods for Quantifying Adipose Tissue Insulin Resistance in Overweight/Obese Humans. *Int J Obes (Lond)* (2017) 41 (8):1288–94. doi: 10.1038/ijo.2017.110
15. Li X, Liu J, Zhou B, Li Y, Wu Z, Meng H, et al. Sex Differences in the Effect of Testosterone on Adipose Tissue Insulin Resistance From Overweight to Obese Adults. *J Clin Endocrinol Metab* (2021) 106(8):2252–63. doi: 10.1210/clinem/dgab325
16. Bell LN, Wang J, Muralidharan S, Chalasani S, Fullenkamp AM, Wilson LA, et al. Relationship Between Adipose Tissue Insulin Resistance and Liver Histology in Nonalcoholic Steatohepatitis: A Pioglitazone Versus Vitamin E Versus Placebo for the Treatment of Nondiabetic Patients With Nonalcoholic Steatohepatitis Trial Follow-Up Study. *Hepatology* (2012) 56(4):1311–8. doi: 10.1002/hep.25805
17. Kim JY, Bacha F, Tfayli H, Michaliszyn SF, Yousuf S, Arslanian S. Adipose Tissue Insulin Resistance in Youth on the Spectrum From Normal Weight to Obese and From Normal Glucose Tolerance to Impaired Glucose Tolerance to Type 2 Diabetes. *Diabetes Care* (2019) 42(2):265–72. doi: 10.2337/dc18-1178
18. Gastaldelli A, Gaggini M, DeFronzo RA. Role of Adipose Tissue Insulin Resistance in the Natural History of Type 2 Diabetes: Results From the San Antonio Metabolism Study. *Diabetes* (2017) 66(4):815–22. doi: 10.2337/db16-1167
19. Hara K, Horikoshi M, Yamauchi T, Yago H, Miyazaki O, Ebinuma H, et al. Measurement of the High-Molecular Weight Form of Adiponectin in Plasma is Useful for the Prediction of Insulin Resistance and Metabolic Syndrome. *Diabetes Care* (2006) 29(6):1357–62. doi: 10.2337/dc05-1801
20. Semnani-Azad Z, Connelly PW, Bazinet RP, Retnakaran R, Jenkins DJA, Harris SB, et al. Adipose Tissue Insulin Resistance Is Longitudinally Associated With Adipose Tissue Dysfunction, Circulating Lipids, and Dysglycemia: The PROMISE Cohort. *Diabetes Care* (2021) 44(7):1682–91. doi: 10.2337/dc20-1918
21. Nakamura K, Sakurai M, Miura K, Morikawa Y, Nagasawa SY, Ishizaki M, et al. HOMA-IR and the Risk of Hyperuricemia: A Prospective Study in non-Diabetic Japanese Men. *Diabetes Res Clin Pract* (2014) 106(1):154–60. doi: 10.1016/j.diabres.2014.07.006
22. Isokuortti E, Zhou Y, Peltonen M, Bugianesi E, Clement K, Bonnefont-Rousselot D, et al. Use of HOMA-IR to Diagnose non-Alcoholic Fatty Liver Disease: A Population-Based and Inter-Laboratory Study. *Diabetologia* (2017) 60(10):1873–82. doi: 10.1007/s00125-017-4340-1
23. Bonora E, Targher G, Alberiche M, Bonadonna RC, Saggiani F, Zenere MB, et al. Homeostasis Model Assessment Closely Mirrors the Glucose Clamp Technique in the Assessment of Insulin Sensitivity: Studies in Subjects With Various Degrees of Glucose Tolerance and Insulin Sensitivity. *Diabetes Care* (2000) 23(1):57–63. doi: 10.2337/diacare.23.1.57
24. Song Y, Sondergaard E, Jensen MD. Unique Metabolic Features of Adults Discordant for Indices of Insulin Resistance. *J Clin Endocrinol Metab*. (2020) 105(8):e2753-e2763. doi: 10.1210/clinem/dgaa265
25. Ryden M, Andersson DP, Arner P. Usefulness of Surrogate Markers to Determine Insulin Action in Fat Cells. *Int J Obes (Lond)* (2020) 44 (12):2436–43. doi: 10.1038/s41366-020-0592-9
26. Perez-Ruiz F, Aniel-Quiroga MA, Herrero-Beites AM, Chinchilla SP, Erauskin GG, Merriman T. Renal Clearance of Uric Acid is Linked to Insulin Resistance and Lower Excretion of Sodium in Gout Patients. *Rheumatol Int* (2015) 35(9):1519–24. doi: 10.1007/s00296-015-3242-0
27. Liu J, Zhang L, Fu J, Wang Q, Wang G. Circulating Prolactin Level is Increased in Metabolically Healthy Obesity. *Endocr Connect* (2021) 10 (4):484–91. doi: 10.1530/EC-21-0040
28. Bian N, Sun X, Zhou B, Zhang L, Wang Q, An Y, et al. Obese Patients With Higher TSH Levels had an Obvious Metabolic Improvement After Bariatric Surgery. *Endocr Connect* (2021) 10(10):1326–36. doi: 10.1530/EC-21-0360
29. Sun H, Wang N, Chen C, Nie X, Han B, Li Q, et al. Cadmium Exposure and its Association With Serum Uric Acid and Hyperuricemia. *Sci Rep* (2017) 7 (1):550. doi: 10.1038/s41598-017-00661-3
30. Zhou BF. Effect of Body Mass Index on All-Cause Mortality and Incidence of Cardiovascular Diseases–Report for Meta-Analysis of Prospective Studies Open Optimal Cut-Off Points of Body Mass Index in Chinese Adults. *BioMed Environ Sci* (2002) 15(3):245–52.
31. Tsushima Y, Nishizawa H, Tochino Y, Nakatsuji H, Sekimoto R, Nagao H, et al. Uric Acid Secretion From Adipose Tissue and its Increase in Obesity. *J Biol Chem* (2013) 288(38):27138–49. doi: 10.1074/jbc.M113.485094
32. Baldwin W, McRae S, Marek G, Wymer D, Pannu V, Baylis C, et al. Hyperuricemia as a Mediator of the Proinflammatory Endocrine Imbalance in the Adipose Tissue in a Murine Model of the Metabolic Syndrome. *Diabetes* (2011) 60(4):1258–69. doi: 10.2337/db10-0916
33. Li F, Chen S, Qiu X, Wu J, Tan M, Wang M. Serum Uric Acid Levels and Metabolic Indices in an Obese Population: A Cross-Sectional Study. *Diabetes Metab Syndr Obes* (2021) 14:627–35. doi: 10.2147/DMSO.S286299
34. Tsunoda S, Kamide K, Minami J, Kawano Y. Decreases in Serum Uric Acid by Amelioration of Insulin Resistance in Overweight Hypertensive Patients: Effect of a Low-Energy Diet and an Insulin-Sensitizing Agent. *Am J Hypertens* (2002) 15(8):697–701. doi: 10.1016/s0895-7061(02)02953-9
35. Fabbrini E, Serafini M, Colic Baric I, Hazen SL, Klein S. Effect of Plasma Uric Acid on Antioxidant Capacity, Oxidative Stress, and Insulin Sensitivity in Obese Subjects. *Diabetes* (2014) 63(3):976–81. doi: 10.2337/db13-1396
36. Wan X, Xu C, Lin Y, Lu C, Li D, Sang J, et al. Uric Acid Regulates Hepatic Steatosis and Insulin Resistance Through the NLRP3 Inflammasome-Dependent Mechanism. *J Hepatol* (2016) 64(4):925–32. doi: 10.1016/j.jhep.2015.11.022

37. Dawson J, Wyss A. Chicken or the Egg? Hyperuricemia, Insulin Resistance, and Hypertension. *Hypertension* (2017) 70(4):698–9. doi: 10.1161/HYPERTENSIONAHA.117.09685
38. Quinones Galvan A, Natali A, Baldi S, Frascerra S, Sanna G, Ciociaro D, et al. Effect of Insulin on Uric Acid Excretion in Humans. *Am J Physiol* (1995) 268 (1 Pt 1):E1–5. doi: 10.1152/ajpendo.1995.268.1.E1
39. Vuorinen-Markkola H, Yki-Jarvinen H. Hyperuricemia and Insulin Resistance. *J Clin Endocrinol Metab* (1994) 78(1):25–9. doi: 10.1210/jcem.78.1.8288709
40. Liu XZ, Li HH, Huang S, Zhao DB. Association Between Hyperuricemia and Nontraditional Adiposity Indices. *Clin Rheumatol* (2019) 38(4):1055–62. doi: 10.1007/s10067-018-4374-x
41. Takahashi S, Yamamoto T, Tsutsumi Z, Moriwaki Y, Yamakita J, Higashino K. Close Correlation Between Visceral Fat Accumulation and Uric Acid Metabolism in Healthy Men. *Metabolism* (1997) 46(10):1162–5. doi: 10.1016/s0026-0495(97)90210-9
42. Gastaldelli A, Harrison SA, Belfort-Aguilar R, Hardies LJ, Balas B, Schenker S, et al. Importance of Changes in Adipose Tissue Insulin Resistance to Histological Response During Thiazolidinedione Treatment of Patients With Nonalcoholic Steatohepatitis. *Hepatology* (2009) 50(4):1087–93. doi: 10.1002/hep.23116
43. Lomonaco R, Ortiz-Lopez C, Orsak B, Webb A, Hardies J, Darland C, et al. Effect of Adipose Tissue Insulin Resistance on Metabolic Parameters and Liver Histology in Obese Patients With Nonalcoholic Fatty Liver Disease. *Hepatology* (2012) 55(5):1389–97. doi: 10.1002/hep.25539
44. Brassard P, Frisch F, Lavoie F, Cyr D, Bourbonnais A, Cunnane SC, et al. Impaired Plasma Nonesterified Fatty Acid Tolerance is an Early Defect in the Natural History of Type 2 Diabetes. *J Clin Endocrinol Metab* (2008) 93 (3):837–44. doi: 10.1210/jc.2007-1670
45. Jorge-Galarza E, Posadas-Romero C, Torres-Tamayo M, Medina-Urrutia AX, Rodas-Diaz MA, Posadas-Sanchez R, et al. Insulin Resistance in Adipose Tissue But Not in Liver Is Associated With Aortic Valve Calcification. *Dis Markers* (2016) 2016:9085474. doi: 10.1155/2016/9085474
46. Chen LK, Lin MH, Lai HY, Hwang SJ, Chiou ST. Uric Acid: A Surrogate of Insulin Resistance in Older Women. *Maturitas* (2008) 59(1):55–61. doi: 10.1016/j.maturitas.2007.10.006
47. Tian S, Liu Y, Feng A, Zhang S. Sex-Specific Differences in the Association of Metabolically Healthy Obesity With Hyperuricemia and a Network Perspective in Analyzing Factors Related to Hyperuricemia. *Front Endocrinol (Lausanne)* (2020) 11:573452. doi: 10.3389/fendo.2020.573452
48. Yuan HJ, Yang XG, Shi XY, Tian R, Zhao ZG. Association of Serum Uric Acid With Different Levels of Glucose and Related Factors. *Chin Med J (Engl)* (2011) 124(10):1443–8. doi: 10.3760/cma.j.issn.0366-6999.2011.10.001
49. Haque T, Rahman S, Islam S, Molla NH, Ali N. Assessment of the Relationship Between Serum Uric Acid and Glucose Levels in Healthy, Prediabetic and Diabetic Individuals. *Diabetol Metab Syndr* (2019) 11:49. doi: 10.1186/s13098-019-0446-6
50. Larsson SC, Burgess S, Michaelsson K. Genetic Association Between Adiposity and Gout: A Mendelian Randomization Study. *Rheumatol (Oxford)* (2018) 57 (12):2145–8. doi: 10.1093/rheumatology/key229

Conflict of Interest: The authors declare that the research was conducted in the absence of any commercial or financial relationships that could be construed as a potential conflict of interest.

Publisher's Note: All claims expressed in this article are solely those of the authors and do not necessarily represent those of their affiliated organizations, or those of the publisher, the editors and the reviewers. Any product that may be evaluated in this article, or claim that may be made by its manufacturer, is not guaranteed or endorsed by the publisher.

frontiers | Frontiers in Endocrinology

ORIGINAL RESEARCH
published: 30 June 2022
doi: 10.3389/fendo.2022.865930

Subcutaneous Adipose Tissue Accumulation Is an Independent Risk Factor of Urinary Stone in Young People

Zixing Ye[1], He Xiao[1], Guanghua Liu[1], Yi Qiao[1], Yi Zhao[1], Zhigang Ji[1], Xiaohong Fan[2], Rongrong Li[3] and Ou Wang[4]*

[1] Department of Urology, Peking Union Medical College Hospital, Beijing, China, [2] Department of Nephrology, Peking Union Medical College Hospital, Beijing, China, [3] Department of Clinical Nutrition, Peking Union Medical College Hospital, Beijing, China, [4] Department of Endocrinology, Peking Union Medical College Hospital, Beijing, China

Background: Urinary stones usually start at a young age and tend to recur. Therefore, preventing stone occurrence and recurrence in young people is crucial. We aimed to investigate the association between subcutaneous adipose tissue, visceral adipose tissue, and stone episodes in young people.

Methods: We retrospectively studied patients aged below 40 years with kidney or ureteral stones. Data on demographic and metabolic characteristics, urolithiasis history, subcutaneous fat area (SFA), and visceral fat area (VFA) were collected. We evaluated the association between SFA or VFA and the occurrence or recurrence of stone episodes using binary logistic regression and Poisson regression analyses.

Results: In total, 120 patients were included. Abdominal obesity, overweight or obesity, dyslipidemia, metabolic syndrome, SFA, and VFA increased with the number of stone episodes (all $p < 0.05$). The increase in SFA was independently associated with episode occurrence ($p = 0.015$). Patients with an SFA > 97 cm^2 had a higher risk of episode occurrence. SFA and VFA accumulation were independently associated with episode recurrence (all $p < 0.05$), and SFA had a stronger association than VFA did.

Conclusions: In young people, SFA accumulation is an independent and early risk factor for the occurrence and recurrence of stone episodes. Subcutaneous fat could be a convenient and effective indicator to assess the risk of stone episodes before the development of metabolic disorders.

Keywords: subcutaneous adipose tissue, metabolic disease, fat distribution, urinary stone, stone episode

OPEN ACCESS

Edited by:
Dirk Müller-Wieland, University Hospital RWTH Aachen, Germany

Reviewed by:
Yong Zhang, Capital Medical University, China
Yi Zhang, Peking University, China

***Correspondence:**
He Xiao
xiaoh@pumch.cn

Specialty section:
This article was submitted to Obesity, a section of the journal Frontiers in Endocrinology

Received: *30 January 2022*
Accepted: *31 May 2022*
Published: *30 June 2022*

Citation:
Ye Z, Xiao H, Liu G, Qiao Y, Zhao Y, Ji Z, Fan X, Li R and Wang O (2022) Subcutaneous Adipose Tissue Accumulation Is an Independent Risk Factor of Urinary Stone in Young People. Front. Endocrinol. 13:865930. doi: 10.3389/fendo.2022.865930

INTRODUCTION

Urolithiasis is one of the diseases that often affect young people. Among people under 40 years of age, nearly 1 in 10 suffers from urolithiasis (1, 2). Young people are the main workforce in society, and an early onset of stones may affect their work and personal lives constantly. The prevention of stone occurrence in young people is also more cost-effective than management of stones in elderly

people. Therefore, it is important to study and reduce the risk factors of urinary stones in young people. Many studies have shown the relationship between urolithiasis and metabolic disorders, especially metabolic syndrome (MetS) (3–5). Therefore, the earlier the metabolic disorder is controlled, the more likely it is to prevent urinary stones. However, most of the metabolic disorders that are found to be related to urinary stones are the result of a long-term decompensation of the metabolic system. Few studies have investigated stone formation in young people. The accumulation of subcutaneous adipose tissue (SAT) occurs when the metabolic imbalance is compensable. Some studies on Asian and African populations have shown a relationship between SAT and MetS (6–8). However, current studies seem to show that visceral adipose tissue (VAT) is more closely related than SAT to stone formation in patients of all ages. Most current studies have investigated the effect of metabolic disorders on the urinary component instead of the stone episodes that really affected young people's quality of life and work.

In this study, we aimed to investigate the association between SAT, VAT, and urinary stone episodes, with the intention of identifying the risk factors of the stone episodes, and then provide effective methods and a theoretical basis for stone prevention among young individuals.

MATERIALS AND METHODS

Patients

This was a retrospective study involving patients from PRE-STONE, a metabolic evaluation database established by Peking Union Medical College Hospital. The inclusion criteria for the patients were as follows: the patients had to be (1) aged 18 years or over but below 40 years; (2) diagnosed with kidney or ureteral stone by either a definite kidney or ureteral stone history or abdominopelvic non-contrast computed tomography (NCCT); and (3) have completed metabolic evaluation in our hospital between May 2016 and January 2019. The exclusion criteria were as follows: (1) patients on lipid-lowering medications; (2) patients taking stone-related medications such as potassium citrate, allopurinol, or thiazides; (3) patients with a known metabolic or anatomic cause of urolithiasis; or (4) patients with a history of bariatric surgery or surgery in the upper urinary tract. A stone episode was defined as the onset of renal colic, hematuria, hydronephrosis, UTI, or flank pain related to urinary stones. The occurrence of stone episodes was defined as the presence of at least one stone episode. Recurrence of stone episodes was defined as the occurrence of at least two episodes. Only stone episodes that occurred in the past 10 years were considered for the purposes of this study.

Data Collection

Demographic and clinical data, including age, gender, history of stone episodes, family history of kidney or ureteral stone, past medical history, medications, vital signs, laboratory blood tests, and imaging examinations were recorded. Two urologists, both with three years of experience in the metabolic evaluation of urinary stones, collected the demographic and clinical data, and evaluated the history of SF with regard to stone episodes by face-to-face consultation. The results of blood tests were collected from clinical laboratory, and imaging examinations were collected from Picture Archiving and Communication Systems (PACS).

Diagnostic Criteria

The definition of MetS proposed by International Diabetes Federation in 2005 (9) was adopted. In this study, a body mass index (BMI) of 28 kg/m^2 or more was considered obesity and a BMI of 24 kg/m^2 or more, but less than 28 kg/m^2, was considered overweight (10). Abdominal obesity was defined as a waist circumference of 90 cm or more in males and 80 cm or more in females (11). Diabetes mellitus (DM) was considered if the patient had a fasting blood glucose level of 7.0 mmol/L or more, or a history of DM, or was taking antidiabetic medications (12). Dyslipidemia was defined as the occurrence of one of the following disorders: hypercholesterolemia (>5.17 mmol/L), hypertriglyceridemia (≥ 1.7 mmol/L), low levels of high-density lipoprotein cholesterol (<1.04 mmol/L for males and <1.30 mmol/L for females), or high levels of low-density lipoprotein cholesterol (>3.36 mmol/L) (13). Renal insufficiency was considered with estimated glomerular filtration rate (eGFR) <90 mL/min (14). The value of eGFR was calculated using the Modification of Diet in Renal Disease (MDRD) Study equation (15).

Visceral and Subcutaneous Adipose Tissue Assessment

Visceral fat area (VFA) and subcutaneous fat area (SFA) were measured at the umbilical level on an NCCT axial slice and used as an indicator to estimate the total amount of abdominal VAT and SAT. The adipose tissue area was delineated by two urologists using ImageJ software (http://rsb.info.nih.gov/ij/). The VFA and SFA were measured as pixels within an attenuation range of −250 to −50 Hounsfield units, also using the ImageJ software (16). The data of SFA and VFA were converted to one tenth of the original value (10 cm^2). All NCCT examinations were performed using a third-generation dual-source computed tomographic (CT) system (Somatom Force, Siemens Healthcare, Forchheim, Germany) with a regular dose of 120 kV and a slice thickness of 5 mm. The scan was performed by technicians in the Department of Radiology of our hospital.

Statistical Analysis

Demographic and clinical data were expressed as means ± standard deviation for continuous variables with a normal distribution and as percentage for categorical variables. Between-group comparisons for categorical variables were performed using chi-squared test. One-way analysis of variance (ANOVA) was used for evaluation of continuous variables with a normal distribution, and non-parametric analysis was performed for continuous variables with an abnormal distribution. The association between the occurrence or recurrence of stone

episode and SFA or VFA was calculated using the binary logistic regression model (age, gender, family history of stone, MetS, and renal insufficiency were included as covariates). The association between SFA or VFA and the number of stone episodes was assessed using Poisson regression. Covariates in Poisson regression included age, gender, family history of stone, MetS, and renal insufficiency. A receiver-operating characteristic (ROC) curve analysis was used to evaluate the effects of SFA and VFA in estimating the occurrence of stone episode. The area under the curve (AUC) was used to evaluate the performance of variables in identifying stone episodes. All tests were of two-tailed type, and a *p* value of <0.05 was considered statistically significant. Statistical analysis was performed using IBM SPSS Statistics for Windows, version 23.0 (IBM Corp., Armonk, NY, USA).

RESULTS

Demographic and Metabolic Characteristics

Based on the inclusion criteria, 131 patients were included in this study. Of these, 11 were excluded, including nine patients who had a known metabolic or anatomic cause of urolithiasis (five patients with polycystic kidney, two with medullary sponge kidney, one with calyceal diverticula, and one with renal tubular acidosis), one patient who was using the lipid-lowering medication atorvastatin, and one who was using stone-related medication potassium citrate. Therefore, a total of 120 patients, including 86 (71.7%) men and 34 (28.3%) women, were enrolled in this study. The patients had an average age of 31.9 ± 5.2 years. We observed that the proportion of abdominal obesity, overweight or obesity, dyslipidemia, and MetS, as well as the values of SFA and VFA, increased significantly with the increase in the number of stone episodes ($p < 0.05$). However, there were no statistical differences between stone episodes and family history, hypertension, DM, or renal insufficiency ($p > 0.05$; **Table 1**).

SFA Accumulation as an Independent Risk Factor of Stone Episode Occurrence and Recurrence

In all SFs, the increase in SFA was significantly associated with the occurrence of stone episodes (OR, 1.150; 95% CI, 1.028–1.286; p = 0.015) after adjustment. These factors, including MetS (OR, 3.271; 95% CI, 0.858–12.463; p = 0.083), were not related to the occurrence of stone episodes. Even in SFs without MetS, the increase in SFA was still significantly associated to the occurrence of stone episodes after adjustment (OR, 1.131; 95% CI, 1.006–1.271; p = 0.039). No significant association was found between VFA and the occurrence of stone episodes ($p > 0.05$; **Table 2**).

SFA and VFA were all associated with the recurrence of stone episodes, and SFA has a stronger association (OR, 1.145; 95% CI, 1.021–1.284; p = 0.021) than VFA (OR, 1.113; 95% CI, 1.035–1.197; p = 0.004) after adjustment. In SFs without MetS, SFA is still associated with the recurrence of stone episode (OR, 1.115; 95% CI, 1.004–1.239; p = 0.042), although the relationship was not statistically significant after the adjustment ($p > 0.05$; **Table 3**).

The Poisson regression in **Table 4** showed a significant association between SFA and number of stone episodes in all SFs (beta, 1.037; 95% CI, 1.000–1.076; p = 0.049). The number of stone episodes increased by 3.7% on average for every 10 cm^2

TABLE 1 | Demographic and metabolic characteristics of SFs with different stone episodes.

Characteristics	All patients	Number of stone episodes			
		Asymptomatic	Once	Twice or more	*p*
Number of patients	120	48	38	34	
Gender (male/female; male [%])	86/34 [71.7]	29/19 [60.4]	29/9 [76.3]	28/6 [82.4]	0.025
Age (year)	31.9 ± 5.2*	30.40 ± 5.26	32.66 ± 5.25	33.1 ± 4.6	0.037
Family history (n [%])	50 [41.7]	21 [43.8]	27 [71.1]	18 [52.9]	0.111
BMI (kg/m^2)	25.4 ± 4.0	24.0 ± 3.9	24.9 ± 3.1	27.7 ± 4.1	< 0.001
Abdominal obesity (n [%])	53 [44.2]	12 [25.0]	17 [44.7]	24 [70.6]	< 0.001
Overweight or obesity (n [%])	79 [65.8]	25 [52.1]	24 [63.2]	30 [88.2]	0.003
Hypertension (n [%])	30 [25.0]	8 [16.7]	11 [28.9]	11 [32.4]	0.215
DM (n [%])	6 [5.8]	0 [0.0]	2 [5.6]	4 [11.8]	0.087
Dyslipidemia (n [%])	80 [66.7]	23 [47.9]	27 [71.1]	30 [88.2]	0.001
MetS (n [%])	35 [29.2]	4 [8.3]	12 [31.6]	19 [55.9]	< 0.001
Renal insufficiency (n [%])	25 [23.1]	9 [23.7]	7 [28.0]	9 [26.5]	0.707
VFA (10 cm^2)	19.2 ± 9.6	17.1 ± 7.7	16.6 ± 7.1	25.0 ± 11.8	0.001
SFA (10 cm^2)	10.5 ± 5.9	8.0 ± 5.1	10.7 ± 5.4	13.9 ± 6.0	< 0.001

**Mean ± SD (all such value).*

Continuous variables with a normal distribution were expressed as means ± standard deviation, categorical variables were expressed as percentage. Chi-squared test was used for between-group comparisons of categorical variables. One-way analysis of variance (ANOVA) was used for evaluation of continuous variables with a normal distribution, and non-parametric analysis was used for continuous variables with an abnormal distribution. The p value was considered significant if less than 0.05.

DM, diabetes mellitus; MetS, metabolic syndrome; SF, stone former; SFA, subcutaneous fat area; VFA, visceral fat area.

TABLE 2 | The relationship between SFA, VFA, and the occurrence of stone episode.

Variables	All SFs				SFs without MetS			
	Unadjusted		Adjusted[¶]		Unadjusted		Adjusted[§]	
	OR (95%CI)	*p*	OR (95%CI)	*p*	OR (95%CI)	*p*	OR (95%CI)	*p*
SFA	1.159 (1.070–1.254)	< 0.001	1.150 (1.028–1.286)	0.015	1.092 (1.013–5.691)	0.047	1.131 (1.006–1.271)	0.039
VFA	1.043 (0.999–1.090)	0.058	1.014 (0.954–1.077)	0.658	0.985 (0.929–1.044)	0.614	0.991 (0.922–1.066)	0.813

[¶]*Adjusted for age, gender, family history of stone, MetS, and renal insufficiency.*
[§]*Adjusted for age, gender, family history of stone, and renal insufficiency.*
The binary logistic regression model was used to assess the association between the occurrence of stone episode and SFA or VFA.
OR, odds ratio; CI, confidence interval; MetS, metabolic syndrome; SF, stone former.

increase in the SFA (p = 0.049) after adjustment. The association between SFA and the number of stone episodes was also significant before adjustment (beta, 1.054; 95% CI, 1.006–1.104; p = 0.026) and less statistically significant after adjustment (beta, 1.058; 95% CI, 0.998–1.121; p = 0.060) in SFs without MetS. However, no significant association was observed between VFA and the number of stone episodes (p > 0.05).

SFA as an Indicator to Identify the Occurrence of Stone Episodes

In this study, ROC curves were plotted to compare between VFA and SFA in terms of the predictive power for the occurrence of the stone episode. The ROC curve analysis with the AUC of VFA and SFA are demonstrated in **Figure 1**. The AUC of SFA (AUC_{SFA} = 0.718; 95% CI, 0.624–0.812) was significantly more than the AUC of VFA (AUC_{VFA} = 0.594; 95% CI, 0.490–0.698), and SFA was adopted as an indicator of the stone episode occurrence. The cutoff point of SFA for predicting the occurrence of stone episode was 97 cm^2 in all SFs based on ROC curve analysis, with sensitivity of 72.2%, specificity of 66.7%, and the Youden index of 0.389; while the cutoff point of VFA was 174 cm^2, with a sensitivity of 61.1%, specificity of 56.2%, and a Youden index of 0.173.

DISCUSSION

Many studies have shown the association between urolithiasis and MetS or its components (3–5). VAT seems to have a closer relationship with urinary stone than SAT does among people of all ages (17–19). SAT is insulin-sensitive and is considered an "energy sink" to store excess energy physiologically, the visceral fat begins to increase when the subcutaneous adipose tissue is unable to handle the calorie surplus due to excess energy accumulation (6).Thus, the accumulation of SAT should happen earlier than the increase in VAT and MetS. Theoretically, it should be more effective to reduce the risk of

TABLE 3 | The relationship between SFA, VFA, and the recurrence of stone episode.

Variables	All SFs				SFs without MetS			
	Unadjusted		Adjusted[¶]		Unadjusted		Adjusted[§]	
	OR (95%CI)	*p*	OR (95%CI)	*p*	OR (95%CI)	*p*	OR (95%CI)	*p*
SFA	1.162 (1.069–1.262)	< 0.001	1.145 (1.021–1.284)	0.021	1.115 (1.004–1.239)	0.042	1.142 (0.981–1.328)	0.086
VFA	1.100 (1.045–1.156)	< 0.001	1.113 (1.035–1.197)	0.004	1.052 (0.981–1.129)	0.155	1.075 (0.977–1.183)	0.137

[¶]*Adjusted for age, gender, family history of stone, MetS, and renal insufficiency.*
[§]*Adjusted for age, gender, family history of stone, and renal insufficiency.*
The binary logistic regression model was used to assess the association between the recurrence of stone episode and SFA or VFA.
OR, Odds ratio; CI, Confidence interval; MetS, metabolic syndrome; SF, stone former.

TABLE 4 | The relationship between SFA, VFA, and the number of stone episodes in all SFs and those without MetS.

Variables	All SFs				SFs without MetS			
	Unadjusted		Adjusted[¶]		Unadjusted		Adjusted[§]	
	Exp(β) (95% CI)	*p*	Exp(β) (95% CI)	*p*	Exp(β) (95% CI)	*p*	Exp(β) (95% CI)	*p*
SFA	1.056 (1.027–1.085)	< 0.001	1.037 (1.000–1.076)	0.049	1.054 (1.006–1.104)	0.026	1.058 (0.998–1.121)	0.060
VFA	1.026 (1.009–1.044)	0.002	1.018 (0.997–1.039)	0.100	1.007 (0.972–1.042)	0.709	1.011 (0.971–1.051)	0.599

[¶]*Adjusted for age, gender, family history of kidney stone, MetS, and renal insufficiency.*
[§]*Adjusted for age, gender, family history of kidney stone, and renal insufficiency.*
Poisson regression was used to evaluate the association between the number of stone episodes and SFA or VFA.
CI, confidence interval; MetS, metabolic syndrome; SF, stone former.

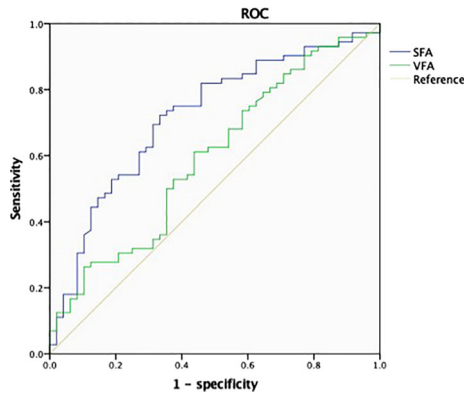

FIGURE 1 | Receiver operating characteristic (ROC) analysis and area under the curve (AUC) for the predictors of the occurrence of stone episode. The AUC values of subcutaneous fat area (SFA) and (visceral fat area) VFA were 0.718 and 0.594 with 95% confidence interval (CI) of 0.624–0.812 and 0.490–0.698, respectively. The cutoff point of SFA was 97 cm^2 and that of VFA was 174 cm^2. ROC analysis was performed for the occurrence of stone episode based on sensitivity of 72.2%, specificity of 66.7%, and the Youden index of 0.389 for SFA and sensitivity of 61.1%, specificity of 56.2%, and the Youden index of 0.173 for VFA.

stone episodes by reducing the SAT when the SFs are young. However, few studies have reported the association between SAT and stone episodes among young people.

Metabolic disorders are associated with stone episodes. Demographic results in this study showed that the prevalence of abdominal obesity, overweight or obesity, dyslipidemia, and MetS significantly increased with the number of stone episodes in young SFs ($p < 0.05$). This is consistent with the current understanding that metabolic disorders are associated with urolithiasis in SFs of all ages (3, 20). However, there are still some controversies on the effect of hypertension and DM on urolithiasis (21). A prospective study showed that hypertensive patients tended to have a higher risk of stone formation; however, SFs in this hypertensive group also had a higher unadjusted BMI, which was also the risk factor of urolithiasis (22). The prospective studies performed by Madore also showed that kidney stones preceded the development of hypertension (23, 24). In our study, the proportion of DM and hypertension increased with stone episodes; however, statistical significance was not achieved. This result may partly be attributed to the fact that urolithiasis and hypertension may share some risk factors, and a larger sample size is needed in further studies.

Accumulation of SAT was independently related to the occurrence of stone episodes in young SFs. In our study, we found that SFA was related to the occurrence of stone episodes independent of MetS in young SFs. This was consistent with the fact that SAT accumulation occurs earlier than MetS (6). Previous studies did not show the relationship between SFA and episode occurrence in SFs of all ages. This may be because as the SAT increases with age, the difference of SAT reduces among elder SFs. Therefore, it would be more effective to reduce SAT accumulation than to treat MetS to prevent the occurrence of stone episodes. Furthermore, the ROC curve showed that SFA is superior to VFA as an indicator of the occurrence of stone episodes in young SFs. Only one cutoff value of VFA had been proposed prior to our study to evaluate the risk of urolithiasis, and VFA categorization was not based on the predictive efficacy of VFA on real-world stone episodes or 24-h urinary abnormalities (25). Based on our results of the AUC analysis, we proposed the first cutoff value of SFA to predict the occurrence of stone episode, and suggested that SFs with an SFA of >97 cm^2 were more likely to experience stone episodes. The clinical value of our results is that young SFs may be able to prevent stone episodes that may affect their quality of life by reducing SFA.

Fujimura et al. found that visceral fat accumulation was significantly related to stone formation in male patients (95% CI, 1.009–1.021; $p < 0.001$) (17). Some studies also showed that VFA was related to abnormal urine components. Fram et al. suggested that VFA was significantly associated with an increased excretion of urine sodium in male patients with either normal or increased BMI (19). However, our study showed no significant association between the VFA and the occurrence of stone episodes. This may be explained by the fact that the accumulation of VAT occurs later than that of SAT and the increasing of VAT is generally not so evident among young SFs. Moreover, the patients' work and quality of life were not affected by abnormal urine components. Few studies have studied the effect of VAT on stone episodes in young SFs. Further investigation may be required to determine the clinical significance of VAT in young SFs.

Both SFA and VFA were independently related to the recurrence of stone episodes, and SFA had a closer relationship with stone recurrence than VFA did in our study. Yamashita and Bos both found that recurrent SFs had a higher %VFA (% VFA=VFA/[VFA + SFA]) than first-time SFs of all ages (16, 26). Several studies have shown a correlation between metabolic disorders and stone recurrence as well (27, 28). However, the SFs in above-mentioned studies were in their fifties, much older than SFs in our study. The accumulation of SAT begins earlier than VAT, thus the difference in SFA between SFs with and without recurrence of stones tends to be more significant than the difference in VFA. Similarly, we found that the SFA was associated with the number of stone episodes in all SFs, which increased at an average of 3.7% per 10 cm^2 of SFA. This suggested that a slight increment in the SFA might increase the risk of stone episodes, which highlights the significance of controlling the SAT in young SFs. Although the association between SFA and the number of stone episodes was less significant after adjustment, this might due to the small sample size.

Race may also be an important factor for the closer relationship of the occurrence and recurrence of stone episodes with SFA. Previous studies have shown that VFA or %VFA were associated with stone formation or recurrence; however, most of these studies were performed in Caucasian populations (16, 19). Some studies showed that SAT was related to MetS in Asians and Africans (7, 8). Therefore, more studies are needed to verify the relationship between SAT and urinary stones in both young and elderly Chinese individuals.

We found that SFA was a better independent indicator than VFA in assessing the risk of occurrence and recurrence of stone episodes and the number of stone episodes in young SFs. Based on this finding, young SFs could assess their risk of occurrence and recurrence of stone episodes simply by measuring their abdominal subcutaneous fat in a quick test. This will enable young SFs to take actions to prevent future stone episodes as early as the compensation state of metabolic imbalance, instead of waiting until MetS develops.

Our study has a few limitations. First, it was a single-center retrospective study, and all subjects enrolled in this study were SFs. Patients who did not or were unwilling to complete the metabolic evaluation were not included. Second, the number of patients enrolled in this study was relatively small; therefore, a larger sample size is needed to verify the results.

CONCLUSION

The accumulation of SFA is an independent risk factor for the occurrence and recurrence of stone episodes in young people. Self-measurement of subcutaneous fat may be a very simple and effective method to assess the risk of stone episodes and could help prevent their occurrence or recurrence even before the development of metabolic disorders. The association between stone episodes and SFA may also help further explore the mechanism of urolithiasis.

DATA AVAILABILITY STATEMENT

The raw data supporting the conclusions of this article will be made available by the authors, without undue reservation.

ETHICS STATEMENT

This study was reviewed and approved by the Institutional Review Board of Peking Union Medical College Hospital (Protocol number: S-K1961). All data was collected after obtaining signed informed consent of the patients.

AUTHOR CONTRIBUTIONS

Study design: ZY, YQ, and HX; data collection: YZ, HX, GL, YQ, YZ, ZJ, XF, RL, and OW; data analysis: ZY, HX, and GL; statistical analysis and data interpretation: ZY and YZ; literature search: ZY, HX, GL, YQ, YZ, XF, RL, and OW; generation of figures: ZY and HX; writing of the manuscript: ZY and HX. All authors had final approval of the submitted and published versions.

FUNDING

This research was supported by The National Key Research and Development Program of China (2021YFC2009300, 2021YFC2009306).

ACKNOWLEDGMENTS

The author would like to thank everyone who participated in the study.

REFERENCES

1. Sakhaee K, Maalouf NM, Sinnott B. Clinical Review. Kidney Stones 2012: Pathogenesis, Diagnosis, and Management. *J Clin Endocrinol Metab* (2012) 97 (6):1847–60. doi: 10.1210/jc.2011-3492
2. Wang W, Fan J, Huang G, Li J, Zhu X, Tian Y, et al. Prevalence of Kidney Stones in Mainland China: A Systematic Review. *Sci Rep* (2017) 7:41630. doi: 10.1038/srep41630
3. Khan SR, Pearle MS, Robertson WG, Gambaro G, Canales BK, Doizi S, et al. Kidney Stones. *Nat Rev Dis Primers* (2016) 2:16008. doi: 10.1038/nrdp.2016.8
4. West B, Luke A, Durazo-Arvizu RA, Cao G, Shoham D, Kramer H. Metabolic Syndrome and Self-Reported History of Kidney Stones: The National Health and Nutrition Examination Survey (NHANES III) 1988-1994. *Am J Kidney Dis* (2008) 51(5):741–7. doi: 10.1053/j.ajkd.2007.12.030
5. Jeong IG, Kang T, Bang JK, Park J, Kim W, Hwang SS, et al. Association Between Metabolic Syndrome and the Presence of Kidney Stones in a Screened Population. *Am J Kidney Dis* (2011) 58(3):383–8. doi: 10.1053/j.ajkd.2011.03.021
6. Després J-P, Lemieux I. Abdominal Obesity and Metabolic Syndrome. *Nature* (2006) 444(7121):881–7. doi: 10.1038/nature05488
7. Goel K, Misra A, Vikram NK, Poddar P, Gupta N. Subcutaneous Abdominal Adipose Tissue Is Associated With the Metabolic Syndrome in Asian Indians Independent of Intra-Abdominal and Total Body Fat. *Heart (British Cardiac Soc)* (2010) 96(8):579–83. doi: 10.1136/hrt.2009.183236
8. Matsha TE, Ismail S, Speelman A, Hon GM, Davids S, Erasmus RT, et al. Visceral and Subcutaneous Adipose Tissue Association With Metabolic Syndrome and its Components in a South African Population. *Clin Nutr ESPEN* (2019) 32:76–81. doi: 10.1016/j.clnesp.2019.04.010
9. Alberti KG, Zimmet P, Shaw J. The Metabolic Syndrome–a New Worldwide Definition. *Lancet (London England)* (2005) 366(9491):1059–62. doi: 10.1016/S0140-6736(05)67402-8
10. Zhou BF. Predictive Values of Body Mass Index and Waist Circumference for Risk Factors of Certain Related Diseases in Chinese Adults–Study on Optimal Cut-Off Points of Body Mass Index and Waist Circumference in Chinese Adults. *Biomed Environ Sci BES* (2002) 15(1):83–96.
11. World Health Organization. Regional Office for the Western Pacific. (2000). The Asia-Pacific Perspective : Redefining Obesity and Its Treatment. Sydney: *Health Communications Australia*. Available at: https://apps.who.int/iris/handle/10665/206936.
12. Orgnization WH. *Definition and Diagnosis of Diabetes Mellitus and Intermediate Hyperglycemia: Report of a WHO/IDF Consultation*. Geneva: WHO Document Production Services (2006).
13. Grundy SM, Cleeman JI, Merz CN, Brewer HB Jr., Clark LT, Hunninghake DB, et al. Implications of Recent Clinical Trials for the National Cholesterol Education Program Adult Treatment Panel III Guidelines. *J Am Coll Cardiol* (2004) 44(3):720–32. doi: 10.1016/j.jacc.2004.07.001
14. National Kidney Foundation. K/DOQI Clinical Practice Guidelines for Chronic Kidney Disease: Evaluation, Classification, and Stratification. *Am J Kidney Dis* (2002) 39(2 Suppl 1):S1–266.
15. Levey AS, Bosch JP, Lewis JB, Greene T, Rogers N, Roth D. A More Accurate Method to Estimate Glomerular Filtration Rate From Serum Creatinine: A New Prediction Equation. *Modification Diet Renal Dis Study Group Ann Intern Med* (1999) 130(6):461–70. doi: 10.7326/0003-4819-130-6-199903160-00002
16. Bos D, Dason S, Matsumoto E, Pinthus J, Allard C. A Prospective Evaluation of Obesometric Parameters Associated With Renal Stone Recurrence. *Can Urol Assoc J* (2016) 10(7-8):234–8. doi: 10.5489/cuaj.3876
17. Fujimura M, Sakamoto S, Sekita N, Mikami K, Ichikawa T, Akakura K. Visceral Fat Accumulation is a Risk Factor for Urinary Stone. *Int J Urol* (2014) 21(11):1184–5. doi: 10.1111/iju.12556
18. Kim JH, Doo SW, Yang WJ, Song YS, Hwang J, Hong SS, et al. The Relationship Between Urinary Stone Components and Visceral Adipose

Tissue Using Computed Tomography–Based Fat Delineation. *Urology* (2014) 84(1):27–31. doi: 10.1016/j.urology.2014.01.026
19. Fram EB, Agalliu I, DiVito J, Hoenig DM, Stern JM. The Visceral Fat Compartment Is Independently Associated With Changes in Urine Constituent Excretion in a Stone Forming Population. *Urolithiasis* (2015) 43(3):213–20. doi: 10.1007/s00240-015-0770-8
20. Wong Y, Cook P, Roderick P, Somani BK. Metabolic Syndrome and Kidney Stone Disease: A Systematic Review of Literature. *J Endourol* (2016) 30 (3):246–53. doi: 10.1089/end.2015.0567
21. Taylor EN, Stampfer MJ, Curhan GC. Diabetes Mellitus and the Risk of Nephrolithiasis. *Kidney Int* (2005) 68(3):1230–5. doi: 10.1111/j.1523-1755.2005.00516.x
22. Borghi L, Meschi T, Guerra A, Briganti A, Schianchi T, Allegri F, et al. Essential Arterial Hypertension and Stone Disease. *Kidney Int* (1999) 55 (6):2397–406. doi: 10.1046/j.1523-1755.1999.00483.x
23. Madore F, Stampfer MJ, Rimm EB, Curhan GC. Nephrolithiasis and Risk of Hypertension. *Am J Hyperten* (1998) 11(1 Pt 1):46–53. doi: 10.1016/S0895-7061(97)00371-3
24. Madore F, Stampfer MJ, Willett WC, Speizer FE, Curhan GC. Nephrolithiasis and Risk of Hypertension in Women. *Am J Kidney Dis Off J Natl Kidney Found* (1998) 32(5):802–7. doi: 10.1016/S0272-6386(98)70136-2
25. Zhou T, Watts K, Agalliu I, DiVito J, Hoenig DM. Effects of Visceral Fat Area and Other Metabolic Parameters on Stone Composition in Patients Undergoing Percutaneous Nephrolithotomy. *J Urol* (2013) 190(4):1416–20. doi: 10.1016/j.juro.2013.05.016
26. Yamashita S, Iguchi T, Nishizawa S, Iba A, Kohjimoto Y, Hara I. Recurrent Stone-Forming Patients Have High Visceral Fat Ratio Based on Computed Tomography Images Compared to First-Time Stone-Forming Patients. *Int J Urol* (2018) 25(6):569–73. doi: 10.1111/iju.13564
27. Kang HW, Seo SP, Kim WT, Kim YJ, Yun SJ, Lee SC, et al. Hypertriglyceridemia is Associated With Increased Risk for Stone Recurrence in Patients With Urolithiasis. *Urology* (2014) 84(4):766–71. doi: 10.1016/j.urology.2014.1006.1013
28. Kim YJ, Park MS, Kim WT, Yun SJ, Kim WJ, Lee SC. Hypertension Influences Recurrent Stone Formation in Nonobese Stone Formers. *Urology* (2011) 77 (5):1059–63. doi: 10.1016/j.urology.2010.07.492

Conflict of Interest: The authors declare that the research was conducted in the absence of any commercial or financial relationships that could be construed as a potential conflict of interest.

Publisher's Note: All claims expressed in this article are solely those of the authors and do not necessarily represent those of their affiliated organizations, or those of the publisher, the editors and the reviewers. Any product that may be evaluated in this article, or claim that may be made by its manufacturer, is not guaranteed or endorsed by the publisher.

Advantages of publishing in Frontiers

OPEN ACCESS
Articles are free to read for greatest visibility and readership

FAST PUBLICATION
Around 90 days from submission to decision

HIGH QUALITY PEER-REVIEW
Rigorous, collaborative, and constructive peer-review

TRANSPARENT PEER-REVIEW
Editors and reviewers acknowledged by name on published articles

Frontiers
Avenue du Tribunal-Fédéral 34
1005 Lausanne | Switzerland

Visit us: www.frontiersin.org
Contact us: frontiersin.org/about/contact

REPRODUCIBILITY OF RESEARCH
Support open data and methods to enhance research reproducibility

DIGITAL PUBLISHING
Articles designed for optimal readership across devices

FOLLOW US
@frontiersin

IMPACT METRICS
Advanced article metrics track visibility across digital media

EXTENSIVE PROMOTION
Marketing and promotion of impactful research

LOOP RESEARCH NETWORK
Our network increases your article's readership